

Mathematische Modellierung von Influenza Virus Replikation in Säugerkellen

Dissertation zur Erlangung des akademischen Grades

Doktoringenieur

(Dr.-Ing.)

von M. Sc. Yury Sidorenko

geb. am 3. März 1979 in Moskau/Russland

genehmigt durch die Fakultät für Verfahrens- und Systemtechnik
der Otto-von-Guericke-Universität Magdeburg

Gutachter:

Prof. Dr.-Ing. Udo Reichl

Prof. Dr.-Ing. Gennady Bocharov

Promotionskolloquium am 29.09.2005

Table of Contents

Acknowledgements	8
Abstract	9
Abbreviations	11
Nomenclature	13
1 Introduction	21
1.1 Classification of Mathematical Models of Virus Dynamics.....	22
1.1.1 Classification by Abstraction Level.....	23
1.1.2 Classification by Modeling Principles	24
1.2 Modeling Approaches for Virus Replication in the Cells of Different Types...	25
1.3 Modeling of Influenza Virus Dynamics	27
1.4 Objectives of The Present Study.....	29
1.5 Biological Properties of Mammalian Cells.....	29
1.5.1 Structure of Cellular Membranes.....	31
1.5.1.1 Structure and Functions of Membrane Proteins.....	33
1.5.2 Compartmentalization of Mammalian Cells.....	34
1.5.2.1 Structure of Cellular Nucleus.....	34
1.5.2.2 Structure of the Endoplasmic Reticulum and Golgi Apparatus.....	36
1.5.2.3 Membrane-Bound and Free Ribosomes.....	37
1.5.2.4 Structure of Mitochondria, Peroxisomes and Lysosomes.....	38
1.5.3 Movement of Proteins Between Cellular Compartments	39
1.5.4 Intracellular Vesicular Transport	41
1.5.4.1 Uptake of Macromolecules by Receptor-Mediated Endocytosis.....	43
1.5.4.2 Exocytosis	44
1.5.5 Apoptosis	45
1.6 Molecular Biology and Infection Cycle of Influenza A Virus	45
1.6.1 Virus Entry into the Host Cell. Structure of the HA Protein	49

1.6.2 vRNP Uncoating and Transport into the Nucleus. Roles of HA and M2 Proteins	50
1.6.3 Transcription (vmRNA Production)	52
1.6.4 Viral Genome Replication	54
1.6.5 Capsid and Nonstructural Protein Production.....	56
1.6.6 Envelope Protein Production	57
1.6.7 Packaging.....	57
1.6.8 Virus Budding and Release.....	58
2 Model Formulation	60
2.1 Virus Entry into the Host Cell	62
2.2 vRNP Uncoating and Transport into the Nucleus.....	64
2.3 Transcription (vmRNA Production)	65
2.4 Viral Genome Replication	67
2.5 Capsid and Nonstructural Protein Production.....	69
2.6 Envelope Protein Production	71
2.7 Packaging.....	72
2.8 Virus Budding and Release.....	73
2.9 Reduced Model	74
2.10 Model with Reinfection	78
2.11 Model for Continuous Infection.....	80
2.12 Population Model.....	81
3 Initial Conditions, Kinetic Parameters, and Modeling Assumptions	89
4 Results	94
4.1 Overall Dynamics	94
4.2 Dynamics of Virus Entry	95
4.3 Dynamics of vmRNA Production.....	96
4.4 Dynamics of Viral Protein Synthesis.....	98
4.5 Dynamics of Viral Genome Replication.....	100
4.6 Dynamics of the Production of M1-vRNP Complexes.....	103
4.7 Dynamics of Progeny virus Release	104
4.7.1 Exponential Stage	104
4.7.2 Polynomial Stage	105

4.8 Use of Cellular Resources.....	106
4.9 Limiting Factors.....	108
4.10 Influence of Initial Condition Changes on Virus Growth and Limiting Factors.....	110
4.10.1 Theoretical Confirmation.....	113
4.11 Influence of Parameter Changes on the Virus Yield and Limiting Factors...	116
4.11.1 Variations of Switch Parameters.....	117
4.11.1.1 Influence on Limiting Factors.....	118
4.11.1.2 Influence on the Virus Yield.....	119
4.11.1.3 Switch Parameters and vmRNA Dynamics	121
4.11.2 Variations of Internalization Dynamics	122
4.11.2.1 Variations of Rate Constants of Dissociation	125
4.11.3 Variations of Rate Coefficients of Transport.....	125
4.11.3.1 Minimal Value of the Delay of Virus Release.....	126
4.11.4 Combined Variations of Rate Coefficients of Internalization and Transport	127
4.11.5 Variations of Macromolecule Synthesis Rates	129
4.11.6 Variations of Rate Constants of Virus Assembly	130
4.11.7 Variations of Rate Coefficients of Virus Release.....	131
4.11.8 Variations of Rate Constants of Degradation	132
4.11.8.1 Degradation of Incoming Virus Particles	132
4.11.8.2 vmRNA Degradation	133
4.11.8.3 vRNA and cRNA Degradation	135
4.11.8.4 Viral Protein Degradation	135
4.12 Model Reduction.....	138
4.12.1 Dynamics of Viral Component Production.....	139
4.12.2 Limiting Factors.....	142
4.12.3 Variations of Model Parameters and Initial Conditions	143
4.13 Reinfection.....	145
4.14 Continuous Infection. Optimal Strategy of Infection	146
4.15 Population Modeling.....	148
4.15.1 Dynamics of Cell and Virus Populations.....	148
4.15.1.1 Estimation of the Average Lifetime of a Cell.....	150
4.15.2 Influence of MOI Changes on Population Dynamics.....	151

4.15.3 Influence of Parameter Changes on Population Dynamics.....	155
5 Discussion.....	164
5.1 Agreement with Other Models.....	165
5.2 Importance of a Reinfection.....	167
5.3 Maximal Number of Produced Virions.....	168
5.4 Dynamics of Transcription and Genome Replication.....	170
5.4.1 Redundancy of Genome Segments	170
5.4.2 Redundancy of Polymerase Complexes.....	172
5.4.3 General Case	172
5.4.4 Choice of Model Assumption	173
5.4.5 Particularities of Transcription Dynamics	174
5.5 Dynamics of Viral Protein Production.....	176
5.6 Mechanisms of Viral Genome Packaging.....	177
5.6.1 Method to Identify the Mechanism of Packaging.....	179
5.7 Influence of NP Proteins on Virus Dynamics.....	180
5.7.1 Are Incoming NP Proteins Favorable for Virus Production?.....	181
5.8 Limiting Factors. Hierarchy of Redundantly Produced Viral Components	182
5.8.1 NP Proteins are the Second Critical Component at the Assembly of M1-vRNP Complexes.....	183
5.8.2 Relation Between the Number of NS2 Proteins, Polymerase Complexes, and vRNA Molecules.....	184
5.8.3 Viral Components at the Budding Site	185
5.9 Are There Any Other Possible Laws of Virus Growth?.....	187
5.9.1 Duration of the Exponential Stage.....	187
5.10 Further Modifications of the Detailed Single Cell Model	189
5.11 Methods to Increase the Number of Virions Produced in a Cell	191
5.12 Strategies for Antiviral Therapies and Vaccine Production Optimization	192
5.13 Limits of Population Model Applicability.....	193
5.14 Use of the Reduced Model.....	193
5.14.1 Is a Further Model Reduction Possible?.....	194
5.14.2 “Simplest Model” for Virus Production	195
5.15 Possible Reasons for Cell Death.....	197
5.16 Directions for Further Experimental Work.....	199

6 Summary	200
References	204
Appendix	218
A1. Dynamics of the Assembly of Simple Components to Complex Particles.....	218
A2. Infection Probability for Virus Particles Containing Eight Genome Segments	227
A3. Method to Calculate the Average Lifetime of a Cell	228
A4. Estimation of Cellular Pools	229
A5. Experimental Data for Virus Release and Cell Detachment.....	231

Acknowledgements

I am gratefully thankful to the Max Planck Society, to the Otto von Guericke University Magdeburg, and to my scientific supervisor, Prof. Dr.-Ing. Udo Reichl for providing me the opportunity and excellent conditions to work on the present study. Besides that, I would like to thank Udo Reichl for his kindness and readiness to help me during the whole period of the preparation of this thesis, for suggestions and useful discussions. For consultations and a lot of advice I am also very thankful to Prof. Dr. Gennady Bocharov.

I thank the whole bioprocess engineering group of the Max Planck Institute and Otto von Guericke University Magdeburg for the fruitful collaboration. Especially, I am grateful to Dr. Yvonne Genzel for providing me a series of important information and data, and to Dr. Heiner Sann for the proof reading of this thesis. Furthermore, I thank Richard Hanke for his numerous consultations concerning the technical problems.

Finally, I would like to thank my family for a plenty of help, support, and encouragement.

Abstract

Intracellular events that take place during influenza virus replication in mammalian cells are well understood qualitatively. However, to better understand the complex interaction of the virus with its host cell and to quantitatively analyze the use of cellular resources for virion formation or the overall dynamics of the entire infection cycle, a mathematical model for influenza virus replication has to be formulated. Developed in the present study is the first structured model for the single cell reproductive cycle of influenza A virus in mammalian cells that accounts for all the individual steps of the process, such as attachment, internalization, genome replication and translation, and progeny virion assembly.

The model describes an average cell surrounded by a small quantity of medium and infected by a low number of virus particles. It makes possible to determine the basic laws that control the dynamics of virus replication. The model allows estimating the number of cellular resources consumed by virus replication and to reveal factors that limit the growth rate of progeny virus particles and virus release. Based on the model it is also possible to analyze effects of parameter changes on the dynamics of virus replication, and, using this knowledge, to formulate hypotheses concerning the optimization of vaccine production processes.

The single cell model and the results of simulations based on it provide the prerequisite for several useful model modifications. One of such modifications is a population model, taking into account the populations of uninfected, infected, and dead cells, as well as the population of free virus particles. The population model, particularly, provides a possibility to investigate the dynamics of virus production by a cellular system at different number of seeded virions per cell. Furthermore, having revealed the most critical steps of virus replication, it is possible to formulate a reduced single cell model, which adequately reproduces the dynamics of the process. Possessing a simple structure, the reduced model can be used for the development of structured population balance models describing the interaction of infected cells.

The single cell model for the influenza virus life cycle and its modifications facilitate future studies of influenza virus replication at a cellular level. A more detailed insight into the interactions of viruses and host cells might help to improve the understanding of virus-related diseases, to develop therapies against them, and to identify possible targets for molecular engineering. Model equations can be easily modified to include new experimental results, as well as to examine different hypotheses concerning cellular or viral replication mechanisms. Finally, the model can be used as a starting point for modeling infection cycles of other viruses.

Abbreviations

ATP	Adenosine triphosphate
CGN	<i>Cis</i> Golgi network
cRNA	Complementary RNA
DNA	Deoxyribonucleic acid
ER	Endoplasmic reticulum
h	Hour
HA	Hemagglutinin
HIV	Human immunodeficiency virus
HTLV	Human T-cell leukemia virus
IAP	Inhibitor of apoptosis (protein)
L	Litter
MDCK	Madin Darby canine kidney
m	Meter
min	Minute
MOI	Multiplicity of infection
mRNA	Messenger RNA
NA	Neuraminidase
NES	Nuclear export signal
NEP	Nuclear export protein
NLS	Nuclear localization signal
NP	Nucleoprotein
ODE	Ordinary differential equation
ORF	Open reading frame
p.i.	Post infection
rER	Rough ER
RNA	Ribonucleic acid
rRNA	Ribosomal RNA
sER	Smooth ER
TGN	<i>Trans</i> Golgi network

vmRNA	Viral mRNA
vRNA	Viral RNA
vRNP	Viral ribonucleoprotein

Nomenclature

a_{NP}	influence of NP proteins on vmRNA production (<i>cells/NP protein</i>)
b_{NP}	influence of NP proteins on genome replication (<i>NP proteins/cell</i>)
C_c	number of cRNA segments (<i>nucleotides/cell</i>)
C_{cell}	number of free cellular nucleotides (<i>nucleotides/cell</i>)
C_{cyt}	number of vmRNA molecules in the cytoplasm (<i>nucleotides/cell</i>)
$C_{c,i}$	number of i -th cRNA segments (<i>nucleotides/cell</i>)
$C_{m,cell}$	number of cellular precursor mRNA molecules (<i>nucleotides/cell</i>)
$C_{i,nuc}$	number of vmRNA molecules encoding i -th proteins in the nucleus (<i>nucleotides/cell</i>)
$C_{i,cyt}$	number of vmRNA molecules encoding i -th proteins in the cytoplasm (<i>nucleotides/cell</i>)
C_{nuc}	number of vmRNA molecules in the nucleus (<i>nucleotides/cell</i>)
C_{seg}	average number of nucleotides in one vRNA segment (<i>nucleotides/vRNA molecule</i>)
C_T	total number of nucleotides produced per hour (<i>nucleotides/h</i>)
C_v	number of vRNA segments (<i>nucleotides/cell</i>)
$C_{v,i}$	number of i -th vRNA segments (<i>nucleotides/cell</i>)
C_{vir}	number of nucleotides in one virus particle (<i>nucleotides/virion</i>)
d_{rib}	distance between ribosomes processing a vmRNA molecule (<i>nucleotides</i>)
E	number of cellular endosomes (<i>endosomes/cell</i>)
F_i	continuous nonnegative function ($mL^{-1} \cdot h^{-1}$ or h^{-1})
F_{C_v}	continuous nonnegative function (h^{-1})
$F_{C_{Pol,nuc}}$	continuous nonnegative function (h^{-1})

$F_{P_{Pol,cyt}}$	continuous nonnegative function (h^{-1})
H	number of nuclear pores (<i>pores/cell</i>)
i	index (-)
j	index (-)
$K_{C_{v,i},v-c}$	half-saturation function (<i>nucleotides/cell</i>)
$K_{C_{v,i},v-vm}$	half-saturation function (<i>nucleotides/cell</i>)
$K_{P_{Pol,muc},v-c}$	half-saturation function (<i>amino acids/cell</i>)
$K_{P_{Pol,muc},v-vm}$	half-saturation function (<i>amino acids/cell</i>)
$k_{ap,in}$	rate coefficient of the apoptosis of infected cells (h^{-1})
$k_{ap,un}$	rate coefficient of the apoptosis of uninfected cells ($nL \cdot h^{-1}$)
k_{bud}	rate constant of progeny virus assembly (h^{-1})
$k_{bud-rel}$	rate coefficient of progeny virus release ($nL^{-1} \cdot h^{-1}$ or h^{-1})
$k_{bud-rel,V_{bud}}$	rate coefficient of progeny virus release (h^{-1})
$k_{bud-rel,V_{rel}}$	rate coefficient of progeny virus release ($nL^{-1} \cdot h^{-1}$)
$k_{bud,P_{j,bud}}$	rate constant of progeny virus assembly (h^{-1})
$k_{bud,P_{NA,bud}}$	rate constant of progeny virus assembly (h^{-1})
$k_{bud,S_{un,bud}}$	rate constant of progeny virus assembly (h^{-1})
$k_{bud,V_{bud}}$	rate constant of progeny virus assembly (h^{-1})
$k_{c-deg r}$	rate constant of cRNA degradation (h^{-1})
k_{c-v}	rate coefficient of vRNA synthesis (h^{-1})
$k_{c-v,max}$	rate coefficient of vRNA synthesis, maximum value (h^{-1})
$k_{cyt-nuc}$	rate coefficient of vRNP nuclear import (h^{-1})
k_{dt}	rate constant of cell detachment from microcarriers (h^{-1})
$k_{end-cyt}$	rate constant of vRNP uncoating (h^{-1})
$k_{end-cyt,S_{cyt}}$	rate constant of vRNP uncoating (h^{-1})
$k_{end-cyt,V_{end}}$	rate constant of vRNP uncoating (h^{-1})

$k_{end-deg r}$	rate constant of “inactive” virus degradation (h^{-1})
k_{ex-s}	rate coefficient of virus binding ($nL \cdot h^{-1}$ or h^{-1})
$k_{ex-s, V_{ex}}$	rate coefficient of virus binding ($nL \cdot h^{-1}$)
k_{ex-s, V_s}	rate coefficient of virus binding (h^{-1})
k_{feed}	rate of virus supply (<i>virions</i> /($nL \cdot h$))
$k_{i, cyt-deg r}$	rate constant of i -th protein degradation in the cytoplasm (h^{-1})
$k_{i, cyt-nuc}$	rate coefficient of i -th protein nuclear import (h^{-1})
$k_{i, deg r}$	rate constant of i -th protein degradation (h^{-1})
$k_{i, nuc-deg r}$	rate constant of i -th protein degradation in the nucleus (h^{-1})
$k_{i, synt}$	rate coefficient of i -th protein synthesis (h^{-1})
$k_{j, bud-deg r}$	rate constant of j -th protein degradation at the budding site (h^{-1})
$k_{j, ER-bud}$	rate constant of j -th protein transport to the budding site (h^{-1})
$k_{j, ER-deg r}$	rate constant of j -th protein degradation in the ER (h^{-1})
$k_{M2, bud}$	constant factor (<i>amino acids</i> / h)
$k_{NA, bud-deg r}$	rate constant of NA protein degradation at the budding site (h^{-1})
$k_{NA, ER}$	constant factor (<i>amino acids</i> / h)
$k_{NA, ER-bud}$	rate constant of NA protein transport to the budding site (h^{-1})
k_{pck}	rate constant of viral component packaging (h^{-1})
k_{pck, C_v}	rate constant of viral component packaging (h^{-1})
k_{pck, P_i}	rate constant of viral component packaging (h^{-1})
$k_{pck, V_{rel}}$	rate constant of viral component packaging ($nL^{-1} \cdot h^{-1}$)
k_{pl}	rate of RNA strand elongation (<i>nucleotides</i> / h)
k_{Rib}	rate of polypeptide chain elongation (<i>amino acids</i> / h)
k_{s-end}	rate coefficient of endocytosis (h^{-1})
k_{s-ex}	rate constant of virus dissociation from the cellular surface (h^{-1})
$k_{s-ex, V_{ex}}$	rate constant of virus dissociation from the cellular surface (h^{-1})

k_{s-ex,V_s}	rate constant of virus dissociation from the cellular surface (h^{-1})
k_{spl}	rate constant of vRNP splitting (h^{-1})
k_{spl,C_v}	rate constant of vRNP splitting (h^{-1})
$k_{spl,C_v,red}$	rate constant of vRNP splitting ($nL \cdot h^{-1}$)
k_{spl,P_i}	rate constant of vRNP splitting (h^{-1})
$k_{spl,P_i,red}$	rate constant of vRNP splitting ($nL \cdot h^{-1}$)
$k_{spl,P_i,nuc}$	rate constant of vRNP splitting (h^{-1})
$k_{spl,S_{nuc}}$	rate constant of vRNP splitting (h^{-1})
$k_{spl,V_{ex}}$	rate constant of vRNP splitting (h^{-1})
k_{un}	rate constant of M1-vRNP assembly (h^{-1})
k_{un,C_v}	rate constant of M1-vRNP assembly (h^{-1})
k_{un-in}	rate coefficient of infection (h^{-1})
$k_{un,nuc-bud}$	rate coefficient of M1-vRNP nuclear export (h^{-1})
$k_{un,P_i,nuc}$	rate constant of M1-vRNP assembly (h^{-1})
$k_{un,P_{NS1},nuc}$	rate constant of M1-vRNP assembly (h^{-1})
$k_{un,S_{un},nuc}$	rate constant of M1-vRNP assembly (h^{-1})
k_{vd}	rate constant of virus degradation ($nL \cdot h^{-1}$)
k_{v-c}	rate coefficient of cRNA synthesis (h^{-1})
$k_{v-c,i}$	rate coefficient of i -th cRNA synthesis (h^{-1})
$k_{v-c,max}$	rate coefficient of cRNA synthesis, maximum value (h^{-1})
$k_{v-deg r}$	rate constant of vRNA degradation (h^{-1})
k_{v-vm}	rate coefficient of vmRNA synthesis (h^{-1})
$k_{v-vm,i}$	rate coefficient of the synthesis of vmRNA molecules encoding i -th proteins (h^{-1})
$k_{v-vm,i,max}$	rate coefficient of the synthesis of vmRNA molecules encoding i -th proteins, maximum value (h^{-1})

$k_{vm, cyt-deg r}$	rate constant of vmRNA degradation in the cytoplasm (h^{-1})
$k_{vm, i, cyt-deg r}$	rate constant of the degradation of vmRNA molecules encoding i -th proteins in the cytoplasm (h^{-1})
$k_{vm, i, nuc-cyt}$	rate coefficient of the nuclear export of vmRNA molecules encoding i -th proteins (h^{-1})
$k_{vm, i, nuc-deg r}$	rate constant of vmRNA degradation in the nucleus (h^{-1})
$k_{vm, nuc-cyt}$	rate coefficient of vmRNA nuclear export (h^{-1})
$k_{vm, nuc-deg r}$	rate constant of vmRNA degradation in the nucleus (h^{-1})
$L_{vm, i}$	length of the vmRNA molecule encoding i -th proteins (<i>nucleotides</i>)
$L_{v, i}$	length of the i -th vRNA segment (<i>nucleotides</i>)
MOI_1	value of the MOI (<i>virions/cell</i>)
MOI_2	value of the MOI (<i>virions/cell</i>)
MOI_{opt}	optimal value of the MOI (<i>virions/cell</i>)
m_i	number of terms in the right-hand side of the i -th equation (-)
N_{cells}	number of cells (<i>cells</i>)
N_{seg}	number of genome segments in one virus particle (<i>molecules</i>)
$N_{v, i}$	number of i -th vRNA segments produced per hour (<i>molecules/h</i>)
n	number of model equations describing the dynamics of viral components (-)
P_{cell}	number of free cellular amino acids (<i>amino acids/cell</i>)
P_i	number of i -th proteins (<i>amino acids/cell</i>)
P_{inf}	probability for a virus particle to be infectious (-)
$P_{inf, exp}$	probability for a virus particle to be infectious, experimental value (-)
$P_{i, cyt}$	number of i -th proteins in the cytoplasm (<i>amino acids/cell</i>)
$P_{i, nuc}$	number of i -th proteins in the nucleus (<i>amino acids/cell</i>)
$P_{i, seg}$	number of i -th proteins in one M1-vRNP complex (<i>amino acids/M1-vRNP complex</i>)
$P_{i, vir}$	number of i -th proteins in one virus particle (<i>amino acids/virion</i>)

$P_{j,bud}$	number of j -th proteins at the budding site (<i>amino acids/cell</i>)
$P_{j,ER}$	number of j -th proteins in the ER (<i>amino acids/cell</i>)
P_{M1}	number of M1 proteins (<i>amino acids/cell</i>)
$P_{M1,nuc}$	number of M1 proteins in the nucleus (<i>amino acids/cell</i>)
$P_{M1,vir}$	number of M1 proteins in one virus particle (<i>amino acids/cell</i>)
$P_{M2,bud}$	number of M2 proteins at the budding site (<i>amino acids/cell</i>)
$P_{NA,bud}$	number of NA proteins at the budding site (<i>amino acids/cell</i>)
$P_{NA,ER}$	number of NA proteins in the ER (<i>amino acids/cell</i>)
$P_{NP,nuc}$	number of NP proteins in the nucleus (<i>amino acids/cell</i>)
$P_{Pol,nuc}$	number of polymerase complexes in the nucleus (<i>amino acids/cell</i>)
R_0	number of cellular ribosomes (<i>ribosomes/cell</i>)
R_{sf}	number of cellular receptors (<i>receptors/cell</i>)
S_{cyt}	number of vRNP complexes in the cytoplasm (<i>vRNP complexes/cell</i>)
S_{nuc}	number of vRNP complexes in the nucleus (<i>vRNP complexes/cell</i>)
$S_{un,bud}$	number of M1-vRNP complexes at the budding site (<i>M1-vRNP complexes/cell</i>)
$S_{un,nuc}$	number of M1-vRNP complexes in the nucleus (<i>M1-vRNP complexes/cell</i>)
t	time (h)
t_0	time point of the intersection of virus growth curves corresponding to different values of the MOI (h)
T	lifetime of a cell (h)
T_{max}	lifetime of a cell, maximum value (h)
U_r	volume of medium containing N_{cells} cells (nL)
V_{bud}	number of virus particles at the budding site (<i>virions/cell</i>)
V_{end}	number of virus particles in the endosome (<i>virions/cell</i>)
V_{ex}	number of virus particles in the extracellular medium (<i>virions/nL</i>)
V_{ex0}	number of virus particles in the extracellular medium, initial value

	(<i>virions/nL</i>)
$V_{ex,red}$	number of extranuclear virus particles (<i>virions/cell</i>)
V_i	function staying in the left-hand side of the i -th equation (<i>virions/nL</i> or <i>virions/cell</i>)
V_{rel}	number of released virus particles (<i>virions/nL</i>)
$V_{rel,1}$	number of released virus particles at $MOI=MOI_1$ (<i>virions/nL</i>)
$V_{rel,2}$	number of released virus particles at $MOI=MOI_2$ (<i>virions/nL</i>)
$V_{rel,opt}$	number of released virus particles at $MOI=MOI_{opt}$ (<i>virions/nL</i>)
$V_{rel,red}$	number of virus particles assembled in the cell (<i>virions/cell</i>)
V_s	number of surface virus particles (<i>virions/cell</i>)
Z	number of cells (<i>cells/nL</i>)
Z_0	number of uninfected cells, initial value (<i>cells/nL</i>)
Z_d	number of dead cells (<i>cells/nL</i>)
Z_{in}	number of infected cells (<i>cells/nL</i>)
Z_{un}	number of uninfected cells (<i>cells/nL</i>)
$\mu_{c-v,i}$	synthesis rate of i -th vRNA segments (<i>nucleotides/h</i>)
$\mu_{v-c,i}$	synthesis rate of i -th cRNA segments (<i>nucleotides/h</i>)
μ_{v-vm}	vmRNA synthesis rate (<i>nucleotides/h</i>)
$\mu_{v-vm,i}$	synthesis rate of vmRNA molecules encoding i -th proteins (<i>nucleotides/h</i>)
$\mu_{v-vm,prod}$	vmRNA synthesis rate corresponding to the number of viral components produced in the cell (<i>nucleotides/h</i>)
$\mu_{v-vm,vir}$	vmRNA synthesis rate corresponding to the number of viral components delivered with incoming virus particles (<i>nucleotides/h</i>)
$\tau_{att-end}$	time interval between the beginning of attachment and the beginning of internalization (h)
$\tau_{i,j}$	time delay of the step represented by the j -th term in the right-hand side of the i -th equation (h)
σ_{M1}	fraction of mRNA nucleotides encoding M1 proteins in the 7 th genome

	segment (-)
σ_{M2}	fraction of mRNA nucleotides encoding M2 proteins in the 7 th genome segment (-)
σ_{NS1}	fraction of mRNA nucleotides encoding NS1 proteins in the 8 th genome segment (-)
σ_{NS2}	fraction of mRNA nucleotides encoding NS2 proteins in the 8 th genome segment (-)
ω_{end}	change in cell population sizes by the beginning of endocytosis (-)
ω_i	fraction of nucleotides contained in mRNA molecules encoding i -th proteins (-)
ω_{HA}	fraction of nucleotides contained in mRNA molecules encoding HA proteins (-)
ω_{M1}	fraction of nucleotides contained in mRNA molecules encoding M1 proteins (-)
ω_{M2}	fraction of nucleotides contained in mRNA molecules encoding M2 proteins (-)
ω_{NA}	fraction of nucleotides contained in mRNA molecules encoding NA proteins (-)
ω_{NP}	fraction of nucleotides contained in mRNA molecules encoding NP proteins (-)
ω_{NS1}	fraction of nucleotides contained in mRNA molecules encoding NS1 proteins (-)
ω_{NS2}	fraction of nucleotides contained in mRNA molecules encoding NS2 proteins (-)
ω_{pl}	fraction of nucleotides contained in mRNA molecules encoding polymerase complex subunits (-)
ω_{rel}	change in cell population sizes by the beginning of virus release (population model) (-)

1 Introduction

Viruses are small obligate intracellular parasites, which extensively use host cell resources for their replication. They contain either a DNA or RNA genome, surrounded by coat proteins, forming a nucleocapsid. In many animal viruses this nucleocapsid is enclosed by a membrane containing viral glycoproteins required for specific virus-host cell interactions. Viruses are widely used as live attenuated, killed-virus or recombinant protein vaccines. Additionally, the development of viral vectors has a great potential for gene therapy. As synthesis of viral components is carried out by cellular systems, viruses can also serve as powerful tools for investigating cellular metabolism, in particular macromolecular synthesis.

The growth of viruses in their host cells is a complex, highly organized process. For a quantitative understanding of virus replication dynamics, mathematical modeling plays a crucial role. Based on a mathematical model and a set of initial conditions, it is possible to predict the behavior of the system at any moment of time, or to identify possible targets for molecular engineering to improve the yield in vaccine production processes. Detailed insights into virus-host cell interactions might also help to improve the understanding of virus-mediated diseases and to develop antiviral strategies. Besides that, a mathematical model provides a possibility to analyze the sensitivity of the system with respect to variations of its parameters. The importance of such an analysis results from the challenge to quantify how the functional properties of genetic and protein components of the virus correlate with the overall dynamics of virus growth. For example, what happens with the rate of virus production if the virus is modified to express a polymerase complex operating twice faster than the wild-type polymerase complex? Finally, without a mathematical model it is practically impossible to interpret some experimental results, particularly, an increase of the number of virions produced by the cell with a decrease of the number of virions added per cell at the time of infection. While this study deals with virus propagation in a single cell and in cellular populations (e.g., in bioreactors), two other fields, in which mathematical methods for the investigation of the spread of virus

infections have been widely applied, are epidemiology (Sahai and Khurshid, 1995; Daly et al., 2004) and immunology (Nowak and May, 2001; Wodarz et al., 1999; Bocharov and Romanyukha, 1994).

This section considers basic principles of model classification, gives an overview of existing modeling approaches for the infection of bacterial, insect, and mammalian cells by different viruses, and formulates the main objectives of the present study. The rest of the section describes the major components of the biological system to be modeled, i.e., mammalian cells and influenza virus particles.

Section 2 formulates a model that is mainly used to achieve purposes posed in this section (the single cell model), as well as its modifications: the reduced model, the model with the reinfection of the cell by progeny virions, and the model for continuous infection. Besides that, it describes the population model, which allows revealing basic laws of virus spread through the population of cells. Presented in section 3 are basic model assumptions and the values of parameters used for modeling. The results of modeling are reported in section 4. Their importance and compatibility with the results obtained by other research groups are, in turn, discussed in section 5. Finally, section 6 summarizes the major achievements of the present study.

1.1 Classification of Mathematical Models of Virus Dynamics

According to the set of modeling assumptions and the data sources used, mathematical models of virus dynamics can be classified by several aspects, the most common of which are abstraction level and modeling principles.

1.1.1 Classification by Abstraction Level

Complex cellular systems are quantitatively described by using different types of abstractions. In other words, the model takes into account only important in the current investigation cellular components and processes. The other, minor parts are not considered. Thus, it is possible to distinguish two types of modeling approaches: structured and unstructured (Fig. 1.1) (Bailey, 1998; Fredrickson et al., 1970). An unstructured model does not consider intracellular phenomena. For example, the basic dynamics of virus growth in bioreactors could be modeled by a system of three differential equations, which describe how the numbers of uninfected cells, infected cells and free virus particles change over time (Moehler et al., in press). In a structured model, different state variables are used to model virus replication in different cellular compartments such as membrane, endosome, cytoplasm or nucleus. Based on genetic and molecular mechanistic data, rate equations are expressed for viral transcription, translation, protein expression, and for reactions catalyzed by virus-encoded enzymes (Sidorenko and Reichl, 2004). An alternative way of model structuring consists in the individual consideration of multiple chemical components of cell material, e.g., DNA, RNA, proteins, etc. (Nadeau et al., 2000).

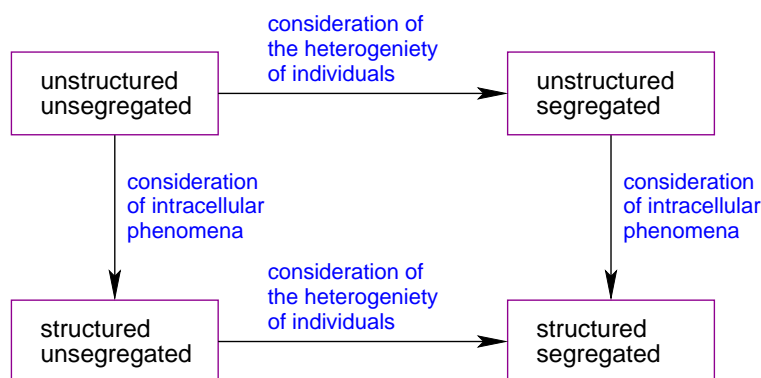


Figure 1.1 Classification of mathematical models of cell population dynamics by abstraction level.

Besides that, modeling approaches can be considered in respect to the presence of heterogeneous individuals in the population of cells. A model accounting for the heterogeneous population of cells is referred to as a segregated model, whereas an

unsegregated model treats the cell population as a uniform mass of “average cells”. Most of the models dealing with the interaction of viruses with their host cells belong to the unsegregated class (see sections 1.2, 1.3).

1.1.2 Classification by Modeling Principles

Complex interactions between elementary processes taking place during the virus replication cycle, e.g., virus entry into the host cell, transcription and replication of the viral genome, and the assembly of progeny virus particles, can be quantitatively interpreted by either a deterministic model (based usually on a system of ordinary differential equations (ODEs)) or a stochastic model (Srivastava et al. (2002)). Deterministic models can provide the ideas concerning the relationships between the numbers of viral components in different intracellular compartments. However, since a deterministic model is unsegregated, it can be applied only for the cases when the number of virions is higher than the number of cells to be infected; it cannot adequately describe the situation when the infection of the cell culture is initiated by a single virus particle that delivers its genome into one cell of the whole population. In the later case, applying of a stochastic model can provide the dynamics of viral components qualitatively different from that provided by a deterministic model. The study of Srivastava et al. (2002) deals with the comparison of deterministic and stochastic modeling approaches for the investigation of the intracellular kinetics of a generic virus. Both approaches are based on the reactions of synthesis and depletion of viral structural proteins and nucleic acids. Deterministic and stochastic simulations provide different transient kinetics and different steady state levels of viral components, particularly for low values of the multiplicity of infection (MOI), when the infection of the cell is initiated by a low number of virus particles (the exact definition of the MOI is given in section 4.10 below).

1.2 Modeling Approaches for Virus Replication in the Cells of Different Types

Mathematical models have been developed for virus infection cycles in bacteria, insect and mammalian cells. A structured mathematical model for bacterial viruses, considered by Endy et al. (1997), examines the replication of the bacteriophage T7 in *Escherichia coli*. The model provides a complete picture for the phage growth cycle. It describes individual steps of infection, including the entry of the viral genome into the host cell, transcription and replication of DNA, translation of mRNA, and progeny phage assembly. Among the unstructured approaches for the modeling of bacteriophage infections are the studies of Schwienhorst et al. (1996) and Beretta and Kuang (1998). Developed in the former work is a basic two-stage model for the bacteriophage infection cycle, in which the adsorption and the intracellular stages are taken into account, whereas the latter model accounts for the influence of a “virus replication factor” (the average number of virus particles released per cell) on the dynamics of the infection.

Other research groups are working on unstructured and structured models of baculovirus replication in insect cells (Dee and Shuler, 1997; Jang et al., 2000; Hu and Bentley, 2000; Licari and Bailey, 1992; De Gooijer et al., 1992). A comprehensive overview of possible approaches to model baculovirus infection is given by Power and Nielsen (1996).

Most of the structured models either deal only with initial steps of the virus infection cycle or omit some intermediate steps. For example, a deterministic model from Dee and Shuler (1997) considers virus attachment, internalization, endosomal fusion, and delivery of the virus genome to the nucleus. However, neither viral protein synthesis nor the assembly and release of progeny virus particles are taken into account. Earlier a similar method was applied to describe the replication of Semliki Forest virus in baby hamster kidney cells (Dee et al., 1995). Another structured model was proposed by Jang et al. (2000). It considers the whole processes of the infection cycle of baculovirus, but being focused mainly on recombinant protein production and the effect of the infection on the host cell metabolism, it does not address some other

steps of infection, such as endosomal sorting, endosomal fusion, and nuclear import of the viral genome.

A study of Licari and Bailey (1992) deals with a stochastic model capable to simulate the dynamics of a population of baculovirus-infected insect cells, the behavior of the number of extracellular virions, and the virus yield. The model deals with the infection of a cell population with high numbers of virus particles (up to five virions per cell). The authors applied a Poisson distribution to approximate the probability that the cell is infected by more than one virus particle. As the model takes into account cell growth, besides the optimal for virus production value of the MOI it can also predict the optimal infection time (the early exponential growth phase). Another probabilistic approach, demonstrated by Hu and Bentley (1999), is the first study that takes into account the process of the formation of progeny baculovirus particles. The authors present a statistical population model characterizing baculovirus infection, protein synthesis and the assembly of virus-like particles (empty virus particles, containing only the outer viral proteins) in insect cells. Like in the earlier study (Licari and Bailey, 1992), the probability of infection is assumed to obey a Poisson distribution, and the function describing the population of cells depends on three variables: the time post infection (p.i.), the number of infecting virions, and the time-delay parameter τ . However, in the model of Hu and Bentley (1999) the number of infecting viruses per host cell is not limited by five, which seems to be essential to describe properly the distribution of the number of virus particles per cell. Another essential advantage of this approach is that it makes possible to consider the virus yield not only as a function of the MOI, but also as a function of the infecting cell density (the concentration of cells to be infected).

So far, virus replication in mammalian cells has mainly been modeled by unstructured approaches. A number of papers are focused on hepatitis virus (Marchuk et al., 1991; Medley et al., 2001; Zhao et al., 2000; Neumann A. et al., 2000), human immunodeficiency virus (HIV) (Funk et al., 2001; Habtemariam et al., 2001; Krogstad et al., 1999), and human T-cell leukemia virus (HTLV) *in vivo* dynamics (Eshima et al., 2001; Wodarz et al., 1999). For example, the study of Funk et al. (2001) is concerned with a basic model for different forms of HIV infection, which

enables determining the basic reproductive rate of the virus (the average number of cells, secondarily infected by one virus-producing cell) as a quantitative measure of the replication capacity of the virus. Another model, formulated by Habtemariam et al. (2001), examines the interaction between the population of cells (CD4) and HIV. Two unstructured models of influenza virus replication *in vivo* are demonstrated by Bocharov and Romanyukha (1994) and Beauchemin et al. (2005). Both studies deal with the immunological aspects of the infection; the former considers a deterministic ODE model, and the later, based on a two-dimensional cellular automaton model, describes the process of infection as a sequence of stochastic events.

At the same time, structured modeling is not so widespread. A detailed mathematical description of HIV-1 infection of CD4 cells was given by Reddy and Yin (1999). All major steps of the virus growth cycle after its internalization to the host cell, e.g., reverse transcription, integration of viral DNA molecules into the genome of the host cell, transcription, splicing of viral mRNA (vmRNA) molecules, genome replication, and formation of progeny virus particles are addressed in detail. Another example of a structured approach is the work of Dee et al. (1995) for Semliki Forest virus dynamics, which mainly considers the initial steps of the infection.

1.3 Modeling of Influenza Virus Dynamics

The present study focuses on modeling of influenza virus replication in mammalian cell culture. Influenza virus is a lipid-enveloped RNA virus that belongs to the *Orthomyxoviridae* family. The membrane of the virion is embedded by molecules of *hemagglutinin* (HA), a glycoprotein containing the receptor binding and the membrane fusion activities, and *neuraminidase* (NA), possessing the receptor destroying activity. Among the three types of influenza (A, B and C), influenza A virus is the best characterized and represents the most significant threat. It causes respiratory infections that result in severe human and animal suffering and high economic losses.

Influenza virus replication was thoroughly investigated by many groups and a number of excellent books and reviews describe its replication in host cells (Nicholson et al., 1998; Flint et al., 2000; Portela and Digard, 2002; Ludwig et al., 1999; Whittaker et al., 1996; Lamb and Choppin, 1983). However, most studies focus on qualitative aspects of virus attachment, endocytosis, protein expression, genome replication, budding and release.

Structured mathematical models developed so far describe only initial steps, such as virus binding and endocytosis. For example, Nunes-Correia et al. (1999) developed a detailed mass kinetic model for the internalization of influenza virus into Madin Darby canine kidney (MDCK) cells, which focuses on virus attachment and endosomal fusion. Together with experimental data, the model enabled the authors to determine several rate coefficients, particularly those for virus binding to the membrane of the cell and virus endocytosis.

Other studies, dealing with the mathematical modeling of hemagglutinin (HA)-mediated fusion between HA-expressing cells and erythrocytes (Mittal and Bentz, 2001; Schreiber et al., 2001), consider in detail all basic steps of the process involved (e.g., lateral diffusion of HA proteins and receptors, reversible formation of HA-receptor contact, and irreversible transformation of HA-receptor contacts into stable bonds between HA proteins and the membrane) and can be applied to describe the attachment of influenza virions to their host cells. The former work is concerned with a deterministic model of the process, whereas the authors of the later article consider the formation of fusion pores as a stochastic event (a very small number of virions infecting a population of host cells is considered).

A detailed mathematical model related to the whole infection cycle of influenza virus has not yet been reported.

1.4 Objectives of The Present Study

Developed in the present study is a structured unsegregated deterministic mathematical model, which describes the complete life cycle of influenza A virus in mammalian cells. According to the work of Bailey (1998), any mathematical model is meaningless if it is not preceded by the explicit definition of its purpose. It must be particularly defined what the use of the model is, i.e., what problems the model is intended to solve. The objective of the model consists in the following: a) to reveal basic laws that control the process of virus replication (particularly, to analyze virus growth dynamics), b) to better understand the complex mechanisms underlying the interaction of virions with their host cells, and c) to use this knowledge for the optimization of virus yields in vaccine production processes. Moreover, the population model is aimed to reveal the dynamics of virus spread in the cell population. Evidently, for the achievement of such purposes it is necessary to describe individually all the steps of the infection cycle, such as virus attachment, internalization, transcription and replication of the viral genome, synthesis of viral proteins, and assembly of newly produced viral components into progeny virions.

1.5 Biological Properties of Mammalian Cells

Cells are building blocks of all living creatures. The cell represents a compartment filled with a watery solution of chemical substances. The simplest form of life is represented by solitary cells, which propagate by division into two daughter cells. In higher organisms, however, cells are subdivided into different groups with certain functions, interconnected by complex systems of communication.

All living cells are subdivided into *procaryotic* and *eucaryotic* cells. Representatives of procaryotic cells are bacteria, the simplest organisms found in the natural environment, and their close relatives. In contrast to procaryotes, which possess a single cytoplasmic compartment, eucaryotic cells (e.g., epithelial cells, Fig. 1.2) have a *nucleus*. The nucleus of eucaryotic cells is a separate internal compartment, enclosed by a double layer of a membrane and containing most of the cellular DNA

molecules. The rest of cellular compartment, where most of the metabolic reactions occur, is called *cytoplasm*. The cytoplasm is filled with a variety of *organelles*, the most noticeable of which are *mitochondria* (and *chloroplasts* in cells, which are able to carry out photosynthesis). These organelles have their own double layer membranes chemically different from the nuclear membrane. Additionally, eucaryotic cells have a *cytoskeleton*, a system of protein filaments. Together with adjacent proteins, the cytoskeleton provides the cell with the mechanical strength, controls the shape of the cell, and guides cellular movements.

Another basic feature of all eucaryotic cells is a plenty of internal membranes. Besides surrounding the nucleus, mitochondria, and chloroplasts, membranes form a twisted structure of the *endoplasmic reticulum (ER)*, the compartment responsible for the synthesis of membrane lipids and proteins, as well as the materials to be excreted from the cell. Flattened sacs of the *Golgi apparatus*, which serves for the transport and modification of molecules synthesized in the ER, are also formed by membranes. Implementing intracellular digestion *lysosomes* are surrounded by a membrane to avoid the attacks of their contents to the cellular macromolecules elsewhere in the cell. For the similar purpose membranes surround *peroxisomes*, which produce and degrade highly reactive hydrogen peroxide during the oxidation processes occurring with the participation of O_2 . Besides that, membranes form in the cytoplasm small vesicles. All membrane-bounded organelles usually occupy about a half of the total cellular volume. The remaining compartment of the cytoplasm is referred to as *cytosol*.

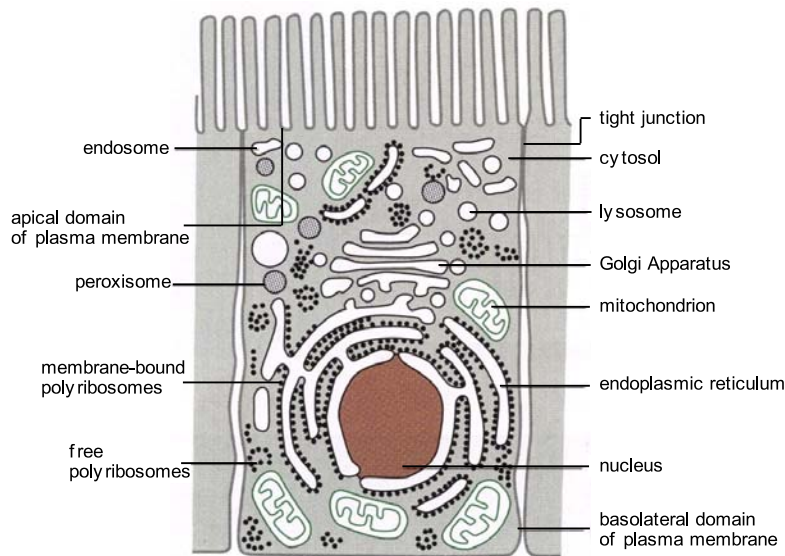


Figure 1.2 Epithelial cell and its major intracellular compartments. Adapted from Alberts *et al.*, 2002.

This section focuses on mammalian cells, which represent a constituent of the biological system considered in the present study. The main attention will be paid on the properties of cells that virus particles use for their replication. Considered will be the basic characteristics of cellular compartments, their functions, as well as the transfer of substances between different compartments. In the end of the section the process of apoptosis (programmed cell death) will be briefly described.

1.5.1 Structure of Cellular Membranes

Membranes play a variety of essential roles in the lifecycle of mammalian cells. For example, the *plasma membrane* defines the boundaries of the cell and maintains the characteristic differences between the cytosol and the extracellular environment. Similarly, inside the cell membranes of organelles, e.g., Golgi apparatus or mitochondria, are responsible for the maintenance of the difference between the contents of the organelle and the cytosol. Additionally, plasma membrane contains proteins that are called *receptors* and serve as sensors of external and internal signals. Receptors are responsible for the transfer of information across the membrane that

allows the cell to adjust its behavior in accordance with possible changes of environmental conditions.

Each biological membrane represents a thin film of lipid and protein molecules (Fig. 1.3). Lipids make up about 50% of the membrane mass, proteins constituting almost all the remaining (Alberts et al., 2002). Lipid molecules form a continuous double layer, called a *lipid bilayer*, with a thickness of approximately 5 nm. Among all the components making up a lipid bilayer phospholipids are the most numerous. Besides phospholipids, cholesterol and glycolipids are also contained in essential amounts. A lipid bilayer is the universal basis of the structure of a cellular membrane. Representing a two-dimensional liquid, in which the molecules possess the ability of lateral movement, it defines the fluid structure of the membrane. Besides that, it serves as a barrier for the transfer of water-soluble molecules into the intracellular compartment. As influenza virus particles acquire the lipid bilayer of their membrane from the plasma membrane of the cell, the structure and the composition of cellular and viral membranes resemble each other.

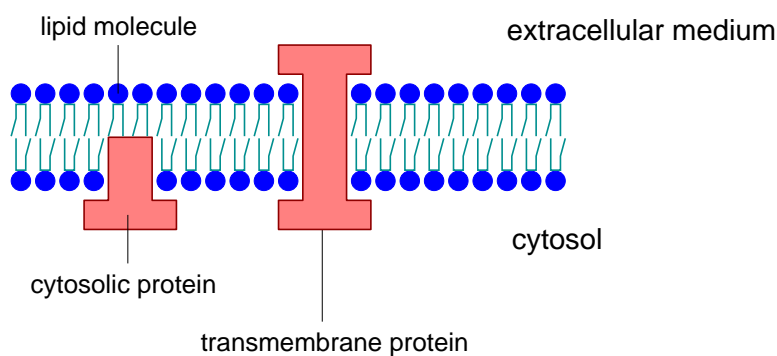


Figure 1.3 Structure of a cellular membrane. Transmembrane proteins extend through the lipid bilayer. Other membrane proteins are entirely located in one compartment, being associated with the corresponding monolayer of the lipid bilayer.

Protein molecules inserted into the lipid bilayer perform all the other functions of a membrane, such as the transport of specific molecules across it or the catalysis of membrane-associated reactions (e.g., ATP synthesis). In the plasma membrane part of the proteins serves as structural links connecting the cytoskeleton to either the

extracellular medium or adjacent cells. The other part represents receptors responsible for the detection of chemical signals in the extracellular medium. For the cell to function and to interact with its environment a variety of membrane proteins is required. Consequently, it is not surprising that approximately 30% of the proteins encoded by the genome of a mammalian cell are membrane proteins.

1.5.1.1 Structure and Functions of Membrane Proteins

The set of membrane proteins defines the characteristic functional properties of each type of cellular membranes. There are several possible mechanisms for the association of proteins with the membrane (Fig. 1.3) (Alberts et al., 2002). For example, some membrane proteins, called *transmembrane proteins*, extend through the lipid bilayer, disposing parts of their mass on each side. Some transmembrane proteins, such as *porin proteins*, form large transmembrane channels. Since the main function of channel proteins is the transport of inorganic ions, these proteins are usually called *ion channels*. Similar to the cell, influenza virus particles possess ion channel proteins embedded into their membrane (*M2 proteins*). The transport of H⁺ into the interior of the virion, performed by these proteins is essential for the release of viral genome from the endosome to the cytoplasm (see section 1.6.2). There is an essential difference between the parts of transmembrane proteins situated on the two sides of the membrane. Since the vast majority of these proteins in mammalian cells are glycosylated (see section 1.5.2.2), the parts of proteins on the noncytosolic side of the membrane always possess the oligosaccharide chains (Gahmberg and Tolvanen, 1996).

Other membrane proteins are entirely located either in the cytosol or at the external cell surface, being associated with the corresponding monolayer of the lipid bilayer. Finally, many membrane proteins do not extend into the lipid bilayer at all; they are bound to the membrane by noncovalent interactions with other membrane proteins (Driscoll and Vuidepot, 1999). Most of these proteins, called *peripheral membrane proteins*, can be released from the membrane by slight changes of the environmental conditions that influence protein-protein interactions, e.g., by the decrease of the pH.

The other membrane proteins that cannot be released from the membrane by this way, i.e., transmembrane proteins and proteins attached to the lipid bilayer, are referred to as *integral membrane proteins*. As well as M2 ion channels, HA and NA proteins of influenza virus are integral membrane proteins.

The functions of a membrane protein are defined by the nature of its association with the lipid bilayer. For example, cellular surface receptors are transmembrane proteins that bind signal molecules from the extracellular medium and can generate corresponding intracellular signals on the opposite side of the plasma membrane. Proteins responsible for the intracellular signaling are, in contrast, associated only with the cytosolic part of the plasma membrane.

1.5.2 Compartmentalization of Mammalian Cells

All eucaryotic cells are subdivided into functionally different, membrane-enclosed compartments (organelles), containing their own set of specialized molecules. The major intracellular compartments of mammalian cells are presented in Figure 1.2. The most essential determinants of the structural and functional properties of the organelle are its proteins, which catalyze chemical reactions and selectively transport small molecules into and out of the organelle interior (*lumen*). Additionally, proteins function as surface markers mediating the delivery of macromolecules to the organelle. A mammalian cell contains in average approximately 10^{10} molecules of proteins of about 10^4 kinds (Alberts et al., 2002). The synthesis of the most of these molecules starts in the cytosol, and each newly synthesized protein is then specifically transported to the compartment where it is required.

1.5.2.1 Structure of Cellular Nucleus

The *nucleus* represents the site of nucleic acid (DNA and RNA) synthesis and contains the major part of cellular genome. Its envelope consists of two concentric

membranes, the inner membrane being structurally supported by a protein network, called *nuclear lamina*. The outer membrane of the nucleus represents the continuation of the membrane of the ER, and the space between the inner and the outer nuclear membranes (the *perinuclear space*) is continuous with the ER lumen. The cytosolic surface of the outer nuclear membrane, similar to that of the ER, contains a plenty of membrane-bound *ribosomes*, which are responsible for the synthesis of proteins needed in the perinuclear space.

There is continuous bidirectional traffic between the cytosol and the nucleus. A plenty of proteins functioning in the nucleus, e.g., DNA and RNA polymerases, gene regulatory proteins, are imported into the nucleus from the cytosol, where they are synthesized. On the other hand, mRNA molecules synthesized in the nuclear compartment are exported to the cytosol. Both nuclear import and export are selective processes and proceed through the *nuclear pore complexes*, piercing the envelope of the nucleus. A nuclear pore complex represents an elaborate structure made up by more than 100 different proteins (*nucleoporins*) (Allen et al., 2000). The number of nuclear pore complexes is thought to define the activity of the nucleus in transcription, more active nuclei containing higher numbers of pores. The envelope of mammalian cell nucleus contains in average 3000-4000 nuclear pore complexes (Alberts et al., 2002).

Small molecules (smaller than 5000 Daltons) are able to pass through the nuclear pore complex by diffusion; it was shown that in respect to free diffusion a nuclear pore was equivalent to a water-filled cylindrical channel, about 15 nm long and 9 nm in diameter (Stoffler et al., 1999). At the same time, complex protein and nucleic acid molecules are transported into and out of the nucleus actively, by specific receptor proteins binding to them. For instance, the proteins to be imported into the nucleus carry *nuclear localization signals* (NLSs), recognized by *nuclear import receptors* (Goerlich and Mattaj, 1996). The system of nuclear export, in turn, relies on *nuclear export signals* (NESs), carried by exported macromolecules, and on complementary *nuclear export receptors*. During their replication cycle influenza viruses extensively use cellular transport machinery for the nuclear export and import of their mRNA molecules and proteins, as well as for the delivery of their genome into the nucleus. Necessary for that NLSs and NESs are carried by correspondent viral proteins (see

sections 1.6.2 and 1.6.7).

The nucleus is surrounded by the cytoplasm, which comprises the cytosol and cytoplasmic organelles. The cytosol is the main site of protein synthesis and degradation. Most of the intermediary metabolism of the cell, e.g., the synthesis of building blocks for macromolecules, also takes place in the cytosol.

1.5.2.2 Structure of the Endoplasmic Reticulum and Golgi Apparatus

The ER comprises about half of the total area of cellular membrane and extends from the nucleus throughout the entire cytosol. Its net-like labyrinth represents an arrangement of interconnected tubules and sacs. The membrane of the ER encloses a single internal space that occupies about 10% of the total cellular volume (Alberts et al., 2002) and is called the *ER lumen*. The membrane of the ER mediates the selective transport of molecules between the ER lumen and the cytosol.

Bound to its cytosolic surface ribosomes are involved in the synthesis of membrane proteins. After influenza infection ER-bound ribosome also synthesize viral HA, NA, and M2 proteins. ER regions that are covered by ribosomes form the *rough ER (rER)*, whereas the other part of the ER, lacking ribosomes, is referred to as the *smooth ER (sER)*. Since the sER contains budding sites of vesicles transporting newly synthesized macromolecules to the Golgi apparatus, it is also called the *transitional ER*. Besides producing proteins, the ER synthesizes lipids for the rest of the cell. Produced in the ER are all major classes of lipids, including phospholipids and cholesterol, required for the production of new cellular membranes.

Another essential biosynthetic function of the ER is the covalent addition of sugars to proteins. This process is known as *protein glycosylation*, and glycosylated proteins are, correspondingly, referred to as *glycoproteins*. Almost all soluble and membrane-bound proteins made in the ER, including proteins to be transported to the Golgi apparatus, lysosomes, plasma membrane, and extracellular medium, are

glycoproteins. The majority of cytosolic proteins are, in contrast, not glycosylated. Protein glycosylation has an important role in the control of protein folding in the lumen of the ER, so that only properly folded proteins are able to leave the ER (Parodi, 2000). However, even being glycosylated, about 80% of proteins translocated into the ER fail to achieve their properly folded state. Proteins that do not fold correctly are excreted into the cytosol, where they are degraded by proteasomes. Additionally, protein glycosylation seems to be important for the protein sorting in the *trans* Golgi network (TGN, see below).

Many proteins and lipids synthesized in the ER are sent by COPII-coated transport vesicles (see section 1.5.4 below) to the *Golgi apparatus* (Klumperman, 2000; Glick, 2000). The Golgi apparatus consists of organized stacks of four to six disc-like membrane-enclosed compartments (*Golgi cisternae*). In most cells it is situated close to the nucleus and lies on the exit route from the ER. The major function of the Golgi apparatus is the synthesis of carbohydrates, an essential part of which is attached in glycosylation reactions to many proteins and lipids delivered from the ER as oligosaccharide side chains. Having acquired the appropriate oligosaccharides, proteins and lipids can be recognized for targeting into transport vesicles going to a variety of cellular sites. Thus, the Golgi apparatus serves as a sorting station for the products of the ER.

Each Golgi stack has two faces, a *cis face* (entry face) and a *trans face* (exit face). *Cis* and *trans* faces are closely associated with corresponding compartments, the *cis Golgi network (CGN)* (or *intermediate compartment*) and the *TGN*, each representing the network of interconnected tubular and cisternal structures (*cis* cisternae and *trans* cisternae respectively). Proteins and lipids enter the CGN and exit from the TGN, where they are packaged into transport vesicles and then transported to their specific destinations. Both networks seem to be important for the sorting of macromolecules.

1.5.2.3 Membrane-Bound and Free Ribosomes

Ribosomes are complex catalytic machines performing protein synthesis. They are

made from about 50 different proteins (*ribosomal proteins*) and several RNA molecules (*ribosomal RNA molecules, rRNA molecules*). Besides ribosomes attached to the cytosolic part of the ER (or nuclear) membrane, there is a separate population of free cytosolic ribosomes. A typical mammalian cell contains in its cytosol about 10^7 ribosomes (Alberts et al., 2002). While membrane-bound ribosomes catalyze the synthesis of proteins to be translocated into the ER (or into the nucleus), free ribosomes synthesize all other proteins encoded by the genome (during the infection cycle of influenza virus they also synthesize capsid and nonstructural viral proteins). There is no functional difference between free and membrane-bound ribosomes; the location of the ribosome is defined only by the protein it produces at the given moment of time. For example, if a protein carries an ER signal sequence, the ribosome is directed to the ER membrane.

Usually, several ribosomes are bound to a single mRNA molecule, forming a *polyribosome* (or a *polysome* complex). If the mRNA molecule to be translated encodes a protein carrying an ER signal sequence, the polyribosome is directed to the ER membrane. The growing polypeptide chain is then translocated into the ER lumen by threading its loop across the ER membrane. When finishing the translation, individual ribosomes can return to the cytosol, however the mRNA molecule remains bound to the membrane of the ER by a changing population of ribosomes. In the case when the synthesized protein lacks an ER signal sequence, the polyribosome and, correspondingly, the mRNA molecule, are free in the cytosol. Thus, mRNA molecules, similar to ribosomes, can be either attached to the membrane of the ER or free. Individual ribosomes are suggested to move randomly between these two mRNA populations.

1.5.2.4 Structure of Mitochondria, Peroxisomes and Lysosomes

Mitochondria represent double-membrane-enclosed organelles that are aimed to generate ATP, exploited by the cell to drive the reactions requiring the input of free energy. Used for this purpose is the energy derived from electron transport and

oxidative phosphorylation. *Peroxisomes* are small vesicular compartments that contain enzymes catalyzing a variety of oxidative reactions and, together with mitochondria, represent the major site of molecular oxygen utilization. Unlike mitochondria, they are surrounded by only one membrane layer.

Lysosomes are membrane-enclosed compartments containing hydrolytic enzymes (*acid hydrolases*) used for the controlled intracellular digestion of needless (e.g., damaged) intracellular organelles, macromolecules (e.g., sugars, proteins, nucleic acids, and lipids), or particles taken from the extracellular medium by endocytosis. Contained in lysosomes are about 40 types of digestive enzymes including proteases, lipases, nucleases, phosphatases, etc. (Luzio et al., 2003). The lysosomal membrane has an ATP-driven H^+ pump responsible for the maintenance of the acidic pH in the interior. An acid environment is required for the activity of acid hydrolases; the lysosomal pH is maintained at a level of about 5.0 by pumping H^+ into its lumen. At the cytosolic pH, equal to approximately 7.2, the digestive enzymes of lysosome cannot cause significant damages; consequently, their possible leakage would not be severely harmful for the contents of the cytosol. Products of macromolecule degradation are further used as precursors for cellular anabolic pathways.

1.5.3 Movement of Proteins Between Cellular Compartments

The fate of cellular proteins, the most of which are synthesized in the cytosol by ribosomes, is defined by *sorting signals* contained in their amino acid sequence (von Heijne, 1990). Sorting signals mediate the transport of proteins to their final destinations outside the cytosol, and proteins deprived of sorting signals remain in the cytosol. Additionally, sorting signals direct the delivery of proteins from the ER to other destinations.

There are three possible mechanisms, by which proteins are transported from one compartment to another: *gated transport*, *transmembrane transport*, and *vesicular transport*. Gated transport relates to protein trafficking between the cytosol and the

nucleus. It implies that the spaces on both sides of the membrane are topologically equivalent. The nuclear pore complexes present an example of selective gates actively transporting specific macromolecules into and out of the nucleus. By transmembrane transport specific proteins are directly transferred across a membrane to a topologically distinct space. This way relates, for example, to the transport of selected proteins from the cytosol to the ER interior. Vesicular transport delivers proteins from one compartment to another by membrane-enclosed transport intermediates (Fig. 1.4). A transport vesicle, loaded with molecules from the lumen of the first compartment, pinches off from the membrane of this compartment and discharges to the second compartment after fusing with its membrane. An example of vesicular transport is the transfer of soluble proteins from the ER to the Golgi apparatus. Transported proteins do not cross a membrane; consequently, vesicular transport can move proteins only between topologically equivalent compartments.

Sorting signals are recognized by complementary sorting receptors that deliver the protein to the appropriate target organelle. For example, for its nuclear import a protein must have a sorting signal (NLS) recognized by receptor proteins that guide it through the nuclear pore complex (see section 1.5.2.1). Similarly, sorting signals of proteins to be transported directly across a membrane are recognized by the translocator of this membrane. At last, proteins to be loaded to a vesicle must possess sorting signals recognized by complementary receptors in the appropriate membrane.

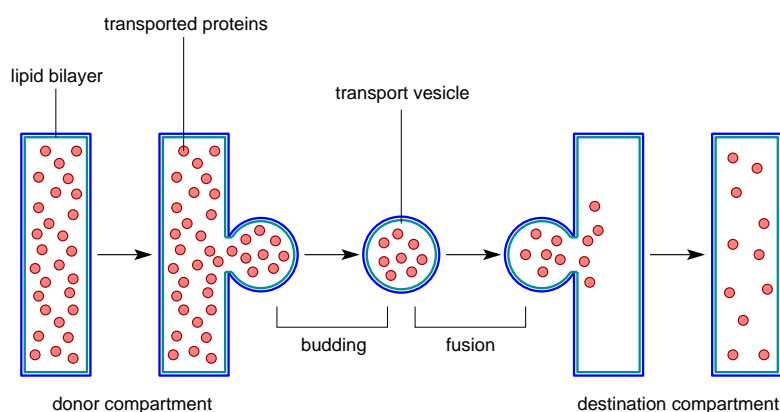


Figure 1.4 Movement of proteins by intracellular vesicular transport. A transport vesicle buds from the donor compartment and fuses with the destination compartment.

1.5.4 Intracellular Vesicular Transport

The plasma membrane of the cell permits indispensable molecules to enter and waste molecules to leave the cellular interior. The nature of this barrier is defined by existence of specific transport processes, as well as physical properties of the lipid bilayer, making up the membrane. Thus, a number of molecules, e.g. water and dissolved gases, can freely cross the membrane. On the other hand, many metabolites, such as nucleotides and ATP, cannot pass through the membrane in this way. Ions, sugars and amino acids are taken up by *permeases*, integral membrane proteins, whereas macromolecules and large particles, such as viruses and bacteria, are usually transported into the cell by *endocytosis*.

In mammalian cells the consumption of specific macromolecules from the extracellular medium by *endocytosis* (*endocytic pathway*) and their digestion, as well as the regulation of the export of newly produced macromolecules by *exocytosis* (*biosynthetic-secretory pathway*), is performed by a complex system of internal membranes. The lumens of all membrane-enclosed compartments involved in endocytosis and exocytosis are topologically equivalent, which allows the communication of compartments by vesicular transport (see section 1.5.3). The traffic of transport vesicles occurs along highly organized directional routes. For instance, the endocytic pathway leads inward from the plasma membrane, while the biosynthetic secretory pathway leads outward from the ER to the cell surface. Most of the transport vesicles are formed as *coated vesicles* from specialized coated domains of membranes. The coat represents a curved lattice, and its formation allows molding the form of the vesicle by the corresponding deformation of the membrane. Additionally, the coat concentrates specific membrane proteins in a certain patch of the membrane, which is destined to form the membrane of the vesicle. Before the fusion of vesicular and target membranes the coat disintegrates to allow the direct interaction of two cytosolic membrane surfaces.

Several types of coated vesicles are distinguished with respect to their coat proteins, the best characterized of which are *clathrin-coated*, *COPI-coated*, and *COPII-coated* vesicles. Clathrin-coated vesicles usually carry out the transport of molecules (*ligands*) from the plasma membrane and from the Golgi apparatus, COPI-coated vesicles transfers ligands from endosomes and Golgi apparatus, and COPII-coated vesicles mediate transport from the ER.

Among the three mentioned types of coated vesicles, clathrin-coated vesicles are the most thoroughly studied. A clathrin-coated vesicle is formed by two major protein components: fibrous protein called *clathrin* and a multisubunit complex referred to as *adaptin* (Schmid, 1997). Clathrin subunits that possess the ability of spontaneous self-assembly into polyhedral cages are responsible for the formation of *coated pits* on the cytosolic surface of the membrane. Clathrin-coated pits are known to include up to 2% of the surface area of a cell (Flint et al., 2000). Adaptin is, in turn, required to bind the clathrine coat to the membrane and to capture transmembrane receptors that bind the molecules to be transported. Growing clathrin-coated buds invaginate and finally pinch off from the membrane (Fig. 1.5). As soon as the vesicle is released, the clathrin coat is rapidly (in a few seconds) removed from the vesicle membrane by special proteins, attached to the vesicle.

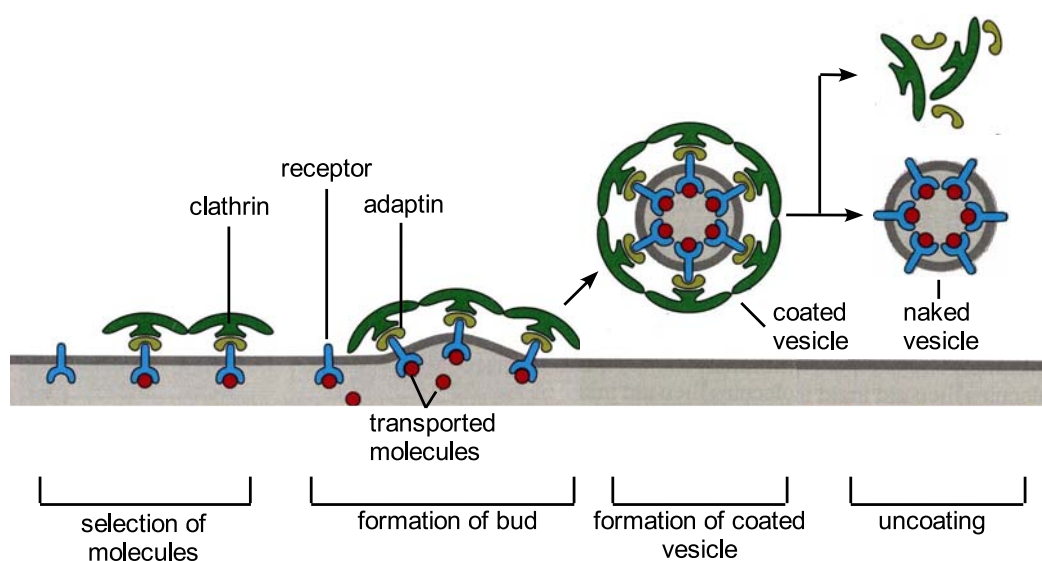


Figure 1.5 Formation and release of a clathrin-coated vesicle.

1.5.4.1 Uptake of Macromolecules by Receptor-Mediated Endocytosis

By endocytosis the cell consumes from the extracellular medium specific substances, macromolecules and sometimes other cells or their fragments. The particles to be transported into the intracellular compartment are first enclosed by a portion of the plasma membrane, which is then invaginates and finally pinches off, forming a particle-containing *endocytic vesicle* in the cytosol. In respect to the size of ingested particles, two main types of endocytosis are distinguished: *phagocytosis*, which relates to the ingestion of large particles, and *pinocytosis*, which, in contrast, involves the uptake of fluids containing suspended small particles.

Phagocytosis and pinocytosis are nonspecific processes, which means that any particle of appropriate size can be delivered into the cell. The import of specific macromolecules from the extracellular medium occurs mainly by *receptor-mediated endocytosis*, the pathway performed by clathrin-coated vesicles. The ligands bind to complementary transmembrane receptors, form clathrin-coated pits, and enter the cell as ligand-receptor complexes within clathrin-coated vesicles (see section 1.5.4). Unlike phagocytosis and pinocytosis, receptor-mediated endocytosis represents a selective mechanism. In respect to the internalization of particular ligands it is hundredfold more effective than mentioned above nonspecific processes. About 25 different types of receptors are known to take part in receptor-mediated endocytosis and the part of plasma membrane belonging to one coated pit can accommodate up to 1000 receptors of different types (Mellman, 1996). Many receptors enter coated pits free of their specific ligands.

Being separated from the plasma membrane and getting rid of its coat, the vesicle delivers its receptor-ligand complexes into the compartment of the *early endosome*, a small smooth-walled organelle, usually located near the cellular surface. Early endosomes are the main sorting station in the endocytic pathway. The membrane of the early endosome, similar to that of the lysosome, possesses a proton pump

implementing an energy-dependent transport of protons into the lumen of the endosome. The endosomal environment is, hence, acidic. At low pH most of the internalized receptor proteins undergo conformational changes and, as a result, dissociate from their ligands. Ligands free of their receptors are directed to lysosomes, where they are degraded. Most of the receptors are recycled back to their initial place in the plasma membrane by *recycling endosomes*. Ligands that remain bound to their receptors share the fate of receptors.

The way from the early endosome to the lysosome starts with the delivery of endocytosed ligands to the *late endosome*. The late endosome is then converted to the lysosome; it fuses with the acid hydrolase-carrying transport vesicle from the TGN, which results in a decrease of its pH. Being delivered to late endosomes, influenza virus particles (except for "inactive" ones, see section 1.6.2) are not degraded in lysosomes. Instead, fusion activity of their HA proteins mediates the fusion of viral and endosomal membranes, which results in the release of viral genome to the cytoplasm.

1.5.4.2 Exocytosis

By *exocytosis* the cell carries out the transfer of newly produced macromolecules from the TGN to the extracellular space. Transport vesicles, budding from the TGN and destined for the plasma membrane, contain membrane proteins and lipids, as well as soluble proteins to be excreted to the extracellular medium (Keller and Simons, 1997).

Most of cells in the tissue are *polarized*, i.e., they have two distinct domains of the plasma membrane (Alberts et al., 2002). For instance, the membrane of epithelial cells comprises an *apical domain* bordering with the extracellular medium and a *basal domain* covering the rest of the cell. Apical and basal domains are separated by a ring of *tight junction* preventing proteins and lipids of one domain from the diffusion to the other (Fig. 1.2). Directed to the two considered domains must be different sets of membrane proteins and lipids. This is achieved in the TGN, where the proteins and lipids from the ER are sorted in accordance with their destinations and packaged to

transport vesicles delivering them to corresponding domains of the plasma membrane (Traub and Kornfeld, 1997).

1.5.5 Apoptosis

Eucaryotic cells contain the seeds of their own destruction, waiting for the signal to destroy the cell. *Apoptosis*, or *programmed cell death*, is a thoroughly regulated process of the activation of the intracellular death program. The intracellular machinery responsible for apoptosis depends on the family of special proteolytic enzymes, called *caspases* (Potten and Wilson, 2004). Caspases exist in the cell in their inactive form, as *procaspases*. They are usually activated via the cleavage by other caspases, forming an amplifying caspase cascade. Activated caspases cleave key proteins of the cell including nuclear lamina and proteins that hold DNA-degrading enzymes (DNAses) in their inactive form. As a result, active DNAses start cutting up the DNA in the cellular nucleus. Caspase activation is strongly regulated by proteins from *IAP* (inhibitor of apoptosis) and Bcl-2 families, some of which inhibit and the others promote caspase activation (Eckert et al., 1999).

1.6 Molecular Biology and Infection Cycle of Influenza A Virus

Influenza A virions are roughly spherical with a diameter of 70-120 nm (Fig. 1.6). The genome of influenza A virus consists of eight negative-stranded RNA segments of different size, encapsidated by *nucleoproteins* (*NP*) (approximately 20 nucleotides per one protein subunit). Associated with each segment are *polymerase complexes* (RNA-dependent RNA polymerases), containing 3 protein subunits: *PB1*, *PB2* and *PA*. The PB1 subunit of the polymerase complex carries both a transcriptase, which catalyses nucleotide addition during the elongation of the RNA transcript, and a cap-dependent endonuclease, which performs the cleavage of capped RNA fragments to generate primers for vmRNA synthesis. The PB2 subunit is, in turn, responsible for

the binding of the cap of cellular precursor mRNA molecules. The PA protein is essential for viral genome replication, however its actual role is not fully understood. The arrangement of a viral genomic RNA molecule (vRNA molecule), NP protein and three polymerase protein subunits is referred to as a *viral ribonucleoprotein (vRNP) complex*. The NP protein represents the most abundant its component (Table 1.1). A vRNP complex represents a 10-20 nm wide panhandle structure, in which the vRNA segment coated by NP proteins forms a loop, and polymerase complexes bind to the partially complementary ends of the vRNA molecule. Eight vRNP complexes are surrounded by a shell of *matrix proteins M1*, the most abundant among all viral proteins (Table 1.1). This M1 protein layer, providing the rigidity of the virion, is, in turn, bound to the lipid membrane of the virion, derived from the host cell. Inserted into the viral membrane are three *envelope proteins: HA, NA, and M2*. Serological differences of HA and NA proteins provide the basis for influenza A virus classification. To date 15 different HA- and 9 different NA-subtypes are known. Finally, virus particles contain *NS2 proteins*, also called *nuclear export proteins (NEPs)*, associated with M1 proteins. NS2 proteins represent a minor component of the virion.

Table 1.1 Stoichiometry of Influenza A virus (A/PR/8/34) (*Knipe et al., 2001*).

Segment	Protein	vRNA, nt	vmRNA, nt	Peptide, aa	MW, Da	Mlc/virion
1	PB2	2341	2320	759	85700	30-60
2	PB1	2341	2320	757	86500	30-60
3	PA	2233	2211	716	84200	30-60
4	HA	1778	1757	566	61468	500
5	NP	1565	1540	498	56101	1000
6	NA	1413	1392	454	50087	100
7	M1	1027	1005	252	27801	3000
	M2		315	97	11010	20-60
8	NS1	890	868	230	26815	0
	NS2		395	121	14216	130-200

nt: Nucleotides

aa: Amino acids

mlc: Molecules

MW: Molecular weight

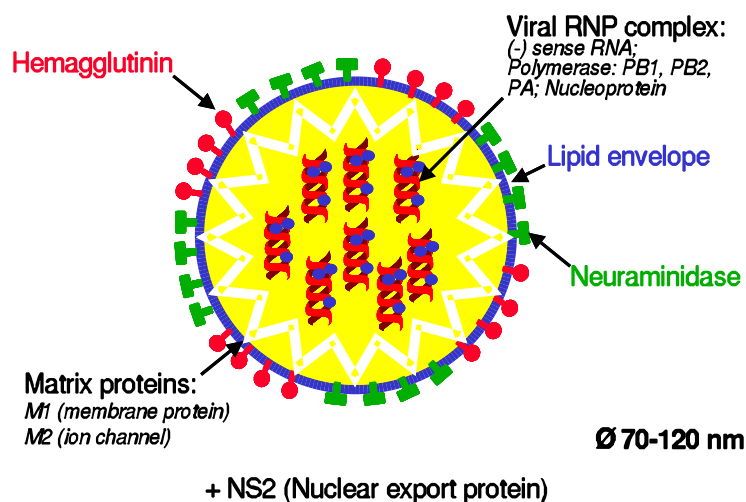


Figure 1.6 Structure of influenza A virus. *U. Reichl.*

The total coding capacity of influenza A virus genome makes up approximately 13 kb (Ludwig et al., 1999). Encoded by eight genome segments are ten viral proteins, nine of which (structural viral proteins) are incorporated into a virus particle. *NS1 proteins* (*nonstructural viral proteins*), particularly responsible for vRNA splicing (Nicholson et al., 1998; Juan, 1998; Ortin, 1998), are not incorporated into the virion. Each of the first six segments of the viral genome encodes one viral protein. Thus, vRNA segments 1, 2, and 3 give rise to polymerase complex subunits PB1, PB2, and PA, respectively; hemagglutinin and neuraminidase are correspondingly derived from segments 4 and 6; and segment 5 encodes NP proteins. The other two segments (the shortest in the genome), each containing two open reading frames (ORFs), code for two proteins. A collinear reading frame of segment 7 encodes M1 proteins, while a spliced mRNA molecule of the same segment expresses M2 proteins (Lam and Choppin, 1983). Similarly, segment 8 contains the coding sequences for NS1 proteins and for NS2 proteins. Recently discovered was a novel protein *PB1-F2*, which is encoded by an ORF within an alternative reading frame of segment 1 (encoding PB1 proteins) (Chen et al., 2001). This 87-residue protein, localizing at the inner mitochondrial membrane of infected cells (Gibbs et al., 2003), seems to permeabilize and destabilize the mitochondrial membranes of the cell, which leads to the leakage of macromolecules and apoptosis (Chanturiya et al., 2004). Besides that, it functions to kill host immune cells responding to influenza virus infections. The PB1-F2 protein was shown to be non-essential for virus replication *in vitro* and, therefore, is not

considered in the model the present study deals with.

Unlike influenza virus, large DNA viruses, such as poxviruses or herpes, express about 200 gene products (Flint et al., 2000). However, despite the relatively small coding capacity of its genome, influenza A viruses are able to successfully infect and multiply in a wide range of mammalian and avian species. They replicate in the epithelial cells of the upper respiratory tract of humans, horses and pigs. *In vitro* they can also infect many other cell types that possess surface glycoproteins containing sialic acid moieties (Julkunen et al., 2001). By multiple interactions between viral and cellular proteins influenza A viruses extensively use and manipulate host cell functions. An increasing amount of information concerning the roles of viral and cellular factors in transcription and replication of the viral genome, nuclear import and export of viral components, and assembly of the virus particle has accumulated in recent years. Relying on this data, the model developed in the present study quantitatively describes virus infections of mammalian cells, such as MDCK or Vero (African Green Monkey kidney) cells, used in vaccine production. It considers the major steps of the virus replication cycle (Fig. 1.7), which is the focus of the current section.

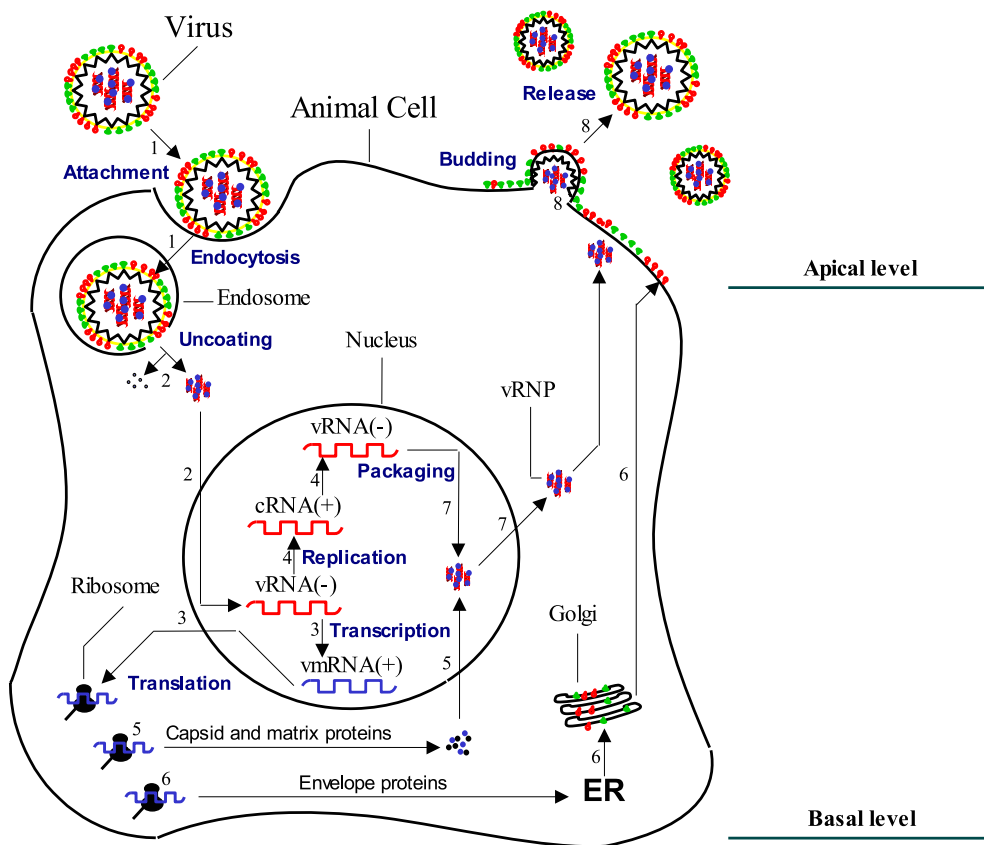


Figure 1.7 Replication cycle of influenza A virus. The numbers designating the steps of the replication cycle correspond to the numbers of subsections in section 1.6. *Sidorenko and Reichl, 2004.*

1.6.1 Virus Entry into the Host Cell. Structure of the HA Protein

Influenza virus particles attach to sialic acid-containing receptors at the apical membrane of polarized epithelial cells (Fig. 1.2) via viral HA glycoproteins (Fig. 1.7, step 1) (Nicholson et al., 1998). Each monomer of the trimeric HA spike consists of two subunits: a globular head (HA1), which carries sialic acid-binding sites, and a long helical stem (HA2), by which the molecule is anchored in the membrane (Fig. 1.8). It is a globular head of the HA protein that mediates binding of the virus to the receptors at the surface of the cell. At the N-terminal tip of the HA2 protein there is a sequence, known as a fusion peptide, which further mediates fusion of viral and

cellular membranes (see section 1.6.2).

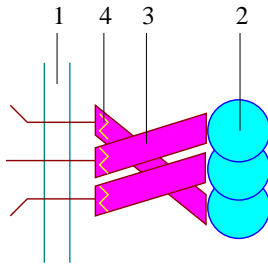


Figure 1.8 Schematic drawing of the HA trimer. 1 – viral membrane; 2 – globular head (HA1 subunit); 3 – helical stem (HA2 subunit); 4 – fusion peptide.

After attachment to the surface receptors, virions penetrate into the cell mainly by clathrin-dependent receptor-mediated endocytosis (see sections 1.5.4.1). The clathrin-dependent endocytic pathway of virus entry seems to be the most common, although several other entry pathways for influenza virus are also reported (Sieczkarski and Whittaker, 2002a; Sieczkarski and Whittaker, 2002b). It was particularly suggested that about one third of virions were internalized by clathrin-independent pathways (Rust et al., 2004).

1.6.2 vRNP Uncoating and Transport into the Nucleus. Roles of HA and M2 Proteins

As mentioned above, the viral genome is stored in the virion in form of vRNP complexes. Internalization of a virus-receptor complex by the endocytic pathway is followed by the release of vRNP complexes from the endosome into the cytoplasm (Fig. 1.7, step 2). To perform this step of its replication cycle, influenza virus has evolved a special mechanism adapted to the acidic pH of the endosome, which involves two viral proteins: HA and M2 ion channel. The import of H^+ into the interior of the virion results in the acidification of the virion first to approximately 6.0 in the early endosome and then to approximately 5.0 in the late endosome (Lakadamyali et al., 2004). As a result of the second acidification, HA proteins undergo an acid-catalyzed conformational rearrangement (proteolytic cleavage)

(Skehel and Wiley, 2000). While in the native HA the fusion peptide is deeply buried inside the molecule, in the low-pH HA structure it is moved to the top of the molecule. Exposed fusion peptides mediate fusion of viral and endosomal membranes, allowing the penetration of vRNP complexes into the cytoplasm.

As mentioned above, influenza virus vRNP complexes interact with viral M1 proteins, which are, in turn, in contact with the internal tails of HA and NA proteins at the viral envelope. Such an arrangement gives rise to two problems. On one hand, the release of vRNP complexes into the cytoplasm is impossible until M1-vRNP interactions are disrupted (Bui et al., 1996). On the other hand, influenza A viruses follow a nuclear replication strategy, consequently, vRNP complexes must be imported to the nucleus for the transcription and replication of their vRNA segments. As the size of the vRNP complex exceeds the size limit for passive import into the nucleus, nuclear import of vRNP complexes through nuclear pore complexes occurs actively, by NLSs, carried by NP proteins (O'Neill et al., 1995; Neumann G. et al., 1997; Portela and Digard, 2002). However, by masking NLSs, M1 proteins inhibit the nuclear import of vRNP complexes (Martin and Helenius, 1991a; Martin and Helenius, 1991b; Bui et al., 1996). Consequently, detachment of M1 proteins from vRNP complexes plays a crucial role at this step: being bound with M1 proteins, a vRNP complex cannot enter the nucleus.

The solution to both problems is provided by influenza virus M2 proteins, proteins with ion channel activity (Pinto et al., 1992, Nicholson et al., 1998). At the viral envelope there is a small number of M2 protein molecules (14 to 68), the native form of which is a homotetramer. The activation of the M2 ion channel is caused by the low pH of the endosome and precedes the fusion between the viral envelope and the endosomal membrane. Due to M2 ion channel activity, protons are able to enter the interior of the virion. The reduced pH of the virion interior is believed to mediate conformational changes in the M1 protein, thus disrupting M1-vRNP interactions. As a result, as soon as viral and endosomal membranes are fused, vRNP complexes are released into the cytoplasm free of M1 proteins and separated from each other (Bui et al., 1996), and can be then efficiently imported to the nucleus by cellular transport machinery. The hypothesis concerning the crucial role of M2 proteins in the delivery of vRNP complexes into the cytoplasm is supported by the fact, that in the presence of

amantadine, the anti-influenza virus drug inhibiting M2 ion channel activity, virus particles are still capable to enter the cellular endosomes and undergo HA-mediated membrane fusion, but their vRNP complexes are no longer able to escape from the endosomal membrane.

As pointed out in section 1.5.4.1, the primary acidification of virions in early endosomes is accompanied by the endosomal sorting of cellular surface receptors. Being secondarily acidified in late endosomes, most of the virions, in turn, perform the release of their genomes into the cytoplasm. However, some virus particles are unable to accomplish this step. Such virions are, for example, those with a defective M2 ion channel (Flint et al., 2000). In the next step, "inactive" virus particles are degraded in lysosomes (Martin and Helenius, 1991a).

1.6.3 Transcription (vmRNA Production)

The genomes of all RNA viruses meet one common requirement. Within the infected cell they must be efficiently copied, providing both genomes for the assembly into progeny virus particles and mRNA molecules for the synthesis of viral proteins. To catalyze the synthesis of new genomes and mRNA molecules most of the RNA viruses encode a trimeric RNA-dependent RNA polymerase. Being an RNA virus with a negative stranded genome, influenza A virus must carry the RNA polymerase in the virion. Otherwise, the incoming vRNA molecules could be neither translated nor copied by the cellular machinery. Additionally, there are two essential requirements for the mechanisms of vRNA synthesis. First of all, during its replication the RNA genome must be copied from one end to the other with no loss of nucleotide sequences. The second requirement refers to the production of vmRNA molecules that must be efficiently translated by the cellular protein synthetic machinery.

Three types of viral RNA molecules are synthesized in cellular nucleus: vmRNA molecules of positive polarity, viral genomic RNA molecules (vRNA molecules) of negative polarity, and complementary RNA molecules (cRNA molecules) of positive

polarity. Like the vast majority of cellular mRNA molecules, influenza virus vRNA molecules contain cap structures at their 5' ends and poly(A) tails at their 3' ends. Cap structures are taken from cellular precursor mRNA molecules, whereas poly(A) tails result from the polyadenylation, reiterative copying of poly(U) stretch, contained at the 5' ends of the negative strand genomic vRNA molecules.

Thus, the synthesis of influenza virus vRNA molecules (Fig. 1.7, step 3) involves three major components: viral polymerase complexes (i.e., their PB1 and PB2 subunits), negative genomic vRNA strands, and cellular precursor mRNA molecules. It comprises several steps. The process starts with the cleavage of capped RNA fragments from the 5' ends of cellular nuclear mRNA molecules, transcripts of cellular RNA polymerase II. These fragments then serve as primers for vRNA synthesis; resembling the cap structures peculiar to the 5' ends of cellular mRNA molecules (processed by cellular translation machinery), they are needed for the efficient transport out of the nucleus and the translation of vRNA molecules. The requirement for capped mRNA 5' ends to function as primers in vRNA production most likely explains the dependency of virus replication on RNA polymerase II activity (Ludwig et al., 1999).

All vRNA molecules possess the characteristic sequence (AGCAAAGCAGG) near their 5' ends, immediately downstream of the sequence snatched from capped cellular mRNA molecules (Flint et al., 2000). Binding of the viral RNA polymerase to this sequence occurs in a specific manner, providing the safety of vRNA molecules from the cleavage by the endonuclease of the viral polymerase complex. The 5' ends of host cell mRNA molecules are deprived of such a protection and are, therefore, efficiently cleaved, providing the primers for vRNA synthesis.

Two viral gene products, M2 and NS2 proteins, are encoded by spliced vRNA molecules. Splicing of M and NS vRNA molecules also occurs in the nucleus. The fraction of spliced to unspliced transcripts from segments 7 and 8 was shown to be controlled by certain virus-encoded factors (Lamb et al., 1981). The major function in the regulation of this segment-specific splicing is most likely carried by viral NS1 proteins (Nicholson et al., 1998; Juan, 1998), although the participation of cellular or

other viral proteins is also not excluded.

Another important role of NS1 proteins in vmRNA production is the inhibition of cellular pre-mRNA splicing (Lamb et. al., 1981). As discussed before, the initiation of vmRNA strands depends on the availability of capped 5' end structures for the cleavage of capped fragments, and most of the cellular mRNA transcripts are retained in the nucleus until they are spliced (Legrain and Rosbash, 1989). Consequently, the inhibition of pre-mRNA splicing results in an increase of the nuclear concentration of capped cellular mRNA molecules that can be used by viral polymerases for the initiation of transcription.

Newly synthesized vmRNA molecules are efficiently exported from the nucleus into the cytoplasm through nuclear pore complexes.

1.6.4 Viral Genome Replication

Genome replication represents the synthesis of full-length vRNA and cRNA strands (Fig. 1.7, step 4). Unlike vmRNA production, this process is independent of the presence of cellular mRNA molecules. vmRNA production and the replication of the viral genome are carried out by functionally different forms of the viral RNA polymerase. During vmRNA synthesis the PB2 cap-binding protein is required for the initiation of vmRNA chains by mRNA primers, derived from the host cell mRNA molecules, and the PA subunit does not have any function. During genome replication, in contrast, the PB2 protein has no role, whereas the PA protein is postulated to be required for the initiation of both positive and negative strands without a primer. Besides that, it was recently proposed that the PA protein possessed protease activity (Hara et al., 2003). However, the role of this activity for the process of infection is still not elucidated.

It is generally assumed that cRNA molecules serve as templates for vRNA synthesis, while newly replicated vRNA molecules are used for the further production of vmRNA and cRNA molecules, as well as for the assembly of vRNP complexes.

Nevertheless, it was experimentally shown that cRNA molecules could also serve as templates for vRNA synthesis (Azzeh et al., 2001). In cells infected with influenza A virus, there is an excess of negative vRNA strands over positive cRNA strands (Flint et al., 2000). The possible reason for this event is that full-length positive strands are synthesized for only a short period at the early stages of the infection. During the infection these positive cRNA molecules remain in the nucleus and serve as templates for genomic vRNA synthesis. The mechanism for the temporal regulation of cRNA synthesis is still not clearly understood.

Since the production of both vRNA molecules and exact copies of genomic vRNA molecules is of vital importance for their life cycle, influenza A viruses have evolved a mechanism for the switch from vRNA synthesis to genome replication. This mechanism may be reversible. Indeed, as new virus particles are assembled, structural protein levels can possibly decrease. In this situation vRNA molecules must be made at the expense of genomic vRNA molecules. The switch from vRNA synthesis to genomic vRNA production is regulated at the polyadenylation step of vRNA synthesis (Flint et al., 2000). According to experimental data, an increasing concentration of NP proteins that are not associated with vRNP complexes plays an important role in this regulation (Portela and Digard, 2002; Shapiro and Krug, 1988; Flint et al., 2000). NP proteins bind to some of the elongating RNA strands and block poly(A) addition. Besides that, they seem to define the activity of the vRNA polymerase. In the presence of NP proteins the PB1 subunit of the polymerase, the enzyme responsible for the replication, initiates the synthesis of full-length positive and negative strand RNA molecules *de novo*, i.e., without a primer, and reads all the way from the 3' end to the 5' end of the genomic vRNA through the polyadenylation and termination signals used for vRNA production. Although the PA protein is assumed to be important for viral genome replication, the exact mechanism regulating the initiation properties of this polymerase subunit and its responsiveness to NP proteins is still unclear. Copying of a positive cRNA strand into a negative vRNA strand also occurs with the participation of NP proteins. Consequently, intracellular concentrations of NP proteins are an important determinant of whether vRNA or genomic vRNA strands are synthesized.

As discussed above, the production of vRNA molecules and the replication of the

viral genome take place in the nucleus of the host cell. One possible reason for that could be the need to produce capped primers from cellular mRNA molecules. However, such mRNA molecules exist not only in the nucleus, but also in the cytoplasm, and other viruses, such as bunya viruses, use them in the similar process of cap snatching. Therefore, a more likely explanation why the nucleus is the site of influenza virus RNA synthesis is the necessity of nuclear RNA splicing machinery for the production of spliced vmRNA molecules (Cros and Palese, 2003).

1.6.5 Capsid and Nonstructural Protein Production

In the next step of the infection cycle (Fig. 1.7, step 5) viral PB1, PB2, PA, NP, NS2 and M1 proteins (capsid proteins) as well as NS1 proteins (nonstructural proteins) are produced by cellular ribosomes in the cytoplasm. As influenza virus particles are internalized into the cell, the rate of cellular protein production drastically decreases (Park and Katze, 1995), accompanied by the efficient selective translation of vmRNA molecules. Indeed, cellular gene expression is strongly modulated by influenza virus on a post-transcriptional level; in approximately 3 h p.i. the synthesis of cellular proteins is practically ceased despite the presence of functional cellular mRNA molecules in the cytoplasm (Katze and Krug, 1984). At the same time, cellular ribosomes organized in polysome complexes effectively synthesize viral proteins.

The reasons for the event described above and the factors it is affected by are not clearly understood. Cassetti et al. (2001) challenged the hypothesis that the translation machinery of infected cells efficiently processes only mRNA molecules possessing the viral 5' untranslated region. Nevertheless, the translation of vmRNA molecules is still predominant over the translation of cellular mRNA molecules. There are three possible mechanisms for the inhibition of cellular protein synthesis (Park and Katze, 1995). The first involves the degradation of newly synthesized cellular mRNA molecules in the nucleus. Another possibility is the inhibition of the translation of cellular mRNA molecules at the initiation and elongation steps. Finally, cellular protein production can be suppressed by retarding the transport of cellular mRNA molecules to the cytoplasm. It was shown that the last mechanism was performed with

the participation of NS1 proteins, which retain cellular RNA polymerase II transcripts in the nucleus (Fortes et al., 1994; Nemeroff et al., 1998).

Newly synthesized polymerase complexes, as well as NP proteins, matrix and nonstructural proteins, are transported to the nucleus, where they participate in the splicing of M and NS vRNA molecules, transcription, and genome replication. Additionally, some of them are consumed for the production of new M1-vRNP complexes.

1.6.6 Envelope Protein Production

The synthesis of M2, HA and NA proteins (Fig. 1.7, step 6) is carried out by ribosomes bound to the membranes of the ER. Newly synthesized precursors of mature HA and NA proteins follow the cellular exocytotic transport pathway (see section 1.5.4.2) from the ER via the Golgi apparatus and the TGN, where they are glycosylated and acylated (Gambaryan et al., 1998; Fischer et al., 1998; Saito et al., 1995). In polarized epithelial cells (e.g. MDCK cells), HA and NA are transported to the apical surface of the cell, thus defining the site of virus release. The translation of M2-encoding mRNA molecules is followed by the phosphorylation of M2 proteins (Gregoriades et al., 1990). Additionally, M2 viral proteins were shown to be acylated (Holsinger et al., 1995).

1.6.7 Packaging

The formation of vRNP complexes takes place in the nucleus of the cell. It represents the binding of newly synthesized PB1, PB2, PA, NP, M1 and NS2 proteins (capsid proteins) to vRNA molecules (Fig. 1.7, step 7). By the cellular transport machinery newly synthesized viral RNP complexes are exported to the cytoplasm. According to experimental data, the nuclear export of the viral genome requires the presence of M1 proteins, which are known to be associated with vRNP complexes (Huang et al., 2001; Martin and Helenius, 1991b; Bui et al., 1996). Besides that, for newly

synthesized vRNP complexes to be delivered into the cytoplasm, they must be associated with NS2 proteins (O'Neill et al., 1998). The arrangement of a vRNP complex and the two viral proteins involved is usually referred to as an M1-vRNP complex. Necessary for the binding with vRNP complexes M1 and NS2 proteins migrate to the nucleus from the cytoplasm, where they are synthesized (Watanabe et al., 2001). The association of some of vRNA molecules with M1 proteins results in the reduction of vRNA production (Perez and Donis, 1998). Furthermore, it halts viral genome replication and mediates the encapsidation of vRNA molecules by NP proteins (Baudin et al., 2001; Huang et al., 2001). According to experimental data, NP proteins can be organized into a helical structure only in the presence of both vRNA and M1. The NS2 protein, in turn, contains a leucine-rich NES, by which it interacts with nuclear pore complexes (Neumann G. et al., 2000; O'Neill et al., 1998). In spite of these observations, the arrangement of two viral proteins, M1 and NS2, is believed to mediate the nuclear export of vRNP complexes associated with them.

As stated above (see section 1.6.2), M1 proteins possess a property to mask NLSs, carried by NP proteins. In the cytoplasm they inhibit the reimport of vRNP complexes into the nucleus. Therefore, newly synthesized vRNP complexes, being associated with M1 proteins, are unable to return into the nucleus. Another possible mechanism of cytoplasmic retention of vRNP complexes is based on the ability of NP and M1 viral proteins to associate with the actin cytoskeleton of the cell (Avalos et al., 1997; Digard et al., 1999). This association can also reflect a role of M1 proteins for the targeting of vRNP complexes to virus budding sites at the plasma membrane of the cell.

1.6.8 Virus Budding and Release

Influenza virus particles bud from the apical membrane of polarized epithelial cells (Fig. 1.2). The lipid bilayer of the viral membrane is derived from the plasma membrane of the cell. According to experimental results, sorting signals of viral envelope proteins (HA, NA, and M2) are not the only factor that defines the location of the budding site (Barman et al., 2003). Besides them, the selection of the site of

virus budding involves other factors, presumably, both cellular and viral. At the budding site M1-vRNP complexes interact with the cytoplasmic tails of M2, HA, and NA proteins, which leads to the formation of a bud (Fig. 1.7, step 8). The major viral component that drives virus budding seems to be the M1 protein (Gomez-Puertas et al., 2000). It was particularly shown that in the transfected culture coexpressing just three viral proteins, M1, HA, and NA, particles resembling true virions in both density and general morphology could be formed. Neither vRNP complexes, nor NS2 proteins are needed for their assembly. Owing to the enzymatic activity of NA proteins to cleave sialic acid receptors on the surface of the cell (Luo et al., 1993), the bud separates from the membrane and a progeny virion is released to the extracellular medium.

NA proteins of influenza virus have a tetrameric structure and appear on the surface of the virion as mushroom-shaped spikes. Similar to an HA molecule, each NA monomer comprises transmembrane and cytoplasmic domains: a thin stalk, and a globular head. It is the globular head of the NA protein that defines its enzymatic activity and antigenic property. The function of NA proteins to remove terminal sialic acids not only promotes virus release from the host cell, but also prevents self-aggregation of virus particles (Rudneva et al., 2003). A series of studies emphasize that for efficient entry of virus particles into the cell and their release from the cell the cleavage activity of NA proteins must be in balance with the binding activity of HA proteins (Baigent and McCauley, 2001; Wagner et al., 2002; Rudneva et al., 2003). The disturbance of the functional balance between HA and NA proteins usually results in the decrease of the viral replicative ability.

There are two divergent ideas concerning the mechanism of vRNP packaging: genome segments can be either selectively or randomly incorporated into progeny virus particles (see section 5.6). The model assumes that influenza virus vRNP complexes are packaged in a random, nonspecific manner (Bancroft and Parslow, 2002), although the hypothesis of specific packaging has been also supported (Fujii et al., 2003).

2 Model Formulation

The main part of this section describes a system of model equations underlying the detailed single cell model by the successive formulation of the equations relating to individual steps of the infection cycle (Sidorenko and Reichl, 2004). In the rest of the section several model modifications, i.e., a reduced model, a model with reinfection, a model for continuous infection, and a population model, will be presented.

Considered in the detailed single cell model is an average cell, surrounded by a small quantity of medium and infected by a low number of virus particles (parental virions) (Fig. 2.1). The major properties of the cell and the virus considered are summarized in Table 2.1. Only one replication cycle is taken into account - the progeny virus particles are not supposed to infect the same cell again. Additionally, it is assumed that cells do not divide after infection, which is supported by the fact that growth of adherent MDCK cells is contact inhibited at the time of infection in large-scale culture, and more than 90% of the cells detach and die within 48 h p.i. (Y. Genzel, personal communication, see Appendix A5).

The model is represented by a system of nonlinear ODEs. All the state variables and rate coefficients, which will be addressed below are time-dependent functions.

Table 2.1 Basic properties of cells and influenza A virus used for modeling.

Parameter	Value	Source
Cell		
Number of receptors (<i>receptors/cell</i>)	10^4 - 10^5	1
Number of endosomes (<i>endosomes/cell</i>)	200	2
Number of ribosomes (<i>ribosomes/cell</i>)	$5 \cdot 10^6$	2
Distance between ribosomes on mRNA (<i>nucleotides</i>)	80	2
Number of nuclear pores (<i>pores/cell</i>)	3000-4000	3
Dry weight of an MDCK cell (<i>ng/cell</i>)	0.54	4
Number of free nucleotides (<i>nucleotides/cell</i>)	$1.3 \cdot 10^{10}$	2, 5
Number of nuclear precursor mRNAs (<i>nucleotides/cell</i>)	$2.2 \cdot 10^5$	2, 5
Average number of nucleotides per mRNA (<i>nucleotides</i>)	6000	2, 5
Number of free amino acids (<i>amino acids/cell</i>)	$3.1 \cdot 10^{10}$	2, 6
Virus (Influenza A, A/PR/8/34)		
Number of genome segments (<i>segments/virion</i>)	8	7
Full length of the genome (<i>nucleotides/virion</i>)	13588	7
Average length of one genome segment (<i>nucleotides</i>)	1699	7
Total number of amino acids (<i>amino acids/virion</i>)	$2.4 \cdot 10^6$	7

- 1: Wickham et al., 1990
- 2: Alberts et al., 2002
- 3: Flint et al., 2000
- 4: U. Reichl, personal communication
- 5: Kaufman et al., 2000
- 6: Nelson et al., 2000
- 7: Knipe et al., 2001

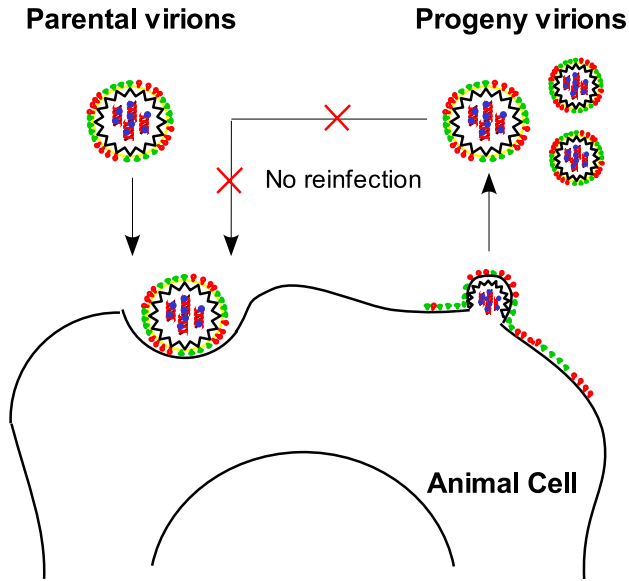


Figure 2.1 Scheme of the process addressed by the single cell model. Extracellular virions are differentiated into parental and progeny virions. The reinfection of the cell is not assumed.

2.1 Virus Entry into the Host Cell

$$(2.1.1) \quad \frac{dV_{ex}}{dt} = -k_{ex-s, V_{ex}} V_{ex} + k_{s-ex, V_{ex}} V_s$$

$$(2.1.2) \quad \frac{dV_s}{dt} = k_{ex-s, V_s} V_{ex} - k_{s-ex, V_s} V_s - k_{s-end} V_s$$

$$(2.1.3) \quad \frac{dV_{end}}{dt} = k_{s-end} V_s - k_{end-cyt, V_{end}} V_{end} - k_{end-degr} V_{end}$$

Here, t (h) is the time, V_{ex} (*virions/nL*), V_s (*virions/cell*), and V_{end} (*virions/cell*) represent the numbers of infectious virus particles in the extracellular medium, on the cellular surface and in the endosome, respectively.

The term $k_{ex-s, V_{ex}} V_{ex}$ in (2.1.1) describes the binding of extracellular virions to the cellular surface, and the term $k_{s-ex, V_{ex}} V_s$ is the rate of the release of surface virions to the extracellular medium due to dissociation. Every term, presenting the transfer of substance (i.e., viral components) from one compartment to another is usually

proportional to the number of the substance in the first compartment with a certain rate coefficient. Accordingly, the former term is proportional to the number of extracellular virus particles, and the latter one to the number of virions, attached to the surface of the cell. The right-hand side of equation (2.1.2) contains two terms ($k_{ex-s,V_s} V_{ex}$ and $k_{s-ex,V_s} V_s$), similar to those from equation (2.1.1), but, naturally, with opposite signs and different units of the corresponding rate constants (see below). The model does not take into account the exact mechanism of virus entry (coated pit formation, see section 1.5.4.1); virus particles are supposed to be transported from the cellular surface directly to the endosome. Accordingly, $k_{s-end} V_s$ in (2.1.2), as well as the corresponding term in (2.1.3), expresses the rate of endocytosis. Finally, the two negative terms in (2.1.3) ($k_{end-cyt,V_{end}} V_{end}$ and $k_{end-degr} V_{end}$) describe the escape of vRNP complexes from the endosome, and the degradation of inactive virus particles, respectively.

The rate coefficient of virus binding is $k_{ex-s,V_{ex}}$ ($mL \cdot h^{-1}$). Under normal *in vitro* conditions, individual cells are infected with a small number of virions. Therefore, the number of cellular receptors, which is in the range $10^4 - 10^5$ receptors per cell (Wickham et al., 1990), significantly exceeds the number of particles bound to the cell surface and does not represent a limiting factor for virus entry. Consequently, Monod-type kinetics is not considered, and it is assumed that $k_{ex-s,V_{ex}}$ is a constant. The rate constant of virus dissociation from the surface is $k_{s-ex,V_{ex}}$ (h^{-1}). The rate coefficients k_{ex-s,V_s} (h^{-1}) and k_{s-ex,V_s} (h^{-1}) are related to $k_{ex-s,V_{ex}}$ ($mL \cdot h^{-1}$) and $k_{s-ex,V_{ex}}$ (h^{-1}), respectively, via

$$k_{ex-s,V_s} = \frac{U_r}{N_{cells}} k_{ex-s,V_{ex}}$$

and

$$k_{s-ex,V_s} = \frac{U_r}{N_{cells}} k_{s-ex,V_{ex}},$$

where U_r (nL) is the volume of medium containing N_{cells} cells ($N_{cells} = 1$ cell in the model). The rate coefficient of endocytosis is k_{s-end} (h^{-1}). There are approximately 200 endosomes per cell, of which only a small fraction contains virus (Alberts et al.,

2002). Consequently, it can be assumed that k_{s-end} remains constant. The uncoating of vRNP complexes and the degradation of inactive viruses are described by the rate constants $k_{end-cyt, V_{end}}$ (h^{-1}) and $k_{end-degr}$ (h^{-1}), respectively.

2.2 vRNP Uncoating and Transport into the Nucleus

$$(2.2.1) \quad \frac{dS_{cyt}}{dt} = k_{end-cyt, S_{cyt}} V_{end} - k_{cyt-nuc} S_{cyt}$$

$$(2.2.2) \quad \frac{dS_{nuc}}{dt} = k_{cyt-nuc} S_{cyt} - k_{spl, S_{nuc}} S_{nuc}$$

Here, S_{cyt} (vRNP complexes/cell) and S_{nuc} (vRNP complexes/cell) are the total numbers of vRNP complexes in the cytoplasm and in the nucleus, respectively.

Similar to the corresponding term in (2.1.3), $k_{end-cyt, S_{cyt}} V_{end}$ in (2.2.1) expresses the rate of vRNP uncoating. The term $k_{cyt-nuc} S_{cyt}$ in (2.2.1) describes the nuclear import of vRNP complexes, and $k_{spl, S_{nuc}} S_{nuc}$ in (2.2.2), proportional to the number of vRNP complexes in the nucleus, represents the splitting of vRNP complexes into vRNA molecules, NP proteins and polymerase complexes.

The rate constants of vRNP uncoating $k_{end-cyt, S_{cyt}}$ (h^{-1}) and $k_{end-cyt, V_{end}}$ (h^{-1}) (see equation (2.1.3)) are related to each other by

$$k_{end-cyt, S_{cyt}} = N_{seg} k_{end-cyt, V_{end}},$$

where N_{seg} (molecules) is the number of genome segments (or the number of vRNP complexes) contained in one virus particle (in the model $N_{seg} = 8$ molecules). The rate coefficient of the nuclear import of vRNP complexes is $k_{cyt-nuc}$ (h^{-1}). There are approximately 3000-4000 pores in a nuclear membrane (Flint et al., 2000). With a small number of virions entering only a low percentage of them are involved in the delivery of vRNP complexes to the nucleus. This also applies for the whole average

life span of infected cells (approximately 12 h; Roy et al., 2000; J. Schulze-Horsel, Y. Genzel, personal communication) including processes related to the nuclear export and import of viral proteins and vmRNA molecules (shown in section 4.8 below). Thus, $k_{\text{cyt-nuc}}$ is not limited by the number of pores. The rate constant $k_{\text{spl},S_{\text{nuc}}}$ (h^{-1}) describes the separation of vRNP complexes into vRNA molecules, NP proteins and polymerase complexes.

2.3 Transcription (vmRNA Production)

$$(2.3.1) \quad \frac{dC_{i,\text{nuc}}}{dt} = k_{v\text{-vm},i} P_{\text{Pol},\text{nuc}} - k_{\text{vm},i,\text{nuc-cyt}} C_{i,\text{nuc}} - k_{\text{vm},i,\text{nuc-degr}} C_{i,\text{nuc}}$$

$$(2.3.2) \quad \frac{dC_{i,\text{cyt}}}{dt} = k_{\text{vm},i,\text{nuc-cyt}} C_{i,\text{nuc}} - k_{\text{vm},i,\text{cyt-degr}} C_{i,\text{cyt}}$$

$$i \in \{Pol, NP, M1, NS1, NS2, M2, HA, NA\}$$

Here, the numbers of vmRNA molecules encoding the i -th protein in the nucleus and in the cytoplasm are described by functions $C_{i,\text{nuc}}$ (*nucleotides/cell*) and $C_{i,\text{cyt}}$ (*nucleotides/cell*), respectively. All three polymerase subunits are always considered as one unit, as well as the vmRNA molecules encoding them. The number of polymerase complexes in the nucleus is $P_{\text{Pol},\text{nuc}}$ (*amino acids/cell*).

The term $k_{v\text{-vm},i} P_{\text{Pol},\text{nuc}}$ in (2.3.1) is the rate of vmRNA synthesis. Polymerase complexes are assumed to operate at the same speed (k_{p_i} (h^{-1})), consequently this term is proportional to $P_{\text{Pol},\text{nuc}}$. The terms $k_{\text{vm},i,\text{nuc-cyt}} C_{i,\text{nuc}}$ and $k_{\text{vm},i,\text{nuc-degr}} C_{i,\text{nuc}}$ are, correspondingly, the rates of the nuclear export and the degradation of nuclear vmRNA molecules. Described by $k_{\text{vm},i,\text{cyt-degr}} C_{i,\text{cyt}}$ in (2.3.2) is the degradation of cytoplasmic vmRNA molecules.

In general, the rate coefficient of vmRNA synthesis $k_{v\text{-vm},i}$ (h^{-1}) depends on C_v (the number of vRNA molecules, defined by equation 2.4.2) - vRNA molecules serve as templates - and on $P_{\text{NP},\text{nuc}}$ (the number of NP molecules in the nucleus, defined by

equation 2.5.2). Based on dry weight and chemical composition of a typical mammalian cell ($0.54 \text{ mg}/10^6$ cells, MDCK cells; U. Reichl, personal communication), it was estimated that a cell possessed a pool of approximately $C_{cell} = 1.3 \cdot 10^{10}$ free nucleotides (0.4% of cellular wet weight, 330 Dalton average weight of nucleotides) and about $3.0 \cdot 10^6$ nuclear precursor mRNA molecules, with an average length of 6000 nucleotides (see Appendix A4). As the total number of nucleotides is significantly higher than that required for vmRNA synthesis and genome replication (see section 4.8 below), the influence of the number of free cellular nucleotides and cellular mRNA molecules on the transcription rate of vRNA molecules $k_{v-vm,i}$ is neglected. It is also assumed that the rate of the process is not limited by C_v (every polymerase complex is involved in transcription and all polymerase complexes operate at the same speed):

$$P_{Pol,nuc} \ll C_v.$$

The correctness of this assumption will be discussed in section 5.4 below. As mentioned above, NP proteins inhibit the production of vmRNA molecules. Consequently, $k_{v-vm,i}$ should be maximal when $P_{NP,nuc} = 0$, and tend to zero when $P_{NP,nuc} \rightarrow \infty$. Taking into account all the assumptions, it can be assumed that

$$k_{v-vm,i} = k_{v-vm,i,max} \frac{1}{1 + a_{NP} P_{NP,nuc}},$$

where a_{NP} (*cells/NP protein*) is a positive parameter. a_{NP} represents an inverse concentration of NP proteins, at which

$$k_{v-vm,i} = \frac{1}{2} k_{v-vm,i,max}.$$

Therefore, a_{NP} defines the influence of NP proteins on vmRNA production. The rate coefficients of vmRNA nuclear export and degradation are $k_{vm,i,nuc-cyt}$ (h^{-1}) and $k_{vm,i,nuc-degr}$ (h^{-1}), respectively. The rate constant of cytoplasmic vmRNA degradation is $k_{vm,i,cyt-degr}$ (h^{-1}). The splicing of M and NS vmRNA molecules is not considered in the model.

Cytoplasmic and nuclear vmRNA molecules could be considered as two pools of nucleotides, irrelative to the individual types of vmRNA molecules. Such an

approach, particularly applied for the formulation of the reduced model (see section 2.9 below), results in the reduction of the number of differential equations underlying the model without limiting the generality of the model. However, several studies revealed that vmRNA processing might depend on the type of the vmRNA to be processed (e.g., early and late genes were discussed: Watanabe et al., 2001; Julkunen et al., 2001; Whittaker et al., 1996), particularly, on signals carried by noncoding sequences of the vmRNA involved (Luytjes et al., 1989). Additionally, M and NS vmRNA molecules are known to undergo splicing in the nucleus (see section 1.6.3). Thus, the numbers of vmRNA molecules of different types are still described by different functions to keep the possibility of model modifications.

2.4 Viral Genome Replication

$$(2.4.1) \quad \frac{dC_c}{dt} = k_{v-c} P_{Pol,nuc} - k_{c-degr} C_c$$

$$(2.4.2) \quad \frac{dC_v}{dt} = k_{c-v} P_{Pol,nuc} + k_{spl,C_v} S_{nuc} - k_{un,C_v} C_v \prod_l P_{l,nuc} - k_{v-degr} C_v$$

$$l \in \{Pol, NP, M1, NS2\}$$

Here, C_c (*nucleotides/cell*) is the number of cRNA molecules, C_v (*nucleotides/cell*) is the number of vRNA molecules, and $P_{l,nuc}$ (*amino acids/cell*) is the number of molecules of the l -th protein in the nucleus.

The terms $k_{v-c} P_{Pol,nuc}$ in (2.4.1) and $k_{c-v} P_{Pol,nuc}$ in (2.4.2) describe the synthesis of cRNA and vRNA, respectively. The terms $k_{c-degr} C_c$ in (2.4.1) and $k_{v-degr} C_v$ in (2.4.2) express, correspondingly, the rates of degradation processes for cRNA and vRNA molecules. The term $k_{spl,C_v} S_{nuc}$ in (2.4.2) is the rate of splitting of incoming vRNP complexes, as well as the corresponding term in (2.2.2). At last, the term $k_{un,C_v} C_v \prod_l P_{l,nuc}$ in (2.4.2) describes the assembly of new M1-vRNP complexes. It is proportional to the number of all viral components (i.e., vRNA, polymerase

complexes, NP, M1, and NS2 viral proteins) to be incorporated into M1-vRNP complexes.

The rate coefficients of cRNA and vRNA synthesis are k_{v-c} (h^{-1}) and k_{c-v} (h^{-1}), respectively. It is assumed that all vRNA molecules are synthesized at similar rates (Yamanaka et al., 1988); therefore it is not necessary to describe their numbers by different functions. Furthermore, every polymerase complex is assumed to participate in either positive or negative strand synthesis. Neither C_v nor C_c limit the rate of the corresponding process because their number exceeds the number of polymerase complexes:

$$P_{Pol,nuc} \ll C_v ; P_{Pol,nuc} \ll C_c$$

(see section 5.4 below for a discussion of this assumption). Since NP proteins promote genome replication, k_{v-c} and k_{c-v} should have maximum values when $P_{NP,nuc} \rightarrow \infty$, and be equal to zero when $P_{NP,nuc} = 0$. Thus, they are described by the following expressions:

$$k_{v-c} = k_{v-c,max} \frac{P_{NP,nuc}}{b_{NP} + P_{NP,nuc}}$$

and

$$k_{c-v} = k_{c-v,max} \frac{P_{NP,nuc}}{b_{NP} + P_{NP,nuc}},$$

where b_{NP} (*NP proteins/cell*) is a positive parameter that defines the influence of NP proteins on virus genome replication. The parameter b_{NP} represents the concentration of NP proteins, at which

$$k_{v-c} = \frac{1}{2} k_{v-c,max}$$

and

$$k_{c-v} = \frac{1}{2} k_{c-v,max}.$$

The rate constants of cRNA and vRNA degradation are k_{c-degr} (h^{-1}) and k_{v-degr} (h^{-1}), respectively. The rate constants of vRNP splitting k_{spl,C_v} (h^{-1}) and $k_{spl,S_{nuc}}$ (h^{-1}) (see equation 2.2.2) are connected with each other by

$$k_{spl,C_v} = C_{seg} k_{spl,S_{nuc}},$$

where C_{seg} (*nucleotides/vRNA molecule*) is the average number of nucleotides, contained in one segment. An influenza A (A/PR/8/34) virion consists of about $C_{vir} = 13588$ nucleotides (Knipe et al., 2001); therefore, the number of nucleotides contained in one segment is approximately

$$C_{seg} = \frac{C_{vir}}{N_{seg}} = 1699 \text{ nucleotides.}$$

The rate constant for the assembly of new M1-vRNP complexes is k_{un,C_v} (h^{-1}).

2.5 Capsid and Nonstructural Protein Production

$$(2.5.1) \quad \frac{dP_{i,cyt}}{dt} = k_{i,synt} \frac{C_{i,cyt}}{d_{rib}} - k_{i,cyt-nuc} P_{i,cyt} - k_{i,cyt-degr} P_{i,cyt}$$

$$(2.5.2) \quad \frac{dP_{i,nuc}}{dt} = k_{i,cyt-nuc} P_{i,cyt} + k_{spl,P_{i,nuc}} S_{nuc} - k_{un,P_{i,nuc}} C_v \prod_l P_{l,nuc} - k_{i,nuc-degr} P_{i,nuc}$$

$$i \in \{Pol, NP, M1, NS1, NS2\}, \quad l \in \{Pol, NP, M1, NS2\}$$

Here, $P_{i,cyt}$ (*amino acids/cell*) and $P_{i,nuc}$ (*amino acids/cell*) are the numbers of molecules of the i -th protein in the cytoplasm and in the nucleus, respectively.

The term $k_{i,synt} \frac{C_{i,cyt}}{d_{rib}}$ in (2.5.1), proportional to the number of vRNA molecules (see below), describes viral protein synthesis, and the two negative terms ($k_{i,cyt-nuc} P_{i,cyt}$ and $k_{i,cyt-degr} P_{i,cyt}$) represent, correspondingly, the rates of the nuclear import and the degradation of cytoplasmic proteins. The term $k_{spl,P_{i,nuc}} S_{nuc}$ in (2.5.2), responsible for vRNP splitting, is contained as well in (2.2.2); and a term, like $k_{un,P_{i,nuc}} C_v \prod_l P_{l,nuc}$, expressing the rate of new vRNP assembly, appears also in (2.4.2). The term $k_{i,nuc-degr} P_{i,nuc}$ expresses the rate of viral protein degradation in the nucleus.

The synthesis of viral proteins is carried out by ribosomes, making up polysome complexes. Like viral polymerase complexes, ribosomes are also assumed to operate at the same speed (k_{Rib} (h^{-1})), and the distance between ribosomes in a polysome complex is about $d_{rib} = 80$ nucleotides (Alberts et al., 2002). The rate coefficient $k_{i,synt}$ (h^{-1}) describes the synthesis of the i -th viral protein by cellular ribosomes. The influence of the number of cellular ribosomes on viral protein synthesis is neglected, assuming that a mammalian cell contains about $R_0 = 5 \cdot 10^6$ ribosomes (Alberts et al., 2002), which is significantly higher than the number of vRNA molecules to be processed (see section 4.8 below). Thus, $k_{i,synt}$ is assumed to be constant. The number of newly synthesized viral proteins increases proportional to $\frac{C_{i,cyt}}{d_{rib}}$, the number of ribosomes translating viral proteins. Furthermore, it is assumed that $k_{i,synt}$ does not depend on P_{cell} as uninfected cells contain a pool of approximately $P_{cell} = 3.1 \cdot 10^{10}$ free amino acids (0.4% of cellular wet weight, 138 Dalton average weight of amino acids see Appendix A4), which would be sufficient to produce about $1.3 \cdot 10^4$ virions (about $2.4 \cdot 10^6$ amino acids per virion, influenza A/PR/8/34). Additionally, it is known that soon after infection by influenza viruses an inhibition of cellular protein synthesis takes place (Park and Katze, 1995). Thus, the pool of cellular amino acids is not exhausted during virus replication, and $k_{i,synt}$ is a constant. The rate coefficient of the nuclear import of i -th proteins and the rate constant of their degradation in the cytoplasm are $k_{i,cyt-nuc}$ (h^{-1}) and $k_{i,cyt-deg}$ (h^{-1}), respectively. As the number of nuclear pores is also not reduced significantly during infection (see section 4.8 below), $k_{i,cyt-nuc}$ is also considered to be constant. The rate constant $k_{spl,P_i,nuc}$ (h^{-1}) is related to $k_{spl,S_{nuc}}$ (h^{-1}) (see equation 2.2.2) by

$$k_{spl,P_i,nuc} = P_{i,seg} k_{spl,S_{nuc}},$$

where $P_{i,seg}$ is the average number of i -th proteins, contained in one vRNP. The rate constant for the assembly of new M1-vRNP complexes (k_{in}) is discussed below (see equations 2.4.2, 2.7.1). The rate constant of the degradation of i -th proteins in the

nucleus is $k_{i,nuc-degr}$ (h^{-1}). NS1 proteins are absent in M1-vRNP complexes and, therefore,

$$k_{un,P_{NS1,nuc}} = 0.$$

On the other hand, at the early stages of the infection, M1, NS1, and NS2 proteins are not delivered into the nucleus together with vRNP complexes, that is

$$k_{spl,P_i,nuc} = 0, \quad i \in [M1, NS1, NS2].$$

Besides that, M1 proteins that are imported to the nucleus by passive diffusion do not seem to be involved in virus replication (Martin and Helenius, 1991a).

2.6 Envelope Protein Production

$$(2.6.1) \quad \frac{dP_{j,ER}}{dt} = k_{j,synt} \frac{C_{j,cyt}}{d_{Rib}} - k_{j,ER-bud} P_{j,ER} - k_{j,ER-degr} P_{j,ER}$$

$$(2.6.2) \quad \frac{dP_{j,bud}}{dt} = k_{j,ER-bud} P_{j,ER} - k_{bud,P_j,bud} S_{un,bud} \prod_l P_{l,bud} - k_{j,bud-degr} P_{j,bud}$$

$$j, l \in \{M2, HA, NA\}$$

Here, $P_{j,ER}$ (*amino acids/cell*) and $P_{j,bud}$ (*amino acids/cell*) express, correspondingly, the numbers of molecules of the j -th protein in the ER and at the budding site, and $S_{un,bud}$ (*M1-vRNP complexes/cell*) is the number of newly synthesized M1-vRNP complexes at the budding site.

The right-hand side of equation (2.6.1), similar to the right-hand side of equation (2.5.1) describes the synthesis of envelope proteins, their transport to the budding site, and the degradation in the ER. The number of envelope proteins at the budding site decreases due to the incorporation of these proteins to progeny virus particles and due to their degradation. The former process is described by the term $k_{bud,P_j,bud} S_{un,bud} \prod_l P_{l,bud}$ in (2.6.2), which is proportional to the number of all molecules (vRNP complexes, M2, HA, and NA viral proteins) forming virions; and the latter is presented by $k_{j,bud-degr} P_{j,bud}$.

$k_{j,ER-bud}$ (h^{-1}) and $k_{j,ER-degr}$ (h^{-1}) are, correspondingly, the rate constants of the transport of j -th proteins to the budding site and their degradation in the ER, $k_{bud,P_j,bud}$ (h^{-1}) is the rate constant of progeny virus particle assembly, and $k_{j,bud-degr}$ (h^{-1}) is the rate constant of the degradation of j -th proteins at the budding site.

2.7 Packaging

$$(2.7.1) \quad \frac{dS_{un,nuc}}{dt} = k_{un,S_{un,nuc}} C_v \prod_l P_{l,nuc} - k_{un,nuc-bud} S_{un,nuc}$$

$$(2.7.2) \quad \frac{dS_{un,bud}}{dt} = k_{un,nuc-bud} S_{un,nuc} - k_{bud,S_{un,bud}} S_{un,bud} \prod_s P_{s,bud}$$

$$l \in \{Pol, NP, M1, NS2\}, \quad s \in \{M2, HA, NA\}$$

Here, $S_{un,nuc}$ (*M1-vRNP complexes/cell*) and $S_{un,bud}$ (*M1-vRNP complexes/cell*) are, correspondingly, the numbers of newly synthesized M1-vRNP complexes in the nucleus and at the budding site. Assuming that vRNP complexes are packaged randomly (see section 1.6.8), M1-vRNP complexes carrying different genome segments are not distinguished here; their total number at the given cellular compartment is described by one state variable.

Similar to equations (2.4.2) and (2.5.2), equation (2.7.1) contains in its right-hand side the rate of M1-vRNP complex assembly ($k_{un,S_{un,nuc}} C_v \prod_l P_{l,nuc}$). The term $k_{un,nuc-bud} S_{un,nuc}$ in (2.7.1) describes the nuclear export of newly assembled M1-vRNP complexes. The term $k_{bud,S_{un,bud}} S_{un,bud} \prod_s P_{s,bud}$ in (2.7.2) expresses the rate of progeny virus particle assembly. Such a term also appears in (2.6.2).

The rate constant of the assembly of new M1-vRNP complexes $k_{un,S_{un,nuc}}$ (h^{-1}) is related to k_{un,C_v} (h^{-1}) and $k_{un,P_{l,nuc}}$ (h^{-1}) corresponding to equations (2.4.2) and (2.5.2) by:

$$k_{un,C_v} = C_{seg} k_{un,S_{un,nuc}}$$

and

$$k_{un,P_{i,nuc}} = P_{i,seg} k_{un,S_{un,nuc}}.$$

Here, $P_{i,seg}$ (*amino acids/M1-vRNP complex*) is the number of i -th proteins, contained in one M1-vRNP complex. The rate coefficient of the nuclear export of newly assembled M1-vRNP complexes is $k_{un,nuc-bud}$ (h^{-1}). The rate constants of the assembly of progeny virus k_{bud} (h^{-1}) are discussed in the section 2.8 (see equation 2.8.1).

2.8 Virus Budding and Release

$$(2.8.1) \quad \frac{dV_{bud}}{dt} = k_{bud,V_{bud}} S_{un,bud} \prod_l P_{l,bud} - k_{bud-rel,V_{bud}} V_{bud}$$

$$l \in \{M2, HA, NA\}$$

$$(2.8.2) \quad \frac{dV_{rel}}{dt} = k_{bud-rel,V_{rel}} V_{bud}$$

Here, V_{bud} (*virions/cell*) and V_{rel} (*virions/nL*) are the numbers of budding and released virions, respectively.

The term $k_{bud,V_{bud}} S_{un,bud} \prod_l P_{l,bud}$ in (2.8.1) describes the rate of progeny virus assembly. The term $k_{bud-rel,V_{bud}} V_{bud}$ in (2.8.1), as well as the corresponding term in (2.8.2), expresses the rate of progeny virus release to the extracellular medium.

The rate constant of the assembly of progeny virus particles ($k_{bud,V_{bud}}$ (h^{-1})) is related to $k_{bud,P_{j,bud}}$ (h^{-1}) and $k_{bud,S_{un,bud}}$ (h^{-1}) (see equations (2.6.2) and (2.7.2)) via formulas:

$$k_{bud,P_{j,bud}} = P_{j,vir} k_{bud,V_{bud}}$$

and

$$k_{bud,S_{un,bud}} = N_{seg} k_{bud,V_{bud}}.$$

Here, $P_{j,vir}$ (*amino acids/virion*) is the number of molecules of j -th envelope proteins in the virus particle, and $k_{bud-rel,V_{bud}}$ is the rate coefficient of progeny virus release.

The rate coefficients $k_{bud-rel,V_{rel}}$ ($mL^{-1} \cdot h^{-1}$) and $k_{bud-rel,V_{bud}}$ (h^{-1}) are related via

$$k_{bud-rel,V_{bud}} = \frac{U_r}{N_{cells}} k_{bud-rel,V_{rel}} .$$

In total, the single cell model is formulated based on equations (2.1.1-3), (2.2.1-2) – (2.8.1-2).

2.9 Reduced Model

The biological system considered is described by a system of 43 ODEs. However, to use the model as a starting point for the development of structured population balance models¹, as well as to reduce the number of unknown rate coefficients and to make the model easier in handling, it is useful to reduce the number of model variables and, correspondingly, the number of model equations. In the reduced model developed here, which comprises only 10 ODEs, only the most essential steps of the replication cycle, namely those representing the branch points of the process of the infection, are taken into account. All the steps making up linear sequences without branch points are lumped together.

All the processes concerned with virus entry, vRNP uncoating, and transport into the nucleus constitute a linear sequence without branch points, and, therefore, can be lumped together. Additionally, as the dissociation of virus particles from the surface of the cell is not essential for virus replication (in particular, the virus yield is not sensitive to variations of its rate constants, see section 4.11.2.1 below), the corresponding terms in (2.1.1) ($k_{s-ex,V_{ex}} V_s$) and (2.1.2) will be neglected. Finally, the term $k_{end-deg} V_{end}$ in (2.1.3) will be also omitted. If necessary, the effect of the

¹ The numbers of viral components are considered as structure parameters of the cell population, i.e., the concentration of cells is a function of the number of vRNA molecules, viral proteins, etc.

degradation of “inactive” virions on virus production can be taken into account by decreasing the initial concentration of extracellular virions (see section 4.10). Thus, equations (2.1.1), (2.1.2), (2.1.3), (2.2.1), (2.2.2) can be reduced to one equation

$$(2.9.1) \quad \frac{dV_{ex,red}}{dt} = -k_{spl,V_{ex}} V_{ex,red}$$

Unlike function V_{ex} (*virions/nL*) in equation (2.1.1), function $V_{ex,red}$ (*virions/cell*) in equation (2.9.1) is related to the cell. It does not account only for extracellular virions, but rather represents the total number of extranuclear virus particles (virus particles with a genome still not delivered into the nucleus). The term $k_{spl,V_{ex}} V_{ex,red}$ in (2.9.1) expresses the rate of separation of delivered with incoming virions vRNP complexes into vRNA molecules, NP proteins, and polymerase complexes. It is proportional to the number of extranuclear virions with the rate constant $k_{spl,V_{ex}}$ (h^{-1}).

The delivery of the viral genome into the nucleus is followed by the beginning of three different processes that must be considered separately: vmRNA production, genome replication, and viral protein synthesis. In respect to the production of viral components vmRNA molecules of different types are indistinguishable. Consequently, all vmRNA molecules produced can be considered as a single pool of nucleotides to be processed by ribosomes, individual vmRNA strands constituting the certain fraction of this pool (ω_i , defined in section 3 below). Equations (2.3.1) and (2.3.2), considering the concentrations of all individual vmRNA molecules, can be, therefore, rewritten for the total number of vmRNA molecules in the nucleus and in the cytoplasm:

$$(2.9.2) \quad \frac{dC_{nuc}}{dt} = k_{v-vm} P_{Pol} - k_{vm,nuc-cyt} C_{nuc} - k_{vm,nuc-degr} C_{nuc}$$

$$(2.9.3) \quad \frac{dC_{cyt}}{dt} = k_{vm,nuc-cyt} C_{nuc} - k_{vm,cyt-degr} C_{cyt}$$

Here, C_{nuc} (*nucleotides/cell*) and C_{cyt} (*nucleotides/cell*) are the functions representing the total numbers of vmRNA molecules in the nucleus and in the cytoplasm, respectively. Thus, rate coefficients of the right-hand sides of equations (2.9.2) and (2.9.3), unlike those of the right-hand sides of equations (2.3.1) and (2.3.2) are deprived of index “i”, identifying individual types of vmRNA molecules. Besides

that, as the cytoplasmic and nuclear pools of viral proteins are not distinguished in the reduced model (see below), the term $k_{v-vm}P_{Pol}$ in (2.9.2), expressing the rate of vmRNA synthesis, is proportional to the total number of polymerase complexes.

Two equations describing the replication of the viral genome (equations (2.4.1) and (2.4.2)) are introduced into the reduced model as

$$(2.9.4) \quad \frac{dC_c}{dt} = k_{v-c}P_{Pol} - k_{c-degr}C_c$$

$$(2.9.5) \quad \frac{dC_v}{dt} = k_{c-v}P_{Pol} + k_{spl,C_v,red}V_{ex,red} - k_{pck,C_v}C_v \prod_l P_l - k_{v-degr}C_v$$

$$l \in \{Pol, NP, M1\}$$

Like $k_{v-vm}P_{Pol}$ in (2.9.2), the terms $k_{v-c}P_{Pol}$ in (2.9.4) and $k_{c-v}P_{Pol}$ in (2.9.5), representing, correspondingly, the rates of cRNA and vRNA synthesis, are proportional to the total number of polymerase complexes. As in the reduced model the steps of the infection cycle from vRNP formation to progeny virus assembly are considered together (see below), the rate constants of packaging k_{pck,C_v} (h^{-1}) in (2.9.5) and k_{um,C_v} (h^{-1}) in (2.4.2) differ from each other. The rate constant k_{pck,C_v} describes the packaging of viral components directly to progeny virions, whereas k_{um,C_v} refers to the assembly of vRNP complexes. Taking into account the corresponding equations of the detailed model and the relation between their rate coefficients, it can be seen that the rate constants of vRNP splitting $k_{spl,C_v,red}$ (h^{-1}) and $k_{spl,V_{ex}}$ (h^{-1}) (see equation 2.9.1) are connected by

$$k_{spl,C_v,red} = C_{vir}k_{spl,V_{ex}}.$$

Here, C_{vir} (*nucleotides/virion*) is the number of nucleotides contained in the virion ($C_{vir} = 13588$ nucleotides).

Among the viral proteins taking part in the nuclear phase of virus replication considered in the reduced model will be only M1 proteins, limiting virus replication (see section 4.9 below), NP proteins, essentially influencing the switch from vmRNA production to viral genome replication (see sections 1.6.3 and 1.6.4), and polymerase complexes, directly involved in transcription and genome replication. As NS1 and

NS2 proteins do not limit virus replication (see section 4.9 below) and are also not assumed to have any essential effects on the production of viral components, their number is not taken into account. Additionally, only one (nuclear) pool of each type of viral proteins will be considered; the nuclear import of newly synthesized proteins will be omitted. Thus, equations (2.5.1) and (2.5.2) can be rewritten as

$$(2.9.6) \quad \frac{dP_i}{dt} = k_{i,\text{synt}} \omega_i \frac{C_{\text{cyt}}}{d_{\text{rib}}} + k_{\text{spl},P_i,\text{red}} V_{\text{ex},\text{red}} - k_{\text{pck},P_i} C_v \prod_l P_l - k_{i,\text{deg r}} P_i$$

$$i \in \{Pol, NP, M1\}, \quad l \in \{Pol, NP, M1\}$$

Here, P_i (*amino acids/cell*) is the total number of i -th proteins. Taking into account that the number of vRNA molecules of the i -th type is $\omega_i C_{\text{cyt}}$ (see section 3 below),

it is evident that $k_{i,\text{synt}} \omega_i \frac{C_{\text{cyt}}}{d_{\text{rib}}}$ in (2.9.6) resembles $k_{i,\text{synt}} \frac{C_{i,\text{cyt}}}{d_{\text{rib}}}$ in (2.5.1). The

connection between the rate constants $k_{\text{spl},V_{\text{ex}}} (h^{-1})$ and $k_{\text{spl},P_i,\text{red}} (h^{-1})$ is similar to that between $k_{\text{spl},V_{\text{ex}}}$ and $k_{\text{spl},C_v,\text{red}}$. It is expressed by

$$k_{\text{spl},P_i,\text{red}} = P_{i,\text{vir}} k_{\text{spl},V_{\text{ex}}}.$$

Here, $P_{i,\text{vir}}$ (*amino acids/virion*) is the average number of i -th proteins contained in the virion.

As shown in sections 4.9 and 4.11.1.1, it is the number of vRNP complexes that represents the bottleneck of virus replication at virus budding. It remains limiting at any variation of model parameters. The other viral components, namely, envelope proteins, are produced in redundant amounts and, therefore, do not limit virus production. It will be also revealed that the number of produced virions is not significantly influenced by variations of the rate constant of the virus assembly k_{bud} (see section 4.11.6). For these reasons, the functions representing the number of envelope proteins and, accordingly, equations (2.6.1) and (2.6.2), describing their change, are omitted in the reduced model. The role of envelope proteins in the infection cycle is expressed only in the rate coefficients of the model (e.g., the rate coefficients of internalization depend on the binding activity of HA proteins).

Thus, the dynamics of virus assembly is not influenced by changes of the number of envelope proteins and repeats the dynamics of vRNP complex formation with the

certain time delay concerned with the finite rate of virus assembly. Consequently, all the processes relating to the last steps of the infection cycle, starting with vRNP formation can be lumped together, and it is possible to reduce equations (2.7.1), (2.7.2), (2.8.1), and (2.8.2) to equation

$$(2.9.7) \quad \frac{dV_{rel,red}}{dt} = k_{pck,V_{rel}} C_v \prod_l P_l$$

The meaning of function $V_{rel,red}$ (*virions/cell*) in equation (2.9.7) differs from that of function V_{rel} (*virions/nL*) in equation (2.8.2). Function $V_{rel,red}$ is related to the cell. It does not account only for the number of released virions, but rather represents the total number of virions assembled in the cell.

As follows from the corresponding equations of the detailed model and the relations between their rate coefficients, the connection of the rate constants k_{pck,C_v} (h^{-1}) and k_{pck,P_i} (h^{-1}) (see equations (2.9.5) and (2.9.6)) with the rate constant $k_{pck,V_{rel}}$ (h^{-1}) is given by

$$k_{pck,C_v} = C_{vir} k_{pck,V_{rel}}$$

and

$$k_{pck,P_i} = P_{i,vir} k_{pck,V_{rel}},$$

respectively.

Thus, the formulation of the reduced model is based on equations (2.9.1) – (2.9.7).

2.10 Model with Reinfection

So far it was assumed that progeny virus particles did not infect the cell repeatedly. The number of virions to enter the cell and the number of virions released from the cell were described by two different functions (V_{ex} and V_{rel}). However, based on the detailed single cell model formulated above, it is also possible to see what happens in the case when a reinfection of the cell by released virions is taken into account (Fig. 2.2). For this purpose the model must be reformulated to consider all the virions in the

surrounding the cell volume of medium as one pool, a single function being used to describe the total number of extracellular virions.

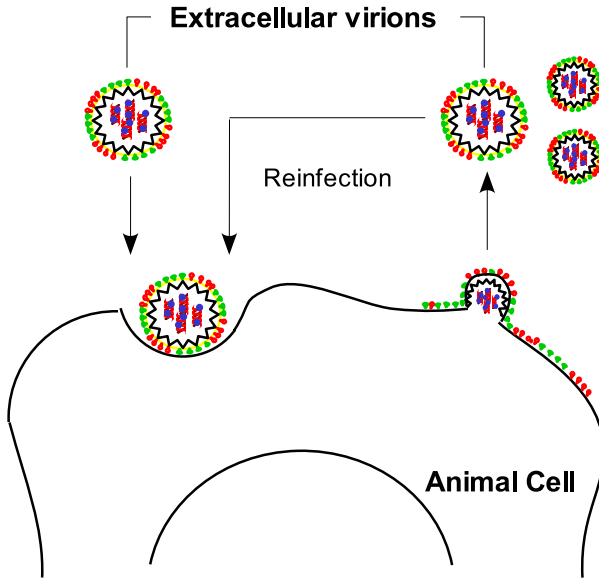


Figure 2.2 Scheme of the process addressed by the model with reinfection. Released virions can enter the cell again, and all extracellular virions are, hence, indistinguishable.

If equation (2.1.1) is modified to include an additional term ($k_{bud-rel,V_{rel}} P_{inf} V_{bud}$) representing the rate of virus release (similar to equation (2.8.2))

$$(2.1.1'') \quad \frac{dV_{ex}}{dt} = -k_{ex-s,V_{ex}} V_{ex} + k_{s-ex,V_{ex}} V_s + k_{bud-rel,V_{rel}} P_{inf} V_{bud}$$

function V_{ex} will describe the total number of extracellular virions. At the same time, function V_{rel} in (2.8.2) still remains meaningful; it represents the total number of produced by the cell virions. Experimental data shows that the total number of released virus particles contains only a small fraction of infectious virions (H. Sann, personal communication, not shown). For this reason, $k_{bud-rel,V_{rel}} P_{inf} V_{bud}$ in (2.1.1'') differs from the corresponding term in (2.8.2) by the factor P_{inf} (-), equal to the probability for a virion to be infectious. The value of P_{inf} is equal to approximately

$$P_{inf} \approx \frac{1}{150}.$$

Thus, the model with reinfection is represented by equations (2.1.1''), (2.1.2-3), (2.2.1-2) – (2.8.1-2).

2.11 Model for Continuous Infection

Another situation that can be found in practice is the continuous infection of the cell. Assume that in the extracellular medium, besides the number of parental (initially seeded) virus particles there is a continuous supply of virus particles from an external source (e.g. other infected cells) (Fig. 2.3). To adjust the detailed single cell model to account for the considered case, equation (2.1.1) must be modified to include the term representing the rate of virus supply k_{feed} (virions/(nL · h)):

$$(2.1.1^*) \quad \frac{dV_{ex}}{dt} = -k_{ex-s, V_{ex}} V_{ex} + k_{s-ex, V_{ex}} V_s + k_{feed}$$

k_{feed} will be supposed to remain constant throughout the whole process of the infection.

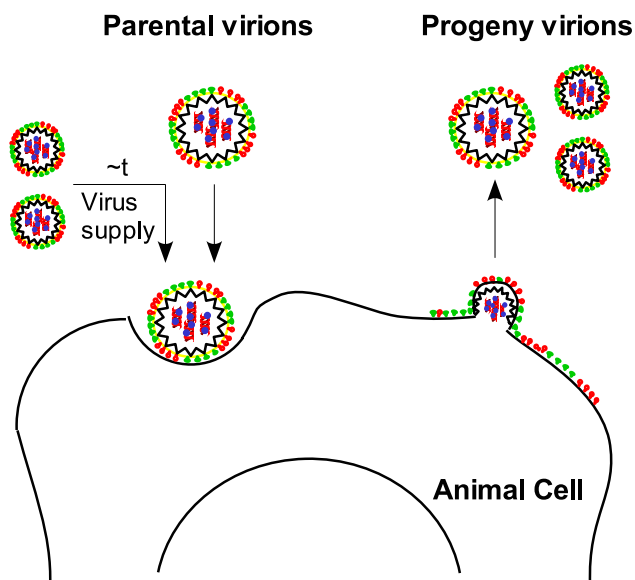


Figure 2.3 Scheme of the process addressed by the model for continuous infection. The cell is infected by both parental (initially seeded) virions and virions from the continuous supply.

The model for continuous infection is represented by equations (2.1.1^{*}), (2.1.2-3), (2.2.1-2) – (2.8.1-2).

2.12 Population Model

Based on the single cell model formulated in sections 2.1 – 2.8, it is possible to develop a population model, which considers the populations of uninfected, infected, and dead cells, as well as the population of free virions.

Like the single cell model, the population model considered here is unsegregated, i.e., concerned with the mass of average cells. It accounts for the processes of influenza virus production in microcarrier cultures, described by Genzel et al. (2004). The process comprises several stages; it starts with the cultivation and scale up of mammalian cells, followed by cell growth on microcarriers (Fig. 2.4). After medium change and infection virus replication occurs. It is the stage of virus replication that the model is mainly concerned with. After cell growth and virus replication further downstream processing is required. This comprises the clarification of virus culture by using 5 μm and 1 μm depth filters, concentration by ultrafiltration, and, finally, purification by gel filtration.

The major components of the biological system considered are MDCK cells and equine influenza virus (H3N8). MDCK cells are polarized epithelial cells (see section 1.5.4.2). For their growth they need a surface, which is supplied by microcarriers (Cytodex 1), small beads of about 200 μm in diameter. At the end of cell growth microcarriers are completely covered by uninfected cells, whereas at virus harvesting most of the cells are killed by virus infection and, therefore, separated from microcarriers (Fig. 2.4).

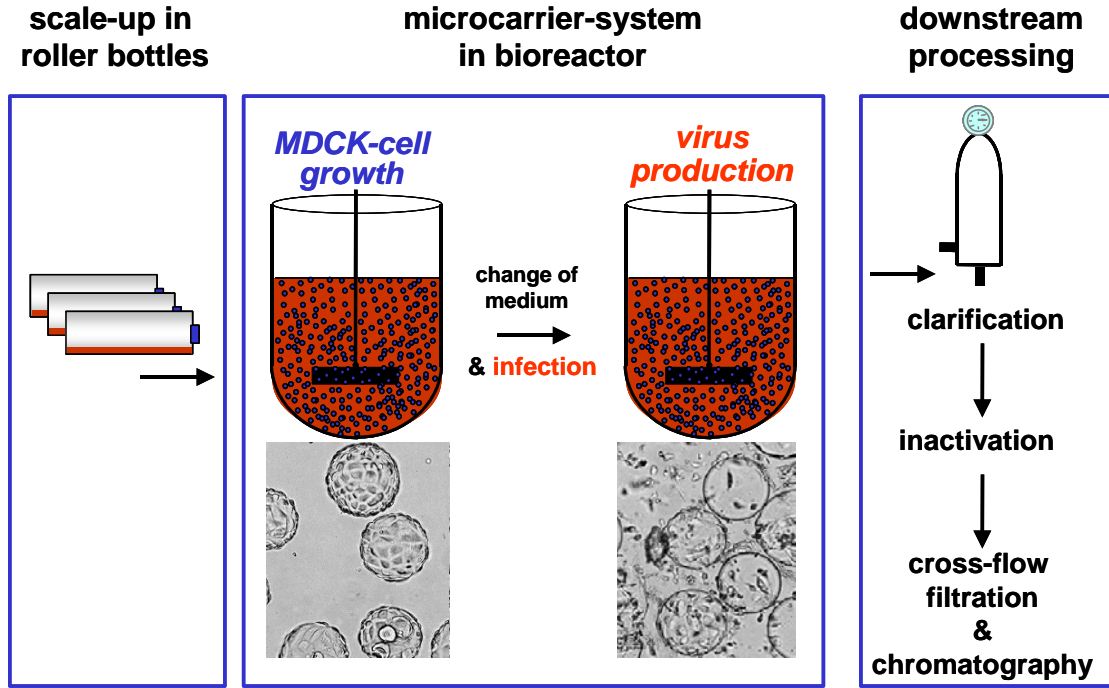


Figure 2.4 Scheme of the process of influenza virus production in microcarrier systems. The population model mainly focuses on the stage of virus replication, which starts as microcarriers are covered by a confluent monolayer of uninfected cells (left image) and finishes as virus infection kills most of the cells (resulting in the detachment of cells from microcarriers, right image). *Genzel et al., 2004.*

A mathematical formulation of the population model can be posed by taking the system of equation underlying the detailed model for a single cells, substituting equations (2.1.1), (2.8.1), and (2.8.2), correspondingly, by equations (2.1.1**), (2.8.1**), and (2.8.2**), and adding equations (2.12.1) – (2.12.3).

$$(2.1.1^{**}) \quad \frac{dV_{ex}}{dt} = -k_{ex-s,V_{ex}} V_{ex} + k_{s-ex,V_{ex}} V_s + k_{bud-rel,V_{rel}} P_{inf} \frac{Z_{in}}{Z_0} V_{bud}$$

$$(2.8.1^{**}) \quad \frac{dV_{bud}}{dt} = k_{bud,V_{bud}} S_{un,bud} \prod_l P_{l,bud} - k_{bud-rel,V_{bud}} \frac{Z_{in}}{Z_0} V_{bud}$$

$$(2.8.2^{**}) \quad \frac{dV_{rel}}{dt} = k_{bud-rel,V_{rel}} \frac{Z_{in}}{Z_0} V_{bud} - k_{vd} V_{rel} Z_d$$

$$(2.12.1) \quad \frac{dZ_{un}}{dt} = -k_{un-in} V_s Z_{un} - k_{ap,un} Z_{un} Z_{in} - k_{dt} Z_{un}$$

$$(2.12.2) \quad \frac{dZ_{in}}{dt} = k_{un-in} V_s Z_{un} - k_{ap,in} Z_{in}$$

$$(2.12.3) \quad \frac{dZ_d}{dt} = k_{dt} Z_{un} + k_{ap,un} Z_{un} Z_{in} + k_{ap,in} Z_{in}$$

Here, functions Z_{un} (*cells/nL*), Z_{in} (*cells/nL*), and Z_d (*cells/nL*) represent, correspondingly, the numbers of uninfected, infected, and dead² cells. Z_0 (*cells/nL*) is the total number of cells (or the initial number of uninfected cells):

$$Z_0 = Z_{un} + Z_{in} + Z_d.$$

The term $k_{bud-rel,V_{rel}} P_{inf} \frac{Z_{in}}{Z_0} V_{bud}$ in (2.1.1^{**}) and the corresponding terms in (2.8.1^{**}) and (2.8.2^{**}) represent the rate of virus release. Like in the model with reinfection (see section 2.10), it is added to take into account the probability of infection by newly produced virions. Equation (2.8.2^{**}) describes the dynamics of the total number of released virions (including secondarily internalized virions). The term $k_{vd} V_{rel} Z_d$ is the rate of virus degradation (k_{vd} ($nL \cdot h^{-1}$) is its rate constant). As virus degradation is induced by proteases released from dead cells, the considered term is proportional not only to the number of released virions itself, but also to the number of dead cells.

Equations (2.12.1) – (2.12.3) express the population balances for uninfected, infected, and dead cells, respectively. The term $k_{un-in} V_s Z_{un}$ in (2.12.1) describes the infection of uninfected cells by attached virions. k_{un-in} (h^{-1}) is the rate coefficient of infection. Infected cells were shown to release to the extracellular medium signaling components, such as double-stranded RNA molecules (Ludwig et al., 2003) that might induce the apoptosis of uninfected cells. This process is considered by the term $k_{ap,un} Z_{un} Z_{in}$ in (2.12.1), proportional to the number of uninfected cells and to the

² During the process dead cells continuously undergo lysis. However, for the formulation of the model it is not necessary to describe degraded cells by an independent function; function Z_d represents the total number of both dead and degraded cells.

number of infected cells; its rate coefficient is $k_{ap,un}$ ($nL \cdot h^{-1}$). The term $k_{dt}Z_{un}$ in (2.12.1) represents the detachment of uninfected cells from microcarriers. The rate constant of detachment is k_{dt} (h^{-1}). Because of the high cell density on microcarriers, detached cells are not supposed to attach again; they finally die within approximately 24 h (Y. Genzel, personal communication, not shown). The term $k_{ap,in}Z_{in}$ in (2.12.2) describes the death of infected cells due to the apoptosis induced by influenza virus infection. The rate coefficient of the apoptosis of infected cells is $k_{ap,in}$ (h^{-1}). Finally, equation (2.12.3) expresses the increase of the total number of dead cells due to the detachment of cells from microcarriers and the apoptosis of both uninfected and infected cells.

The formulation of the population model does not imply any assumptions concerning cell-to-cell or microcarrier-to-microcarrier spread of virus particles. Instead, it is assumed that all the components of the biological system considered are homogeneously mixed. As the ratio of the number of uninfected, infected, and dead cells continuously changes in time, for the precise description of the population dynamics it would be necessary to multiply each term in the right-hand sides of model equations (2.1.1**), (2.1.2-3), (2.2.1-2) – (2.7.1-2), (2.8.1** -2**) by a certain additional factor. This factor is equal to the ratio of the number of cells participating in the step of the infection cycle described by the considered term to the number of cells, in which the virions involved in the considered step have passed through the previous step of the infection cycle.

For example, the term $k_{s-end}V_s$ in (2.1.2) representing the rate of endocytosis might be multiplied by factor

$$(2.12.4) \quad \omega_{end} = \frac{Z_{un}(t) + Z_{in}(t)}{Z_{un}(t - \tau_{att-end}) + Z_{in}(t - \tau_{att-end})},$$

where $\tau_{att-end}$ (h) is the time interval between attachment and internalization. Indeed, virus particles taken up by endocytosis attach to the number of cells that stays in the denominator of formula (2.12.4) (both attachment and endocytosis seem to be

executed only by living (uninfected and infected) cells). At the same time, some of living cells that are involved in virus attachment become dead by the beginning of endocytosis. Consequently, the number of cells participating in endocytosis (staying in the numerator of formula (2.12.4)) is lower than the number of cells, to which the considered virions attached.

In general, model equations describing the dynamics of viral components (e.g., vRNA molecules or viral proteins) would have the following form:

$$(2.12.5) \quad \frac{dV_i(t)}{dt} = F_i(V_1(t), \dots, V_n(t), Z_{in}(t, t - \tau_{i,1}, \dots, t - \tau_{i,m_i}), \\ Z_{in}(t, t - \tau_{i,1}, \dots, t - \tau_{i,m_i})) \\ i = 1 \dots n$$

Here, n is the number of equations (i.e., the number of process steps considered in the model), m_i is the number of terms in the right-hand side of the i -th equation, V_i ($i = 1 \dots n$) (*virions/nL* or *virions/cell*) is the function defined by the i -th equation, $\tau_{i,j}$ ($j = 1 \dots m_i$) (h) is the time interval separating the beginning of the step represented by the j -th term in the right-hand side of the i -th equation and the beginning of the preceding step, F_i ($i = 1 \dots n$) ($nL^{-1} \cdot h^{-1}$ or h^{-1}) are continuous nonnegative functions.

The system of ODEs underlying the present population model represents a simplification of the system of time-delayed differential equations (2.12.5). Actually, instead of the real biological system it describes a certain model system, which, nevertheless, allows estimating the real number of newly produced virions and intracellular viral components (see below). The essential difference of the considered model system from the real system is that all the cells it contains (uninfected, infected, and dead cells) perform all the steps of the infection cycle until virus release (in reality, uninfected and dead cells, naturally, do not perform any steps). Virus release is, in contrast, assumed to occur only from infected cells, as it does in the real system. Thus, the only terms that must be multiplied by an additional factor are those

responsible for virus release, i.e., the term $k_{bud-rel,V_{rel}} P_{inf} \frac{Z_{in}}{Z_0} V_{bud}$ in (2.1.1^{**}) and the corresponding terms in (2.8.1^{**}) and (2.8.2^{**}). The factor is, evidently, equal to

$$(2.12.6) \quad \omega_{rel} = \frac{Z_{in}(t)}{Z_0}.$$

The denominator corresponds to the assumption that all the cells are involved in the process, and the numerator shows that only infected cells produce virions. An essential advantage of the considered approach is that the denominator does not depend on time, and, consequently, the resulting system of equations does not contain time delays.

As mentioned before, in the model system uninfected and dead cells, side by side with infected cells, are supposed to synthesize viral components. Consequently, a significant part of viral components produced by this model system is not produced in the reality. However, the assumption that only infected cells perform virus release (multiplying of corresponding terms by factor (2.12.6)) allows cutting off most of the “sham” viral components³. Consequently, the number of virions produced by the model system represents a reasonable approximation for the number of virions produced in the reality. Further in this section it will be also discussed how the formulated population model allows estimating the real concentrations of the intracellular viral components.

Throughout the whole process of virus replication (except the first 1-2 h) it is the total number of released virions (V_{rel}) that represents the size of the population of free virions. Indeed, most of the parental virions internalize, and the rest of them make up an infinitesimal part of the total number of extracellular virions. The number of released virions participating in the infection of cells also seems to be much lower than their total number. At the same time, function V_{ex} takes into account virus

³ To exclude all such components and to derive the more precise value for the number of released virions, multiplication of correspondent terms by additional factors might be carried out at every step of the infection cycle, as described by system (2.12.5).

internalization to dead cells, and, consequently, cannot be considered to characterize virus population. Function V_{rel} and functions Z_{un} , Z_{in} , and Z_d , which represent, correspondingly the populations of uninfected, infected, and dead cells, are four major output functions of the considered population model.

Other functions, describing the dynamics of intracellular viral components (intermediate functions), were investigated in detail in the single cell model. For the modeling of the population dynamics their exact meanings are not essentially important. Consequently, model assumption made above that all the cells are involved in virus production is relevant for the population modeling; it does not significantly influence the behavior of function V_{rel} , disturbing only the meanings of intermediate functions. On the other hand, as discussed in section 5.13, the lag between the beginning of the infection and the beginning of virus release is quite short in comparison with the duration of virus replication process. Consequently, even the number of viral components represented by intermediate functions can be estimated from the population model involved. To derive the value of the real concentration of the considered viral component at the given time point, the meaning of the function describing it must be multiplied by the factor ω_{rel} , given by formula (2.12.6)⁴.

After all, the general model, in which the dynamics of viral components is represented by the system of equations (2.12.5), is also approximate. It accounts for the size of considered cell and virus populations only in the finite set of time points, whereas the infection of uninfected cells and cell death occur continuously.

In the population model formulated here, like in the model with reinfection, the experimental fact that not all the released virions are infectious (see section 5.6 below) is taken into account by introducing into the term $k_{bud-rel,V_{rel}} P_{inf} \frac{Z_{in}}{Z_0} V_{bud}$ in

⁴ It does not refer to the functions describing the number of viral components at the steps of virus entry and penetration into the nucleus (V_{ex} , V_s , V_{end} , S_{cyt} , S_{nuc}). These viral components, unlike other viral components, are not produced by a cell; consequently the correspondent factor is already taken into account for them, when describing the step of virus release.

(2.1.1^{**}) the probability that a virion is infectious (the factor P_{inf}). There is also another method to formulate the equations of the population model, which does not require the introduction of the factor P_{inf} . It consists in the consideration of the probability of infection caused by a virion when choosing the values of the kinetic coefficients staying in the right-hand sides of population balance equations (2.12.1) – (2.12.3) (e.g., k_{un-in}). In this case, however, the number of parental extracellular virions (V_{ex0}), which in the single cell model accounts for the number of infectious virions per cell, would imply the presence of noninfective virions. To keep the consistency of the population model with the other modifications of the single cell model, this approach is not used.

Thus, the formulation of the population model is based on equations (2.1.1^{**}), (2.1.2-3), (2.2.1-2) – (2.7.1-2), (2.8.1^{**}-2^{**}), (2.12.1-3).

3 Initial Conditions, Kinetic Parameters, and Modeling Assumptions

All simulations based on the detailed single cell model, the reduced model, the model with reinfection, and the model for continuous infection were performed for the initial virus concentration $V_{ex0} = 10 \text{ nL}^{-1}$, and a cell surrounded by $U_r = 1 \text{ nL}$ of medium. All the parental virions are assumed to be infectious. Additionally, it is assumed that the average lifetime of a cell is about $T=12 \text{ h}$ p.i. (according to experimental data for Mv-1 lung cells (Roy et al., 2000) and for MDCK cells (J. Schulze-Horsel, Y. Genzel, personal communication, not shown), the average lifetime of a cell after infection is in the range from 10 to 12 hours, depending on experimental conditions).

The values for several kinetic parameters were taken from the literature (Table 3.1). The rate for endocytosis was taken as $k_{s-end} = 2.6 \cdot 10^{-4} \text{ s}^{-1} = 0.936 \text{ h}^{-1}$ (Nunes-Correia et al., 1999). The rate of peptide chain elongation was adjusted to $k_{Rib} = 5.0 \text{ s}^{-1}$ and the rate of RNA synthesis to $k_{Pl} = 30.0 \text{ s}^{-1}$ (Alberts et al., 2002). Other parameters, particularly at the early steps of infection, were estimated based on the general information available from the literature concerned with the dynamics of the influenza virus infection cycle (see section 4.1 below). To estimate the kinetic parameters for the transfer of vRNP complexes into the nucleus, particularly the rate coefficient of endosomal virus degradation ($k_{end-degr}$) (Fig. 1.7, step 2), it was also taken into account that "active" virus particles (able to be released from the endosome) made up 65-70% of the total number of endosomal viruses⁵ (Martin and Helenius, 1991a). The nuclear concentration of NP proteins defines the switch from vmRNA production to genome replication, and the switch parameters were estimated as $a_{NP} = 2.0 \cdot 10^{-5}$ and $b_{NP} = 1.0 \cdot 10^6$ (to achieve the appropriate number of released

⁵ The rate coefficient of vRNP nuclear export ($k_{cyt-nuc}$) was put equal to zero, and the ratio of the number of segments in the cytoplasm to the number of internalized virions (S_{cyt}/V_{ext}) was controlled.

virions at 12 h p.i.). All data for the stoichiometry of influenza A virus (A/PR/8/34; the lengths of polypeptides and vmRNA molecules encoding viral proteins, the numbers of viral proteins in the virion, etc.) were taken from Knipe et al. (2001) (Table 1.1).

Rate coefficients, contained in the right hand sides of model equations, and the time scale of the process are closely related to each other. Since the matrix of coefficients for the system of differential equations considered is a sparse matrix, one can adjust rate coefficients, relying on the overall time scale (see section 4.1). The results of these estimations are summarized in Table 3.2.

Table 3.1 Kinetic parameters, reported in the literature.

Parameter	Value	Source
Rate constant for endocytosis k_{s-end} (s^{-1})	$2.6 \cdot 10^{-4}$	1
Rate of peptide chain elongation k_{rib} (s^{-1})	5.0	2
Rate of RNA synthesis k_{Pl} (s^{-1})	30.0	2

1: Nunes-Correia et al., 1999

2: Alberts, 2002

Table 3.2 Estimated rate coefficients.

Rate coefficient	Value	Rate coefficient	Value
k_{ex-s,V_s} (h^{-1})	100.0	$k_{v-deg r}$ (h^{-1})	100.0
k_{s-ex,V_s} (h^{-1})	0.1	$k_{i,cyt-nuc}$ (h^{-1})	1.0
k_{s-end} (h^{-1})	0.936	$k_{i,cyt-deg r}$ (h^{-1})	0.01
$k_{end-cyt,V_{end}}$ (h^{-1})	14.0	$k_{i,nuc-deg r}$ (h^{-1})	5.0
$k_{end-deg r}$ (h^{-1})	6.0	$k_{j,ER-bud}$ (h^{-1})	1.0
$k_{cyt-nuc}$ (h^{-1})	5.0	$k_{j,ER-deg r}$ (h^{-1})	0.01
$k_{spl,S_{nuc}}$ (h^{-1})	1.0	$k_{j,bud-deg r}$ (h^{-1})	5.0
$k_{vm,i,nuc-cyt}$ (h^{-1})	1.0	$k_{un,S_{un,nuc}}$ (h^{-1})	1.0
$k_{vm,i,nuc-deg r}$ (h^{-1})	0.1	$k_{un,nuc-bud}$ (h^{-1})	1.0
$k_{vm,i,cyt-deg r}$ (h^{-1})	0.01	$k_{bud,V_{bud}}$ (h^{-1})	1.0
$k_{c-deg r}$ (h^{-1})	100.0		

The same data set and the dynamics of viral component productions obtained from the detailed model allowed estimating the rate coefficients of the reduced model (Table 3.3). The parameters were adjusted in a way that at 12 h p.i. the number of virions assembled in a cell in the reduced model fitted the number of virions released per nanoliter in the detailed model.

Table 3.3 Estimated rate coefficients (reduced model).

Rate coefficient	Value	Rate coefficient	Value
$k_{spl,V_{ex}}$ (h^{-1})	0.6	$k_{c-deg r}$ (h^{-1})	10.0
$k_{vm,nuc-cyt}$ (h^{-1})	0.17	$k_{v-deg r}$ (h^{-1})	10.0
$k_{vm,nuc-deg r}$ (h^{-1})	0.04	$k_{i,deg r}$ (h^{-1})	3.25
$k_{vm,cyt-deg r}$ (h^{-1})	0.01	$k_{pck,V_{rel}}$ (h^{-1})	0.082

For the simulations based on the population model the concentration of cells was still considered equal to 1 cell/nL (10^6 cells/mL). However, the concentration of virions was assumed to be 10^5 virions/mL, which corresponds to the value of the MOI equal to 0.1 virions/cell (a typical value for the considered fermentation experiments is 0.025 virions/cell, Genzel et al., 2004). The default values for the rate coefficient of the apoptosis of uninfected cells ($k_{ap,un}$) and for the rate constant of virus detachment (k_{dt}) were put equal to zero (see section 4.15.3). The other rate coefficients of the population model, i.e., rate coefficients of infection (k_{un-in}), apoptosis of infected cells ($k_{ap,in}$), virus release ($k_{bud-rel}$), and virus degradation (k_{vd}) were estimated based on experimental data concerning the overall dynamics of cell and virus populations (see section 4.15.1 below). Their estimates are given in Table 3.4. Reasoned by the difference in the structure of corresponding equations ((2.8.2) and (2.8.2**)), the meaning of the rate coefficient of virus release ($k_{bud-rel}$) in the population model differs from that in the detailed single cell model.

Table 3.4 Estimated rate coefficients (population model). The values of the other rate coefficients are given in Table 3.2.

Rate coefficient	Value	Rate coefficient	Value
k_{un-in} (h^{-1})	0.7	$k_{bud-rel}$ (h^{-1})	0.013
$k_{ap,in}$ (h^{-1})	0.1	k_{vd} ($nL \cdot h^{-1}$)	0.003

In section 2.5 it is assumed that all ribosomes operate at a constant rate and that vmRNA molecules are translated by several ribosomes, separated by $d_{rib} = 80$ nucleotides (Alberts et al., 2002). Therefore, the synthesis rate is the same for all viral proteins and equal to k_{Rib} (*amino acids/h*). The model also implies that the viral polymerase complexes process all 8 genome segments at the same rate k_{pl} (*nucleotides/h*). Therefore, the vmRNA molecule coding for the i -th viral protein is synthesized at the rate $\omega_i k_{pl}$, where ω_i (-) is the fraction of the nucleotides making up vmRNA molecules encoding i -th viral proteins from the entire number of nucleotides produced. For vmRNA molecules encoding polymerase complexes

$$\omega_{pl} = \frac{3}{8}$$

(three polymerase subunits encoded by three genome segments), and for NP, HA and NA vmRNA molecules

$$\omega_{NP} = \omega_{HA} = \omega_{NA} = \frac{1}{8}.$$

For vmRNA molecules encoding M1 and M2 proteins

$$\omega_{M1} = \frac{1}{8} \sigma_{M1};$$

$$\omega_{M2} = \frac{1}{8} \sigma_{M2}.$$

Here, σ_{M1} is a fraction of M1 encoding nucleotides in the 7th genome segment and

$$\sigma_{M2} = 1 - \sigma_{M1}.$$

The same applies to nucleotides encoding NS1 and NS2 proteins in the 8th genome segment:

$$\omega_{NS1} = \frac{1}{8} \sigma_{NS1};$$

$$\omega_{NS2} = \frac{1}{8} \sigma_{NS2}.$$

Numerical algorithms to solve the given system of ODEs were provided by DIVA (Kroener et al., 1990) and ProMoT (Traenkle et al., 1999), a software package to build structured dynamic simulation models.

4 Results

Presented in this section will be the results obtained from the single cell model (Sidorenko and Reichl, 2004). Considered in the beginning are the overall dynamics of virus replication and the behavior of the number of viral components in different cellular compartments, particularly, the dynamics of progeny virus release. After that, it will be shown how virus infection depends on the pools of cellular resources, and what bottlenecks limit virus replication. Further, the sensitivity of the system in respect to changes of model parameters and initial conditions will be described. Finally, results provided by model modifications (the model with reinfection, the model for continuous infection, and the population model) will be reported in a similar way.

4.1 Overall Dynamics

According to literature (Roy et al., 2000; Nunes-Correia et al., 1999) and simulation results, most of the virions are attached to the cellular membrane within 2 to 5 min p.i.⁶. Internalization via receptor-mediated endocytosis is accomplished in about 10 min⁶. As a consequence, within 15 to 20 min p.i. all the virions enter the cell⁷. As soon as the first vRNP complexes reach the nucleus (about 30 min p.i.)⁸, vmRNA molecules are being transcribed in high numbers of copies. The switch from vmRNA production to virus genome replication takes place at about 3 h p.i., when a significant

⁶ The rate coefficients of attachment (k_{ex-s}) and detachment (k_{s-ex}) were adjusted in such a way that in 5 min p.i. about 99% of the virions are internalized (V_{ex} makes up about 1% of its initial value) and in 10 min p.i. the number of endosomal virions (V_{end}) reaches its maximum.

⁷ It can be seen by putting the rate coefficient of virus release from the endosome ($k_{end-cyt}$) equal to zero and controlling the time point when about 99% of internalizing virions reach the endosome.

⁸ The time point when the number of vRNP complexes in the nucleus reaches half of its maximal value (adjusted by $k_{cyt-nuc}$).

amount of newly produced NP proteins accumulate in the nucleus. As a result, vRNA molecules start being intensively replicated by viral polymerase complexes, followed by the assembly of new vRNP complexes. At approximately 4 h p.i., newly produced virus particles are released into the extracellular medium⁹. The cell produces about 8000 virions before it dies at about 12 h p.i. due to the virus interfering with basic cellular processes or apoptosis (see section 5.15).

4.2 Dynamics of Virus Entry

Functions, describing the virus entry into the host cell show a similar dynamic behavior. Indeed, at the early stages of the infection a certain amount of incoming viral components is successively transported from one compartment to another (from the extracellular medium to the surface of the cell, from the cellular surface to the endosome, etc. – see equations (2.1.1), (2.1.2), (2.1.3), (2.2.1), (2.2.2), (2.4.2)). During such transport processes an exponential increase of the number of the corresponding component caused by the import of the component from the previous compartment is followed by an exponential decrease due to the export to the next compartment (naturally, the number of extracellular virions exponentially decreases from the beginning of the infection) (Fig. 4.1). Finally, as the incoming vRNP complexes reach the nucleus, the number of vRNA molecules arising from the vRNP splitting also starts to exponentially increase.

⁹ Adjusted by the choice of the rate coefficients of transport.

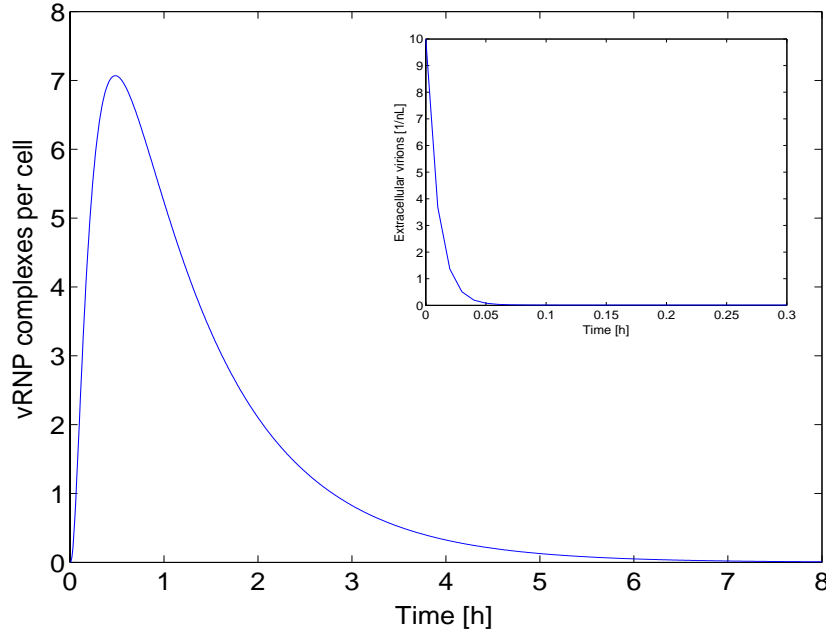


Figure 4.1 Internalization of viral components. The exponential increase of the number of cytoplasmic vRNP complexes (S_{cyt}) caused by the release of the viral genome from the endosome is followed by the exponential decrease due to nuclear import. Inset: exponential decrease of the number of extracellular virions (V_{ex}).

4.3 Dynamics of vmRNA Production

At the early stages of the infection (0.0 – 0.5 h p.i.) the total number of vmRNA molecules produced increases exponentially in time (Fig. 4.2). Indeed, since the number of NP proteins is small at this period:

$$(4.3.1) \quad a_{NP} P_{NP,nuc} \ll 1 \quad (\text{exponential stage})$$

the term $k_{v-vm,i,max} \frac{1}{1 + a_{NP} P_{NP,nuc}} P_{Pol,nuc}$ in (2.3.1), describing the increase of the

number of vmRNA molecules, is proportional only to the number of polymerase

complexes. At the same time, the term $k_{i,synt} \frac{C_{i,cyt}}{d_{rib}}$ in (2.5.1), which describes the

increase of the number of viral capsid proteins (including the number of polymerases), is proportional to the number of corresponding vmRNA molecules. The solution to such a system of equations represents exponentially increasing functions of time for both the number of viral proteins and the number of vmRNA molecules.

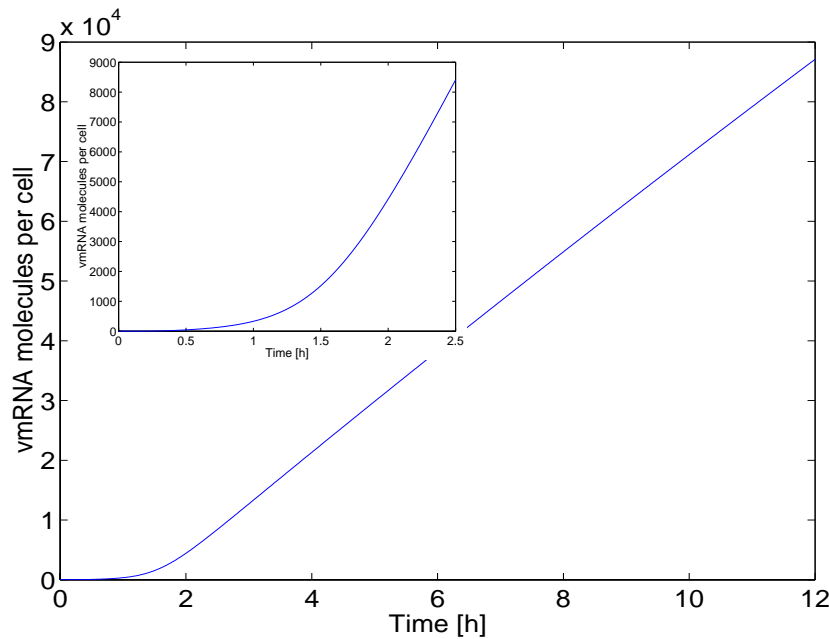


Figure 4.2 Total number of vmRNA molecules. The number of vmRNA molecules, after initial exponential stage (0 – 0.5 p.i., see inset), increases linearly. Transitional stage takes place at about 0.5 - 2.0 h p.i.

At the next stage of the infection the number of NP proteins becomes high enough to inhibit vmRNA synthesis (2.0 – 12.0 h p.i.) (Fig. 4.2):

$$(4.3.2) \quad a_{NP} P_{NP,nuc} \gg 1 \quad (\text{linear stage})$$

It can be shown, that at this stage the number of vmRNA molecules increases obeying a polynomial law. Indeed, the process of vmRNA synthesis is affected by two factors; its rate is proportional to the number of polymerase complexes and inversely proportional to the number of NP proteins (see equation (2.3.1)). The model implies that the proportion, in which viral proteins are produced, is kept constant throughout the whole process of the infection. Consequently, the factors considered are cancelled by each other, resulting in the certain constant rate of vmRNA synthesis. As the rate constant of vmRNA degradation is assumed to be quite low, it can be concluded that at moderate values of time (2.0 – 12.0 h p.i.) the number of vmRNA molecules increases linearly in time.

At the late stages of the infection, when the number of vmRNA molecules produced is high, the degradation of vmRNA molecules can become appreciable. In this situation (not achieved at 12 h p.i. at the considered set of model parameters), the number of

vmRNA molecules tends to constant (see equations (2.3.1) and (2.3.2)).

Thus, the number of vmRNA molecules has two growth stages: initial exponential and late polynomial. The first stage turns to the second through the transitional stage (approximately 0.5 – 2.0 h p.i.), which is defined by the value of the switch parameter a_{NP} . The transitional stage satisfies the relation

$$(4.3.3) \quad a_{NP} P_{NP,nuc} \approx 1 \quad (\text{transitional stage})$$

4.4 Dynamics of Viral Protein Synthesis

As it can be seen from $k_{i,synt} \frac{C_{i,cyt}}{d_{rib}}$ in (2.5.1) and the corresponding term in (2.6.1), the rate of viral protein synthesis is proportional to the number of vmRNA molecules. Since the rate constant of protein degradation is assumed to be high, the number of viral proteins in the nucleus (except M1 proteins, representing a limiting factor during the assembly of M1-vRNP complexes, see section 4.9), similar to the number of vmRNA molecules, exponentially increases at the early stages (0 – 2.0 h p.i.) (Fig. 4.3), linearly increases as the growing number of NP proteins becomes essentially inhibiting vmRNA synthesis (4.0 – 12.0 h p.i.) (relation (4.3.2) is satisfied), and, finally, tends to constant at the latest stages (beyond the average lifetime of the cell, not shown) (see equations (2.5.1), (2.5.2), and section 4.3). The difference between the time courses of vmRNA and viral protein production results from the finite rates of the nuclear export of vmRNA molecules and the nuclear import of viral proteins.

Unlike nuclear viral proteins, those incorporated into progeny virus particles are not influenced by nuclear protein degradation. Consequently, the number of proteins, consumed for virus production (and, consequently, the number of produced viral proteins and the total number of viral proteins in the system) after initial exponential increase grows first proportional to the second and then to the first power of time (beyond the average lifetime of the cell) (Fig. 4.4).

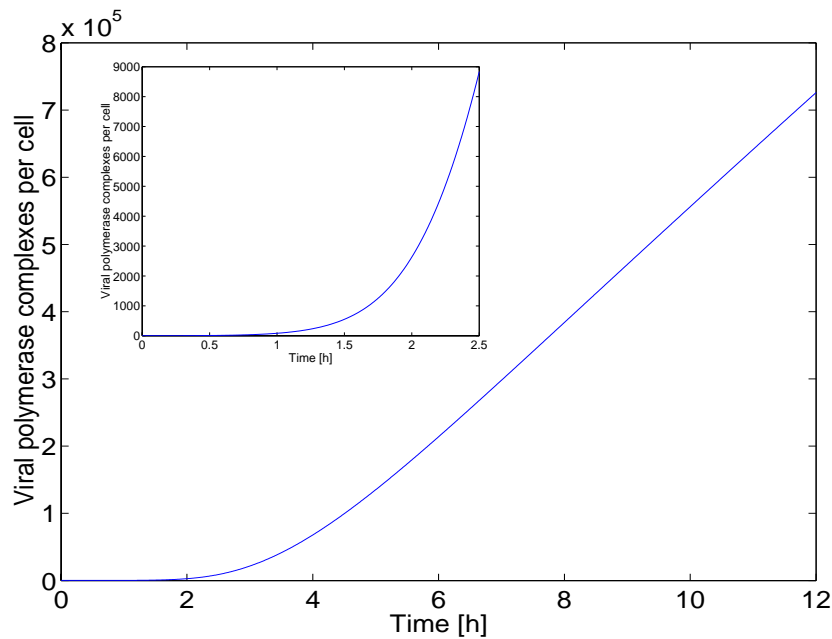


Figure 4.3 Polymerase complexes in the nucleus. The number of polymerase complexes in the nucleus ($P_{Pol,nuc}$) (as well as the number of other proteins except M1) increases first exponentially (0 – 2.0 h p.i., see inset), then linearly (4.0 – 12.0 h p.i.).

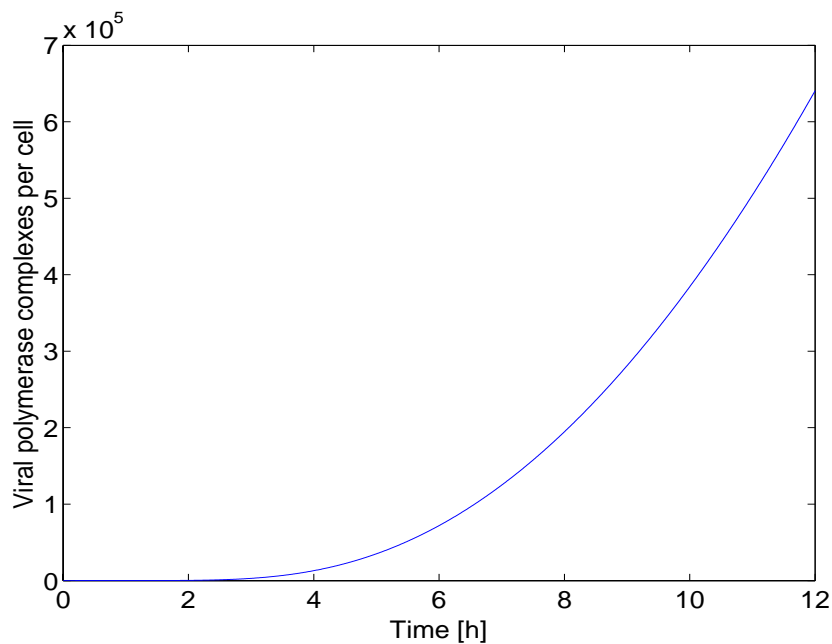


Figure 4.4 Polymerase complexes incorporated into progeny virions. The initial exponential stage is followed by the second order polynomial increase.

The dynamics of envelope protein synthesis is similar to that of capsid protein synthesis. Since envelope proteins are not limiting at the stage of virus particle formation (the bottleneck at this stage is the number of M1-vRNP complexes, see

section 4.9), they accumulate at the budding site in the same manner, as capsid proteins do in the nucleus (Fig. 4.3).

4.5 Dynamics of Viral Genome Replication

Among all the functions considered, the one describing the number of vRNA segments (C_v) in the nucleus has the most complex behavior. As shown in section 4.2, it increases first exponentially due to virus internalization (0.0 – 0.3 h p.i.) (Fig. 4.5). This initial stage is followed by a short interval of linear growth (approximately 0.3 – 1.0 h p.i.). During the considered interval only a certain fixed number of internalized vRNA segments is replicated, providing the constant rate of vRNA synthesis. Later, the law of the increase changes again to exponential (approximately 1.0 – 4.0 h p.i.). Indeed, as revealed in section 4.3, the number of polymerases increases exponentially at the early stages of the infection (when relation (4.3.1) is

satisfied) and, consequently, the term $k_{c-v,max} \frac{P_{NP,nuc}}{b_{NP} + P_{NP,nuc}} P_{Pol,nuc}$ in (2.4.2) also

increases in the same manner. As NP proteins become inhibiting vmRNA synthesis (relation (4.3.2) is satisfied), the number of vRNA molecules starts increasing parabolically (proportional to the 2nd power of time) (approximately 4.0 – 7.0 h p.i.). The matter is that the mentioned above term is now proportional to two linear factors

($\frac{P_{NP,nuc}}{b_{NP} + P_{NP,nuc}}$ and $P_{Pol,nuc}$, see section 4.4). Additionally, it is assumed that the rate

constant of genomic vRNA degradation is high, which does not permit an increase proportional to the third power of time. After changing of the relationship between b_{NP} and $P_{NP,nuc}$ (see below) only one linear factor remains in the term

$k_{c-v,max} \frac{P_{NP,nuc}}{b_{NP} + P_{NP,nuc}} P_{Pol,nuc}$ in (2.4.2), another factor tending to constant. As a result,

vRNA growth turns to its second linear stage. Finally, at the latest stages of the infection both factors tend to constant (see sections 4.4), and, correspondingly, the number of genomic vRNA molecules also tends to constant.

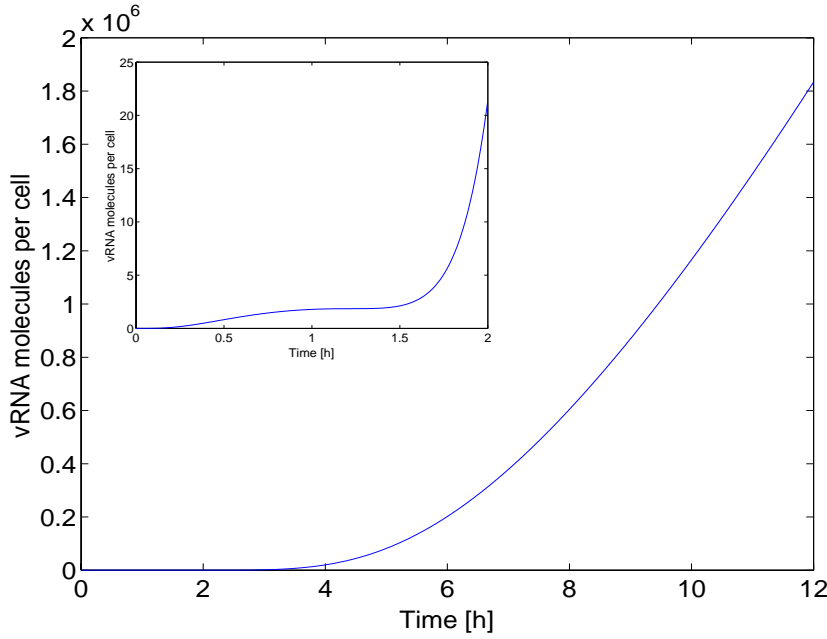


Figure 4.5 Synthesis of vRNA molecules. The increase of vRNA number (C_v) comprises several stages: two exponential (0 – 0.3 h p.i. and 1.0 – 4.0 h p.i.) and two polynomial (0.3 – 1.0 h p.i. and 4.0 – 12.0 h p.i.). Inset: initial exponential and linear stages.

The transition from the parabolic to the linear growth stage of genomic vRNA number is determined by the number of NP proteins in the nucleus. If

$$(4.5.1) \quad P_{NP,nuc} \ll b_{NP} \quad (\text{parabolic stage})$$

both factors making up $k_{c-v,max} \frac{P_{NP,nuc}}{b_{NP} + P_{NP,nuc}} P_{Pol,nuc}$ in (2.4.2) are linear and the

number of vRNA molecules increases proportional to the second power of time (due to the high value of the rate constant of vRNA degradation). In the opposite case, i.e., when

$$(4.5.2) \quad P_{NP,nuc} \gg b_{NP} \quad (\text{linear stage})$$

the rate of vRNA production becomes proportional to only one linear factor, and, consequently, the number of vRNA molecules itself starts to increase linearly. At

$$(4.5.3) \quad P_{NP,nuc} \approx b_{NP} \quad (\text{transitional stage})$$

the transitional stage of vRNA growth takes place. At some sets of model parameters it can happen that relations (4.3.2) and (4.5.1) are not satisfied together at any time interval. In this case the second exponential stage of vRNA growth turns directly to the linear stage, bypassing the parabolic stage.

The value of b_{NP} chosen for the simulations is $b_{NP} = 10^6$, whereas at 12 h p.i. the number of NP protein molecules in the nucleus is about $P_{NP,nuc}(12) = 6 \cdot 10^5$ (not shown). The transitional stage of vRNA growth (relation (4.5.3) is satisfied) starts at about 7 h p.i. (not shown), whereas the linear stage (relation (4.5.2) is satisfied) cannot be achieved within the lifetime of the cell. Thus, the time point when the cell dies (12 h p.i.) corresponds to the transitional stage between the parabolic and linear stages.

Similar to viral proteins incorporated into progeny virus particles, vRNA molecules consumed for virus production are also not influenced by nuclear degradation. At the parabolic stage of nuclear vRNA increase the number of packaged genomic vRNA molecules could grow proportional to the third power of time (see equations (2.4.1), (2.4.2)). However, since at these stages viral proteins are produced proportional to the square of time (see section 4.4), the number of vRNA molecules incorporated into virions must grow in the same manner, the redundant amount of produced vRNA molecules being degraded in the nucleus. It is also remarkable, that the number of packaged proteins goes on growing exponentially until NP proteins become inhibiting vRNA production (while relation (4.3.1) is satisfied), lacking the first linear growth phase, peculiar to the number of vRNA molecules. Consequently, during its linear growth stage the number of vRNA molecules consumed for virus formation also increases exponentially in time, the redundancy of vRNA molecules accumulating and degrading in the nucleus.

Unlike vRNA segments, cRNA segments are not delivered into the nucleus with incoming virus particles. Thus, the increase of cRNA number lacks the first linear stage, taking place for the increase of vRNA number. Instead, initial exponential increase goes on continuously until turning to the parabolic stage. Further behavior of cRNA number is similar to that of vRNA number (Fig. 4.6).

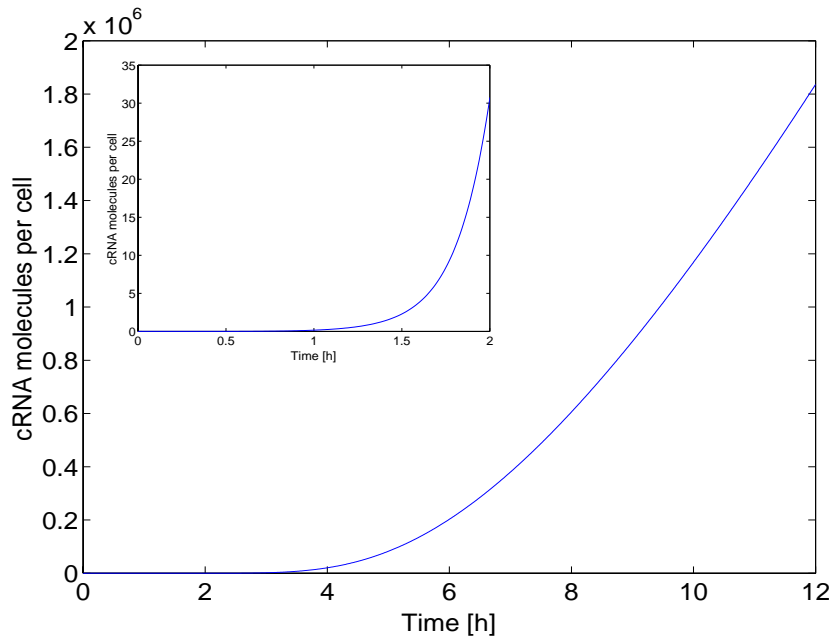


Figure 4.6 Synthesis of cRNA molecules. The law of the increase of cRNA number (C_c) is similar to that of vRNA number, however it lacks the first linear stage. The initial exponential increase (see inset) directly turns to the second order polynomial stage.

4.6 Dynamics of the Production of M1-vRNP Complexes

The function describing the number of newly produced M1-vRNP complexes, as well as other functions presenting virus release, behaves similar as the function describing the number of progeny virus particles (Fig. 4.14). For this reason it will not be considered individually. Indeed, being limiting during virus budding (see section 4.9), it is the number of M1-vRNP complexes that defines the dynamics of virus release. Since the rates of transport of viral components (nuclear export of vmRNA molecules, nuclear import of viral proteins, and nuclear export of M1-vRNP complexes) and the rate of virus budding are limited, the difference can be only in the time scale of the considered processes. The time behavior of the number of progeny virions will be considered below (section 4.7).

4.7 Dynamics of Progeny virus Release

Finally, having made clear the dynamics of viral component synthesis, it is possible to make a series of conclusions concerning the behavior of the number of released virions. In this section it will be shown, that at the given set of model parameters the number of progeny virus particles increases exponentially at the early stages of the infection, whereas at the late stages it obeys a polynomial law. Besides that, the conditions peculiar to each stage will be specified, and further (see section 5.9 below) it will be discussed if other qualitatively different solutions to the considered system of equations are possible for the number of produced virus.

4.7.1 Exponential Stage

As shown in sections 4.4 and 4.5, at the early stages of the infection (when the number of NP proteins is low, see relation (4.3.1)) the number of viral components (viral proteins and vRNA molecules) consumed for virus production increases exponentially. Consequently, the number of progeny virions itself also increases exponentially at this stage.

The exponential stage of virus release goes on until the number of NP proteins becomes high enough to inhibit vmRNA synthesis. As relation (4.3.3) starts being satisfied, the number of progeny virions turns to the transitional stage, at which its behavior changes from exponential to polynomial. The time interval corresponding to the transitional stage of virus release, similar to that corresponding to the transitional stage of vmRNA production (see section 4.3) depends on the value of the switch parameter a_{NP} . An increase of a_{NP} makes the transitional stage shorter, and a decrease of a_{NP} elongates it. It is remarkable, however, that the “middle” of the transitional phase is not influenced by variations of a_{NP} (see section 4.11.1.3 below). To a lower extent, the transition from the exponential to the polynomial stage is also influenced by virus internalization dynamics. When the process of virus internalization is fast the polynomial stage of virus growth begins as soon as the rate

of vmRNA synthesis becomes constant (relation (4.3.2) starts being satisfied), whereas a slow delivery of the viral genome into the nucleus delays the transitional stage.

4.7.2 Polynomial Stage

The stage of polynomial growth consists of two phases. During its first phase the number of virus particles produced is proportional to the square of time. It corresponds to the situation, when the number of vmRNA molecules increases linearly (relation (4.3.2) is satisfied), without a significant influence of degradation. Indeed, as it is seen from sections 4.4 and 4.5, in this case the number of all viral components incorporated into progeny virus particles, and, consequently, the number of virions itself increases parabolically.

The second phase of polynomial growth is the phase of the linear increase of progeny virus number. It starts, when the degradation of vmRNA molecules becomes appreciable and the number of vmRNA molecules tends to constant. In this situation the number of viral components produced increases linearly (see section 4.4), which results in a linear increase of the number of produced virions.

At the conditions chosen for simulations, the linear phase of progeny virus release is not achievable. It would start as late as at about 150 h p.i. (not shown), which is definitely beyond the lifetime of the cell. However, as it will be seen later (see section 4.11.8.1) at certain sets of model parameters a linear phase of virus growth can be found within the cellular lifetime.

The change of vmRNA dynamics by the increasing number of NP proteins (which happens within 0.5 – 1.5 h p.i., see section 4.3) becomes influencing the dynamics of virus release within 4.0 – 7.0 h p.i. (not shown). The time delay results from the finiteness of transport rates of viral components. Consequently, the transitional stage between the exponential and polynomial stages of virus growth occurs at the period 4.0 – 7.0 h p.i. At 7.0 h p.i. the number of released virions starts growing proportional

to the square of time, remaining in the parabolic phase until reaching the time point of cell death (12 h p.i.) (Fig. 4.14).

Remarkably, the degradation of vmRNA molecules is the only reason that causes the change from the parabolic growth phase to the linear growth phase. In the absence of degradation the polynomial law of progeny virus growth would be parabolic throughout the whole replication cycle.

4.8 Use of Cellular Resources

The model allows an estimation of the number of cellular resources (e.g. surface receptors or amino acids) required for influenza virus replication and a comparison with the total number of these resources in the cell.

As mentioned before (see section 2.1), the cell has about 10^4 to 10^5 binding sites for influenza virus and approximately 200 endosomes, which exceeds by far the number of virus particles bound to the cell and the number of endosomes required for virus incorporation at low multiplicities of infection. Thus the number of cellular receptors and endosomes is not significantly reduced at the beginning of the infection cycle.

In a typical mammalian cell, the nuclear plasma membrane has approximately 3000 to 4000 nuclear pores. Assuming a transfer rate of 10^2 to 10^4 molecules per second, typical for membrane transport proteins (Lodish et al., 2000), 10^9 to 10^{11} viral molecules (vmRNA and vRNA molecules, vRNP complexes, viral proteins) could pass the nuclear membrane per hour. As simulations show, nuclear pores are mainly used for the transfer of newly synthesized viral proteins, e.g. M1 and NP, into the nucleus. The maximum rate of this process is $k_{por,max} \sim 10^7 h^{-1}$. The rates of other processes of viral component transport requiring nuclear pores are significantly lower and can be neglected. Thus, influenza viruses use only a negligible part of the transfer capacity of nuclear pores for their replication.

The number of free cellular nucleotides and amino acids consumed for virus production ($1.7 \cdot 10^8$ nucleotides and $2.2 \cdot 10^{10}$ amino acids) is much lower than the total cellular pool of these components ($1.3 \cdot 10^{10}$ nucleotides and $3.1 \cdot 10^{10}$ amino acids, see Appendix A4) (Fig. 4.7). Even assuming that the synthesis of free cellular nucleotides and amino acids is stopped early during the infection, their total number is much higher than their number necessary for synthesizing 8000 virus particles. Accordingly, Monod-type kinetics is not used in the model for the rate coefficients of viral protein and RNA synthesis.

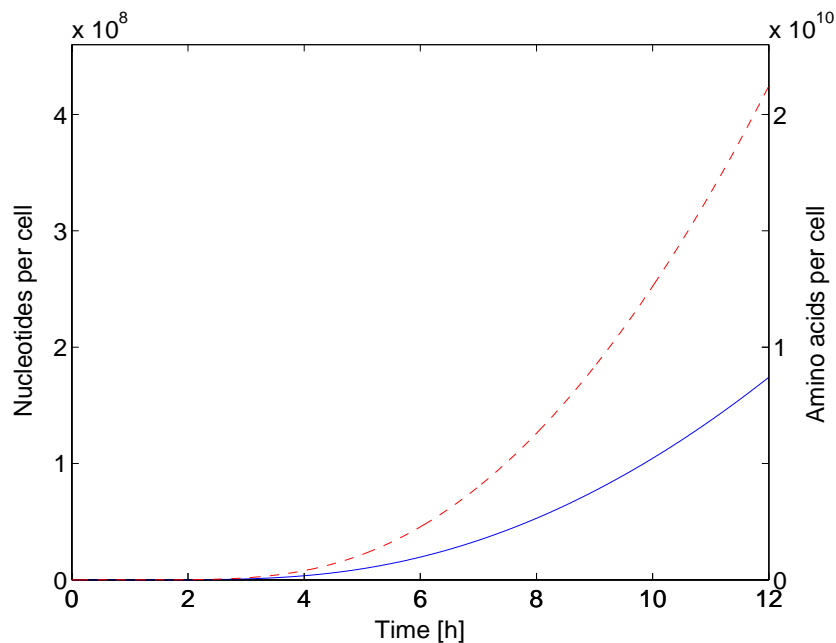


Figure 4.7 Cellular resources consumed for virus replication. Free cellular nucleotides (—) and amino acids (---).

The maximum number of vmRNA molecules in the cytoplasm never exceeds $C_{vm,max} \sim 10^5$ molecules (Fig. 4.2). Therefore, the number of ribosomes involved in the synthesis of viral proteins is significantly smaller than the estimated total number of cellular ribosomes (approximately 10^7). Consequently, the number of cellular ribosomes does not limit viral protein production, and the rate coefficients $k_{i,synt}$ (see equation 2.5.1) and $k_{j,synt}$ (see equation 2.6.1) are considered to be constant. Also, the number of heterogeneous nuclear precursor mRNA molecules, which is about $2.2 \cdot 10^5$ molecules (Kaufman, 2000), is not limiting for vmRNA synthesis (Fig. 4.2).

4.9 Limiting Factors

During several processes of the infection cycle (e.g., the assembly of M1-vRNP complexes and the formation of progeny virus particles), one, more complex viral component, is synthesized from other, simpler viral components. A simple model accounting for this kind of processes is formulated in Appendix A1. It is, particularly, shown that in the case when there are more than two viral components to be assembled, and the considered viral components have different ratios of the rate of their synthesis to the rate of their packaging, one of viral components invariably represents a limiting factor for the process of assembly: the whole amount of it incorporates into complex components, whereas the other simple components accumulate at the place of the assembly.

By now little is known concerning the mechanisms, by which influenza virus regulates the synthesis of its proteins and vRNA molecules, therefore, such mechanisms are not considered in the model. As the balance between the rate of the synthesis of viral components and the rate of their packaging is not assumed to be controlled, the situation described above takes place for all the processes of the incorporation of simple viral components into complex ones; i.e., one of the simple viral components limits the formation of complex components.

The model provides a possibility to reveal factors that limit the rate of progeny virus release. Simulations show that during the assembly of M1-vRNP complexes (Fig. 1.7, step 7), as well as during virus budding (Fig. 1.7, step 8), one of the newly produced viral components is completely consumed for progeny virus particle formation. As a result, the consumption rates of other components and, hence, the rate of the whole correspondent process becomes limited. This leads to the accumulation of viral proteins and vRNA molecules in the nucleus and to the accumulation of viral membrane proteins at the budding site, respectively.

For instance, the formation of M1-vRNP complexes in the nucleus (Fig. 1.7, step 7) it is the number of M1 proteins that represents a limiting factor (Fig. 4.8). M1 proteins

do not accumulate in the nucleus – all their molecules are consumed for the production of M1-vRNP complexes. At the same time, the other viral proteins (NS1, NS2, NP, and polymerase complex subunits), as well as vRNA molecules, are synthesized in redundant amounts. Their incorporation into newly formed M1-vRNP complexes is restricted by the number of M1 proteins produced, while NS1 nonstructural proteins are not incorporated at all. These viral components accumulate in the nucleus; their number increases linearly in time. An insignificant increase of the number of M1 proteins early in the infection (Fig. 4.8) can be explained by a low rate of packaging during this period of time. Indeed, the rate of the assembly of M1-vRNP complexes is proportional to the number of vRNA molecules and all viral proteins making up M1-vRNP complexes (see equation 2.4.2).

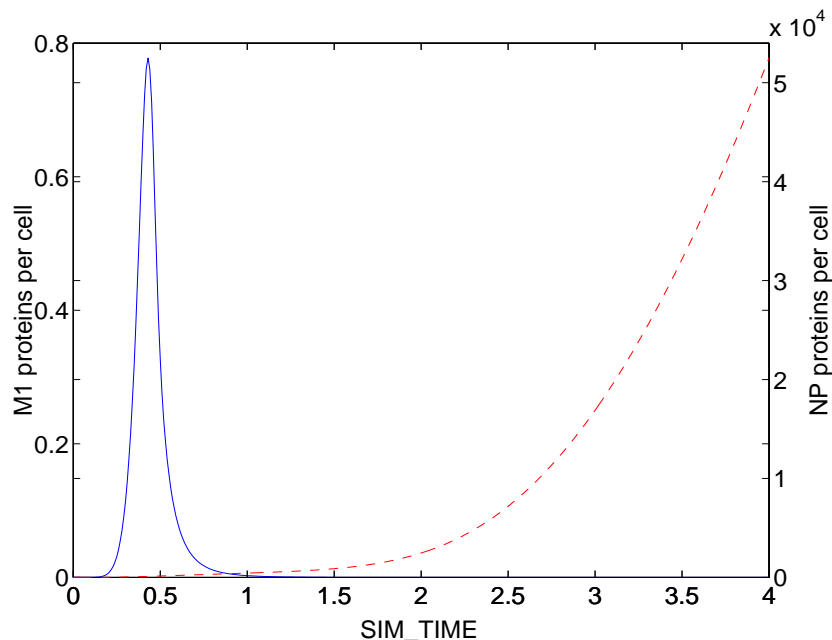


Figure 4.8 Viral components in the nucleus. M1 proteins (—) are limiting the formation of new M1-vRNP complexes, whereas other capsid proteins, e.g. NP proteins (---), and vRNA molecules accumulate in the nucleus.

A similar situation takes place during virus budding (Fig. 1.7, step 8). Newly synthesized M1-vRNP complexes represent a limiting factor (Fig. 4.9). Simulation results show, that the number of M1-vRNP complexes at the budding site is close to zero. The reason for its small increase at the initial stage of the infection is that the rate of budding, proportional to the number of M1-vRNP complexes and all envelope proteins to be incorporated into virions, is not yet high enough at this period. Viral

membrane proteins (HA, NA, and M2) accumulate at the budding site, and, similar to the previous case, their number increases linearly in time (Fig. 4.9). As discussed above, the formation of M1-vRNP complexes is limited by the number of newly produced M1 proteins. Since M1-vRNP complexes are limiting at virus budding, M1 proteins can be considered as the major determinant of the virus yield. This inference is particularly used for the development of the reduced model (see sections 2.9 and 5.14.2).

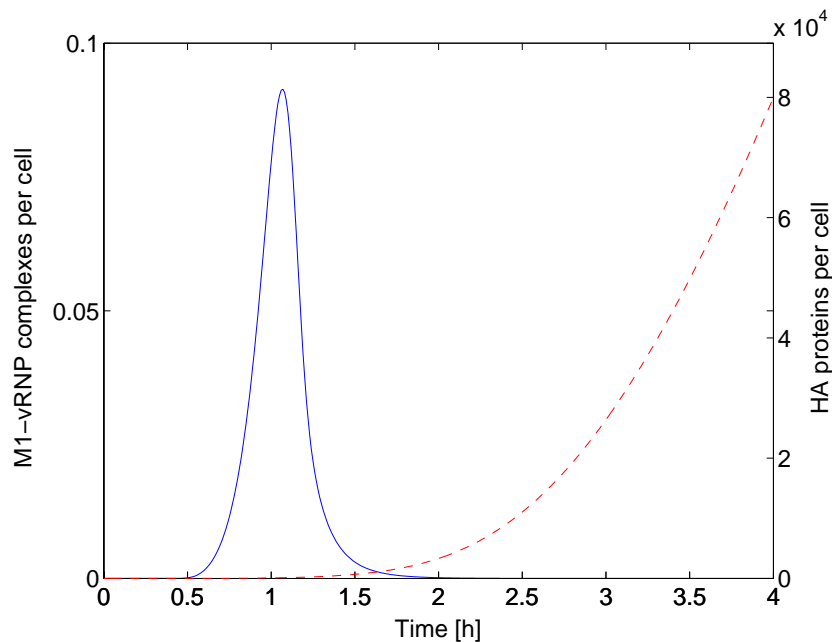


Figure 4.9 Viral components at the budding site. Newly synthesized M1-vRNP complexes (—) represent a limiting factor, while viral envelope proteins (HA proteins, ---) accumulate at the budding site.

4.10 Influence of Initial Condition Changes on Virus Growth and Limiting Factors

For the achievement of purposes of the model mentioned in section 1.4, particularly for the optimization of the virus yield, it is important to investigate the sensitivity of the system behavior to variations of initial conditions. The only nonzero initial condition is the initial concentration of extracellular virions (see section 3):

$$V_{ex}(0) = V_{ex0}.$$

The number of virions and viral components in all cellular compartments is equal to zero. Thus, this section considers the dependency of the number of produced virions on the *MOI* (*virions/cell*), the ratio of the concentration of virus particles added per cell at the time of infection (V_{ex0} , (*virions/nL*)) to the initial concentration of uninfected cells (Z_0 , (*cells/nL*)) (Licari and Bailey, 1992):

$$MOI = \frac{V_{ex0}}{Z_0}.$$

To investigate, how the *MOI* affects the number of virions produced at different time points, consider two values of the *MOI*: MOI_1 and MOI_2 : $MOI_1 < MOI_2$. Let $V_{rel,1}(t)$ and $V_{rel,2}(t)$ denote the number of virions produced at the time point t , corresponding to MOI_1 and MOI_2 respectively. Simulations show, that if MOI_1 and MOI_2 are high enough (higher than 3 virions/cell) there is a time point t_0 , at which $V_{rel,1}(t_0) = V_{rel,2}(t_0)$; for $t < t_0$ $V_{rel,1}(t) < V_{rel,2}(t)$, and for $t > t_0$ $V_{rel,1}(t) > V_{rel,2}(t)$ (Fig. 4.10). In other words, an increase of the *MOI* results in an increase of the number of produced virions at the early stages of the infection and in a decrease of the number of produced virions at the late stages of the infection.

If the values of MOI_1 and MOI_2 are lower than 3 virions/cell, $V_{rel,1}(t)$ and $V_{rel,2}(t)$ do not intersect (Fig. 4.10). In this case $V_{rel,1}(t) < V_{rel,2}(t)$ at any value of t ; an increase of the *MOI* results in an increase of the number of produced virions at any time point. In the situation when $MOI_1 < 3 \text{ virions/cell} < MOI_2$ the existence of the point of intersection for the plots of $V_{rel,1}(t)$ and $V_{rel,2}(t)$ depends on the vicinity of the values of MOI_1 and MOI_2 to the value of 3 virions per cell.

Let now the value of MOI_2 be fixed. Simulations show that when decreasing the value of MOI_1 , the value of t_0 (if $V_{rel,1}(t)$ and $V_{rel,2}(t)$ intersect) increases and at the certain value of MOI_1 turns to infinity ($V_{rel,1}(t)$ and $V_{rel,2}(t)$ do not intersect). Consequently, although for any value of MOI_2 there is a time point t_0 , at which a decrease of the *MOI* becomes profitable for virus production¹⁰ (in the particular case it can be

¹⁰ Results in the increase of the number of released virions at $t \rightarrow \infty$.

infinite), the value of t_0 can be beyond the lifetime of the cell $T=12$ h. Feasible values for t_0 are, hence limited by T :

$$0 \leq t_0 \leq T .$$

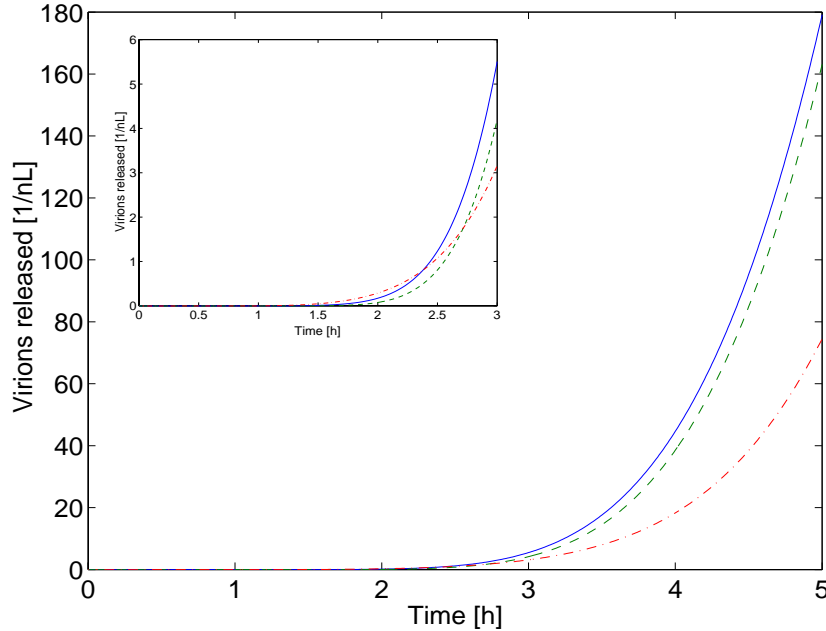


Figure 4.10 The number of released virions (V_{rel}) for different values of the MOI. The maximal number of virions is produced at MOI=3 virions/cell (—). Inset: the curve corresponding to MOI=3 virions/cell (—) intersects the curve corresponding to MOI=100 virions/cell (---) and has no intersection with the curve, corresponding to MOI=1 virion/cell (---).

Therefore, it can be concluded that there is a value of the MOI (MOI_{opt}) optimal for the virus yield. Function $V_{rel,opt}(t)$, corresponding to this value possesses the following property. Every curve $V_{rel,1}(t)$, corresponding to the value $MOI_1 < MOI_{opt}$ intersects the plot of function $V_{rel,opt}(t)$ at the time point $t_0 > T$ (possibly, $t_0 = \infty$), whereas every curve $V_{rel,2}(t)$, corresponding to the value $MOI_2 > MOI_{opt}$ intersects the plot of function $V_{rel,opt}(t)$ at the time point $t_0 < T$ (Fig. 4.10). Consequently, at the time point $t=T$ function $V_{rel,opt}(t)$ in any case provides the maximal number of produced virions.

As the model refers to the infection of a single cell, it is clear that the range of relevant values of the MOI is limited from below by 1 virion/cell. On the other hand, consideration of MOI values higher than 100 virions/cell can bring to the situation when the number of cellular endosomes limits virus replication (the cell contains

about 200 endosomes, Alberts et al., 2002). Thus, it is reasonable to perform simulations for the values of the MOI changing in the range from 1 virion/cell to 100 virions/cell. As follows from simulation data summarized in Table 4.1, the number of produced virions represents a monotonously decreasing function of the MOI in the interval of MOI values from 3 virions/cell to 100 virions/cell, whereas at the interval of MOI values from 1 virion/cell to 3 virions/cell it increases, $MOI_{opt} \approx 3$ virions/cell (the abscissa of the maximum) representing the optimal value of the MOI at the considered set of model parameters. At the same time, table 4.1 shows that the impact of the MOI changes in the range from 1.0 virion/cell to 10.0 virions/cell on the virus yield is rather small. It becomes appreciable only if the MOI is significantly increased (from 10.0 virions/cell to 100.0 virions/cell).

Table 4.1 Virus yield and limiting factors of virus replication for different values of the MOI (virions/cell)

MOI	1.0	2.0	3.0	4.0	5.0	10.0	100.0
V_{rel}	8140	8270	8300	8290	8260	8020	6170
LF	B	B	B	B	A	A	A

LF: Limiting factor

A: M1 proteins

B: vRNA molecules and M1 proteins

Variations of the MOI also have an influence on limiting factors of virus replication. It can be seen from Table 4.1 that if the values of the MOI are lower than approximately 4 virions/cell, genomic vRNA molecules are limiting at the early stages of the infection, M1 proteins becoming limiting only at the late stages. At the same time, for the values of the MOI higher than 4 virions/cell M1 proteins represent a bottleneck of virus production throughout the whole infection cycle.

4.10.1 Theoretical Confirmation

As follows from the conclusions made in section 4.7 and model equations describing the production of viral components, the main determinant of the dynamics of virus release is the rate of vRNA synthesis. Indeed, the synthesis rates of all viral proteins

are proportional to the number of vmRNA molecules encoding them (see equations (2.5.1) and (2.6.1)); at the same time vRNA molecules are redundant at the stage of the assembly of M1-vRNP complexes and do not significantly influence the processes of the infection cycle. As it can be seen from equation (2.3.1), the rate of vmRNA synthesis μ_{v-vm} (*nucleotides/h*), is proportional to the number of viral polymerase complexes in the nucleus and inversely proportional to the number of NP proteins in the nucleus:

$$(4.10.1) \quad \mu_{v-vm} = k_{v-vm,Pol,max} \frac{P_{Pol,nuc}}{1 + a_{NP} P_{NP,nuc}}.$$

Here, the formula for $k_{v-vm,Pol}$ (as an example, the synthesis of vmRNA molecules encoding polymerase complexes is considered) from equation (2.3.1) right-hand side was taken into account. Assuming that the numbers of produced viral proteins are proportional to each other throughout the whole process of the infection (see section 4.3) and taking into consideration formula (4.10.1), it can be concluded that μ_{v-vm} is an increasing function of the number of viral polymerase complexes and NP proteins. It approaches to its maximum, as the concentrations of viral polymerase complexes and NP proteins become high enough. The value of the maximal rate of vmRNA synthesis is defined by the ratio of the numbers of polymerase complexes and NP proteins produced in the cell, and is independent of the numbers of polymerase complexes and NP proteins internalized with incoming virions.

The ratio of the number of polymerase complexes produced in the cell to the number of NP proteins produced in the cell (approximately 1.3, not shown) is much higher than the ratio of the number of polymerase complexes contained in the virion to the number of NP proteins contained in the virion (approximately 0.05, Table 1.1). Consequently, as follows from formula (4.10.1), the maximal rate of vmRNA synthesis $\mu_{v-vm,prod}$ (*nucleotides/h*) corresponding to the ratio of the numbers of viral components produced in the cell significantly exceeds the maximal rate of vmRNA synthesis $\mu_{v-vm,vir}$ (*nucleotides/h*) corresponding to the ratio of the numbers of viral components delivered with incoming virions. As viral proteins start being intensively produced, the rate of vmRNA synthesis changes from its lower value $\mu_{v-vm,vir}$ towards its higher value $\mu_{v-vm,prod}$. The number of vmRNA molecules produced and, hence,

the number of viral proteins produced and the number of virus particles released depend on how fast the rate of vmRNA synthesis approaches to $\mu_{v-vm,prod}$.

On the one hand, the lower the number of viral components internalized with incoming virions the lower the number of newly synthesized viral proteins (viral polymerase complexes and NP proteins) necessary to compensate the difference between $\mu_{v-vm,vir}$ and $\mu_{v-vm,prod}$. On the other hand, however, the more viral components are delivered into the nucleus, the higher the initial rate of vmRNA production, and, accordingly, the initial rate of viral protein production. The behavior of the virus yield as a function of the MOI depends on the relation between two mentioned above effects.

At the MOI changing in the range from 1 virion/cell to 3 virions/cell the increase of the initial rate of vmRNA synthesis is determinant for the behavior of the number of released virions; the virus yield increases with an increase of the MOI (Fig. 4.11). At higher values of the MOI (from 3 virions/cell to 100 virions/cell) an increase of the value of the MOI is, in contrast, not profitable for vmRNA production; the increase of the number of newly synthesized viral proteins necessary to compensate the difference between $\mu_{v-vm,vir}$ and $\mu_{v-vm,prod}$ is predominant over the increase of the initial rate of vmRNA synthesis (Fig. 4.11). As a result, the virus yield decreases with an increase of the MOI.

As discussed in section 4.11.1.1, limiting factors at a delay in the switch from transcription to genome replication (introduced by an increase of b_{NP}) differ from those at the initial set of model parameters. As NP proteins promote the switch (see sections 1.6.3 and 1.6.4), and a decrease of the MOI invariably leads to a decrease of the concentration of incoming NP proteins, it is the delayed switch at low values of the MOI that is responsible for the effect of MOI variations on limiting factors.

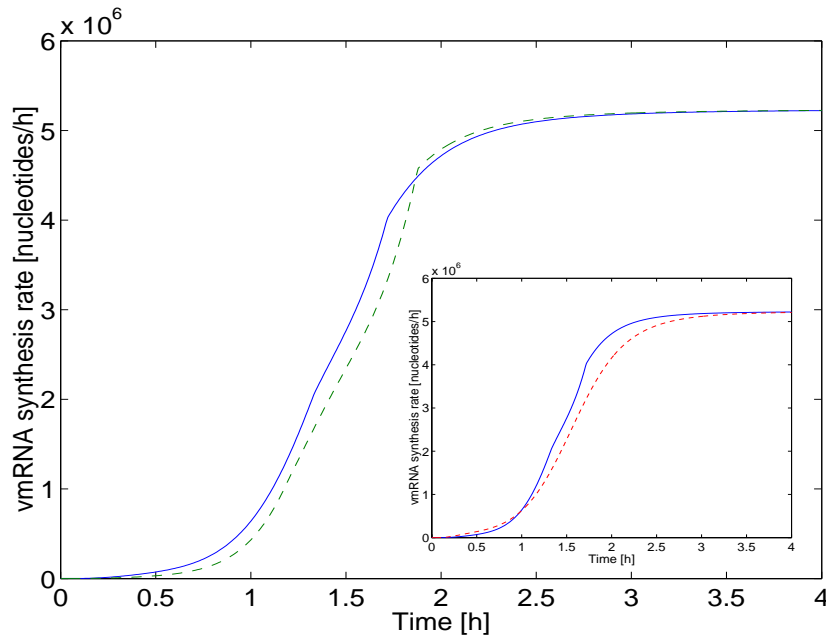


Figure 4.11 The rate of vmRNA synthesis (μ_{v-vm}) for different values of the MOI. At the initial stages of the infection the rate of vmRNA synthesis corresponding to the optimal value of the MOI (MOI=3 virions/cell, —) is higher than vmRNA synthesis rates corresponding to MOI=1 virion/cell (---) and MOI=10 virions/cell (---, see inset). At the late stages of the infection all three curves naturally tend to the same constant, equal to $\mu_{v-vm,prod}$.

4.11 Influence of Parameter Changes on the Virus Yield and Limiting Factors

Both for a better understanding of the dynamics of virus replication and for the identification of possible ways to increase the efficiency of virus replication in a cell it is necessary to explore the influence of parameter changes on the main functions describing the behavior of the considered biological system. Besides that, knowing the set of model parameters, variations of which do not significantly change the behavior of the system, can be helpful for the development of the reduced model, taking into account only the most essential steps of the process (see section 2.9). Particularly important is to reveal the character of changes in the number of produced virions and in the number of viral components limiting virus replication, when the values of model parameters are varied.

All model parameters can be classified into several groups: rate coefficients of internalization (rate coefficients of all processes related to delivery of the viral genome to the nucleus: k_{ex-s} , k_{s-ex} , k_{s-end} , $k_{end-cyt}$, $k_{cyt-nuc}$, k_{spl}), rate coefficients of transport (rate coefficients of all transport processes taking place after viral genome starts being processed: $k_{vm,i,nuc-cyt}$, $k_{i,cyt-nuc}$, $k_{j,ER-bud}$, $k_{un,nuc-bud}$), rate coefficients of macromolecule synthesis (k_{Rib} , k_{Pl} , $k_{v-vm,i}$, k_{v-c} , k_{c-v} , $k_{i,synt}$), rate constants of virus assembly (k_{un} , k_{bud}), rate coefficients of virus release ($k_{bud-rel}$), rate constants of degradation (all rate coefficients supplied with the index “degr”), and switch parameters (a_{NP} , b_{NP}). For the convenience here and further in this section the indexes defining the correspondence of rate coefficients to certain equations are omitted (e.g., for both rate coefficients of virus attachment $k_{ex-s,V_{ex}}$ and k_{ex-s,V_s} the common designation k_{ex-s} is used). Although both the first and the second group of parameters refer to transport processes, it is reasonable to consider rate coefficients of internalization separately. The matter is that the beginning of nuclear phase of virus replication is an essential branch point; it is a starting point of several processes, such as transcription, genome replication, and viral protein production. Additionally, rate coefficients of internalization, unlike other rate coefficients of transport, depend not only on the properties of the cell, but also on the individual features of virus (e.g., binding and fusion activities of HA proteins).

4.11.1 Variations of Switch Parameters

Limiting factors of virus replication, as well as the virus yield, depend on the switch from vmRNA production to genome replication, which is correlated with the nuclear concentration of NP proteins (see section 1.6.4). The extent, in which NP proteins influence the switch, i.e., inhibit vmRNA production and promote vRNA replication, is defined by the ability of NP proteins to bind to elongating vRNA and cRNA strands and to block poly(A) addition (Portela and Digard, 2002), expressed by two model parameters, a_{NP} and b_{NP} (see equations (2.3.1), (2.4.1), and (2.4.2)).

4.11.1.1 Influence on Limiting Factors

Depending on the values of a_{NP} and b_{NP} , two types of system behavior are possible. Previously presented results were obtained for small values of b_{NP} compared to the number of NP protein molecules in the nucleus (about 10^6). It corresponds to a situation when the switch occurs relatively early (vRNA molecules start being intensively produced at about 1.0 h p.i., see section 4.5). As shown in section 4.9, in this case M1 proteins are limiting all the way.

However in the case when the switch takes place at the late stages of the infection, which corresponds to high values of b_{NP} (e.g. $b_{NP} \approx 10^7$), simulation results become qualitatively different from those described above. Until about 2 h p.i. the level of vRNA production is very low, and vRNA molecules limit virus replication at this stage. M1 proteins are, in contrast, produced in redundant amounts and accumulate in the nucleus. At about 2.5 h p.i., when the switch is accomplished, vRNA molecules start being intensively produced, and M1 proteins become limiting (Fig. 4.12).

Variations of the parameter a_{NP} have no influence on limiting factors of virus replication, affecting only the virus yield (see section 4.11.1.2 below).

Limiting factors of virus budding are influenced neither by variations of a_{NP} and b_{NP} , nor by variations of other model parameters. At any set of model parameters M1-vRNP complexes remain limiting throughout the whole infection cycle.

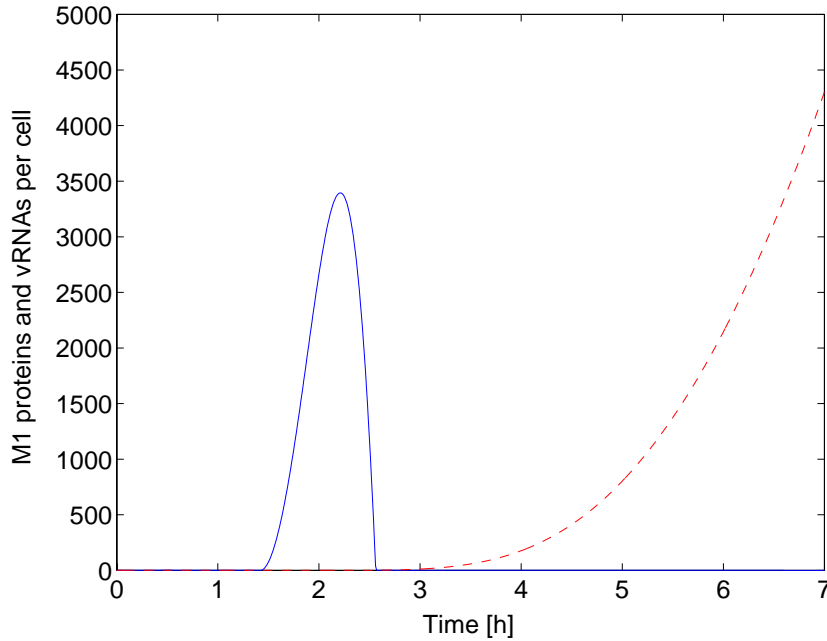


Figure 4.12 Viral components in the nucleus at high values of b_{NP} . M1 proteins (—) limit virus replication after about 2 h p.i. At the early stages of the infection vRNA molecules (---) represent a limiting factor, whereas M1 proteins accumulate.

4.11.1.2 Influence on the Virus Yield

Variations of a_{NP} and b_{NP} also influence the number of released virions. Table 4.2 summarizes the results of simulations for b_{NP} changed by different factors from 0.5 (the earliest switch) to 5.0 (the latest switch). This data shows that if the factor is less than approximately 2.3, the virus yield is slightly sensitive to variations of b_{NP} . Indeed, at the value of b_{NP} changed by a factor of 2.3, the rate coefficient k_{v-c} in (2.4.2) already at the early stages of the infection becomes close to its maximal value. Consequently, any further decrease of b_{NP} cannot significantly change the behavior of the system. In this range M1 proteins are limiting for virus replication throughout the whole period of the infection.

For b_{NP} increased by a factor greater than 2.3, further increase of this parameter results in a decrease of released virus number. b_{NP} increased by a factor of 2.5 and higher corresponds to the situation when vRNA molecules is limiting during the early

stages of the infection. It could be supposed that the delay of the switch, giving M1 proteins the possibility to accumulate in the nucleus, might result in an increase of the virus yield, since the drawback of vRNA molecules can be fast compensated when M1 proteins become limiting. However, as vRNA molecules limit virus production, it is the number of vRNA molecules that defines the number of released virions. And as the delay of the switch leads to a decrease of the number of produced genomic vRNA molecules, the number of released viruses also decreases. Consequently, if the impact of NP proteins on vRNA replication is not strong (which is not the case at the considered set of model parameters, see above), a decrease of b_{NP} can result in an increase of the virus yield.

Table 4.2 Virus yield and limiting factors of virus replication for the switch parameter b_{NP} changed by different factors

Factor	0.5	1.0	2.3	2.5	3.0	4.0	5.0
V_{rel}	8020	8020	8020	8019	8005	7960	7914
LF	A	A	A	B	B	B	B

LF: Limiting factor

A: M1 proteins

B: vRNA molecules and M1 proteins

It can be concluded from Table 4.2 that the impact of variations of b_{NP} on the virus yield is rather small. At the same time, variations of a_{NP} can significantly change the number of virions released. Simulations were performed for a_{NP} changed by the factors 0.1, 0.5 and 2.0. According to simulation data (see Table 4.3), the virus yield increases with a decrease of a_{NP} . Indeed, a decrease of a_{NP} makes the process of vmRNA production faster, and, accordingly, all viral proteins are produced more efficiently. Thus, reducing the inhibitory effect of NP proteins on vmRNA synthesis (i.e., decreasing the value of the parameter a_{NP}) can be considered as an effective way for improving virus production. Furthermore, as shown in section 5.9.1, a decrease of a_{NP} results in an extension of the exponential stage of progeny virus growth, and at low values of a_{NP} the law of virus growth is close to exponential.

Table 4.3 Virus yield for the switch parameter a_{NP} changed by different factors

Factor	0.1	0.5	1.0	2.0
V_{rel}	82980	16510	8020	3810

4.11.1.3 Switch Parameters and vmRNA Dynamics

It could be supposed that by decreasing a_{NP} it is possible to make the rate of vmRNA synthesis μ_{v-vm} being proportional to the first power of time instead of remaining constant, increasing thus the order of the polynomial law of virus release. Indeed, a decrease of a_{NP} makes the rate coefficient of vmRNA synthesis $k_{v-vm,i}$ (see equation (2.3.1)) less sensitive to an increase of the nuclear concentration of NP proteins; higher values for the number of NP proteins are required to essentially increase the denominator in the expression for $k_{v-vm,i}$. However, as discussed above, any decrease of the parameter a_{NP} invariably results in an increase of NP protein concentration. For example, tenfold decrease of a_{NP} value leads to the change of the number of NP proteins (at 12 h p.i.) from approximately $5.5 \cdot 10^5$ to $5.5 \cdot 10^6$, i.e., also by a factor of approximately 10.0. Consequently, the product of the parameter a_{NP} and nuclear concentration of NP proteins does not change.

The time point when the number of vmRNA starts to increase linearly also does not change as a_{NP} is varied. However, the term $k_{v-vm,i,max} \frac{1}{1 + a_{NP} P_{NP,nuc}} P_{Pol,nuc}$ in (2.3.1) is still sensitive to a_{NP} changes. A decrease of a_{NP} makes its increase in time sharper and the value it tends to higher (otherwise, it would not result in an increase of vmRNA and viral protein production).

Thus, variations of the parameter a_{NP} do not provide an option to make vmRNA number increasing faster, than proportional to the first power of time. Accordingly, the maximal order for the polynomial law of viral protein growth, as well as for the polynomial law of virus release, is second.

4.11.2 Variations of Internalization Dynamics

Virus internalization has an essential influence on the number of progeny virus, limiting factors, and the behavior of some viral components. This section shows possible changes in virus replication dynamics caused by variations of internalization rate coefficients, which are mainly defined by binding and fusion activities of viral HA proteins.

As variations of individual rate coefficients of internalization, except the rate constant of dissociation (k_{s-ex}) result in similar effects, it makes sense to increase all these rate coefficients simultaneously by the same factor in each trial. Simulations were performed for internalization rate coefficients changed by factors from 0.5 to 2.0. The number of virions produced in 12 h p.i. for different values of the rate coefficients of internalization is presented in Table 4.4.

Table 4.4 Virus yield and limiting factors of virus replication for the internalization rate coefficients changed by different factors

Factor	0.5	0.6	0.7	1.2	1.3	1.4	2.0
V_{rel}	8009	8069	8069	7999	7995	7997	8071
LF	B	B	A	A	A	A	A
Phase	1	1	2	2	2	3	3

LF: Limiting factor

A: M1 proteins

B: vRNA molecules and M1 proteins

1: Initial increase

2: Decrease

3: Late increase

Simulations show that at the increase of the rate coefficients from 50% of their initial values the number of produced virions first increases, and at about 60-70% of the initial values of the rate coefficients of internalization there is a local maximum. Further increase of the rate coefficients of internalization results in a decrease of the virus yield. The local minimum takes place at the values of internalisation rate coefficients equal to approximately 130% of their initial values. Finally, the increase

of the rate coefficients of internalization from 130% to 200% of their initial values result again in the increase of released virus number. Thus, the behavior of the number of produced virions as a function of the internalization rate coefficients can be subdivided into three phases, the origin of which will be explained below. These phases are initial increase, decrease, and late increase.

Variations of the rate coefficients of internalization also affect limiting factors of virus replication (Table 4.4). If the values of the rate coefficients are greater than approximately 60% of their initial values (which corresponds to the phases of decrease and late increase), M1 proteins are limiting throughout the whole infection cycle (Fig. 4.8). In the opposite case (the phase of initial increase), the bottleneck at the early stages of the infection is represented by vRNA strands, M1 being limiting at the late stages (similar to the case of the delayed switch discussed in section 4.11.1.1, Fig. 4.12).

Initial increase. If the values of the rate coefficients of internalization are low, their increase naturally leads to an increase of the number of released virions. Indeed, to start virus production, the delivery of viral components is required. Additionally, in this situation vRNA molecules are limiting at the early stages of the infection. Since the rate of vRNA production is proportional to the number of NP proteins (see equation (2.4.2)), an increase of NP protein concentration (resulting from an increase of the rate coefficients of internalization) directly leads to an increase of the number of M1-vRNP complexes, and, consequently, to an increase of the number of virions produced.

Decrease and late increase. For the internalization rate coefficients increased by factors from 0.7 to 2.0 M1 proteins represent a limiting factor of virus growth throughout the whole infection cycle. The number of produced virus particles is, hence, no longer directly dependent on vRNA production. It is the number of vmRNA molecules that mainly affects the number of M1 proteins produced.

Incoming virus particles deliver NP proteins and viral polymerase complexes into the nucleus of the cell, the former inhibiting vmRNA synthesis and the latter promoting it. As pointed out in section 4.10.1, the increase of the number of internalized viral

components affects the production of vmRNA molecules depending on the relation between two effects accompanying it: the increase of the number of newly synthesized viral proteins required to compensate the difference between the lower and the higher values of vmRNA synthesis rate ($\mu_{v-vm, vir}$ and $\mu_{v-vm, prod}$, introduced in section 4.10.1) and the increase of the initial rate of vmRNA production.

Thus, in the range of the rate coefficients of internalization from 70% to 130% (corresponding to the *decrease* phase) of their initial values any increase of the internalization rate coefficients does not increase vmRNA production (Fig. 4.13). Newly synthesized viral proteins are transported into the nucleus much earlier than the whole amount of incoming viral components is internalized, and the increased number of newly synthesized viral proteins necessary to compensate the difference between $\mu_{v-vm, vir}$ and $\mu_{v-vm, prod}$ is predominant over the increased initial rate of vmRNA synthesis. As a result, the virus yield decreases with an increase of the rate coefficients of internalization.

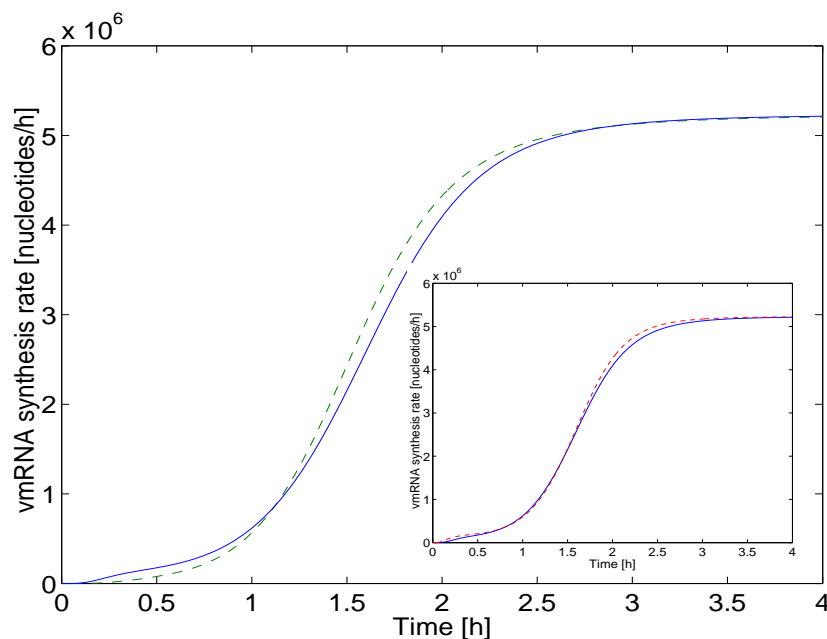


Figure 4.13 The rate of vmRNA synthesis for different values of internalization rate coefficients. Rate coefficients of internalization increased by a factor 1.3 (—) correspond to the minimal rate of vmRNA synthesis. E.g., their variations by factors of 0.7 (---) and 2.0 (---, see inset) result in higher values of vmRNA synthesis rate at the early stages of the infection.

At the rate coefficients of internalization in the interval from 130% to 200% of their initial values (*late increase* phase) an increase of the rate coefficients of internalization causes only an increase of the initial rate of vmRNA synthesis (Fig. 4.13). The number of viral proteins required for the compensations of the difference between $\mu_{v-vm,vir}$ and $\mu_{v-vm,prod}$ remains practically unchanged. Indeed, internalization of incoming viral components is accomplished earlier than the significant amount of newly synthesized viral proteins enters the nucleus and starts changing the rate of vmRNA synthesis towards $\mu_{v-vm,prod}$. Consequently, an increase of the internalization rate coefficients results in an increase of the number of released virions.

4.11.2.1 Variations of Rate Constants of Dissociation

According to simulation results, the behavior of the system, particularly the virus yield is not significantly sensitive to variations of the rate constants of virus dissociation from the cellular surface (k_{s-ex}), correlated with the affinity of viral HA proteins to cellular surface receptors. Even an increase or a decrease of the considered rate constants by a factor of 10.0 does not result in noticeable changes in the number of produced virions (not shown). This observation provides the possibility not to consider virus dissociation in the reduced model (see section 2.9).

4.11.3 Variations of Rate Coefficients of Transport

The model takes into account different cellular compartments involved in the virus replication cycle, such as cytoplasm, nucleus, ER, and budding site. The transfer of viral components from one compartment to another is carried out with a certain finite rate. Side by side with rate coefficients of virus internalization, rate coefficients of transport events, defined by the functional properties of corresponding signal sequences (i.e., NLSs and NESs), also represent an important determinant of virus dynamics.

Simulations allow exploring, what will happen with system behavior (particularly with the number of produced virus particles) if the transport of viral components between cellular compartments is speeded up or slowed down. In each trial all the rate coefficients of transport were increased simultaneously by the same factor. Table 4.5 summarizes the results of simulations for the number of virus particles released after 12 h p.i. Relying on this data it can be concluded that variations of the rate coefficients of transport do not result in any unusual effects; an increase of the transport rate coefficients naturally leads to an increase of the number of produced virions. As this increase of the virus yield is rather appreciable, the increasing of the efficiency of viral component transport might be one of possible ways of virus production optimization. The situation remains the same if the simulations are performed at increased or decreased values of internalisation rate coefficients (not shown). Indeed, the faster the transport of viral components, the faster the beginning of vmRNA processing and the assembly of M1-vRNP complexes. The switch from vmRNA production to genome replication does not depend on the rate coefficients of transport; consequently, any negative effects of the increase of the transport rate coefficients on the virus yield are excluded.

Table 4.5 Virus yield for the transport rate coefficients changed by different factors

Factor	0.5	0.6	0.7	1.0	1.5	2.0
V_{rel}	3170	4270	5340	8020	11070	13010

4.11.3.1 Minimal Value of the Delay of Virus Release

The model also allows estimating the minimal time post-infection when virions can start being produced. According to simulation results, when all the rate coefficients of transport are increased by a factor of 2.0, virus release starts at approximately 3 h p.i. (at the initial values of the rate coefficients of transport it starts at about 4 h p.i.). It can be also seen that at further increase of the transport rate coefficients the time point of the beginning of virus release tends to approximately 1.7 h p.i., which represents the value for the minimal possible time interval between the beginning of the infection and the beginning of virus release. This value is much less than the average

lifetime of the cell ($T=12h$). Therefore it can be concluded that the infected cell produces virions during the major part of its life.

4.11.4 Combined Variations of Rate Coefficients of Internalization and Transport

As pointed out in section 4.11.2, the number of released virions, as a function of the rate coefficients of internalization, has two local extremes. Existence and location of these extremes, however, depend on the other model parameters, particularly on the rate coefficients of transport. To explore this dependency, simulations were performed for the same values of the internalization rate coefficients as in the section 4.11.2 and for the values of the transport rate coefficients changed by factors of 2.0 and 0.5. The results are summarized in Tables 4.6 and 4.7 respectively.

Table 4.6 Virus yield and limiting factors of virus replication for the internalization rate coefficients changed by different factors (the transport rate coefficients are multiplied by 2.0)

Factor	0.5	0.7	0.8	0.9	1.5	2.0	2.5
V_{rel}	12910	13060	13060	13040	12890	12860	12890
LF	B	B	A	A	A	A	A

LF: Limiting factor

A: M1 proteins

B: vRNA molecules and M1 proteins

Table 4.7 Virus yield and limiting factors of virus replication for the internalization rate coefficients changed by different factors (the transport rate coefficients are multiplied by 0.5)

Factor	0.3	0.4	0.5	0.6	1.0	1.5	2.0
V_{rel}	2930	3080	3150	3160	3170	3240	3350
LF	B	B	B	A	A	A	A

LF: Limiting factor

A: M1 proteins

B: vRNA molecules and M1 proteins

Comparing the data from Tables 4.4 and 4.6, it can be concluded that in both cases the abscissa of the maximum corresponds to the point where the distribution of limiting

factors change; on the left from the point of the maximum first vRNA molecules and then M1 proteins are limiting, and on the right from it M1 proteins are limiting throughout the whole infection cycle (this phenomenon is explained in section 4.11.2). It is also seen that at the values of the rate coefficients of transport increased by a factor of 2.0 the decrease comes later and lasts longer, than at their initial values (see below for the explanation).

Table 4.7 shows that a twofold decrease of the rate coefficients of transport leads to a situation when two discussed above extremes no longer appear, and the virus yield represents a monotonously increasing function of the rate coefficients of internalization. With slowing down transport processes, the interval of the decrease of the virus yield diminishes and finally disappears. The observed effect can be explained by the following way. As the nuclear export of newly produced vmRNA molecules and nuclear import of newly produced viral proteins are essentially slowed down, even at low values of the internalization rate coefficients the process of internalization accomplishes earlier than newly synthesized viral proteins are transported in significant amounts into the nucleus, resulting in the increase of the rate of vmRNA synthesis (the situation described in section 4.11.2 for the late increase phase). Additionally, at low values of the rate coefficients of transport there is more time for polymerase complexes internalized with incoming virus particles to produce vmRNA molecules (and, hence, to increase the efficiency of viral protein synthesis), which make the positive effect of faster internalization even more appreciable. As a result, at all considered values of the rate coefficients of internalization the phase of the initial increase is directly followed by the phase of the late increase, the phase of the decrease being bypassed. Since the increase of the rate coefficients of internalization is profitable for vmRNA production, it results in the increase of the number of viral proteins produced (particularly in the increase of the number of limiting for virus replication M1 proteins) and, finally, in the increase of the number of virions released.

For the existence of the decrease of the number of produced virus particles as a function of the rate coefficients of internalization the following criterion can be formulated. The decrease takes place if and only if viral polymerase complexes internalized with incoming virions synthesize the number of vmRNA molecules

sufficient to initiate the synthesis of the number of viral proteins suppressing the increase of the number of viral proteins required for the compensation of the difference between $\mu_{v-vm,vir}$ and $\mu_{v-vm,prod}$. Thus, at low values of the rate coefficients of transport (particularly, if newly produced viral proteins are delivered to the nucleus later than the whole amount of incoming viral components is internalized) there is no decrease phase, and with an increase of the rate coefficients of internalization the virus yield monotonously increases.

4.11.5 Variations of Macromolecule Synthesis Rates

According to the results of simulations, the number of produced virions is mainly influenced by variations of two model parameters: viral polymerase speed, and the translation efficiency of viral proteins. The former parameter expresses the ability of the PB1 subunit of the polymerase complex to catalyze the nucleotide addition to growing viral RNA strands (Flint et al., 2000), whereas the later is mainly defined by the effectiveness of the processing of mRNA molecules (Knipe et al., 2001). Speeding up viral polymerase complexes leads to an accelerated transcription of all types of vRNA molecules, whereas an increased synthesis rate of ribosomes results in the increased production rates of all viral proteins, including M1 proteins, which limit virus replication, and polymerase complexes required for transcription.

The polymerase speed k_{pl} was successively increased by factors of 0.5, 1.5, and 2.0. The results of simulations are summarized in Table 4.8. It is seen that the increase of k_{pl} by a factor of 2.0 causes a more than twofold increase of the number of released virions (Fig. 4.14). Similar results can be obtained by an increase of the translation efficiency of viral proteins (the parameter k_{Rib}).

Thus, one of the most effective ways for obtaining more progeny virus particles are speeding up viral polymerase complexes or increasing of the translation efficiency of viral proteins. Additionally, it can be concluded that one possible reason why viruses

have different replication rates is the difference in their polymerase speed and in their ability to produce proteins.

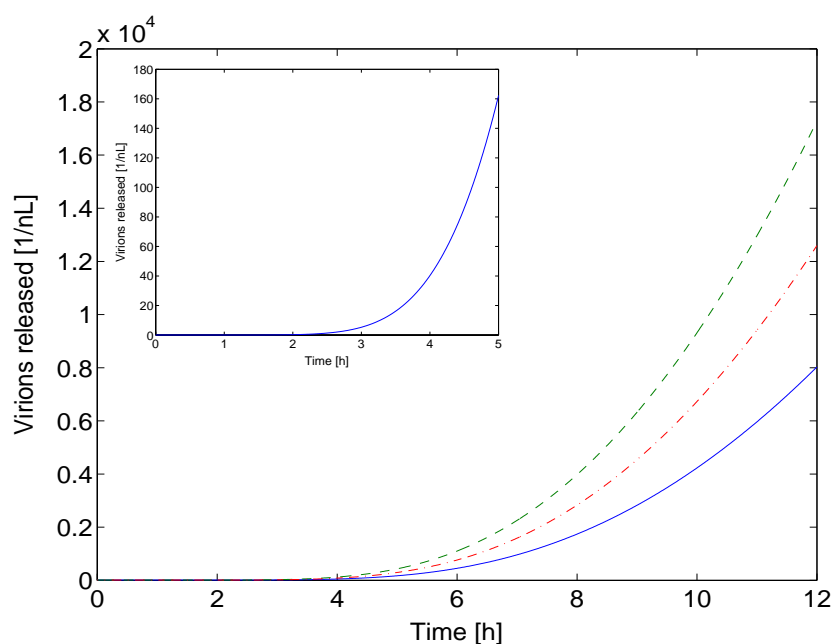


Figure 4.14. The number of released virions for different values of viral polymerase speed. The number of progeny virions, after the initial exponential stage (0.0 – 4.0 h p.i., see inset) and the transitional stage (4.0 – 7.0 h p.i.) increases proportional to the second power of time. Presented plots correspond to a polymerase speed k_{PI} increased by factors of 1.0 (—), 1.5 (---) and 2.0 (---).

Table 4.8 Virus yield for polymerase speed (k_{PI}) changed by different factors

Factor	0.5	1.0	1.5	2.0
V_{rel}	3660	8020	12590	17270

4.11.6 Variations of Rate Constants of Virus Assembly

To investigate the sensitivity of the virus yield to variations of the rate constants of the assembly of M1-vRNP complexes (k_{um}), simulations were performed for the values of these rate constants increased by factors of 0.5 and 2.0. It can be concluded that the number of produced virions is not significantly affected by changes of the rate constants of the assembly of M1-vRNP complexes. Indeed, the production of new M1-vRNP complexes, and, hence, virus release are limited by the production of M1

proteins. Consequently, the rate of virus release cannot be increased by the increase of the rate constants of the assembly of M1-vRNP complexes. The considered rate constants define only the initial increase of the number of M1 proteins preceding the formation of M1-vRNP complexes.

Simulations also show that variations of the rate constants of progeny virus assembly (k_{bud}) slightly influence the number of produced virions, changing only the initial increase of the number of M1-vRNP complexes. In fact, virus production is limited by the rate of the formation of M1-vRNP complexes, and, accordingly, speeding up virus assembly cannot result in an increase of the number of released virus particles.

The negligible sensitivity of the virus yield on the rate constants of viral component assembly makes possible to lump together or even omit the last steps of the process in the reduced model (see section 2.9).

4.11.7 Variations of Rate Coefficients of Virus Release

It is natural to suppose that the number of released virions is sensitive to variations of the rate coefficients of virus release, defined by the cleavage activity of viral NA proteins. Simulations were performed for the rate coefficients of virus release ($k_{bud-rel}$) increased by factors from 0.5 to 2.0. The results are summarized in Table 4.9. The number of released virions naturally increases with an increase of $k_{bud-rel}$. However, if the values of the rate constants of release are high enough, the influence of their further increase becomes less significant.

Table 4.9 Virus yield for the rate coefficients of release ($k_{bud-rel}$) changed by different factors

Factor	0.5	1.0	1.5	2.0
V_{rel}	6420	8020	8690	9050

4.11.8 Variations of Rate Constants of Degradation

The rate constants of viral component degradation express the activity of cellular decomposing enzymes, such as nucleases and proteases. Their variations to a different degree influence the virus yield and limiting factors. As the values of the degradation rate constants used for modeling are not precisely defined, the ranges for their variations were chosen to be quite wide in comparison with those for other model parameters.

4.11.8.1 Degradation of Incoming Virus Particles

As discussed in section 1.6.2, a certain number of virus particles delivered to the endosomes (“inactive” virions) are transported to the lysosomes for degradation. The ratio of “active” and “inactive” virions can be changed by several mechanisms, such as the specific inhibition of M2 ion channel activity by the anti-influenza virus drug *amantadine* (Flint et al., 2000). In the presence of amantadine the interaction of M1 proteins with vRNP complexes is not disrupted, and, accordingly, vRNP complexes cannot be released from the endosomal membrane.

It could be supposed that the virus yield might monotonously decrease with an increase of the rate constant of endosomal virus degradation ($k_{end-deg}$). However, simulations show that this is not the case. Simulations were performed for the value of the rate constant involved changed by different factors. The results are summarized in Table 4.10. It can be seen, that a moderate increase of the rate constant of endosomal virus degradation results in an increase of the number of released virions. Only when the rate constant of endosomal virus degradation becomes approximately 100.0 times higher than its initial value the virus yield becomes less than it is at the initial value of the degradation rate constant.

In section 4.10.1 slowing down of virus production with an increase of the MOI was explained by the difference in the rates of vmRNA production corresponding to the ratios of the number of viral polymerase complexes to the number of NP proteins in

the virion and in the cell after the beginning of intensive viral protein production. Provided that the MOI is high, an increased initial rate of vmRNA synthesis, caused by the increased number of internalized viral components, is suppressed by the increased number of viral proteins to be synthesized for the compensation the difference between $\mu_{v-vm,vir}$ and $\mu_{v-vm,prod}$, whereas at low values of the MOI the former effect is, in contrast, prevalent over the latter. The observed behavior of the virus yield with respect to variations of the rate constant of endosomal virus degradation can be explained in the similar way. A moderate increase of the rate constant of endosomal virus degradation, resulting in a decrease of the number of incoming viral proteins, speeds up vmRNA production, which results in an increase of the number of viral proteins produced. At the same time, at a significant increase of the considered rate constant a resulting strong decrease of the number of internalized viral components is, in contrast, not profitable for vmRNA production and, hence, for the virus yield.

Table 4.10 Virus yield for the rate constant of “inactive” virus degradation ($k_{end-degr}$) changed by different factors

Factor	0.1	0.5	1.0	4.0	5.0	10.0	100.0
V_{rel}	7840	7930	8020	8280	8320	8360	7930
LF	A	A	A	A	B	B	B

LF: Limiting factor

A: M1 proteins

B: vRNA molecules and M1 proteins

4.11.8.2 vmRNA Degradation

An increase of vmRNA degradation rates naturally results in a decrease of virus production. The data from simulations performed for the rate constants of nuclear ($k_{nuc-degr}$) and cytoplasmic ($k_{cyt-degr}$) vmRNA degradation changed by different factors is summarized in Tables 4.11 and 4.12, respectively. From this data it can be seen that variations of the rate constants of nuclear vmRNA degradation have a stronger impact on virus production than variations of the rate constants of cytoplasmic vmRNA

degradation. Indeed, the decrease of the number of cytoplasmic vmRNA molecules can be compensated by the delivery of new vmRNA molecules from the nucleus.

Table 4.11 Virus yield for the rate coefficients of nuclear vmRNA degradation ($k_{vm,i,nuc-degr}$) changed by different factors

Factor	0.1	0.5	1.0	5.0	10.0	100.0
V_{rel}	8580	8320	8020	6180	4780	830

Table 4.12 Virus yield for the rate coefficients of cytoplasmic vmRNA degradation ($k_{vm,i,cyt-degr}$) changed by different factors

Factor	0.1	0.5	1.0	5.0	10.0	100.0
V_{rel}	8200	8120	8020	7280	6500	1930

However, variations of the rate constants of cytoplasmic vmRNA degradation can alter virus dynamics. The increase of these rate constants by a factor of 100.0 results in the situation when the linear phase of virus growth is within the average life span of the cell (Fig. 4.15). Indeed, in the considered situation the number of vmRNA molecules approaches a steady state earlier than at 12 h p.i. As this happens, the number of newly synthesized viral proteins and, accordingly, the number of progeny virions increase linearly in time.

Simulations did not reveal any influence of vmRNA degradation on limiting factors of virus replication.

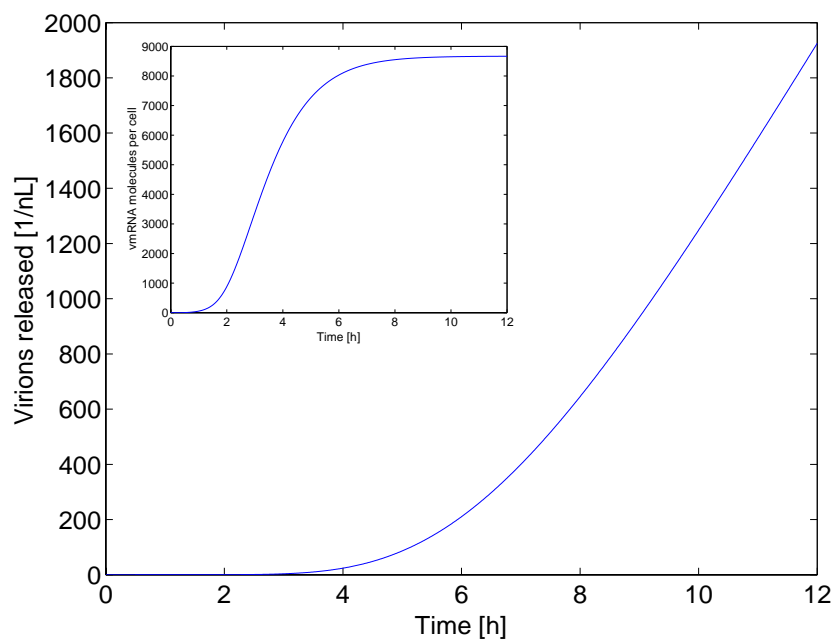


Figure 4.15 Virus production at high values of the rate coefficients of cytoplasmic vmRNA degradation ($k_{vm,l,cyt-degr}$). The picture demonstrates all three phases of virus growth, including the linear phase, which is within the lifetime of the cell. The linear phase starts at about 9 h p.i., when the number of cytoplasmic vmRNA molecules approaches a steady state (see inset).

4.11.8.3 vRNA and cRNA Degradation

Variations of the rate constants of degradation for full-length vRNA and cRNA molecules have no significant effect on the virus yield and do not change limiting factors of virus replication. Actually, even in the case when vRNA degradation is increased by a factor of 100.0, vRNA molecules remain redundant both for the production of progeny virions and for the synthesis of vmRNA molecules by viral polymerase complexes.

4.11.8.4 Viral Protein Degradation

The model shows that the number of released virions as a function of the rate constants of nuclear protein degradation has an extreme. Simulations were performed for the rate constants of nuclear protein degradation (polymerase, NP, M1, NS1, NS2)

changed by different factors. It is assumed that the rate constant of degradation is the same for all viral proteins, and, accordingly, in each trial this rate constant is changed by the same factor. The results are summarized in Table 4.13.

Table 4.13 Virus yield for the rate coefficients of nuclear protein degradation ($k_{i,nuc-degr}$) changed by different factors

Factor	0.1	0.5	0.7	1.0	1.3	1.5	10.0
V_{rel}	7590	7930	7990	8020	8020	8010	5580
LF	A	A	A	A	B	B	B

LF: Limiting factor

A: M1 proteins

B: vRNA molecules and M1 proteins

It could be supposed that slowing down of protein degradation leads to an increase of the virus yield. However, making the values of the rate constants of nuclear protein degradation lower than their initial values results in a decrease of the number of produced virions. Indeed, as discussed in section 5.7, the number of internalized polymerase complexes and, consequently, the rate of their degradation, are much lower than those of NP proteins. Additionally, as shown in section 4.10.1, the lower the number of the internalized viral components kept in the nucleus, the less newly synthesized viral components is required to bring the rate of vmRNA production to its maximal value. Thus, a decrease of the rate constants of protein degradation, resulting to the increase of the number of internalized viral proteins kept in the nucleus and increasing the ratio of the number of internalized polymerase complexes to the number of internalized NP proteins, leads to a decrease of the rate of vmRNA production (Fig. 4.16). A decrease of vmRNA synthesis rate, in turn, results in a decrease of the rate of viral protein production. Limiting factors of virus replication do not seem to be sensitive to a decrease of the rate constants of nuclear protein degradation; M1 proteins remain limiting throughout the whole replication cycle.

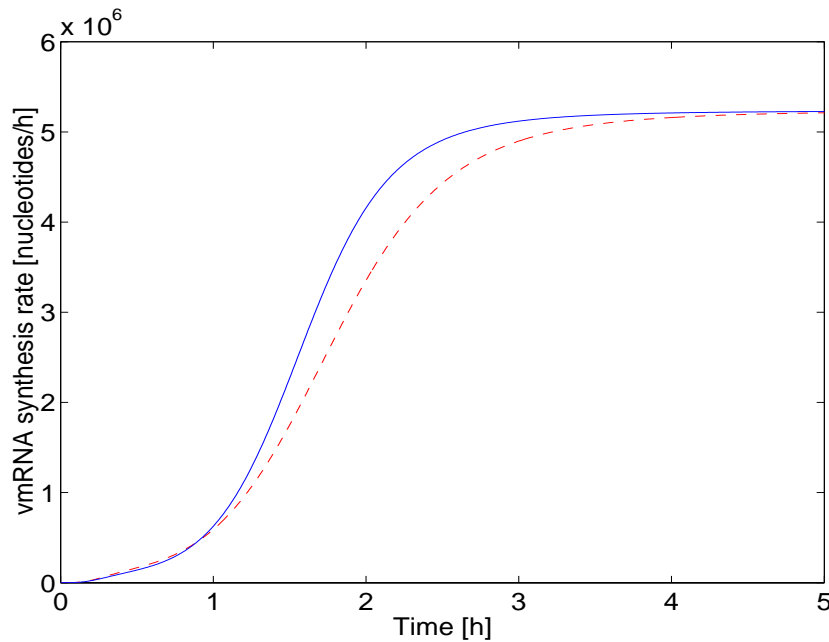


Figure 4.16 The rate of vmRNA synthesis for different values of rate coefficients of nuclear protein degradation. Presented plots correspond to rate coefficients of nuclear protein degradation ($k_{nuc-degr}$) changed by factors of 1.0 (—) and 0.1 (---).

Simulations show that a significant increase of the rate constants of nuclear protein degradation also leads to a decrease of the number of produced virus particles. Indeed, if the rate constants of degradation are high, an essential part of internalized and produced proteins is degraded, and further increase of the degradation rate constants naturally cannot result in an increase of the virus yield. In the considered situation the increase of the ratio of the number of polymerase complexes to the number of NP proteins in the nucleus by newly produced viral proteins is not essential for virus dynamics; the need for internalized viral components is prevalent over it. Due to a low number of NP proteins in the nucleus, at high values of the rate constants of nuclear protein degradation vRNA molecules are limiting at the early stages of the infection (as discussed in sections 1.6.4 and 2.4, NP proteins promote vRNA production).

Thus, it can be concluded that there are optimal (in respect to the virus yield) values for the rate constants of viral protein degradation. The maximal value of the virus yield is achieved at the values of the rate constants of degradation equal to those used for simulations (changed by a factor of 1.0).

The number of degraded cytoplasmic proteins, unlike that of nuclear proteins, cannot be compensated by the transport of proteins from other cellular compartments. For this reason, variations of the rate constants of degradation of cytoplasmic proteins have more significant effect on the virus yield than variations of the rate constants of nuclear proteins degradations. On the other hand, limiting factors of virus replication do not change at speeding up or slowing down the cytoplasmic protein degradation. The simulation data concerning the influence of variations of the rate constants of cytoplasmic protein degradation on the virus yield is summarized in Table 4.14. As it could be expected, the number of released virions represents a monotonously decreasing function of the rate constants involved.

Table 4.14 Virus yield for the rate coefficients of cytoplasmic protein degradation ($k_{i,cyt-degr}$) changed by different factors

Factor	0.1	0.5	1.0	5.0	10.0
V_{rel}	8080	8050	8020	7780	7490

Variations of the rate constants of degradation for the proteins bound to the budding site and to the membrane of the ER have an infinitesimal influence on the number of produced virions. Even in the case when the values of these rate constants are 100.0 times higher than their initial values, the virus yield practically does not change with respect to that at the initial values of the rate constants of degradation. The number of envelope proteins produced is so high in comparison with their number required for virus production that at significantly increased rate constants of degradation it still remains redundant, and the number of released virions is defined by the number of newly synthesized M1-vRNP complexes.

4.12 Model Reduction

As expected, the dynamics of viral component production provided by the reduced model is similar to that provided by the detailed model. For the reduced model it is possible to find a set of parameters, at which the functions representing the number of assembled virions and the number of viral proteins, as well as limiting factors of virus replication, behave similar to the corresponding functions in the detailed model.

However, the reduced model, which does not take into account several process steps, has some peculiarities. For example, the time course of viral component production slightly differs from that in the detailed model. In the following, the dynamics of viral components, as well as specific features of the reduced model will be discussed.

4.12.1 Dynamics of Viral Component Production

The number of extranuclear virions in the reduced model, similar to the number of extracellular virions in the detailed model decreases exponentially in time (Fig. 4.17). However, since extranuclear virions, unlike extracellular virions are delivered directly into the nucleus, the time course of internalization is different in the two models considered. The total number of vmRNA molecules (Fig. 4.18), the number of vRNA and cRNA molecules (Fig. 4.19), and the number of viral proteins in the nucleus (Fig. 4.21) increase in the same way in the reduced model and in the detailed model. The finite rate of vmRNA nuclear export, as it does in the detailed model, defines the difference between the time courses of vmRNA and viral protein production.

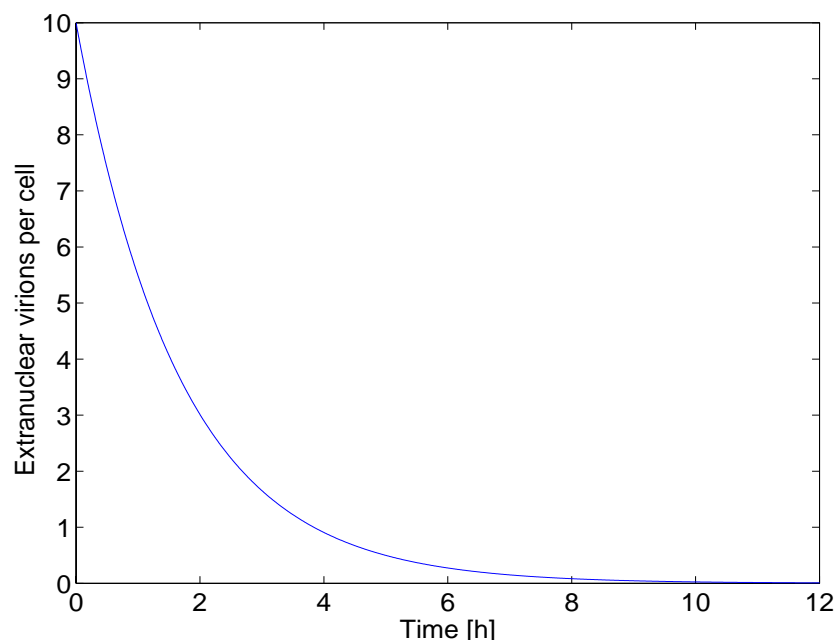


Figure 4.17 Virus internalization. Like the number of extracellular virions from the detailed model, the number of extranuclear virions from the reduced model exponentially decreases in time.

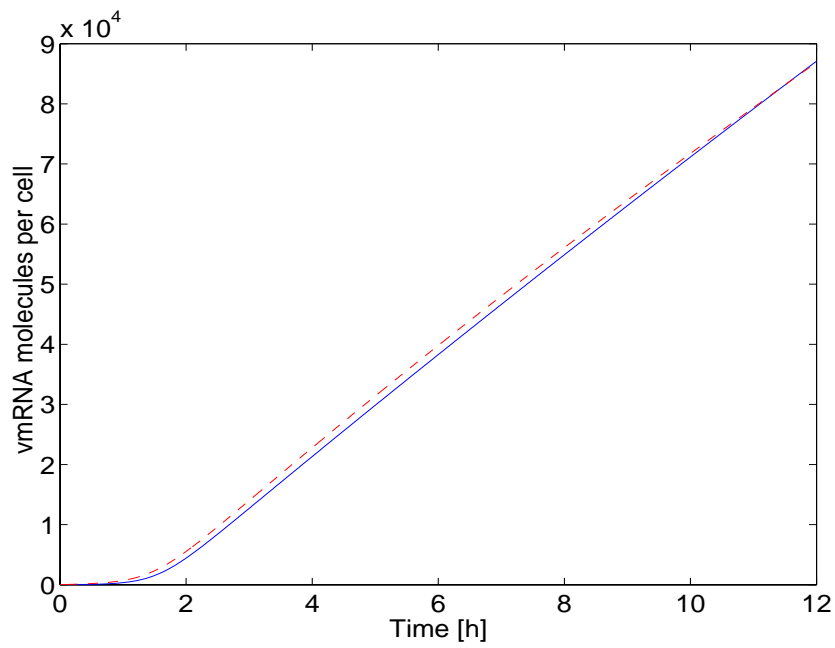


Figure 4.18 The total number of vmRNA molecules (in the nucleus and in the cytoplasm) from the detailed model (—) and the reduced model (- - -).

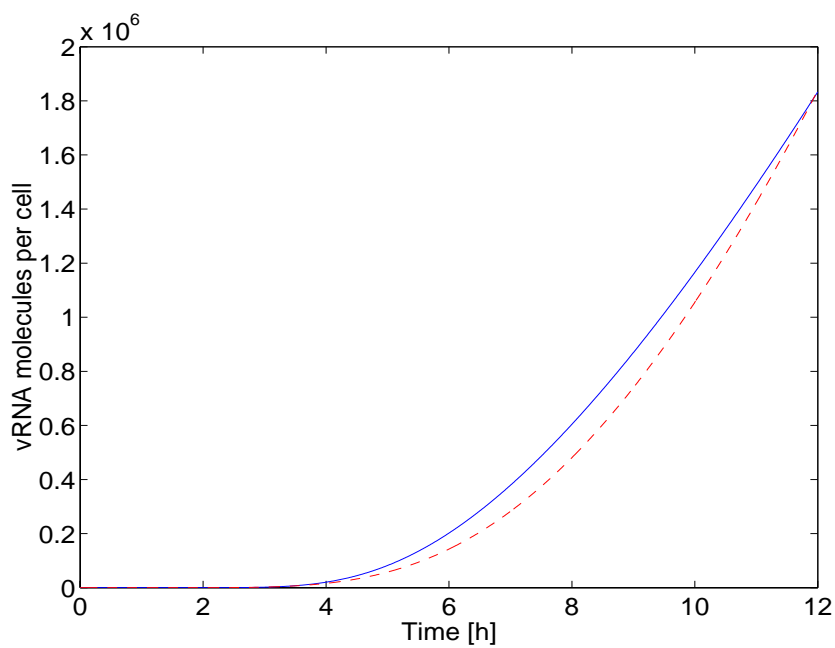


Figure 4.19 The number of vRNA molecules in the nucleus from the detailed model (—) and the reduced model (- - -).

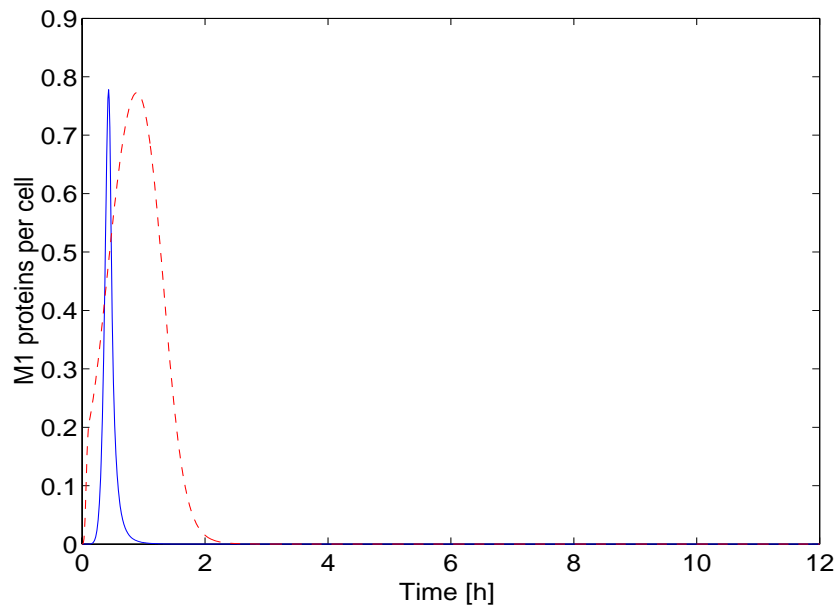


Figure 4.20 The number of M1 proteins in the nucleus from the detailed model (—) and the reduced model (---).

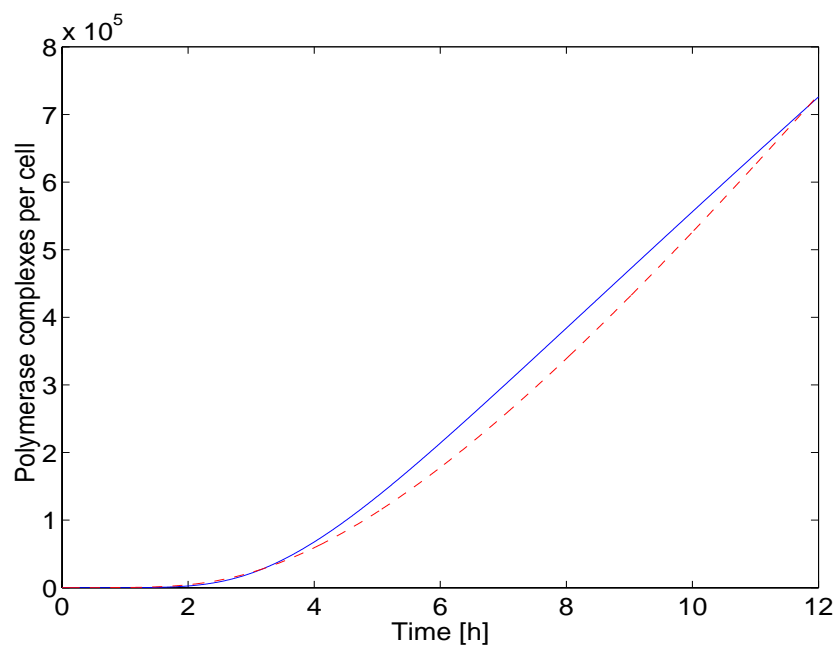


Figure 4.21 The number of polymerase complexes in the nucleus from the detailed model (—) and the reduced model (---).

The number of assembled virions in the reduced model behaves similar to the number of released virions in the detailed model (Fig. 4.22). As in the reduced model newly produced viral proteins are immediately packaged to progeny virions, there is no lag between the beginning of viral protein production and the beginning of virus

assembly. Accordingly, the time course of virus assembly in the reduced model slightly differs from the time course of virus release in the detailed model.

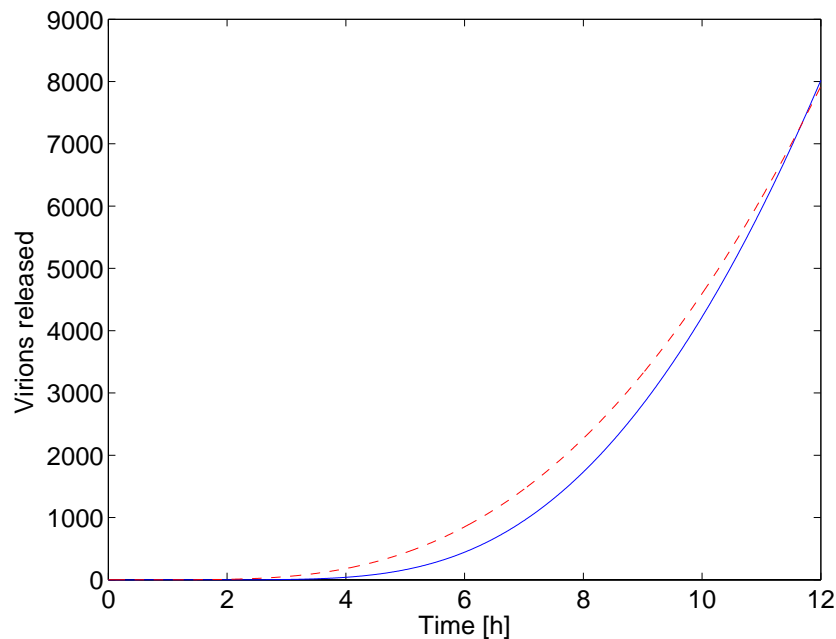


Figure 4.22 The number of released virions from the detailed model (—) and the number of assembled virions from the reduced model (---).

4.12.2 Limiting Factors

Like the detailed model, the reduced model reveals factors limiting virus replication. As viral proteins are packaged to form M1-vRNP complexes, M1 proteins are completely consumed (Fig. 4.20), whereas redundant amounts of polymerase complexes and NP proteins accumulate in the cell (Fig. 4.21).

The increase of the switch parameter b_{NP} from 10^6 (its initial value) to 10^7 (the delay of the switch) in the reduced model, as well as that in the detailed model, results in the situation when M1 proteins become a bottleneck of virus production only at the late stages of the infection, whereas vRNA molecules are limiting at the early stages of the infection.

4.12.3 Variations of Model Parameters and Initial Conditions

As shown in section 4.11.2, the dependency of the number of released virions on the rate coefficients of internalization in the detailed model can be subdivided into three phases (initial increase, decrease, and late increase). Table 4.15 indicates that for the reduced model the situation is not the same. For the rate coefficient of internalization (k_{spl}) changed by factors from 0.5 to 1.5 the number of assembled virions ($V_{rel,red}$) is a decreasing function of k_{spl} , and for higher values of k_{spl} it increases with an increase of k_{spl} . However, the phase of the initial increase is not achievable at moderate variations of k_{spl} . As pointed out in section 4.11.4, an increase of the values of transport rate coefficients in the detailed model results in the expansion of the interval of the decrease. And since in the reduced model all the rate coefficients of transport (except the rate coefficient of vmRNA nuclear export) are omitted or, in other words, assumed to be infinite, it is not surprising that the phase of the decrease is wider than it is in the detailed model.

Table 4.15 The number of assembled virions for the rate coefficients of vRNP splitting (k_{spl}) changed by different factors in the reduced model

Factor	0.5	0.7	1.0	1.5	2.0
V_{rel}	8170	8030	7920	7880	7900

Like in the detailed model, variations of the rate coefficient of transport ($k_{vm,nuc-cyt}$) in the reduced model have a significant influence on the virus yield (the simulation data are presented in Table 4.16); an increase of $k_{vm,nuc-cyt}$ leads to an increase of the number of assembled virions. Simulations performed at high values of $k_{vm,nuc-cyt}$ provide the same value of the minimal delay of virus production as reported in section 4.11.3 (1.7 h p.i.).

Table 4.16 The number of assembled virions for the rate coefficient of vmRNA nuclear export ($k_{vm,nuc-cyt}$) changed by different factors in the reduced model

Factor	0.5	0.7	1.0	1.5	2.0
V_{rel}	4320	5890	7920	10600	12610

Variations of viral polymerase speed and the translation efficiency for viral proteins in the reduced model bring to the same results as those in the detailed model. The two parameters involved have the most significant effect on the number of virions assembled.

In section 4.11.6 it is shown that in the detailed model the virus yield is not significantly influenced by variations of the rate constants of viral component assembly k_{in} and k_{bud} . Similarly, in the reduced model the number of produced virions is not sensitive to variations of the assembly rate constants k_{pck} (as done before, indexes “ C_v ”, “ P_i ”, and “ V_{rel} ” will be omitted, and all the rate coefficients involved will be designated by one symbol). In fact, virus production is limited by M1 protein production, and, hence, an increase of the assembly rate constants cannot result in an increase of the rate of virus release. The rate constants k_{pck} define only the value of the initial increase of the number of M1 proteins.

The impact of variations of the rate constants of the nucleic acid degradation on the virus yield in the reduced model is similar to that in the detailed model. Namely, the number of produced virions represents a monotonously decreasing function of the rate constants of cytoplasmic and nuclear vmRNA degradation and does not significantly change when the rate constants of vRNA and cRNA degradation are varied. The same refers to variations of the rate constants of protein degradation. It can be seen from Table 4.17 that the number of virions assembled, as a function of the rate constants of protein degradation, has a maximum, which corresponds to a factor of about 3.0.

Table 4.17 The number of assembled virions for the rate coefficients of protein degradation ($k_{i,degr}$) changed by different factors in the reduced model

Factor	0.1	1.0	2.0	3.0	4.0	5.0	7.0
V_{rel}	7030	7920	8090	8100	8060	7950	7590

An increase of the values of the switch parameters a_{NP} and b_{NP} in the reduced model, similar to that in the detailed model (see section 4.11.1), results in a decrease of the virus yield.

The dependency of the virus yield on the MOI represents a monotonously decreasing function (Table 4.18). In contrast to the situation, taking place in the detailed model the optimal value of the MOI is less than 1, i.e., beyond the range of relevant values. The difference in the abscissas of the optimum can be explained by the assumption of the reduced model that the incoming virions are delivered directly to the nucleus, which implies earlier in comparison with the detailed model start of viral component production. Consequently, in respect to the vicinity to the optimum, the certain value of the MOI in the detailed model corresponds to the lower value of the MOI in the reduced model.

Table 4.18 The number of assembled virions for different values of the MOI (*virions/cell*) in the reduced model

MOI	1.0	2.0	10.0	100.0
V_{rel}	8850	8750	7920	5760

4.13 Reinfection

Simulations based on the formulated in section 2.10 model with reinfection were performed for the values of the MOI changing in the range from 1 virion/cell to 100 virions/cell. At the given set of model parameters the difference between the simulation data obtained based on the models with reinfection and without reinfection is not significant. For this reason, to investigate the influence of the reinfection on virus dynamics the “amplified” reinfection was considered; the value of factor P_{inf} in (2.1.1”) were put equal to 1.0 (which corresponds to the assumption that all the released virions are infectious). Simulation results are summarized in Table 4.19. Comparing these results with those obtained in the model without reinfection (see section 4.10, Table 4.1), it can be concluded that at the fixed value of the MOI the total number of produced virions is slightly higher when newly produced virions do

not infect the cell again. Indeed, in the case of the reinfection incoming virions deliver into the nucleus an additional portion of polymerase complexes and NP proteins, and, as shown in section 4.10.1, the ratio of the numbers of delivered viral components is lower than the ratio of the numbers of viral components produced in the cell. As a result, vmRNA synthesis, and, consequently, viral protein production is inhibited. The negative effect of incoming virus particles on the virus yield will be also referred to in section 4.14 below.

Table 4.19 Virus yield for different values of the MOI (*virions/cell*) in the model with reinfection

MOI	1.0	2.0	3.0	4.0	5.0	10.0	100.0
V_{rel}	7930	8050	8080	8070	8030	7800	6000

On the other hand, the qualitative dependency of the number of released virions on the MOI in the model with reinfection is similar to that in the model without reinfection (Tables 4.19 and 4.1). Particularly, the virus yield as a function of the MOI also reaches the maximum at the value of the MOI equal to about 3 virions/cell.

4.14 Continuous Infection. Optimal Strategy of Infection

To apply the model formulated in section 2.11 for the investigation of the impact of the continuous infection on the virus yield, simulations were performed for different values of the MOI and the rate coefficient of virus supply (k_{feed}). Particularly, the case of the $MOI=0$ *virions/cell* (when only supplied virions infect the cell) was investigated. As at the values of the MOI more than 3 virions/cell the number of released virions represents a decreasing function of the MOI (see section 4.10), it can be easily shown that at these values of the MOI the virus yield represents a decreasing function of k_{feed} . Indeed, if an increase of the number of internalizing virions leads to a decrease of the number of released virions, the rate of vmRNA production is defined by the ratio of the number of newly synthesized viral polymerases to the number of newly synthesized NP proteins. Internalization of additional viral components will

result in a decrease of this ratio, and, hence, in a decrease in the rate of vmRNA production and the virus yield. Consequently, at the values of the MOI more than 3 virions/cell any increase of the virus yield due to virus supply during the infection cycle cannot be expected.

Simulation results are summarized in Table 4.20. The data for the values of the MOI higher than 3 virions/cell confirms the conclusion made above that in this range the virus yield decreases with an increase of k_{feed} . On the other hand, it can be seen that even at sufficiently low values of the MOI (e.g., 1 virion/cell) virus supply is not favorable for virus production; the maximal virus yield is achieved at the value of the rate coefficient of virus supply equal to zero. At the $MOI=0$ virions/cell the value of the rate coefficient of virus supply corresponding to the maximal number of produced virions, naturally, differs from zero (it is equal to about 3 virions/h). However, the maximal virus yield at the continuous infection at the $MOI=0$ virions/cell is lower than the virus yield at the $MOI=3$ virions/cell (the optimal value of the MOI).

Table 4.20 Virus yield for different values of the rate of virus supply (k_{feed} , virions/(nL · h)) and the MOI (virions/cell) in the model for continuous infection

	$k_{feed}=0.0$	$k_{feed}=1.0$	$k_{feed}=2.0$	$k_{feed}=3.0$	$k_{feed}=4.0$	$k_{feed}=5.0$
MOI=0.0	0	7510	7640	7680	7660	7620
MOI=1.0	8140	8100	8050	8000	7920	7840
MOI=3.0	8300	8230	8150	8070	7980	7900
MOI=5.0	8260	8170	8090	8010	7940	7870

Therefore, a continuous infection does not result in an increase of the number of released virions. Consequently, the optimal way of the infection in respect to the maximization of the virus yield seems to be the infection of the cell at the initial time point without further supply of virions.

The conclusion made here, can be also confirmed from the theoretical point of view. At the late stages of the infection it is the ratio of the numbers of newly synthesized viral proteins that defines the rate of vmRNA synthesis ($\mu_{v-vm,prod}$, defined in section 4.10.1). Consequently, if the certain number of virions, in which the ratio of the numbers of viral components corresponds to the lower value of the rate of vmRNA

synthesis ($\mu_{v-vm,vir}$), internalizes relatively late after the initial infection, vmRNA synthesis, and, accordingly, viral proteins production and progeny virus release will slow down. An increase of the viral yield at the early stages of the infection with an increase of k_{feed} at the $MOI=0$ virions/cell is explained by the need of viral components for the initiation of the process of virus replication.

4.15 Population Modeling

As pointed out in section 2.12, the main state variables of the population model are the numbers of uninfected, infected, and dead cells (Z_{un} , Z_{in} , and Z_d , respectively) and the total number of released virions (V_{rel}). Experimental observations and simulations performed at the time interval 0 – 90 h p.i. (a typical duration of virus replication stage in the considered fermentation experiments is 60-70 h, Genzel et al., 2004) allowed revealing major features of the dynamics of the populations involved (see section 4.15.1). For simulations and the following discussion, the rate coefficients of the degradation of extracellular virions and apoptosis of uninfected cells were put equal to zero. The values of the other model parameters, as well as the initial conditions, are reported in section 3.

4.15.1 Dynamics of Cell and Virus Populations

The number of uninfected cells is, evidently, a decreasing function of time (Fig. 4.23). It decreases first due to a primary infection¹¹ (0 – 4 h p.i.) and further due to a secondary infection (4 – 90 h p.i.). At about 20 h p.i. practically no uninfected cells remain in the system.

¹¹ The term *primary infection* indicates the infection by parental viruses (virus seeds, added to the culture at the time of infection). It differs from the term *initial infection*, which commonly refers to the infection of all uninfected cells (Hu and Bentley, 2000).

The number of infected cells (Fig. 4.23) first increases due to the primary infection (0 – 2 h p.i.). At the time interval between the end of the internalization of parental virions and the beginning of the secondary infection (2 – 8 h p.i.) the number of infected cells decreases due to cell death. A further increase (8 – 20 h p.i.) results from the secondary infection. Finally, as all the cells are infected the number of infected cells is again brought down by cell death (20 – 90 h p.i.). Such a time course of the infection is mainly defined by the rate coefficient of infection (k_{un-in}) and the rate coefficient of cell death due to virus-induced apoptosis ($k_{ap,in}$). It corresponds to experimental observations, particularly to the data from the fluorescence experiments (Genzel et al., 2004; Moehler et al., in press). As expected for low MOI values, the peak corresponding to the secondary infection is higher than that corresponding to the primary infection.

It is clear, that the number of dead cells equals to the difference between the total number of cell in the system and the number of living cells (infected and uninfected cells) monotonously increases in time (Fig. 4.23). Because of the big difference between the number of cells and virions involved in the secondary infection and in the primary infection, the increase corresponding to the secondary infection is much sharper than that corresponding to the primary infection. As pointed out in section 2, more than 90% of cells die within 48 h p.i. (Y. Genzel, personal communication, see Appendix A5).

The number of released virions in the population model, unlike that in the single cell model, is not a monotonously increasing function of time (Fig. 4.24). At about 72 h p.i., when the last cells die, the number of released virions start decreasing due to their degradation. Thus, the time point 72 h p.i., at which the virus yield reaches its maximal value, is the optimal time point for virus harvesting. The maximal number of released virions is in good agreement with experimental observations (HA test; H. Sann, personal communication, not shown).

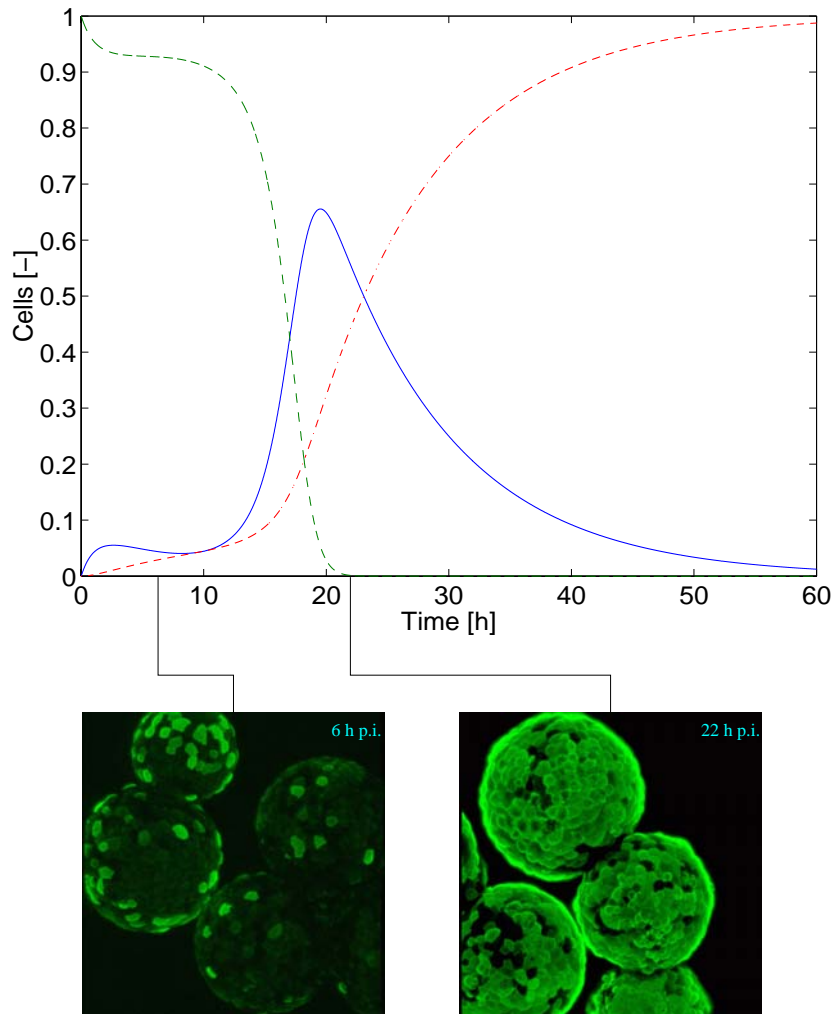


Figure 4.23 Dynamics of cell populations. The number of infected (Z_{in} , —), uninfected (Z_{un} , ---), and dead (Z_d , ---) cells related to the total number of cells in the system. Images (*H. Sann*) show that, for example, at 6 h p.i. only a low number of cells produce virions (fluorescent cells), whereas at 22 h p.i. all cells in the system are infected; they fast die due to virus induced apoptosis and separate from microcarriers.

4.15.1.1 Estimation of the Average Lifetime of a Cell

The dynamics of the population of dead cells obtained based on the population model allows estimating the average lifetime of a cell. The average lifetime of a cell, clearly, decreases with an increase of the MOI. Applying the method reported in Appendix A3, it can be calculated that at the considered MOI ($MOI=0.1$ virions/cell) the average cell of the population survives after infection about 22 h. Furthermore, the average lifetime of an infected cell can be also estimated from the population model.

For a high value of the MOI ($MOI=10.0$ virions/cell), which implies that all the cells of the population are immediately infected, the method indicates that the average lifetime of a cell is approximately 10 h. As expected (see equation (2.12.2)), further increase of the MOI (taking, for example, $MOI=100.0$ virions/cell) has no impact on this estimate.

4.15.2 Influence of MOI Changes on Population Dynamics

The population model, unlike the single cell model, allows considering values of the MOI less than 1 virion/cell (particularly, the initial value of the MOI was taken equal to 0.1 virions/cell, see section 3). While the single cell model reveals the optimal value of the MOI in respect to the virus yield (even in the case when the reinfection is taken into account), simulations based on the population model show that the number of virions produced at the late stages of the process monotonously decreases with an increase of the MOI (Fig. 4.24).

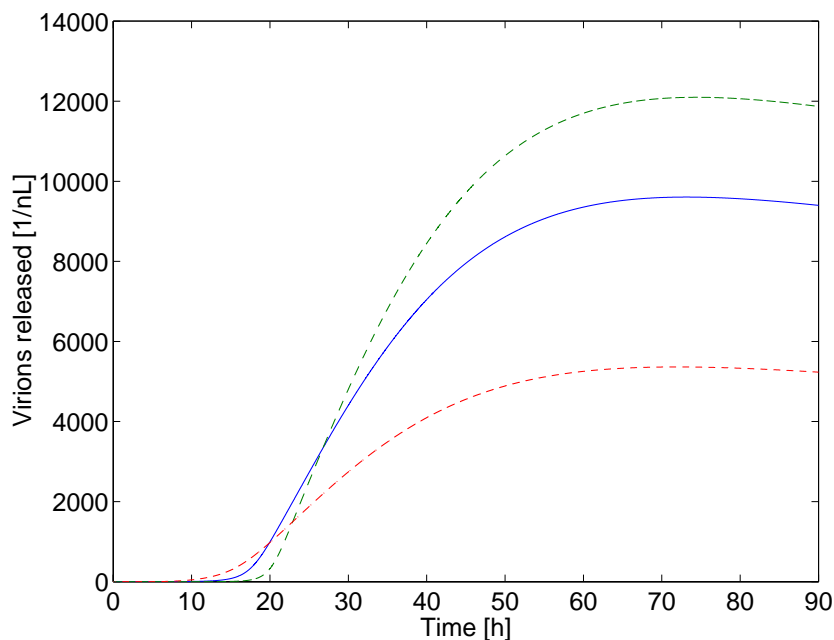


Figure 4.24 The number of released virions (V_{rel}) for different values of the MOI. The MOI is taken equal to 0.01 (---, maximum: 12100 virions/cell), 0.1 (—, maximum: 9600 virions/cell), and 1.0 (---, maximum: 5400 virions/cell).

To explain this dependency, consider two possible scenarios of infection. Suppose first that the MOI is so high that most of the cells in the system are infected during the primary infection. Then the number of virions produced during the secondary infection can be neglected, and only one replication cycle remains. As follows from results obtained for the single cell model for high values of the MOI, a decrease of the MOI value corresponds to an increase of the number of produced virions. Assume now that after infection at low MOI the major part of the cells remains uninfected. It means that at the late stages of the process the virus yield is defined by the number of virions produced during the secondary infection. In the considered case lower values of the MOI correspond to lower numbers of primarily infected cells (Fig. 4.25) and, hence, to lower numbers of virions produced by the end of the primary infection (Fig. 4.24). Assuming that virus particles produced during the primary infection infect all the remaining uninfected cells (which is, particularly, the case for the given set of model parameters), the situation for the secondary infection will resemble the situation the previous case deals with.

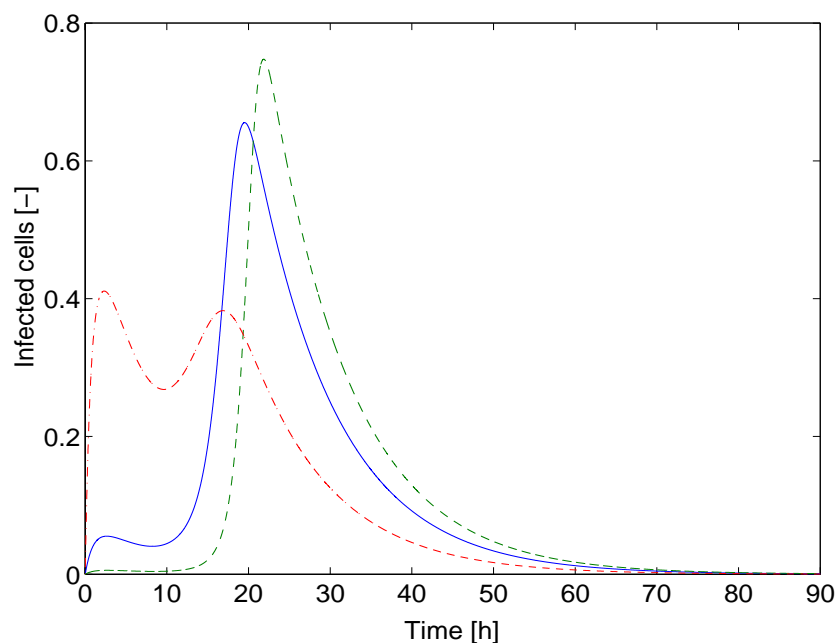


Figure 4.25 The number of infected cells (Z_{in}) related to the total number of cells in the system (Z_0) for different values of the MOI. The MOI is taken equal to 0.01 (---), 0.1 (—), and 1.0 (---).

At low MOI, however, there is also another reason, which causes the decrease of the virus yield with the increase of the MOI. This reason is a consequence of the model structure, i.e., the assumption that viral components are produced by a mass of average cells. As the synthesis of viral components in the average cell starts immediately after infection, the number of virions produced by secondarily infected cells is overestimated. Consequently, these results must be treated cautiously.

Nevertheless, whatever the primary or the secondary infection provides the number of virions making up the major part of the total number of released virions, the virus yield represents a monotonously decreasing function of the MOI. Accordingly, in the cases when the contributions of both considered stages of the infection are comparable, it will also decrease with a decrease of the MOI.

At the early stages of the process higher values of the MOI, in contrast, correspond to higher values of the virus yield. Indeed, an increase of the initial number of virions in the extracellular medium results in an increase of the initial rate of infection (the term $k_{ex-s,V_{ex}} V_{ex}$ in (2.1.1^{**})). Thus, it can be concluded that any two plots of the function $V_{rel}(t)$ corresponding to different values of the MOI always have a point of intersection (Fig. 4.24). For example, those corresponding to values of the MOI equal to 0.1 virions/cell and 1.0 virions/cell intersect at approximately 23 h p.i.

Based on experimental observations (roller bottle experiments) (Y. Genzel, personal communication, see Appendix A5), it was determined that the dynamics of virus release at the early stages of the process depended on the MOI in the same way, as it did according to simulation results. Although no effect of the MOI variations on the maximal number of released virions was revealed by the considered experiments, a series of studies confirmed the model outcome that the maximal number of released virions decreases with an increase of the MOI (see section 5.1).

The data concerning the influence of MOI variations on the number of uninfected, infected, and dead cells are shown on Figures 4.27, 4.25, and 4.26, respectively. At higher values of the MOI the infection and death of the cells occur faster than it does

at lower values of the MOI. However, as discussed above, the maximal number of infected cells at higher MOI values is lower than that at lower MOI values.

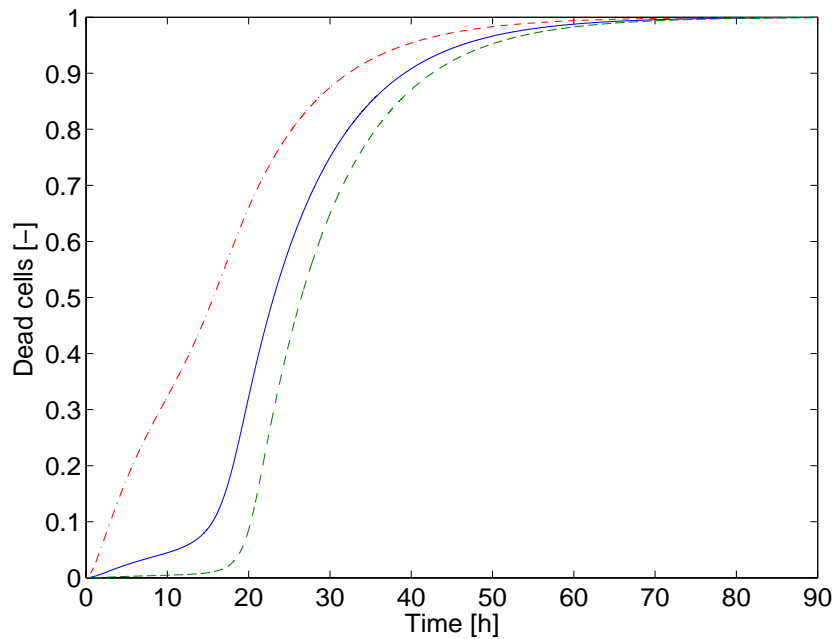


Figure 4.26 The number of dead cells (Z_d) related to the total number of cells in the system (Z_0) for different values of the MOI. The MOI is taken equal to 0.01 (---), 0.1 (—), and 1.0 (---).

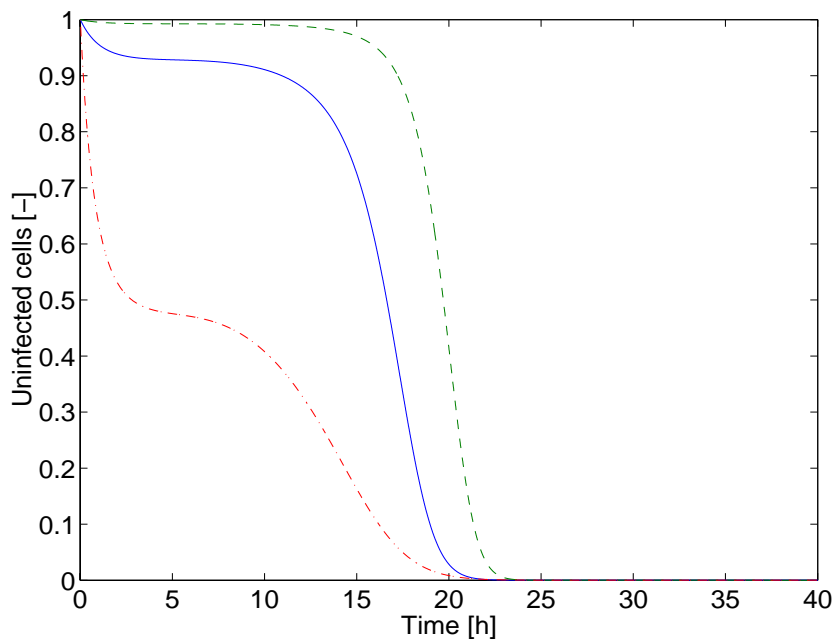


Figure 4.27 The number of uninfected cells (Z_{un}) related to the total number of cells in the system (Z_0) for different values of the MOI. The MOI is taken equal to 0.01 (---), 0.1 (—), and 1.0 (---).

4.15.3 Influence of Parameter Changes on Population Dynamics

The influence of changes of different model parameters on the number of virions produced by a single cell within 12 h was investigated in detail in section 4.11. Now it will be shown how variations of the ability of a single cell to produce virions influence the dynamics of the populations involved (released virions and uninfected, infected, and dead cells). For this purpose, consider the behavior of population sizes for different values of one of model parameters, variations of which have a significant influence on the function describing the number of virions released from a single cell. Such a parameter is, for example, the rate of polymerase operation (k_{pl}). Among all model parameters it has the strongest influence on the virus yield in the single cell model (see section 4.11.5); particularly, its twofold increase results in approximately twofold increase of the virus yield (Fig. 4.14).

Simulations based on the population model show that the number of virions produced in the system increases with an increase of the number of virions produced by a single cell (i.e., with an increase of k_{pl}) (Fig. 4.28). However, the extent, in which variations of k_{pl} influence the virus yield in the population model, is lower than it is in the single cell model; instead of about twofold increase of the number of produced virions in the single cell model, in the population model the twofold increase of k_{pl} results in the increase of the virus yield by a factor of approximately 1.6. Indeed, in the population model the process of virus production is accompanied by cell death, which brings the virus yield down.

An increase of the number of virions produced in the system at the given time point, in turn, leads to an increase of the rate of infection (the term $k_{un-in} V_s Z_{un}$ in (2.12.1)) and, correspondingly, to an increase of the rate of cell death (the term $k_{ap,in} Z_{in}$ in (2.12.2)). Thus, at higher numbers of virions produced by a single cell, the decrease of the number of uninfected cells (Fig. 4.29) and, correspondingly, the increase of the

number of dead cells (Fig. 4.30) occur faster than those at lower numbers of virions produced by a single cell. The number of infected cells in the former case changes faster and have higher maximal values than in the latter case (Fig. 4.31).

The population model contains two parameters that are absent in the single cell model. These parameters are the rate coefficient of infection (k_{un-in}) and the rate coefficient of the death of infected cells due to virus-induced apoptosis ($k_{ap,in}$). Evidently, an increase of the later rate coefficient reduces the size of the population of infected cells and, hence, causes a decrease of the virus yield (Fig. 4.32, 4.33). To demonstrate this tendency, the rate coefficient was changed by the factors 1.0, 1.5, and 2.0. It is also clear that under these circumstances the number of uninfected cells decreases more slowly than it does at the initial value of $k_{ap,in}$ (Fig. 4.34). An increase of the rate coefficient of infection, in contrast, leads to a faster decrease of the number of uninfected cells (Fig. 4.35). Additionally, it results in an increase of the number of primarily infected cells (Fig. 4.36) and, hence (see section 4.15.2), to a decrease of the number of produced virions (Fig. 4.37). It is also clear that at the early stages of the process higher numbers of released virions correspond to higher values of k_{un-in} (Fig. 4.37).

The remaining parameters included in the population model are the rate coefficients of the apoptosis of uninfected cells ($k_{ap,un}$) and the rate constant of the detachment of uninfected cells from microcarriers (k_{dt}). The values of these parameters are not assumed to be high enough to have an essential influence on virus dynamics, and their default values were put equal to zero (it particularly implies that the only reason for cell death is virus infection, see equation (2.12.1)). An increase of $k_{ap,un}$ clearly results in a decrease of the number of uninfected and infected cells and, hence, to a decrease of the virus yield (to demonstrate this tendency, the behavior of the system for $k_{ap,un}$ equal to $0.0 h^{-1}$, $0.1 h^{-1}$, and $0.2 h^{-1}$ was considered, Fig. 4.38, 4.39, 4.40). Similar changes in the system behavior also take place at the increase of k_{dt} .

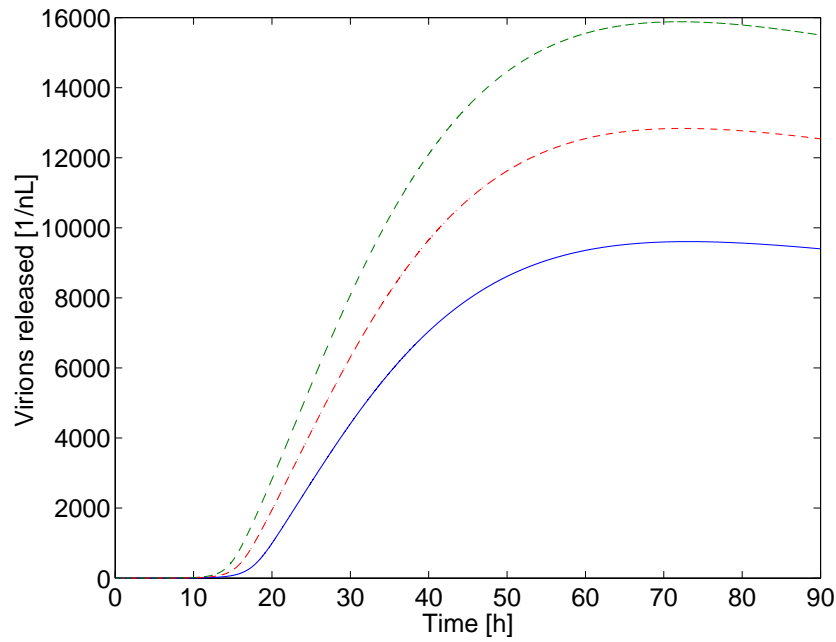


Figure 4.28 The number of released virions (V_{rel}) for different values of viral polymerase speed. Polymerase speed (k_{pi}) is increased by factors of 1.0 (—, maximum: 9600 virions/cell), 1.5 (---, maximum: 12800 virions/cell) and 2.0 (---, maximum: 15900 virions/cell).

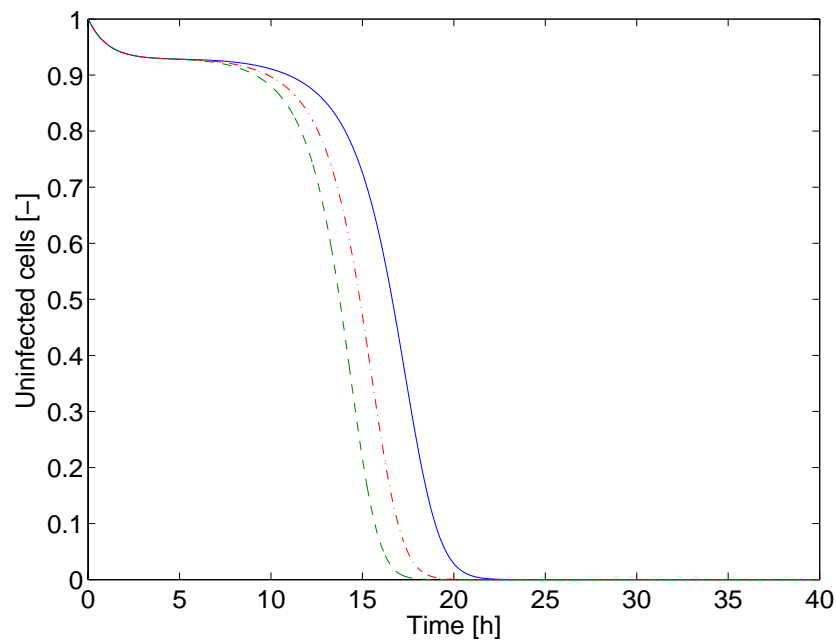


Figure 4.29 The number of uninfected cells (Z_{un}) related to the total number of cells in the system (Z_0) for different values of viral polymerase speed. Polymerase speed (k_{pi}) is increased by factors of 1.0 (—), 1.5 (---) and 2.0 (---).

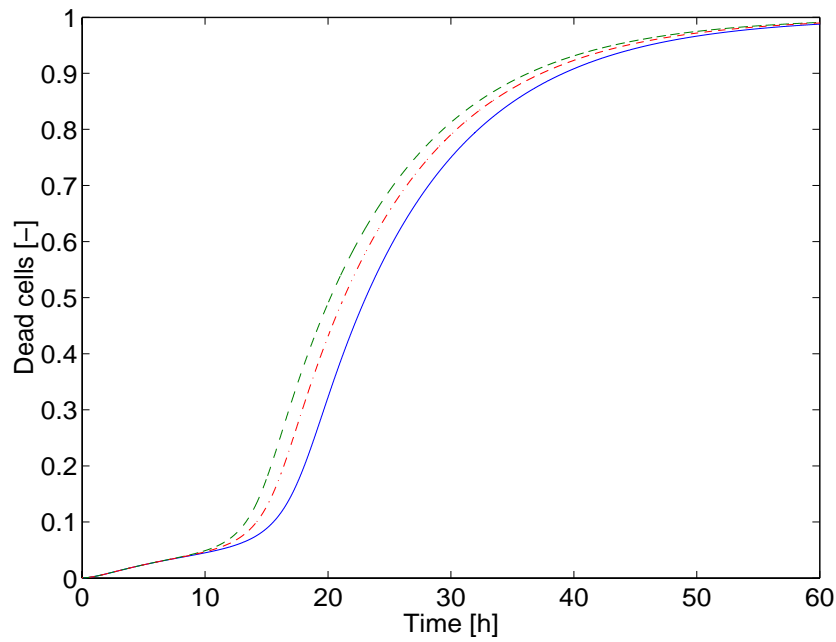


Figure 4.30 The number of dead cells (Z_d) related to the total number of cells in the system (Z_0) for different values of viral polymerase speed. Polymerase speed (k_P) is increased by factors of 1.0 (—), 1.5 (---) and 2.0 (-.-).

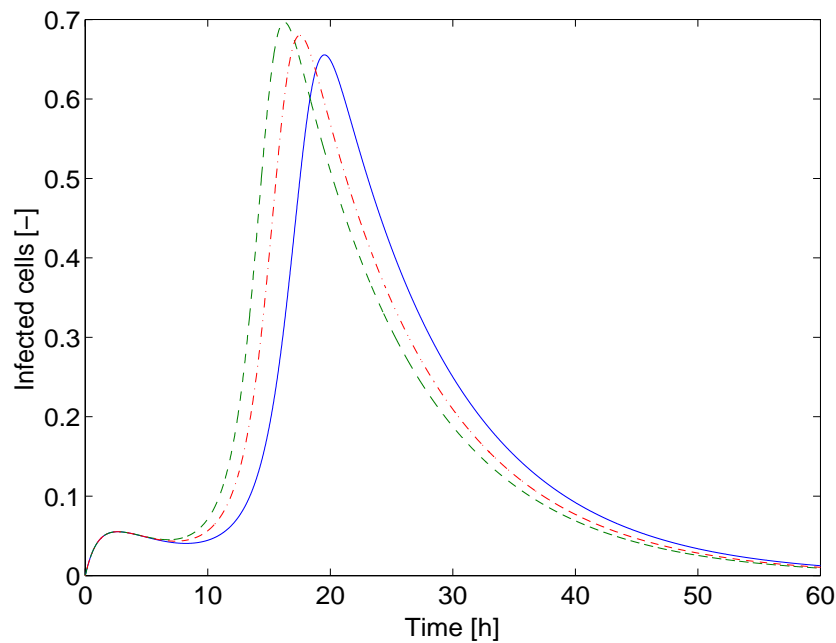


Figure 4.31 The number of infected cells (Z_{in}) related to the total number of cells in the system (Z_0) for different values of viral polymerase speed. Polymerase speed (k_P) is increased by factors of 1.0 (—), 1.5 (---) and 2.0 (-.-).

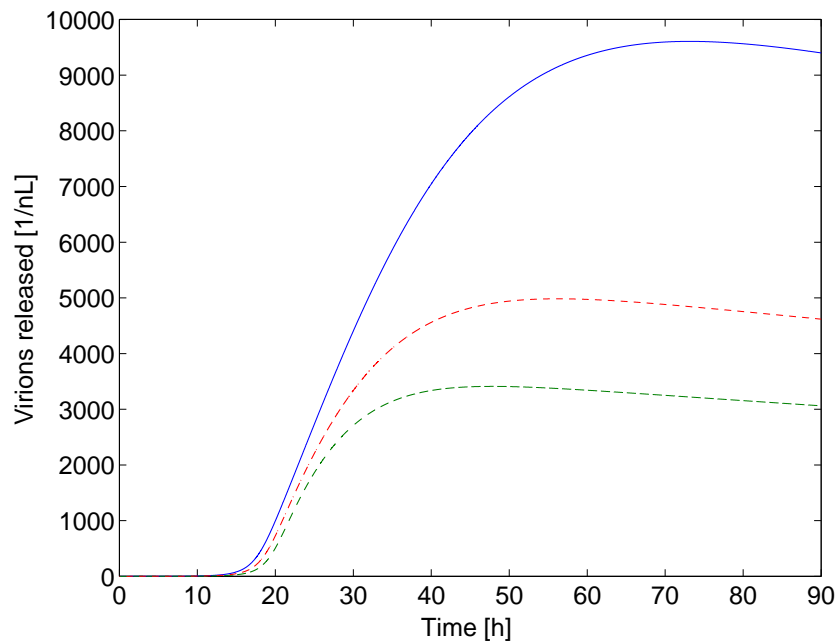


Figure 4.32 The number of released virions (V_{rel}) for different values of the rate coefficient of apoptosis of infected cells. The rate coefficient of apoptosis of infected cells ($k_{ap,in}$) is changed by factors of 1.0 (—, maximum: 9600 virions/cell), 1.5 (---, maximum: 5000 virions/cell) and 2.0 (---, maximum: 3400 virions/cell).

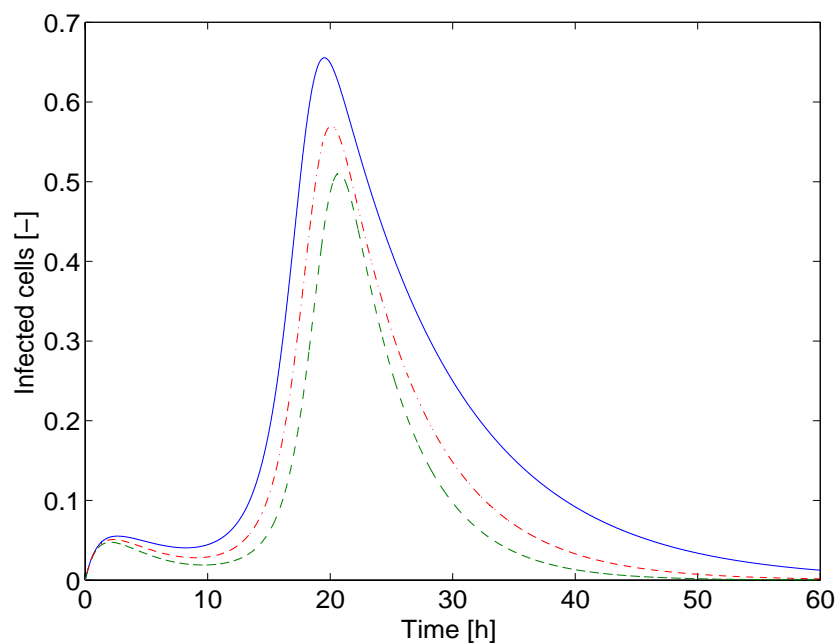


Figure 4.33 The number of infected cells (Z_{in}) related to the total number of cells in the system (Z_0) for different values of the rate coefficient of apoptosis of infected cells. The rate coefficient of apoptosis of infected cells ($k_{ap,in}$) is changed by factors of 1.0 (—), 1.5 (---) and 2.0 (---).

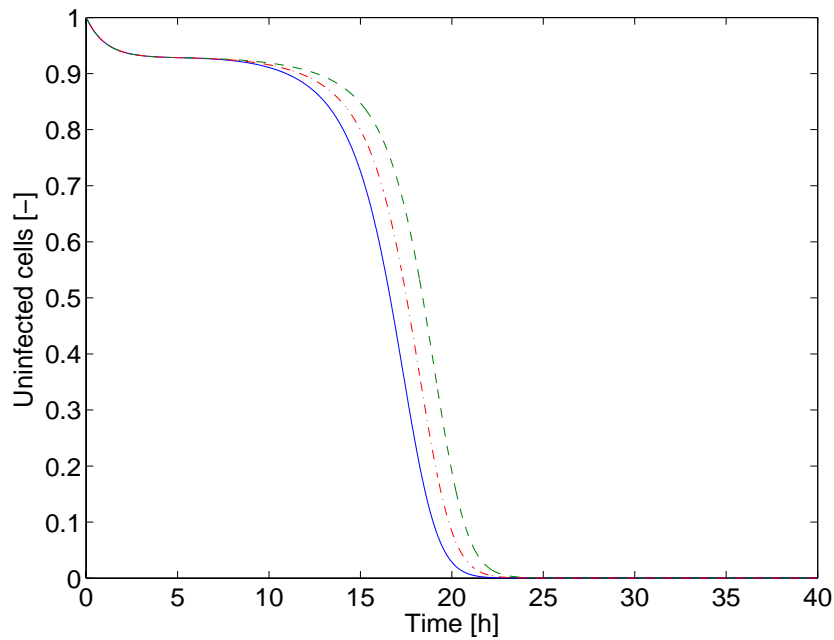


Figure 4.34 The number of uninfected cells (Z_{un}) related to the total number of cells in the system (Z_0) for different values of the rate coefficient of apoptosis of infected cells. The rate coefficient of apoptosis of infected cells ($k_{ap,in}$) is changed by factors of 1.0 (—), 1.5 (---) and 2.0 (---).

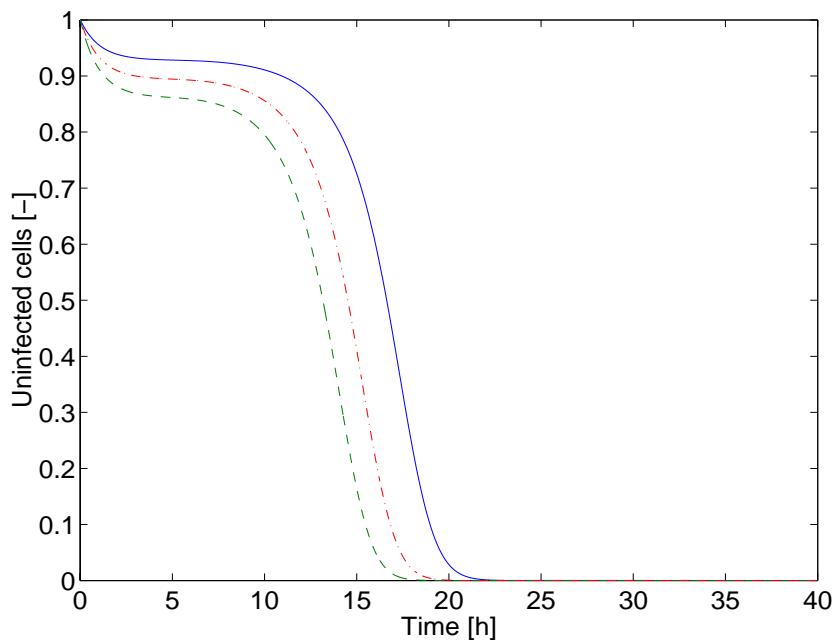


Figure 4.35 The number of uninfected cells (Z_{un}) related to the total number of cells in the system (Z_0) for different values of the rate coefficient of infection. The rate coefficient of infection ($k_{un,in}$) is changed by factors of 1.0 (—), 1.5 (---) and 2.0 (---).

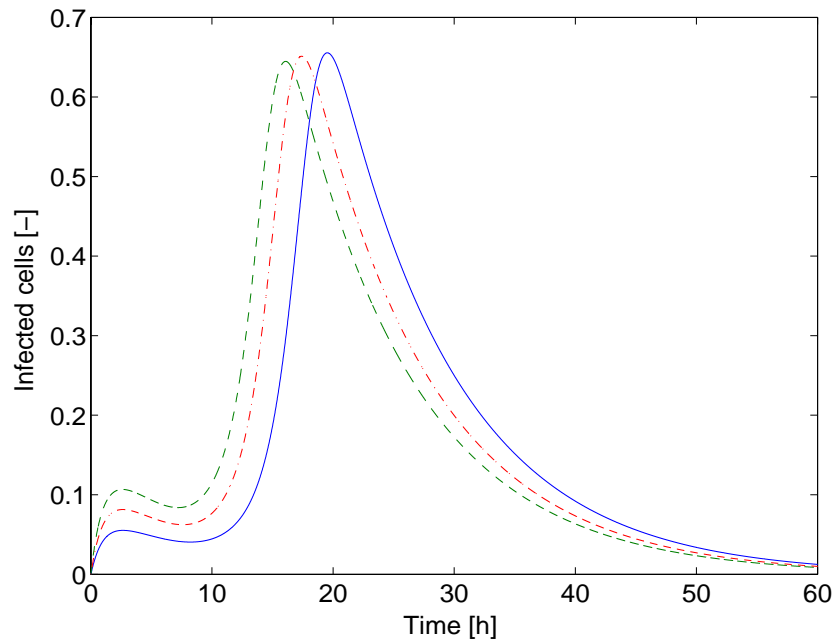


Figure 4.36 The number of infected cells (Z_{in}) related to the total number of cells in the system (Z_0) for different values of the rate coefficient of infection. The rate coefficient of infection ($k_{un-,in}$) is changed by factors of 1.0 (—), 1.5 (---) and 2.0 (---).

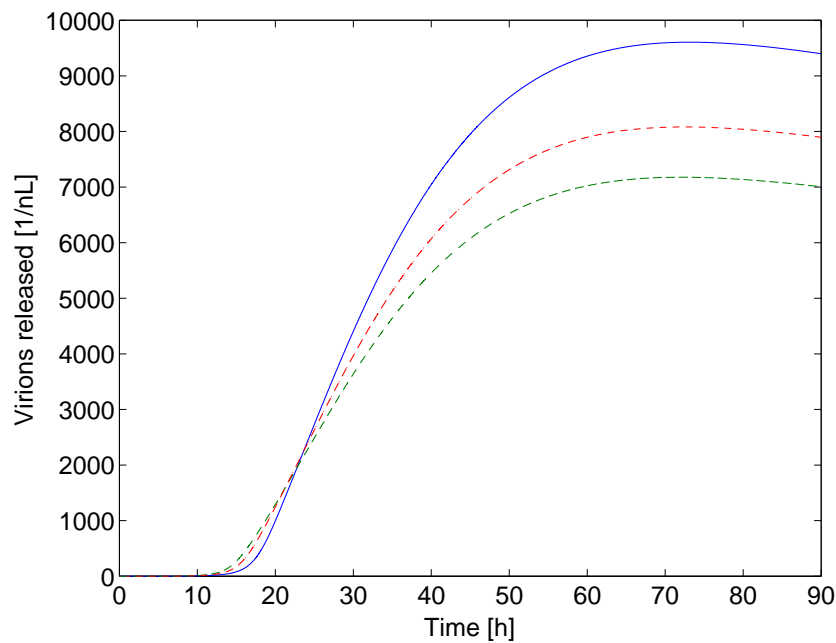


Figure 4.37 The number of released virions (V_{rel}) for different values of the rate coefficient of infection. The rate coefficient of infection ($k_{un-,in}$) is changed by factors of 1.0 (—, maximum: 9600 virions/cell), 1.5 (---, maximum: 8100 virions/cell) and 2.0 (---, maximum: 7200 virions/cell).

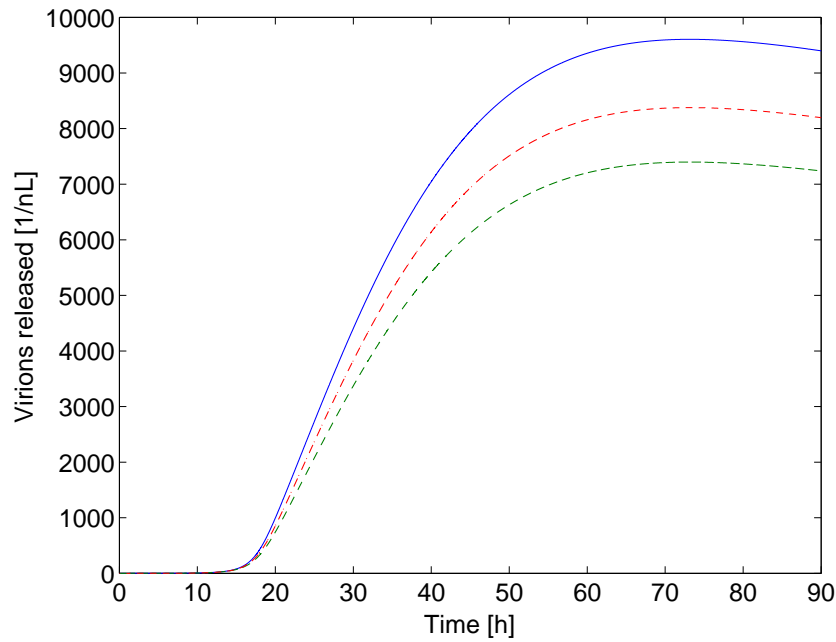


Figure 4.38 The number of released virions (V_{rel}) for different values of the rate coefficient of apoptosis of uninfected cells. The rate coefficient of apoptosis of uninfected cells ($k_{ap,un}$) is taken equal to 0.0 h^{-1} (—, maximum: 9600 virions/cell), 0.1 h^{-1} (---, maximum: 8400 virions/cell), and 0.2 h^{-1} (---, maximum: 7400 virions/cell).

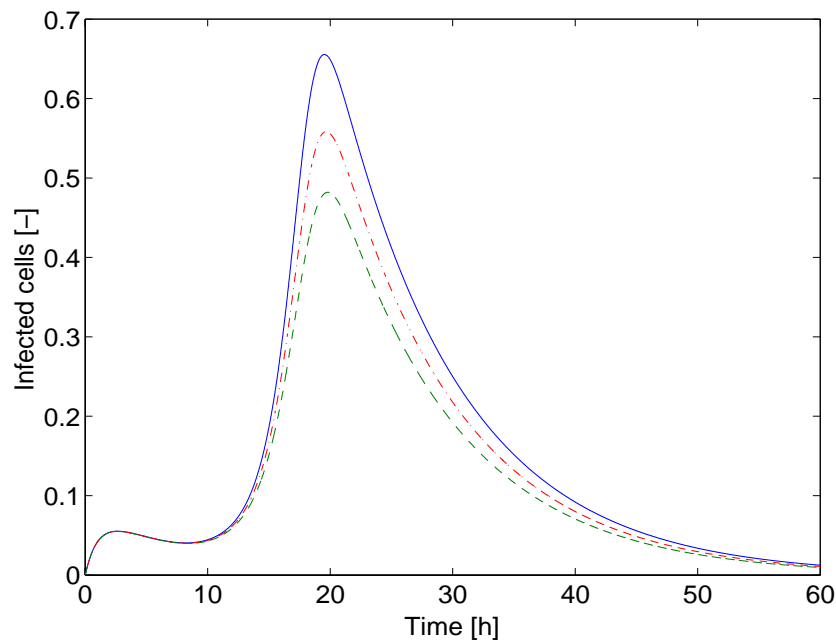


Figure 4.39 The number of infected cells (Z_{in}) related to the total number of cells in the system (Z_0) for different values of the rate coefficient of apoptosis of uninfected cells. The rate coefficient of apoptosis of uninfected cells ($k_{ap,un}$) is taken equal to 0.0 h^{-1} (—), 0.1 h^{-1} (---), and 0.2 h^{-1} (---).

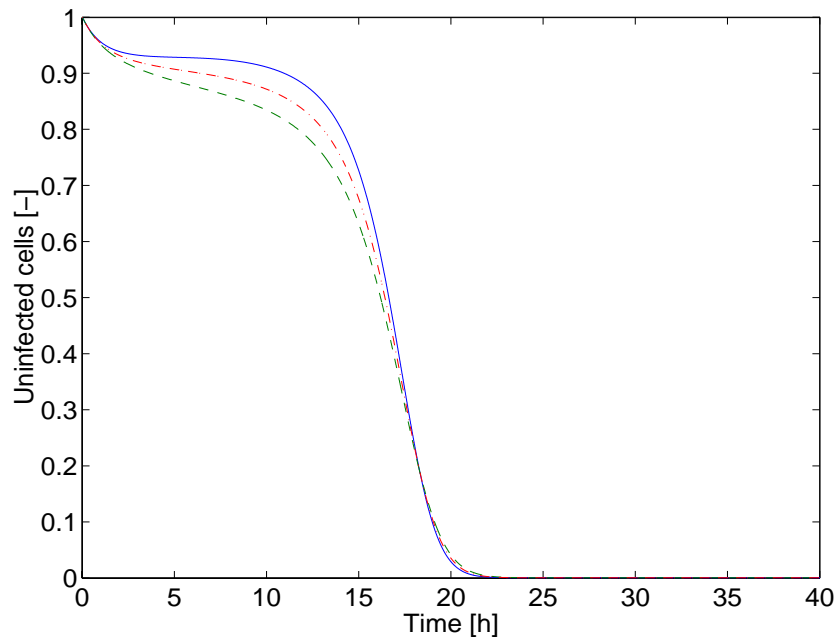


Figure 4.40 The number of uninfected cells (Z_{un}) related to the total number of cells in the system (Z_0) for different values of the rate coefficient of apoptosis of uninfected cells. The rate coefficient of apoptosis of uninfected cells ($k_{ap,un}$) is taken equal to 0.0 h^{-1} (—), 0.1 h^{-1} (---), and 0.2 h^{-1} (---).

5 Discussion

Developed in the present study was a structured model for the reproductive cycle of Influenza A virus in mammalian cells. The single cell model, as well as its possible modifications taking into account the reinfection, the continuous infection, and the dynamics of cell populations (uninfected, infected, and dead cells), were investigated. Unlike most of the existing models of virus infection, which take into account only certain steps of the replication cycle, the present model considers all the steps of the process, from virus entry into the host cell to progeny virus release.

As pointed out in section 1.1.2, when a very small number of virions infect a population of host cells, it is possible to describe the events of the replication cycle by stochastic approaches (Schreiber et al., 2001; Srivastava et al., 2002). However, in the present model stochastic events are not taken into account. Instead, a single cell, which is infected at least by one virion, is considered. As a consequence, virus attachment and entry are described by differential equations, the structure of these equations being similar to that of the equations used to describe other intracellular processes.

In the present section it will be discussed how the results of simulations correlate with the results provided by other models. Further, the importance of the reinfection for the adequate description of virus dynamics will be considered. Sections 5.3 – 5.11 will mainly discuss the detailed single cell model itself. It will be shown, how many virions the cell would be able to produce if it did not die due to apoptosis. Furthermore, different possible mechanisms of transcription, replication, and packaging of the viral genome will be presented; it will be discussed, which of them the most relevant for the considered biological system and the most appropriate for the modeling are. The influence of NP proteins on virus replication dynamics will be investigated. Besides that, addressed again will be limiting factors of virus replication; the relative demands of newly produced viral components for the production of progeny virions will be discussed. Possible changes of the law of virus growth and

several modifications that could be introduced into the model will be also considered here. Further subsections will be concerned with methods to improve the virus yield, as well as with some ideas for the optimization of vaccine production processes and possible targets for antiviral therapies. After that, the particularities of the population model and the reduced model will be addressed. Finally, the end of the section will be devoted to the discussion of virus-induced apoptosis, the most likely reason for the early cell death and with the identification of directions for the further experimental work.

5.1 Agreement with Other Models

The overall dynamics obtained based on the present model agrees well with results obtained by other models. For example, similar results for the dynamics of genome transcription, viral protein production and progeny virus release were obtained from a structured model of HIV-1 infection (Reddy and Yin, 1999). In particular, polynomial increase of the number of released virus particles is reported. However, as the right-hand sides of the equations describing the number of viral proteins in the membrane do not contain any terms responsible for the assembly of progeny virions (the authors consider the total number of newly produced viral proteins), no limiting components were identified during virus assembly.

Unlike the model of Reddy and Yin (1999), which assumes that the virus was already internalized into its host cell (and, thus, does not provide data concerning the initial stages of the infection), a model of Dee and Schuler (1997) focuses on the dynamics of virus entry. The structure of equations underlying this model is similar to the structure of the first equations of the detailed single cell model presented here. Particularly, extracellular, surface, endosomal, and cytoplasmic virions are considered individually. Moreover, baculovirus particles, like influenza virus particles, are partially inactive and degraded in endosomes; therefore a term describing the endosomal sorting of virus particles is taken into account in the model equations. Thus, it is not surprising that the behavior of the functions expressing the number of

extracellular and internalized virus particles resembles that of the corresponding functions in the detailed single cell model. In addition, the process of infection has a similar time scale. Simulation results are also comparable with those obtained for a model of Semliki Forest virus internalization (Dee et al., 1995). However, the time scale of Semliki Forest virus trafficking is clearly different from that of influenza virus and baculovirus replication.

Qualitative data for the replication of bacteriophage T7 in *Escherichia coli* provided by Endy et al. (1997) shows similar results for the number of progeny phages when compared to simulations based on the present model; an initial exponential stage is followed by a polynomial increase of the number of released virions. At the same time, unlike simulation results obtained at the given set of model parameters, in the model of Endy et al. (1997) cellular concentrations of vmRNA molecules and viral proteins achieve steady state within simulation time.

The dynamics of cell populations obtained from the modification of the present model (the population model, see section 2.12) is also comparable with the results obtained from other models. For example, the qualitative behavior and the time scale of the function describing the number of dead cells in the present population model resembles that of the function describing the number of infected cells in the model of Hu and Bentley (1999) for baculovirus infection (this model does not account for cell death, considering a population of dead cells as a part of the population of infected cells). According to both approaches, the infection of uninfected cells and, correspondingly, cell death occur faster at higher MOI. Besides that, the number of uninfected cells decreases obeying similar laws; both models show a faster decrease at higher MOI. The dynamics of virus entry and release presented by Hu and Bentley (1999) and that provided by the population model presented here are also comparable, however, as the present model takes into account virus degradation, simulations reveal a decrease of the number of released virions at the late stages of the process. According to simulations based on the model of Hu and Bentley (1999), the overall virus yield increases with a decrease of the MOI. Moreover, the maximal number of produced virions is achieved earlier at higher MOI, i.e., a decrease of the MOI is

profitable for virus production only at the late stages of the process. Both conclusions closely agree with the results obtained from the present model (see section 4.15.2).

Another study that investigates the optimal conditions for virus production, in particular the MOI (Likari and Bailey, 1992) also shows a dependency of the virus yield on the MOI similar to that obtained from the present model. The dependency of the number of released virions on the MOI agrees well with the data presented in the article when the MOI changes in the range from 0.1 virions/cell to 100 virion/cell. However, for a low MOI (less than 0.1 virions/cell) the authors report that the virus yield represents an increasing function of the MOI. Furthermore, the qualitative behavior of the number of uninfected and infected cells, obtained from the population model presented here, is in agreement with the population dynamics reported by Jang et al. (2000). This article also reveals dependencies of the number of viable cells and the number of produced virions on the MOI, which resemble those obtained in the present model.

5.2 Importance of a Reinfection

Hu and Bentley (1999) pointed out that a reinfection had an influence on the virus concentration and the probability of infection; therefore they incorporated it into a stochastic model. The authors show that a reinfection is particularly important for low values of the MOI.

For a population model formulated in section 2.12 the terms describing the reinfection

($k_{bud-rel,V_{rel}} P_{inf} \frac{Z_{in}}{Z_0} V_{bud}$ in (2.1.1^{**}) and the corresponding term in (2.8.2^{**})) is also

crucial. The reinfection affects the dynamics of cell populations, as well as the number of produced virions. Similar to that in the model of Hu and Bentley (1999), the effect of a reinfection on system behavior is stronger for lower MOI. Indeed, for a high MOI (more than 1 virion/cell) most of the cells are infected by the primary

infection, and the number of virions produced during a secondary infection is negligible.

On the other hand, as follows from the results presented in section 4.13 for the single cell model, a reinfection does not play an important role for the virus dynamics. Indeed, the values of the virus yield provided by single cell models with reinfection (Table 4.19) and without reinfection (Table 4.1) do not differ significantly. Besides that, the factors limiting virus production, as well as the dependency of the number of produced virions on the MOI, are the same for both models.

5.3 Maximal Number of Produced Virions

The single cell model considers a small number of virions infecting the cell (10 virions/cell) and an average lifetime of infected cells of about 12 hours. As discussed in section 4.8, under the initial conditions considered, the initial cellular pools of nucleotides and amino acids are much bigger than the virus requires for its replication. However, if the cell is infected with significantly higher number of virions or if the cell survives longer, cellular resources such as cellular precursor mRNA molecules, free nucleotides and amino acids would be exhausted during virus replication.

Suppose that the lifetime of the cell is not limited by $T=12h$; the cell does not undergo the apoptosis and survives and produces virions until one of its resources is exhausted. Simulation results show that the most critical resource is the number of free amino acids ($P_{cell} = 3.1 \cdot 10^{10}$ amino acids, see section 2.3). As mentioned in section 2.5, the cellular pool of free amino acids would allow the production of about $1.3 \cdot 10^4$ virions (Fig. 5.1), which is in the range of yields typically obtained for equine influenza A virus replication in MDCK cells from large-scale microcarrier cultures (6500 to 13000 virions per cell, data not shown).

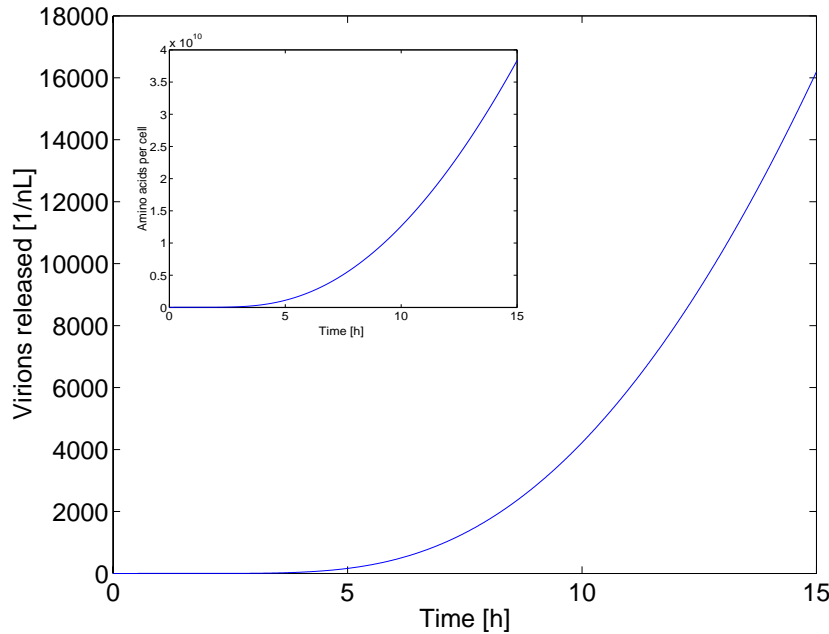


Figure 5.1 The number of released virions (V_{rel}) for the expanded lifetime of the cell. Inset: the number of free cellular amino acids incorporated into progeny virions.

Simulations provide an indication of the lower limit of the lifetime of the cell and the capacity of the cell to produce virions. Assuming that the cell does not die until the exhaustion of one of its resource, and it does not synthesize or take up amino acids, it would survive at least $T_{max}=15 h$ (Fig. 5.1). A more realistic scenario and an estimation of the upper limits for the quantities involved would require the extension of the existing model to include aspects of cell death, as well as other relevant parts of cellular metabolism. In the latter case, Monod-type kinetics rather than constant rate coefficients would be required for the description of the corresponding steps of the infection cycle. For example, the rate coefficient $k_{v-vm,i}$ (see equation (2.3.1)) would not only depend on the nuclear concentration of NP proteins ($P_{NP,nuc}$) but also on the number of cellular precursor mRNA molecules ($C_{m,cell}$) and on the number of free cellular nucleotides (C_{cell}). Additionally, it must be taken into account that according to experimental observations, an increase of amino acid concentrations in the extracellular medium was detected directly after infection (Genzel et al., 2004). The most likely reason for this is that the cell does go on producing new amino acids after infection. However, the excretion of amino acids already existing in the cell (the reduction of intracellular pools of amino acids) is also not excluded.

5.4 Dynamics of Transcription and Genome Replication

The operation of viral polymerase complexes involved in the processes of vRNA production and viral genome replication depends on the ratio of the number of polymerase complexes to the number of template segments (vRNA or cRNA segments). Besides the case when the number of genome segments is much higher than the number of polymerase complexes (assumed in the model), the option that it is comparable or lower than the number of polymerase complexes will be also considered in this section.

5.4.1 Redundancy of Genome Segments

When formulating the model, particularly the equations describing the replication of the viral genome, it is assumed that the number of vRNA molecules significantly exceeds the number of polymerase complexes; all polymerase complexes are supposed to be involved in the process and to operate at the same speed. Under the assumptions made it is possible to consider the whole amount of vRNA segments participating in the genome replication as a uniform mass of nucleotides being processed by the given number of polymerase complexes. The rate of vRNA (cRNA) production is then proportional to the number of polymerase complexes (the terms $k_{v-c} P_{Pol,nuc}$ in (2.4.1) and $k_{c-v} P_{Pol,nuc}$ in (2.4.2)).

Having processed one vRNA (cRNA) segment, the polymerase complex is released and can theoretically process another vRNA (cRNA) segment. Thus, it could be supposed that shorter genome segments lose their polymerase complexes more often than longer segments do, and, hence, their production (in nucleotides per hour) should be slower in respect to the production of longer segments. Nevertheless, the vRNA (cRNA) segment nearest to the polymerase complex is the segment that has just been

processed (or its copy), and, therefore, this segment will most likely be bound and processed again. Consequently, once bound to a vRNA (cRNA) segment, the polymerase complex is supposed to go on processing this segment.

On the other hand, it could be speculated that shorter segments, being produced in higher copy numbers, recruit more newly produced polymerase complexes than longer segments, and, therefore, their synthesis rates (measured in nucleotides per hour) should be higher than those of longer segments. However, it is evident, that at the given initial conditions (one segment of each sort, provided by a polymerase complex processing it) the number of copies of the i -th genome segment produced per hour ($N_{v,i}$, (*molecules/h*)) is inversely proportional to the length of this segment ($L_{v,i}$, (*nucleotides*)):

$$(5.4.1) \quad N_{v,i} \sim \frac{1}{L_{v,i}}.$$

At the same time, the probability that an incoming polymerase complex binds an i -th vRNA segment ($P_{v,i}$, (-)) (according to the assumption made above, the number of i -th vRNA segments bound by other polymerases makes up just a minor part of the total number of these segments) is proportional to the number of nucleotides contained in the copies of this segment:

$$(5.4.2) \quad P_{v,i} \sim N_{v,i} L_{v,i}.$$

Thus, as follows from formulas (5.4.1) and (5.4.2), the probability to be bound by a newly synthesized polymerase complex is equal for all sorts of vRNA (cRNA) segments.

According to the arguments discussed above, the total number of newly produced nucleotides is uniformly distributed among all sorts of segments. To calculate the number of copies of the i -th genome segment produced per hour ($N_{v,i}$, (*molecules/h*)), the total number of nucleotides produced per hour (C_T , (*nucleotides/h*)) must be divided by the number of different genome segments ($N_{seg} = 8$ *molecules*) and by the length of the i -th segment ($L_{v,i}$, (*nucleotides*)):

$$(5.4.3) \quad N_{v,i} = \frac{C_T}{N_{seg} L_{v,i}}.$$

5.4.2 Redundancy of Polymerase Complexes

Consider now the opposite case, i.e., when the number of polymerase complexes significantly exceeds the total number of vRNA and cRNA segments. In this situation it is the number of vRNA and cRNA segments rather than the number of polymerase complexes that defines the rate of segment copying. Now genome segments to be processed can no longer be considered as a uniform mass of nucleotides. Indeed, as soon as vRNA (cRNA) segments are produced, free polymerase complexes immediately bind them, and, therefore, the synthesis rate (measured in nucleotides per hour) is different for different sorts of segments. The synthesis rates of i -th vRNA and cRNA segments (they will be denoted by $\mu_{v-c,i}$ (nucleotides/h) and $\mu_{c-v,i}$ (nucleotides/h), respectively), are proportional to the number of these segments ($C_{v,i}$ (nucleotides/cell) and $C_{c,i}$ (nucleotides/cell), respectively) and inversely proportional to their length ($L_{v,i}$ (nucleotides)). In the considered case, for example, the term $k_{v-c} P_{Pol,nuc}$ in (2.4.1), expressing the synthesis rate of cRNA segments, would be replaced by term

$$(5.4.4) \quad \mu_{v-c,i} = \frac{k_{v-c,i}}{L_{v,i}} C_{v,i},$$

where $k_{v-c,i}$ (h^{-1}) is the rate coefficient of cRNA synthesis, calculated by the formula similar to that for the rate coefficient k_{v-c} in section 2.4.

5.4.3 General Case

In the intermediate case, when the number of vRNA and cRNA segments is comparable with the number of polymerase complexes, the calculation of the synthesis rate of complementary segment becomes more complicated. In general,

cRNA (vRNA) synthesis rate depends on both the number of polymerase complexes and the number of processed vRNA (cRNA) segments. It can be expressed using a Monod-type kinetics:

$$(5.4.5) \quad \mu_{v-c,i} = k_{v-c,i,\max} \frac{P_{NP,nuc}}{b_{NP} + P_{NP,nuc}} \cdot \frac{C_{v,i}}{K_{C_{v,i},v-c}(P_{Pol,nuc}) + C_{v,i}} \cdot \frac{P_{Pol,nuc}}{K_{P_{Pol,nuc},v-c}(C_{v,i}) + P_{Pol,nuc}},$$

where half-saturation functions $K_{C_{v,i},v-c}$ (*nucleotides/cell*) and $K_{P_{Pol,nuc},v-c}$ (*amino acids/cell*) (representing the analogues of Monod constants) depend on the total number of polymerase complexes and the total number of i -th vRNA segments, respectively.

5.4.4 Choice of Model Assumption

In the case of genome segment redundancy all genome segments can be considered as one pool of nucleotides. Consequently, to describe the dynamics of genome replication it is enough to consider only two functions, representing the total numbers of vRNA and cRNA segments (in equations (2.4.1) and (2.4.2) these functions are, correspondingly, C_v and C_c) and calculate the number of copies of the i -th segment by formulas like (5.4.3).

In the case of polymerase complex redundancy, as well as in the general case, the number of copies must be described individually for each sort of segments. Consequently, genome replication dynamics is now described by sixteen functions (instead of two in the previous case): eight functions representing the numbers of vRNA segments and eight functions representing the numbers of cRNA segments. Additionally, as follows from formula (5.4.5), the general case requires the identification of more model parameters in comparison with the particular cases considered before. For example, functions $K_{C_{v,i}}$ and $K_{P_{Pol,nuc}}$ depending on the complex interaction of polymerase complexes with genome segments must be defined.

So far little is known about an individual control of transcription and translation. Therefore, for the simplicity of the model it is reasonable to assume that the number of polymerase complexes is much lower than the number of genome segments. Simulation results show that this assumption is well satisfied for the late stages of the infection cycle, but violated at the early stages of the infection (Fig. 5.2). Nevertheless, the overestimate of the number of vRNA and cRNA segments produced at the early stages of the infection (at this time interval the number of polymerase complexes exceeds the number of vRNA segments) can be compensated by the decreasing of the rate coefficients of vRNA and cRNA synthesis in the right-hand sides of equations (2.4.1) and (2.4.2) (k_{c-v} and k_{v-c} , respectively).

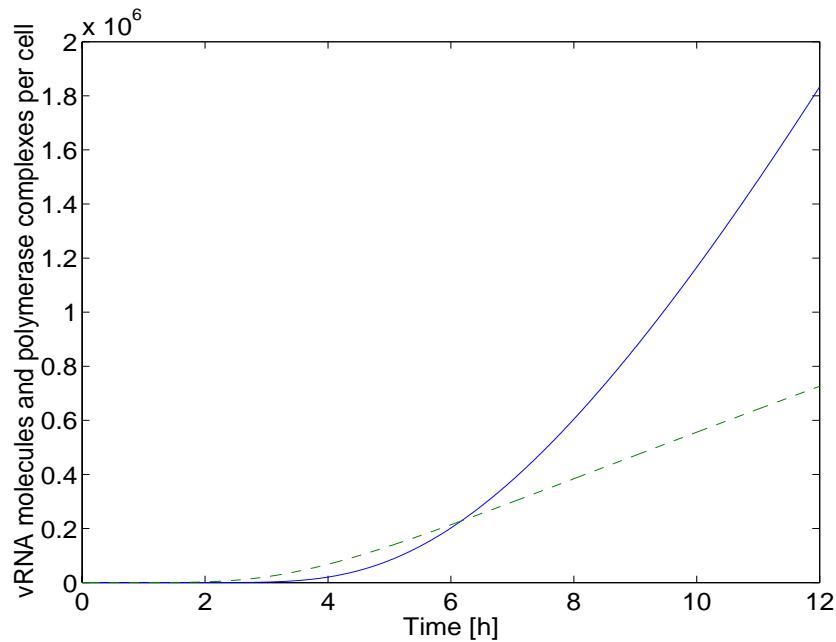


Figure 5.2 vRNA molecules and polymerase complexes in the nucleus. At the late stages of the infection the number of vRNA molecules (C_v) exceeds the number of viral polymerase complexes ($P_{Pol,nuc}$).

5.4.5 Particularities of Transcription Dynamics

As the number of polymerase complexes is supposed to be much lower than the number of vRNA segments to be transcribed, the number of produced vmRNA molecules, like the number of vRNA segments, can be considered as a uniform mass

of nucleotides. The number of nucleotides belonging to vmRNA molecules encoding the i -th protein ($C_{i,cyt}$ (*nucleotides/cell*), used, particularly, in the equations describing viral protein production) is calculated by formula

$$(5.4.6) \quad C_{cyt,i} = \omega_i C_{cyt},$$

where C_{cyt} (*nucleotides/cell*) is the total number of nucleotides in vmRNA molecules produced (see section 3). Such an approach is applied for the formulation of the reduced model (see section 2.9). However, as pointed out in section 2.3, in the detailed model the numbers of vmRNA molecules encoding different proteins are still considered separately to keep the possibility of model modifications. Factors ω_i (-) are taken into account when calculating the rate coefficient of the synthesis of vmRNA molecules encoding the i -th protein.

In the case of polymerase complex redundancy the term $k_{v-vm,i} P_{Pol,nuc}$ in (2.3.1), representing the rate of the synthesis of vmRNA molecules encoding the i -th protein ($\mu_{v-vm,i}$ (*nucleotides/h*)), would be proportional to the number of i -th vRNA segments (for $i = 1 \dots 6$; segments 7 and 8 are spliced), i.e., replaced by term

$$(5.4.7) \quad \mu_{v-vm,i} = \frac{k_{v-vm,i}}{L_{vm,i}} C_{v,i}.$$

Here, $k_{v-vm,i}$ (h^{-1}) is the rate coefficient of vmRNA synthesis, calculated by the same formula, as it is in section 2.3, and $L_{vm,i}$ (*nucleotides*) is the length of the vmRNA molecule encoding the i -th protein. For the calculation of the numbers of vmRNA molecules produced from the 7th and 8th genome segments (encoding M and NS proteins, respectively), the corresponding fractions of nucleotides of the segments involved must be taken into account (like it was done in section 3). At the same time, since in the previous case vmRNA molecules encoding different proteins are also considered separately, the number of equations describing vmRNA production is the same in both particular cases considered.

Finally, the formula for the rate of the synthesis of vmRNA molecules encoding the i -th proteins is similar to formula (5.4.5) for the synthesis rate of cRNA segments:

$$(5.4.8) \quad \mu_{v-vm,i} = k_{v-vm,i,max} \frac{1}{1 + a_{NP} P_{NP,nuc}}.$$

$$\cdot \frac{C_{v,i}}{K_{C_{v,i},v-vm}(P_{Pol,nuc}) + C_{v,i}} \cdot \frac{P_{Pol,nuc}}{K_{P_{Pol,nuc},v-vm}(C_{v,i}) + P_{Pol,nuc}} \cdot$$

5.5 Dynamics of Viral Protein Production

As discussed in sections 1.6.5 and 1.6.6, the synthesis of viral proteins is carried out by the cellular translation machinery. The rate of protein synthesis depends on the relation between the number of cellular ribosomes and the number of cytoplasmic vmRNA molecules to be translated. The former number makes up $R_0 = 5 \cdot 10^6$ *ribosomes/cell*, which significantly exceeds the latter number throughout the whole process of the infection (see sections 2.5 and 4.8). The situation when the number of cytoplasmic vmRNA molecules is higher than the number of cellular ribosomes is excluded and therefore not worth being considered. Consequently, it is reasonable to assume that the rates of viral protein synthesis, expressed by $k_{i,synt} \frac{C_{i,cyt}}{d_{rib}}$ in (2.5.1) and the corresponding term in (2.6.1), are proportional to the number of vmRNA molecules in the cytoplasm. Furthermore, since the number of cellular ribosomes does not seem to be significantly reduced by virus replication, it can be assumed to remain constant, which particularly allows considering the rate coefficients of viral protein synthesis $k_{i,synt}$ as constants.

Cellular ribosomes involved in protein synthesis are organized in polysome complexes (see section 1.5.2.3). In the model a polysome complex is assumed to incorporate the maximal number of ribosomes, i.e., equal to the ratio of the length of a vmRNA molecule to the distance between ribosomes on it (this assumption is taken into account by the term $k_{i,synt} \frac{C_{i,cyt}}{d_{rib}}$ in (2.5.1) and the corresponding term in (2.6.1)).

In reality, however, the number of ribosomes making up a polysome is not necessarily maximal. As reported, for example, by Singh (1996), polysome complexes involved in the translation of vmRNA molecules encoding a given protein have a certain size distribution, which changes in time and depends not only on the length of the

molecules considered, but also on such parameters as the rate of initiation, translocation, and release of ribosomes. Thus, the real number of viral proteins produced seems to be overestimated by the model. To improve this estimate, the rate coefficients $k_{i,synt}$, which are assumed in the model to be constants, should be treated as time-dependent functions of several parameters.

5.6 Mechanisms of Viral Genome Packaging

As pointed out before, the genome of influenza virus consists of 8 different RNA segments. So far, it is not clear if each of viral genome segments is selectively incorporated into a progeny virus particle or packaging of genome segments is a purely random process. Both hypotheses have an experimental support (Bancroft and Parslow, 2002; Fujii et al, 2003). In the case when the packaging of genome segments obeys a selective strategy (Fujii et al, 2003), each virus particle produced by a cell is most likely infectious (it contains 8 different genome segments), whereas random packaging (Bancroft and Parslow, 2002) implies that the number of infectious virus particles makes up just a low percentage of the total number of released virions. In addition, a virion might incorporate more than eight genome segments (Enami et al., 1991), which in the case of random packaging increases the probability that it is infectious.

Experimental data (H. Sann, personal communication, not shown) implies that not all virions are able to infect cells, which is also confirmed by Roy et al. (2000). In the case of selective packaging this fact can be explained by cellular events, e.g., related to virus binding, endocytosis, viral protein synthesis, and genome replication. However, according to experimental data (H. Sann, personal communication, not shown), the total number of released virions exceeds the number of infectious virions so significantly (by about two orders) that purely selective packaging does not seem to take place. It is rather reasonable to assume for modeling that vRNP complexes are packaged in a random, nonspecific manner.

In the model it is assumed for simplicity, that all virus particles contain eight genome segments. If all segments were produced in equal amounts, the probability for a virus particle to be infectious would be $P_{\text{inf}} = \frac{8!}{8^8} = \frac{1}{400}$ (Knipe et al., 2001). However, the real number of produced genome segments might be different. Indeed, the segments of the viral genome have different lengths (e.g. the vRNA encoding PB2 proteins has 2341 nucleotides and the vRNA encoding M1 and M2 proteins has 1027 nucleotides, Table 1.1), and the rates of their synthesis seem to differ from each other. Based on the assumption that viral polymerase complexes operate at the same rate on vRNA molecules of different length, it can be calculated that the probability for a released virion to be infectious is as small as $P_{\text{inf}} \approx \frac{1}{667}$ (see Appendix A2).

On the other hand, according to experimental observations, produced virus particles are infectious with a probability of $P_{\text{inf,exp}} \approx \frac{1}{150}$ (H. Sann, personal communication, not shown), which is appreciably higher than the values derived above for a random packaging of genome segments. There are two possible scenarios explaining this discrepancy.

The value of the infection probability increases, if more than eight segments are assumed to incorporate into progeny virus particles. Such a hypothesis was experimentally supported in 1991 (Enami et al., 1991), when a transfectant influenza virus particle, containing nine genome segments was artificially created. The probability that a virus particle containing nine genome segments has at least one copy of each gene is in the range from $\frac{1}{50}$ to $\frac{1}{90}$ (Roy et al., 2000; own calculations, not shown), which is higher than $P_{\text{inf,exp}}$. Thus, assuming, for example, that released virions can contain either eight or nine genome segments, it could be possible to find the ratio of the number of eight segment-containing virions to the number of nine segment-containing virions, corresponding to the experimental value of the infection probability.

The other scenario is based on the assumption that the packaging of virus genome is not purely random, but rather involves some selective mechanisms. Such mechanisms might be performed with the participation of short noncoding sequences surrounding coding regions of genome segments. It was particularly shown that these noncoding sequences contained signals required for transcription, replication, and packaging of genome segments (Nicholson et al., 1998; Luytjes et al., 1989).

In the model with reinfection and in the population model the presence of noninfective virions were taken into account by introducing the additional factors into the terms $k_{bud-rel,V_{rel}} P_{inf} V_{bud}$ in (2.1.1'') and $k_{bud-rel,V_{rel}} P_{inf} \frac{Z_{in}}{Z_0} V_{bud}$ in (2.1.1''). These factors are equal to the probability that a virion is infectious (P_{inf}), i.e., to its experimental value $P_{inf,exp}$.

5.6.1 Method to Identify the Mechanism of Packaging

It is remarkable that the factors limiting virus production do not depend on the packaging of the viral genome. Indeed, according to section 4.9, M1-vRNP complexes limit virus replication at the stage of virus budding. Under the assumption of random packaging, it means that the whole amount of newly produced M1-vRNP complexes is incorporated into progeny virus particles. Accordingly, when the selective packaging is assumed, completely consumed for progeny virus production are only M1-vRNP complexes of one sort (produced in the lowest amount), while M1-vRNP complexes of other sorts, together with viral envelope proteins, accumulate at the budding site.

Therefore, an experimental method to identify if the packaging of the viral genome is purely random or partially selective would be as follows. If an accumulation of M1-vRNP complexes is not observed at the budding site, the genome segments are packaged randomly; otherwise, a specific selection of appropriate genome segments does take place during virus budding.

5.7 Influence of NP Proteins on Virus Dynamics

The property of NP proteins to inhibit vmRNA production seems to affect virus dynamics at the early stage of the infection. According to the assumptions made so far, the nuclear concentration of NP proteins starts increasing earlier than that of other viral proteins (at approximately 0.3 h p.i.). This early increase is a consequence of the transfer of NP proteins with the incoming virus particles. Indeed, if the corresponding term ($k_{spl, P_{NP, nuc}} S_{nuc}$) is excluded from equation (2.5.2) for NP proteins, the number of NP proteins behaves similar to the number of other viral proteins (except M1 proteins, which are limiting, see section 4.4). About $5 \cdot 10^6$ amino acid residues of NP protein are transported into the cell with 10 virions (Table 1.1), which has an appreciable negative effect on vmRNA synthesis (see equation (2.3.1), $a_{NP} \approx 10^{-6}$). During the first hours after infection an essential part of redundant NP proteins is degraded. The degradation ends at about 1.5 h p.i., when vmRNA molecules and, consequently, viral proteins start being synthesized at the maximal rate.

Besides NP proteins, internalized virus particles deliver viral polymerase complexes to the nucleus. These polymerase complexes are also degraded, however, the system is less sensitive to polymerase degradation, which is, unlike NP protein degradation, not required for the initiation of transcription. Additionally, the number of internalized polymerase complexes and, consequently, the rate of their degradation, are much lower than those of NP proteins. Thus, protein degradation is profitable for vmRNA production; it results to the increase of the ratio of the number of polymerase complexes to the number of NP proteins, and, therefore, to the increase of vmRNA synthesis rate.

The event described in this section provides the example, when the reversibility of the switch from transcription to vRNA production (see section 1.6.4) plays an important role. Indeed, internalisation of the number of NP proteins comparable with the value of b_{NP} (10^6) mediates the direct switch from transcription to genome replication, whereas after the degradation of redundant NP proteins the reverse switch takes place.

As high enough number of viral components is synthesized and transported into the nucleus, the direct switch occurs again. The effect involved takes place for all values of the rate coefficients of internalization from 50% to 200% of their initial values.

5.7.1 Are Incoming NP Proteins Favorable for Virus Production?

To examine the influence the nuclear import of NP proteins on virus dynamics the term presenting the transfer of incoming NP proteins into the nucleus ($k_{spl, NP, nuc} S_{nuc}$) was excluded from (2.5.2) for NP proteins. Since vRNA production is no longer inhibited by the presence of NP proteins, the synthesis of all viral proteins starts earlier (at about 0.4 h p.i.) than in the situation when the incoming NP proteins are taken into account (about 1.5 h p.i.) (not shown). As discussed in section 1.6.2, NP proteins play an important role for the nuclear import of the viral genome (they carry NLSs). However, simulation results indicate that if NP proteins themselves did not enter the nucleus with vRNA segments, the number of produced virions would be approximately 9500 virions per cell (19% higher than in the case when NP proteins enter the nucleus, not shown).

Additionally, if NP proteins from internalized virions were absent in the nucleus, an increase of the rate coefficients of internalization would invariably result in an increase of the virus yield. Indeed, as in the considered situation NP proteins are not internalized at all, the rate of vRNA synthesis corresponding to the ratio of the numbers of internalized viral components is, evidently, higher than that corresponding to the ratio of the numbers of newly synthesized viral components; the faster the internalization of viral components the more efficient the process of vRNA synthesis. This statement is confirmed by simulation data summarized in Table 5.1: simulations, performed for the values of the rate coefficients of internalization changing from 90% to 200% of their initial values show that the virus yield represents a monotonous function of the internalization rate coefficients.

Table 5.1 Virus yield and limiting factors of virus replication for internalization rate coefficients changed by different factors in the case when NP proteins are not delivered into the nucleus ($k_{spl, NP} = 0$)

Factor	0.9	1.0	1.1	1.2	1.5
V_{rel}	9393	9529	9644	9748	10010
LF	B	B	A	A	A

LF: limiting factor

A: M1 proteins

B: vRNA molecules and M1 proteins

5.8 Limiting Factors. Hierarchy of Redundantly Produced Viral Components

As shown in section 4.9, if it is assumed that the influenza virus does not control the synthesis of its proteins and vRNA molecules, some of viral components accumulate in the nucleus and at the budding site. Other viral components are limiting for virus replication. Appendix A1 shows that the numbers of such viral components in most cases tend to zero (complete consumption for the production of new virions); however, in some situations they can also tend to constants or even increase.

Model modifications provide a possibility to reveal, which of the viral components are more critical for virus replication in comparison with others, and which of them are, in contrast, produced in redundant amounts. Based on an analysis of the numerical (and, sometimes, analytical) solution of model equations, it is usually also possible to predict the dynamics of viral components at the modifications involved.

M1 proteins were shown to limit virus production at the step of M1-vRNP complex formation and to be present in the nucleus in extremely low amounts (see section 4.9). This result can be confirmed by several arguments. For example, as pointed out in section 1.6, M1 is a matrix protein; among all proteins, making up a virus particle, it is the most abundant (Table 1.1). Thus, it could be expected that M1 proteins are critical for virus production. Besides that, experimental results show that M1 proteins

are found in the nucleus only in the association with vRNP complexes (Martin and Helenius, 1991b). In other words, M1 proteins do not accumulate in the nucleus and are completely consumed for the production of M1-vRNP complexes, necessary for the formation of progeny virions.

5.8.1 NP Proteins are the Second Critical Component at the Assembly of M1-vRNP Complexes

Suppose now that the number of M1 proteins in the nucleus is artificially maintained to be high enough for the synthesis of new M1-vRNP complexes. In the model this situation can be realized by excluding factor $P_{M1,nuc}$ from the term $k_{in,S_{in,nuc}} C_v \prod_l P_{l,nuc}$, describing the assembly of M1-vRNP complexes in (2.7.1) and

from the corresponding terms in (2.4.2) and in (2.5.2) for NP and NS2 proteins and polymerase complexes. Furthermore, the term $k_{in,P_{M1,nuc}} C_v \prod_l P_{l,nuc}$ in (2.5.2) for M1

proteins has to be removed. As after such a transformation of the model M1 proteins are no longer limiting, one of the other viral components must become a bottleneck for the assembly of M1-vRNP complexes. Simulation results reveal that the most critical viral component is now the number of NP proteins. This is also in agreement with the data from Table 1.1, which shows that NP proteins represent the most abundant component of a vRNP complex. Furthermore, as the number of nuclear NP proteins is coupled with the synthesis rate of vRNA molecules (NP proteins promote the replication of the viral genome, see section 1.6.4 and the terms

$k_{v-c,max} \frac{P_{NP,nuc}}{b_{NP} + P_{NP,nuc}} P_{Pol,nuc}$ in (2.4.1) and $k_{c-v,max} \frac{P_{NP,nuc}}{b_{NP} + P_{NP,nuc}} P_{Pol,nuc}$ in (2.4.2)), virus

production is limited by both viral components involved.

Based on the model it could be concluded that making NP proteins critical for virus production results in a situation when the number of produced virions represents an exponentially increasing function of time. Indeed, at the given set of model parameters the level of NP protein concentration kept in the nucleus is so low that

relation (4.3.1) is satisfied throughout the whole infection cycle. It means that both the number of produced vmRNA molecules and the number of produced polymerase complexes exponentially increase in time (see section 4.9). However, in the considered case the model does not allow predicting the exact dynamics of viral component production. As pointed out in sections 2.3 and 5.4, the behavior of viral components provided by the model is based on the assumption that the number of vRNA molecules exceeds the number of viral polymerase complexes, whereas throughout the whole process of the infection the inverse situation takes place. To obtain a realistic scenario of system behavior at the deficiency of NP proteins model equations might be modified to apply formulas (5.4.4) and (5.4.7) for the rates of genome replication and vmRNA production, respectively.

5.8.2 Relation Between the Number of NS2 Proteins, Polymerase Complexes, and vRNA Molecules

Assume now that NP proteins, side by side with M1 proteins, are contained in the nucleus in such high amounts that they do not limit virus replication. It means that in addition to the modifications of the model described in section 5.8.1, the term $k_{un,P_{NP,nuc}} C_v \prod_l P_{l,nuc}$ in (2.5.2) for NP proteins must be removed, and factors $P_{NP,nuc}$ must be excluded from the terms mentioned in section 5.8.1. According to the results of such simulations, NS2 proteins become limiting for the formation of M1-vRNP complexes. The whole number of NS2 proteins is incorporated into newly produced M1-vRNP complexes, while vRNA molecules and viral polymerase complexes accumulate in the nucleus (see Appendix A1).

Finally, consider the case when the nuclear concentration of NS2 proteins is also maintained to be higher than virions require for their replication. Simulation results show that in this case neither polymerase complexes nor vRNA molecules are completely consumed for the formation of new M1-vRNP complexes. Instead, both viral components involved accumulate in the nucleus. Such a scenario is reasoned by the reduced number of factors in the expression for the rate of packaging (the term

$k_{un,C_v} C_v \prod_l P_{l,nuc}$ in (2.4.2) and the corresponding term in (2.5.2)) resulting from model modifications involved. As follows from the numerical solution of the system of model equations, the order of the increase of the packaging rate remains lower than that of the synthesis rate throughout the whole process. At the same time, the numbers of both viral components ($P_{Pol,nuc}$ (amino acids/cell) and C_v (nucleotides/cell)) represent slowly increasing¹² functions of time (t, h):

$$P_{Pol,nuc}(t) = o(t), \quad t \rightarrow \infty;$$

$$C_v(t) = o(t), \quad t \rightarrow \infty.$$

This situation is similar to that described in Appendix A1 for the absence of the critical sort of system components (see relation (A1.6)). Additionally, as it can be seen from model equations (particularly, equation (2.4.2)), the numbers of polymerase complexes and vRNA molecules are coupled. It might be, consequently, concluded that the considered viral components are equivalent in respect to the incorporation to progeny virions.

5.8.3 Viral Components at the Budding Site

At the step of virus budding the process of virus production is limited by the number of newly produced M1-vRNP complexes. To determine, which of envelope proteins accumulating at the budding site (HA, NA, M2) is more critical for virus production, and which is, in contrast, redundant, let us, first, exclude factor $S_{un,bud}$ from the term

$$k_{bud,P_j,bud} S_{un,bud} \prod_l P_{l,bud}$$

describing the assembly of progeny virus particles in (2.6.2) for all envelope proteins and remove the corresponding term from (2.7.2). Such a modification of the model corresponds to a scenario that the number of M1-vRNP complexes at the budding site does not limit virus production.

¹² By definition, $f(t) = o(g(t))$, $t \rightarrow a$, if $\frac{f(t)}{g(t)} \rightarrow 0$, $t \rightarrow a$.

Unlike NP proteins and viral polymerase complexes, viral envelope proteins do not seem to significantly influence the dynamics of the synthesis of other viral components, and functions representing their numbers are, hence, not coupled. Consequently, newly produced envelope protein, the number of which is the most critical for the formation of virus particles, represents the only limiting factor. Simulation results show that the viral component that limits virus production with a redundancy of M1-vRNP complexes is the number of HA proteins.

Making now HA proteins redundant for virus production, it can be concluded that from the two remaining envelope proteins (M2, NA) NA proteins are more critical for virus production. However, the number of NA proteins does not decrease in time, tending to zero. Instead, it increases, approaching to a constant. Indeed, after model modifications made in this section the equation for the number of NA proteins ($P_{NA,bud}$ (amino acids/cell)) has the form

$$(5.8.1) \quad \frac{dP_{NA,bud}}{dt} = k_{NA,ER-bud} P_{NA,ER} - k_{bud,P_{NA,bud}} P_{NA,bud} P_{M2,bud} - k_{NA,bud-deg r} P_{NA,bud}$$

The number of envelope proteins in the ER (particularly, $P_{NA,ER}$ (amino acids/cell)) increases proportional to the first power of time (t, h):

$$P_{NA,ER} = k_{NA,ER} t,$$

and the number of M2 proteins at the budding site ($P_{M2,bud}$ (amino acids/cell)) also increases linearly:

$$P_{M2,bud} = k_{M2,bud} t$$

(Here, $k_{NA,ER}$ (amino acids/h) and $k_{M2,bud}$ (amino acids/h) are positive constants).

Consequently, equation (5.8.1) at the late stages of the infection reduces to

$$(5.8.2) \quad \frac{dP_{NA,bud}}{dt} = k_{NA,ER-bud} k_{NA,ER} t - k_{bud,P_{NA,bud}} k_{M2,bud} t P_{NA,bud} - k_{NA,bud-deg r} P_{NA,bud}$$

As shown in Appendix A1, equation (5.8.2) corresponds to the situation, when the function $P_{NA,bud}$ described by it tends to a positive constant. Furthermore, the value of the rate constant of packaging $k_{bud,P_{NA,bud}}$ (h^{-1}) is small enough for $P_{NA,bud}$ to represent an increasing function of time.

5.9 Are There Any Other Possible Laws of Virus Growth?

As mentioned in section 4.3, the proportion between the numbers of viral proteins produced is kept throughout the whole process of the infection. Taking this into account, it can be seen from the term $k_{v-vm,i,max} \frac{1}{1 + a_{NP} P_{NP,nuc}} P_{Pol,nuc}$ in (2.3.1) that for any choice of model parameters there is a certain moment of time p.i., when the number of vmRNA molecules starts to grow linearly. The rate of vmRNA production is equal to $\mu_{v-vm,prod}$, which is defined by the ratio of the number of polymerase complexes to the number of NP proteins (see section 4.10.1). It is also clear that at the latest stages of the infection the number of vmRNA invariably tends to constant.

Thus, the polynomial stage of virus growth with its parabolic and linear phases is the property of any solution to the considered system of differential equations. It is evident that the initial exponential stage of virus growth also takes place independently of the set of initial conditions. Consequently, variations of model parameters, e.g., rate constants of degradation or transport, or switch parameters, can influence the time scale of the process, the character and the duration of the transitional stage, but the two major stages of progeny virus growth are always an exponential followed by a polynomial increase.

5.9.1 Duration of the Exponential Stage

The time interval, at which the number of released virions increases exponentially, depends on the ability of NP proteins to suppress vmRNA production, which is defined by a_{NP} . From the analysis of the system of model equations, particularly equations (2.4.2), (2.3.1) and (2.5.1) (the last two equations are considered for viral polymerase complexes)

$$\frac{dC_v(t)}{dt} = k_{c-v}(t)P_{Pol,nuc}(t) - F_{C_v}(t)C_v(t) + o(P_{Pol,nuc}(t)), \quad t \rightarrow \infty$$

$$\frac{dC_{Pol,nuc}(t)}{dt} = k_{v-vm,Pol}(t)P_{Pol,nuc}(t) - F_{C_{Pol,nuc}}(t)C_{Pol,nuc}(t)$$

$$\frac{dP_{Pol,cyt}(t)}{dt} = k_{Pol,synt}(t)\frac{C_{Pol,cyt}(t)}{d_{rib}} - F_{P_{Pol,cyt}}(t)P_{Pol,cyt}(t)$$

($F_i(t)$, $i \in \{C_v, C_{Pol,nuc}, P_{Pol,cyt}\}$ (h^{-1}) are continuous nonnegative functions) it can be easily concluded that if the influence of NP proteins was neglected ($a_{NP} = 0$), the exponential stage of virus growth would go on throughout the whole process of the infection.

It is remarkable that such a conclusion can be made independently on the assumed relation between the number of polymerase complexes and the number of vRNA molecules in the nucleus (see section 5.4). Indeed, if the rates of vRNA and vmRNA synthesis in (2.4.2) and in (2.3.1) are proportional rather to the number of vRNA molecules than to the number of polymerase complexes,

$$\frac{dC_v(t)}{dt} = k_{c-v}(t)C_c(t) - F_{C_v}(t)C_v(t) + o(C_v(t)), \quad t \rightarrow \infty$$

$$\frac{dC_{Pol,nuc}(t)}{dt} = k_{v-vm,Pol}(t)C_v(t) - F_{C_{Pol,nuc}}(t)C_{Pol,nuc}(t)$$

$$\frac{dP_{Pol,cyt}(t)}{dt} = k_{Pol,synt}(t)\frac{C_{Pol,cyt}(t)}{d_{rib}} - F_{P_{Pol,cyt}}(t)P_{Pol,cyt}(t)$$

the solution to the system of model equations for the number of vmRNA molecules (and, hence, for the numbers of all newly produced viral components) will be, obviously, also represented by exponentially increasing functions of time.

Based on the solution to the system of model equation, it could be assumed that the number of released virions could also exponentially increase in time, if the number of nuclear M1 proteins is maintained at such a high level that it does not limit the formation of new M1-vRNP complexes. Such a modification of the considered biological system would make the number of NP proteins critical for virus production, and, hence, insufficient to inhibit vmRNA synthesis. However, as NP proteins at the same time promote genomic vRNA synthesis, the level of vRNA molecules in the nucleus would be very low, and, therefore, the model does not allow adequately describing the system dynamics (see section 5.8.1).

Another reason for the transition from the exponential stage to the polynomial might be the observation that cRNA strands are produced only for a short period of time p.i. (Flint et al., 2000). Taking this into account would, evidently, result in a polynomial increase of the number of vRNA molecules, and, hence, in a polynomial increase of the number of virions released. However, since the mechanism for the inhibition of cRNA synthesis is still not yet understood, it is not considered in the model.

5.10 Further Modifications of the Detailed Single Cell Model

The model allows the simulation of the overall dynamics of virus replication, the analysis of the use of cellular resources and the testing of hypotheses concerning basic virus replication mechanisms, thus, essentially facilitating future studies of influenza viruses at a cellular level. The behavior of the number of newly produced viral components provided by simulations is in close agreement with results obtained by other models. A general rule states that every mathematical model should be as simple as possible and as complex as necessary. It is evident that any extension of the model scope and accuracy invariably leads to an increase of its complexity. However, if it is necessary, the structure of the model can be easily modified to consider additional features of the virus replication cycle.

For example, several equations could be introduced to express the dynamics of splicing of M and NS vRNA molecules and the effect of nuclear NS1 proteins on it (Nicholson et al., 1998; Juan, 1998). By modifying the rate coefficients of vRNA synthesis, it is also possible to take into account that vRNA molecules encoding different viral proteins are processed at different stages of the virus replication cycle (Watanabe et al., 2001). The possibility of such modifications of the model is, particularly, the reason why the numbers of vRNA molecules of different sorts are kept represented by different functions. Furthermore, in the case when a reinfection is taken into account (or when virus internalization occurs slowly) the inhibitive effect

of M1 proteins accumulating in the cytoplasm on the nuclear import of genome segments released from the endosome (Martin and Helenius, 1991b) can be considered. Although the model does not consider in detail endocytotic and exocytotic pathways, it still can take into account (by incorporating several additional equations) certain events taking place during these pathways, e.g., virus binding to different number of cellular surface receptors (addressed, for example, in the study of Dee and Schuler (1997)) and coated pit formation.

As shown in section 4.8, virus replication does not exhaust the pools of cellular resources. However, balance equations for the numbers of cellular precursor mRNA molecules, free nucleotides, and amino acids could be easily introduced into the model to investigate the change of cellular metabolism after infection. It would allow, for example, expressing mathematically the inhibitive effect of the NS1 protein on the splicing of precursor mRNA molecules (Lamb et al., 1981), as well as the action of the NS1 protein as a translational enhancer for vmRNA molecules and its ability to retain cellular precursor mRNA molecules in the nucleus (Fortes et al., 1994; Nemeroff et al., 1998). Additionally, taking into account the balance of cellular resources would allow estimating more precisely the total capacity of the cell to produce virions. For this purpose the synthesis of amino acids and nucleotides after infection can also be considered. Finally, it would be possible to incorporate into the model a balance of energy and thus to observe the impact of virus replication on the cellular pools of ATP and NAD(P)H molecules.

Other modifications and improvements of the model can be made as new details of the influenza virus replication cycle are revealed.

5.11 Methods to Increase the Number of Virions Produced in a Cell

According to simulation results, two parameters, the variations of which mainly increase virus production, are the speed of viral polymerase complexes and the elongation rate of polypeptide chains of viral proteins (see section 4.11.5). Consequently, the most effective ways to increase the virus yield are speeding up viral polymerase complexes (e.g., by using more efficient promoters) or the increasing of the translation efficiency of viral proteins (e.g. by virus mutants, which efficiently inhibit the processing of cellular mRNA molecules). What is more, the process of virus production can be effectively optimized by weakening the ability of NP proteins to bind to elongating RNA strands, which has a strong inhibitive effect on the transcription of virus genome (at low values of the switch parameter a_{NP} the increase of the number of produced virions in time becomes close to exponential, see section 4.11.1.2). As M1 proteins were shown to represent a bottleneck for virus replication (see section 4.9), their supply to the cellular nucleus would also result in an increase of the number of produced virions. Finally, the virus yield can be appreciably increased by increasing the efficiency of the transport of viral components into and out of the nucleus (e.g., by modifying the properties of signal sequences, see section 4.11.3) or by increasing the lifetime of the cell (see section 5.3).

While mentioned above modifications of the considered biological system have significant effects on the virus yield, to a lower extent an increase of the number of produced virions can also be achieved by a series of other variations of system parameters. Such variations are, for instance, the improvement of the impact of NP proteins on genomic vRNA production (see section 4.11.1.2), an increase of internalization and release rate coefficients (e.g., by the increasing of binding and fusion activities of HA proteins and cleavage activity of NA proteins, respectively, see section 4.11.2), as well as a decrease of the degradation rates of vmRNA molecules and cytoplasmic viral proteins (by the regulation of, correspondingly, cellular nuclease and protease activities, see section 4.11.8). Although based on the results of simulations the MOI optimal for virus production was found (see section

4.10), the increase of the virus yield reasoned by bringing the MOI to its optimal value is not very significant.

5.12 Strategies for Antiviral Therapies and Vaccine Production Optimization

The detailed single cell model can be used to identify molecular targets for antiviral therapies. As shown in section 4.9, the number of M1 proteins in the nucleus limits the replication cycle of the virus at the assembly of M1-vRNP complexes. Consequently, virus production could be effectively suppressed by disabling nuclear M1 proteins. Furthermore, as pointed out in section 5.7.1, NP proteins internalized have a negative effect on the virus yield. The delivery of the high number of NP proteins into the nucleus of infected cells would block vmRNA synthesis and, hence, the production of progeny virions. An additional option to reduce the number of virions produced would be the shortening of the lifetime of infected cells (see section 5.3).

Several methods for the increase of the virus yield, discussed in section 5.11, could be applied in practice for the optimization of vaccine production. Such methods are the expansion of the lifetime of a cell, or the delivery of M1 proteins into the nucleus. Other ideas, however, would be difficult to realize. Indeed, vaccines are produced against a certain type of virus, which cannot be modified. One possible way out could be the creation of a reassortment virus, which has a desired property (e.g., improved polymerase complexes), and possesses the HA and NA proteins of the required virus strain.

More hypotheses concerning the optimization of vaccine production in cell cultures can be derived based on the population model. As shown in section 4.15.2, the virus yield can be significantly improved by decreasing of the MOI. Besides that, the population model indicates that the number of produced virions increases if virus-induced apoptosis (of either infected or uninfected cells) is inhibited, or the infection rate is decreased (see section 4.15.3).

5.13 Limits of Population Model Applicability

At the given set of parameters the population model provides an upper estimate for the number of released virions. Indeed, the structure of the system of model equations implies that the synthesis of viral components, the number of which is taken for the calculation of the number of released virions, starts from the beginning of the primary infection. In reality, however, at the late stages of the process primarily infected cells often make up only a minor part of the total number of infected cells, most of the cells being infected by newly produced virions. Consequently, higher precisions of the results provided by the model (especially for low MOI values, see section 4.15.2) correspond to shorter lags between the beginning of the infection and the beginning of virus release. For the model to adequately predict the population dynamics the lag must be much shorter than the duration of the process of virus replication.

According to simulation results, secondarily infected cells start to produce virions at about 10 h p.i. (Fig. 4.23), which is much less than 90 h (the duration of virus replication process). Besides that, little is known concerning the exact values of the rate coefficients of viral component transport. For example, as shown in section 4.11.3.1 for the single cell model, increasing of the efficiency of viral component transport can result in approximately threefold decrease of the lag. Thus, at the given conditions the population model developed here seems to provide reasonable estimates for the virus yield and the size of cell populations. These estimates are to be further confirmed by experiments.

5.14 Use of the Reduced Model

As mentioned in section 2.9, the reduced model is mainly required as a starting point for the development of structured population balance models. A structured population balance model implies that the numbers of viral components in different compartments of the cell are considered as structure parameters of the cell population.

The number of cells Z (*cells/nL*) represents a function of time and the number of vRNA molecules, viral proteins, etc. (parameters i_1, \dots, i_n):

$$Z = Z(t, i_1, \dots, i_n).$$

The total number of virions in the extracellular medium is described by an independent state variable $V_{ex}(t)$ (*virions/nL*), which accounts for the contribution of all cells in the population.

Thus, the reduced model is aimed to provide the data concerning the dynamics of intracellular viral components. Accordingly, it is reasonable to consider all the functions describing the number of viral components, including the number of extranuclear virions and the number of assembled virions, related to the cell. For the same reason, it is not necessary to separate the number of extracellular virions from the total number of extranuclear virions and the number of released virions from the total number of virions assembled in the cell.

On the other hand, the reduced model can be also used as a simplified version of the detailed model. In this case, two additional state variables describing the number of extracellular virions and the number of released virions could be introduced. Another option would be to consider the number of extranuclear virions and the number of assembled virions related to the volume of medium and to use them as approximations for the number of extracellular virions and the number of released virions, respectively.

5.14.1 Is a Further Model Reduction Possible?

All the steps of the infection cycle the reduced model represented by equations (2.9.1) – (2.9.7) takes into account (except the step of the packaging of viral components, see below in section 5.14.2) represent branch points of the process.

It could be thought that the cytoplasmic and nuclear pools of vmRNA molecules can be lumped together. However, lumping these pools together would imply that the nuclear export of the viral genome and its translation are not separated anymore. As a

consequence, all the vmRNA molecules produced would be available for translation. Thus, after such a modification the model would not properly reflect the behavior of the biological system considered. Moreover, as the ribosome operation, defining the rate of viral protein production is fixed and cannot be changed, the lag between the beginning of the infection and the beginning of virus release would not be controlled by any model parameters (see section 4.12). Finally, omitting the step of vmRNA transport from the nucleus into the cytoplasm would deprive the model of the flexibility in respect to further possible modifications, e.g., taking into account the role of NS1 proteins in the nuclear export of cellular and viral mRNA molecules (see sections 1.6.3 and 1.6.5).

For the nuclear and cytoplasmic pools of proteins the situation is similar. Nevertheless, lumping these pools together, i.e., considering together the nuclear import and packaging of viral proteins does make sense. Indeed, it seems that the virus does not have any mechanisms for the specific regulation of the transport of viral proteins from the cytoplasm into the nucleus, and, accordingly, at this step there is no need in model modifications. Additionally, the contribution of the delay of packaging concerned with the nuclear import of viral proteins to the lag of virus production can be taken into account by changing the rate coefficient of the nuclear export of vmRNA molecules.

On the other hand, provided by certain restrictions of modeling purposes, a further reduction of the model still can be possible. For example, at certain sets of model parameters it can be possible to reduce the number of differential equations of the reduced model by one. Such a modification of the reduced model involved, which will be referred to as the “simplest model”, is considered in section 5.14.2.

5.14.2 “Simplest Model” for Virus Production

As shown in section 4.11.6, variations of the packaging rate constant k_{un} , as well as variations of the rate constant k_{bud} , do not influence the number of released virions

significantly. This is explained by the limitation of the formation of M1-vRNP complex by the number of newly produced M1 proteins. Consequently, it would be expected that the virus yield in the reduced model is not sensitive to variations of the rate constant k_{pck} (shown in section 4.12.3); it is completely defined by the number of M1 proteins produced.

In fact, if only the number of assembled virions is to be investigated, differential equation (2.9.7) describing virus release is not required. Instead, for the number of assembled virions it is possible to write an algebraic equation, expressing the proportionality of the number of released virions to the number of M1 proteins produced:

$$(5.14.1) \quad V_{rel,red} = \frac{1}{P_{M1,vir}} P_{M1}.$$

Thus, the “simplest model” is represented by as few as 9 ODEs.

Besides that, $k_{pck,C_v} C_v \prod_l P_l$ in (2.9.5) and the corresponding term in (2.9.6), describing the packaging of viral components are also can be excluded. These terms have no influence on the location of produced proteins. Indeed, the major part of the viral polymerase complexes and the NP proteins is accumulated in the nucleus, and only an insignificant number is required for progeny virus production. On the other hand, all the M1 proteins are incorporated into newly produced virions. Consequently, the two equations considered can be rewritten in the form

$$(5.14.2) \quad \frac{dC_v}{dt} = k_{c-v} P_{Pol} + k_{spl,C_v} V_{ex} - k_{v-degr} C_v$$

$$(5.14.3) \quad \frac{dP_i}{dt} = k_{i,sym} \omega_i \frac{C_{cvt}}{d_{rib}} + k_{spl,P_i} V_{ex} - k_{i,deg} P_i$$

$$i \in \{Pol, NP, M1\}$$

Thus, the behavior of the number of assembled virions at different sets of model parameters can be investigated based on the “simplest model”, represented by equations (2.9.1)-(2.9.4), (5.14.1)-(5.14.3). However, the use of this model is limited by sets of model parameters, at which M1 proteins are limiting throughout the whole infection cycle. As discussed in section 4.11, this is not always the case; limiting

factors at vRNP assembly, unlike those at virus budding, are sensitive to parameter changes.

The reduced model presented by equations (2.9.1)-(2.9.7), in contrast, allows considering virus production independently of the bottlenecks. Additionally, it considers separately viral component assembly, thus making possible both to observe the changing of limiting factors during the infection cycle and to investigate their sensitivity to parameter changes (e.g., changes of the switch parameters a_{NP} and b_{NP}). Thus, the reduced model (2.9.1)-(2.9.7), despite containing one extra differential equation, is more helpful to better understand the dynamics of viral component production than the “simplest model” (2.9.1)-(2.9.4), (5.14.1)-(5.14.3).

5.15 Possible Reasons for Cell Death

According to experimental observations, cells infected with influenza virus die at about 10-12 h p.i. (Roy et al., 2000; J. Schulze-Horsel, Y. Genzel, personal communication). In the detailed single cell model the average lifetime of a cell is assumed to be 12 h. A more precise estimate can be derived based on the behavior of the number of living cells after infection (see Appendix A3). Particularly, the dynamics of the population of dead cells provided by the population model corresponds to the value of the average lifetime of an infected cell equal to approximately 10 h.

The exact mechanisms, by which the virus induces cell damage, finally leading to cell death, are not fully understood. As shown in section 4.8, cellular resources consumed for virus replication, such as the number of free nucleotides and amino acids, make up only an insignificant part of the total number of the cellular resources. Therefore, cell death does not seem to be correlated with the exhaustion of the pools of these resources.

The most likely reason for the early death of influenza virus-infected cells is virus-induced apoptosis, an active process of cellular self-destruction (see section 1.5.5).

The positive role of apoptosis for virus replication was pointed out by Stray and Gillian (2000). It consists in the removal of the cells that have already been infected from those capable of producing more virions. Influenza virus-induced apoptosis is regulated by both cellular and viral factors, as well as by their interactions. Indeed, according to results of several studies, influenza virus, side by side with some other viruses (e.g., baculovirus; Zhou et al., 1998), interacts with the apoptotic response of the host cell by either promoting or inhibiting cell death.

Olsen et al. (1996a) demonstrated that particularly in MDCK cells influenza virus-induced apoptosis is inhibited by the expression of *bcl-2*, a human proto-onco-gene known to inhibit many forms of apoptosis. Other cellular factors commonly involved in apoptotic processes, such as calcium and reactive oxygen species, are, in contrast, involved in triggering the death of influenza virus-infected cells (Olsen et al., 1996b). Among viral factors, viral NS1 proteins were reported to be a major inducer of apoptosis (Schultz-Cherry et al., 2003). It was shown that the expression of NS1 proteins in an inducible system was sufficient for the induction of apoptosis in MDCK cells. It was also shown that cell death was most likely induced by the binding of NS1 proteins to specific cellular RNA molecules or by a complete inhibition of PKR, a double-stranded RNA-dependent kinase, which acts as an antiviral protein inhibiting both cellular and viral protein synthesis. On the other hand, M1 proteins were shown to inhibit viral apoptosis by the specific interaction with caspase-8 in chicken embryos (Zhirnov et al., 2002). A critical role of the activation of caspases in cells infected by equine influenza viruses was discussed by Lin et al. (2002). The impact of the interaction of cellular and viral factors on the process of programmed cell death was investigated, for example, in the study of Morris et al. (1999). It was shown that in MDCK cells NA proteins promoted apoptosis by the mechanism occurring at virus entry into the cell and based on the activation of the growth factor TGF- β , known as an inducer of apoptosis.

Besides the direct interaction of the influenza virus with the apoptotic response of the cell, other scenarios of the induction of apoptosis might also be possible. As discussed in section 1.6.5, the synthesis of cellular proteins drastically slows down after infection (Park and Katze, 1995). Additionally, cellular functions can be

compromised by the consumption of nuclear precursor mRNA molecules, i.e., their cap fragments for vmRNA production. As discussed in section 4.8, the number of precursor mRNA molecules consumed for virus production seems to be negligible. However, as the cap snatching is a random process, it can exhaust some sorts of mRNA molecules present in low numbers of copies.

Presumably, at the presence of influenza virus particles in cell cultures not only infected cells, but also uninfected cells can die due to virus-induced apoptosis (not shown). Apoptosis of uninfected cells is thought to be initiated by specific ligands, such as double-stranded RNA molecules (Ludwig et al., 2003), released by infected cells and binding to the receptor proteins of uninfected cells. To take this into account in the population model the term $k_{ap,un}Z_{un}Z_{in}$ in (2.12.1) was introduced.

The detailed mechanisms of influenza virus-induced apoptosis still have to be experimentally elucidated. Based on such results, simulation time T in the detailed single cell model, which is now set as an initial condition ($T=12 h$), could be used as an additional parameter in simulations, and the influence of the apoptosis on virus yields could be investigated.

5.16 Directions for Further Experimental Work

The model still needs the experimental verification of its parameters, such as rate coefficients, parameters defining the dynamics of the switch from vmRNA production to genome replication, as well as the exact time scale of the individual steps. Experimental work to identify key model parameters and to test several options regarding the structure of the model is in progress. It focuses mainly on the infection of cells under conditions relevant for vaccine production processes, where MDCK cells are grown in static cultures and microcarrier systems (Genzel et al., 2001; Genzel et al., 2003). Having also available comprehensive experimental data on cell metabolism during infection and the analysis of virus propagation in cell populations, it might be possible to better understand basic laws of virus infection both in a single mammalian cell and in a population of cells.

6 Summary

Presented in this study was a structured mathematical model of influenza A virus replication in mammalian cells, which is the first model covering all steps of the infection cycle from virus attachment and internalization to viral protein expression, genome synthesis, assembly of M1-vRNP complexes, and release of progeny virions to the extracellular medium. The major purposes of the present study are an investigation of the dynamics of virus growth and viral component production, a better understanding of the interaction of virions with their host cells, and the formulation of the ideas concerning the improvement of virus yields in vaccine production processes.

Based on the detailed single cell model, it was found that the process of progeny virus release by a single cell consisted of two main stages, an initial exponential and a late polynomial, comprising parabolic and linear phases. Analysis of model equations clearly showed that the existence of the polynomial stage of virus growth was a consequence of the inhibitive effect of NP proteins on the transcription of the viral genome. The ability of NP proteins to suppress vmRNA synthesis is expressed by the parameter a_{NP} , which also defines the duration of the exponential stage. It was shown that certain viral components represented bottlenecks for virus production at different stages of the replication cycle. Namely, M1 proteins represent a limiting factor at the production of M1-vRNP complexes, whereas M1-vRNP complexes themselves are limiting during virus budding. Additionally, it was worked out, which of the remaining viral components were produced in redundant amounts, and which of them were, in contrast, more critical. The dynamics of viral components limiting the production of progeny virions was shown to be sensitive to variations of some model parameters, such as the rate coefficients of virus internalization and the rate constants of the degradation of viral proteins in the nucleus. Besides that, it was shown that the behavior of the system was strongly correlated with the switch from vmRNA

production to genome replication, which, in turn, depends on the values of switch parameters, as well as on the nuclear concentration of NP proteins. At last, analysis of limiting factors of virus replication allowed formulating an experimental method to identify if the incorporation of genome segments into a progeny virion is a purely random process, or some selective mechanisms take place.

The interaction of virus particles with the host cell was mainly analyzed in respect to the consumption of cellular resources by virus replication. Simulations showed that the pools of cellular resources, such as the number of free cellular nucleotides and amino acids, as well as precursor mRNA molecules, are not significantly influenced by virus replication. It was determined that if the cell was able to produce virions until the complete exhaustion of its free amino acids (the most critical resource), even the initial pool of free amino acids would be sufficient to produce about $1.3 \cdot 10^4$ virions, which is approximately two times more than the number of virions released within 12 h p.i. (average lifetime of the cell). It was also shown that transport events did not limit the process. Relying on these arguments, it was particularly concluded that the early death of cells infected by influenza virus was most likely reasoned by virus-induced apoptosis.

Finally, the model allowed revealing the methods to improve the number of virions produced in the cell and formulating the hypotheses concerning the optimization of vaccine production processes, as well as the strategies for antiviral therapies. Thus, all three major purposes of this study were achieved. Besides that, several model modifications, which can be helpful for solving different important tasks, were considered.

From the investigation of the sensitivity of the system behavior to parameter changes it can be concluded that variations of model parameters such as, for example, rate constants of the dissociation of virions from the cellular surface or rate constants of the assembly of M1-vRNP complexes and progeny virus particles, have a negligible effect on both the virus yield and limiting factors of virus replication. Furthermore, several sequences of the steps of the infection cycle contain no branch points and can be, therefore, lumped together. These arguments provided the basis for the model

reduction. The reduced model of virus replication in a single cell has a rather simple structure, comprising as few as 10 differential equations. The dynamics of virus replication obtained from the reduced model resembles that obtained from the detailed model. Consequently, the model can be used for the development of structured population balance models considering the interactions of cells infected by different numbers of virus particles.

Introduction of a reinfection to the model for a single cell shows that the number of produced virions differs only slightly from that in the model without reinfection. What is more, limiting factors of virus production, as well as the optimal value of the MOI in respect to the virus yield, are the same for both models. Thus, it can be concluded that for the single cell model the reinfection is not important.

The model with a continuous infection allowed revealing the optimal way of the infection of cells. It was shown that the continuous supply of virions to the volume of medium surrounding the cell did not increase virus yield, and the optimal strategy of infection with respect to the maximization of the number of released virions seems to be the infection of the cell at the initial moment of time without further supply of virions.

Taking into account the balances for the populations of uninfected, infected, and dead cells allowed simulating the dynamics of virus production in microcarrier systems and to obtain realistic scenarios of the process, which are in good agreement with experimental data. Particularly, relying on simulation results, the optimal time of virus harvesting was estimated. Based on the population model it is possible to predict the changes in the dynamics of cell and virus populations at different variations of model parameters, and to investigate the dependency of the population sizes both on the MOI and on the ability of individual cells to produce virions. The corresponding changes in the dynamics of intracellular viral components can also be investigated. Besides that, the model allowed obtaining estimates for the average lifetime of a cell after infection at different initial conditions; particularly, it was possible to estimate the average lifetime of an infected cell. It was noted that unlike the single cell model,

the population model did not reveal the value of the MOI optimal for virus production; instead, the total number of virions produced by the system represented a monotonously decreasing function of the MOI. Being based on the reasonable and convenient simplifying assumption concerning the number of cells involved in the process of virus production, the population model keeps the simple structure peculiar to the single cell model. It adequately describes the system behavior in the situations when the lag between the beginning of the infection and the beginning of virus release is short in comparison with the duration of virus replication stage in the fermentation process (about 90 h), which takes place for the given set of model parameters. Indeed, cells infected by a secondary infection start to produce virus particles at approximately 10 h p.i. For the cases when virus release starts late after infection the model can provide approximate data concerning the population dynamics, particularly, upper estimates of the virus yield.

Providing the data concerning the overall dynamics of virus replication and making possible the testing of hypotheses concerning basic virus replication mechanisms, the model developed in this study essentially facilitates future studies of influenza viruses at a cellular level. Its structure can be easily modified to incorporate additional details of the virus replication cycle. Experimental work to test several options regarding the structure of the model and to identify key model parameters, such as those defining the time scale of individual steps and the switch from vmRNA production to genome replication is in progress.

References

Alberts B, Bray D, Lewis J. 2002. Molecular biology of the cell. 4th ed. *Garland Publishing, Inc.*

Allen TD, Cronshaw JM, Bagley S, Kiseleva E, Goldberg MW. 2000. The nuclear pore complex: Mediator of translocation between nucleus and cytoplasm. *J. Cell Sci.* 113(10): 1651-1659.

Avalos RT, Yu Z, Nayak DP. 1997. Association of influenza virus NP and M1 proteins with cellular cytoskeletal elements in influenza virus-infected cells. *J. Virol.* 71(4): 2947-2958.

Azzeh M, Flick R, Hobom G. 2001. Functional Analysis of the Influenza A Virus cRNA Promoter and Construction of an Ambisense Transcription System. *Virology.* 289(2): 400-410.

Baigent SJ, McCauley JW. 2001. Glycosylation of haemagglutinin and stalk-length of neuraminidase combine to regulate the growth of avian influenza viruses in tissue culture. *Virus Res.* 79(1-2): 177-185.

Bailey JE. 1998. Mathematical modeling and analysis in biochemical engineering: Past accomplishments and future opportunities. *Biotechnol. Prog.* 14(1): 8-20.

Bancroft CT, Parslow TG. 2002. Evidence for segment-nonspecific packaging of the influenza a virus genome. *J. Virol.* 76(14): 7133-7139.

Baudin F, Petit I, Weissenhorn W, Ruigrok R. 2001. In vitro dissection of the membrane and RNP binding activities of influenza virus M1 protein. *Virology.* 281(1): 102-108.

- Barman S, Adhikary L, Kawaoka Y, Nayak DP. 2003. Influenza A virus hemagglutinin containing basolateral localization signal does not alter the apical budding of a recombinant influenza A virus in polarized MDCK cells. *Virology*. 305(1): 138-152.
- Beauchemin C, Samuel J, Tuszynski J. 2005. A simple cellular automaton model for influenza A viral infections. *J. Theor. Biol.* 232(2): 223-34.
- Beretta E, Kuang Y. 1998. Modeling and analysis of a marine bacteriophage infection. *Math. Biosci.* 149(1): 57-76.
- Bocharov GA, Romanyukha AA. 1994. Mathematical model of antiviral immune response. III. Influenza A virus infection. *J. Theor. Biol.* 167(4): 323-360.
- Bui M, Whittaker G, Helenius A. December, 1996. Effect of M1 protein and low pH on nuclear transport of influenza virus ribonucleoproteins. *J. Virol.* 70(12): 8391-401.
- Cassetti MC, Noah DL, Montelione GT, Krug RM. 2001. Efficient translation of mRNAs in influenza A virus-infected cells is independent of the viral 5' untranslated region. *Virology*. 289(2): 180-185.
- Chanturiya AN, Basanez G, Schubert U, Henklein P, Yewdell JW, Zimmerberg, J. 2004. PB1-F2, an influenza A virus-encoded proapoptotic mitochondrial protein, creates variably sized pores in planar lipid membranes. *J. Virol.* 78(12): 6304-6312.
- Chen W, Calvo PA, Malide D, Gibbs J, Schubert U, Bacik I, Basta S, O'Neill R, Schickli J, Palese P, Henklein P, Bennink JR, Yewdell JW. 2001. A novel influenza A virus mitochondrial protein that induces cell death. *Nat. Med.* 7(12): 1306-1312.
- Cros JF, Palese P. 2003. Trafficking of viral genomic RNA into and out of the nucleus: influenza, Thogoto, and Borna disease viruses. *Virus Res.* 95(1-2): 3-12.

Daly JM, Newton JR, Mumford JA. 2004. Current perspectives on control of equine influenza. *Vet. Res.* 35(4): 411-423.

De Gooijer CD, Koken RHM, Van Lier FLJ, Kool M, Vlak JM, Tramper JA. 1992. Structured dynamic model for the baculovirus infection process in insect-cell reactor configurations. *Biotechnol. Bioeng.* 40(4): 537-548.

Dee KU, Hammer DA, Shuler ML. 1995. A Model of the Binding, Entry, Uncoating, and RNA Synthesis of Semliki Forest Virus in Baby Hamster Kidney (BHK-21) Cells. *Biotechnol. Bioeng.* 46(5): 485-496.

Dee KU, Shuler ML. 1997. A mathematical model of the trafficking of acid-dependent enveloped viruses: Applied to the binding, uptake, and nuclear accumulation of baculovirus. *Biotechnol. Bioeng.* 54(5): 468-490.

Digard P, Elton D, Bishop K, Medcalf E, Weeds A, Pope B. 1999. Modulation of nuclear localization of the influenza virus nucleoprotein through interaction with actin filaments. *J. Virol.* 73(3): 2222-2231.

Driscoll PC, Vuidepot AL. 1999. Peripheral membrane proteins: FYVE sticky fingers. *Curr. Biol.* 9(22): 857-860.

Ekert PG, Silke J, Vaux DL. 1999. Caspase inhibitors. *Cell Death Differ.* 6(11): 1081-1086.

Enami M, Sharma G, Benham C, Palese P. 1991. An influenza virus containing nine different RNA segments. *Virology* 185(1): 291-298.

Endy D, Kong D, Yin J. 1997. Intracellular kinetics of a growing virus: A genetically structured simulation for bacteriophage T7. *Biotechnol. Bioeng.* 55(2): 375-389.

Eshima N, Tabata M, Kikuchi H, Karukaya S, Taguchi T. 2001. Analysis of the infection system of human T-cell leukaemia virus type I based on a mathematical epidemic model. *Stat. Med.* 20(24): 3891-3900.

Fischer C, Schrothdiez B, Herrmann A, Garten W, Klenk HD. 1998. Acylation of the influenza hemagglutinin modulates fusion activity. *Virology.* 248(2): 284-294.

Flint JS, Racaniello VR, Krug R. 2000. Principles of virology: molecular biology, pathogenesis, and control. *American Society for Microbiology.*

Fortes P, Beloso A, Ortin J. Influenza virus NS1 protein inhibits pre-mRNA splicing and blocks mRNA nucleocytoplasmic transport. 1994. *EMBO J.* 13(3): 704-712.

Fredrickson AG, McGee RD, Tsuchiya HM. 1970. Mathematical Models in Fermentation Processes. *Adv. Appl. Microbiol.* 13: 419-465.

Fujii Y, Goto H, Watanabe T, Yoshida T, Kawaoka Y. 2003. Selective incorporation of influenza virus RNA segments into virions. *P. Nat. Acad. Sci. US.* 100(4): 2002-2007.

Funk GA, Fischer M, Joos B, Opravil M, Gunthard HF, Ledergerber B, Bonhoeffer S. 2001. Quantification of in vivo replicative capacity of HIV-1 in different compartments of infected cells. *J. Acq. Immun. Def. Synd.* 26(5): 397-404.

Gahmberg CG, Tolvanen M. 1996. Why mammalian cell surface proteins are glycoproteins. *Trends Biochem. Sci.* 21(8): 308-311.

Gambaryan AS, Marinina VP, Tuzikov AB, Bovin NV, Rudneva IA, Sinitsyn BV, Shilov AA, Matrosovich MN. 1998. Effects of host-dependent glycosylation of hemagglutinin on receptor-binding properties of H1N1 human influenza virus grown in MDCK cells and in embryonated eggs. *Virology.* 247(2): 170-177.

- Genzel Y, Voges L, Reichl U. 2001. Development of bioprocess concepts on vaccine production: influenza virus as an example. *Proceedings from the 17th ESACT meeting: Animal cell technology: From target to market*: 344-346.
- Genzel Y, Behrendt I, Koenig S, Sann H, Reichl U. 2004. Metabolism of MDCK cells during cell growth and influenza virus production in large-scale microcarrier culture. *Vaccine*. 22(17-18): 2202-2208.
- Gibbs JS, Malide D, Hornung F, Bennink JR, Yewdell JW. 2003. The influenza A virus PB1-F2 protein targets the inner mitochondrial membrane via a predicted basic amphipathic helix that disrupts mitochondrial function. *J. Virol.* 77(13): 7214-7224.
- Glick BS. 2000. Organization of the Golgi apparatus. *Curr. Opin. Cell Biol.* 12(4): 450-456.
- Goerlich D, Mattaj JW. 1996. Nucleocytoplasmic transport. *Science*. 271(5255): 1513-1518.
- Gomez-Puertas P, Albo C, Perez-Pastrana E, Vivo A, Portela A. 2000. Influenza virus matrix protein is the major driving force in virus budding. *J. Virol.* 74(24): 11538-11547.
- Gregoriades A, Guzman GG, Paoletti E. 1990. The phosphorylation of the integral membrane M2 protein of influenza virus. *Virus Res.* 16(1): 27-42.
- Habtemariam T, Yu P, Oryang D, Nganwa D, Ayanwale O, Tameru B, Abdelrahman H, Ahmad A, Robnett V. 2001. Modelling viral and CD4 cellular population dynamics in HIV: Approaches to evaluate intervention strategies. *Cell. Mol. Biol.* 47(7): 1201-1208.

Hara K, Shiota M, Kido H, Watanabe K, Nagata K, Toyoda T. 2003. Inhibition of the protease activity of influenza virus RNA polymerase PA subunit by viral matrix protein. *Microbiol. Immunol.* 47(7): 521-526.

Holsinger LJ, Shaughnessy MA, Micko A, Pinto LH, Lamb RA. 1995. Analysis of the posttranslational modifications of the influenza virus M(2) protein. *J. Virol.* 69(2): 1219-1225.

Hu YC, Bentley WE. 2000. Poisson distribution in a kinetic and statistical-thermodynamic model for baculovirus infection and virus-like particle assembly in suspended insect cells. *Chem. Eng. Sci.* 55: 3991-4008.

Huang X, Liu T, Muller J, Levandowski RA, Ye Z. 2001. Effect of influenza virus matrix protein and viral RNA on ribonucleoprotein formation and nuclear export. *Virology.* 287(2): 405-416.

Jang JD, Sanderson CS, Chan LCL, Barford JP, Reid S. 2000. Structured modeling of recombinant protein production in batch and fed-batch culture of baculovirus-infected insect cells. *Cytotechnology.* 34(1-2): 71-82.

Juan O. 1998. Multiple levels of posttranscriptional regulation of Influenza virus gene expression. *Seminars in Virology.* 8: 335-342.

Julkunen I, Sareneva T, Pirhonen J, Ronni T, Melen K, Matikainen S. 2001. Molecular pathogenesis of influenza A virus infection and virus-induced regulation of cytokine gene expression. *Cytokine Growth F. R.* 12(2-3): 171-180.

Katze MG, Krug RM. 1984. Metabolism and expression of RNA polymerase II transcripts in influenza-virus infected cells. *Mol. Cell. Biol.* 4(10): 2198-2206.

- Kaufman RJ. 2000. Overview of vector design for mammalian gene expression. *Mol. Biotechnol.* 16(2): 151-160.
- Keller P, Simons K. 1997. Post-Golgi biosynthetic trafficking. *J. Cell Sci.* 110(24): 3001-3009.
- Klumperman J. 2000. Transport between ER and Golgi. *Curr. Opin. Cell Biol.* 12(4): 445-449.
- Knipe DM, Howley PM, Griffin DE. 2001. Fields' virology. 4th ed. *Lippincott Williams & Wilkins.*
- Kroener A, Holl P, Marquardt W, Gilles ED. 1990. DIVA - An open architecture for dynamic simulation. *Computers Chem. Eng.* 14: 1289-1295.
- Krogstad P, Uittenbogaart CH, Dickover R, Bryson YJ, Plaeger S, Garfinkel A. 1999. Primary HIV infection of infants: the effects of somatic growth on lymphocyte and virus dynamics. *Clin. Immunol.* 92(1): 25-33.
- Lakadamyali M, Rust MJ, Zhuang X. 2004. Endocytosis of influenza viruses. *Microbes Infect.* 6(10): 929-936.
- Lamb RA, Choppin PW. 1983. The gene structure and replication of influenza virus. *Ann. Rev. Biochem.* 52: 467-506.
- Lamb RA, Lai CJ, Choppin PW. 1981. Sequences of messenger RNA species derived from genome RNA segment 7 of influenza virus co linear and interrupted messenger RNA species code for overlapping proteins. *P. Nat. Acad. Sci. US.* 78(7): 4170-4174.
- Legrain P, Rosbash M. 1989. Some *cis* and *trans*-acting mutants for splicing target pre-messenger RNA to the cytoplasm. *Cell.* 57(4): 573-584.

- Licari P, Bailey JE. 1992. Modeling the population dynamics of baculovirus-infected insect cells: Optimizing infection strategies for enhanced recombinant protein yields. *Biotechnol. Bioeng.* 39(4): 432-441.
- Lin C, Holland RE, Donofrio JC, McCoy MH, Tudor LR, Chambers TM. 2002. Caspase activation in equine influenza virus induced apoptotic cell death. *Vet. Microbiol.* 84(4): 357-365.
- Ludwig S, Planz O, Pleschka S, Wolff T. 2003. Influenza-virus-induced signaling cascades: Targets for antiviral therapy. *Trends Mol. Med.* 9(2): 46-52.
- Ludwig S, Pleschka S, Wolff T. 1999. A fatal relationship: Influenza virus interactions with the host cell. *Viral Immunol.* 12(3): 175-196.
- Luo G, Chung J, Palese P. 1993. Alterations of the stalk of the influenza virus neuraminidase: Deletions and insertions. *Virus Res.* 29(2): 141-153.
- Luytjes W, Krystal M, Enami M, Parvin JD, Palese P. 1989. Amplification expression and packaging of a foreign gene by influenza virus. *Cell.* 59(6): 1107-1114.
- Luzio JP, Poupon V, Lindsay MR, Mullock BM, Piper RC, Pryor PR. 2003. Membrane dynamics and the biogenesis of lysosomes. *Mol. Membr. Biol.* 20(2): 141-154.
- Marchuk GI, Petrov RV, Romanyukha AA, Bocharov GA. 1991. Mathematical model of antiviral immune response. I. Data analysis, generalized picture construction, and parameter evaluation for hepatitis B. *J. Theor. Biol.* 151(1): 1-40.
- Martin K, Helenius A. 1991a. Transport of incoming influenza virus nucleocapsids into the nucleus. *J. Virol.* 65(1): 232-244.

- Martin K, Helenius A. October, 1991b. Nuclear transport of influenza virus ribonucleoproteins: the viral matrix protein (M1) promotes export and inhibits import. *Cell* 67(1): 117-30.
- Medley GF, Lindop NA, Edmunds WJ, Nokes DJ. 2001. Hepatitis-B virus endemicity: heterogeneity, catastrophic dynamics and control. *Nat. Med.* 7(5): 619-624.
- Mellman I. 1996. Endocytosis and molecular sorting. *Annu. Rev. Cell Dev. Biol.* 12: 575-625.
- Mittal A, Bentz J. September, 2001. Comprehensive kinetic analysis of influenza hemagglutinin-mediated membrane fusion: Role of sialate binding. *Biophys. J.* 81(3): 1521-1535.
- Moehler L, Flockerzi D, Sann H, Reichl U. A Mathematical Model of Influenza A Virus Production in Large-Scale Microcarrier Culture. *Biotechnol. Bioeng.* Accepted.
- Morris SJ, Price GE, Barnett JM, Hiscox SA, Smith H, Sweet C. 1999. Role of neuraminidase in influenza virus-induced apoptosis. *J. Gen. Virol.* 80(1): 137-146.
- Nadeau I, Jacob D, Perrier M, Kamen A. 2000. 293SF metabolic flux analysis during cell growth and infection with an adenoviral vector. *Biotechnol. Prog.* 16(5): 872-884.
- Nelson DL, Cox MM, Lehninger AL. 2000. Lehninger principles of biochemistry. 3rd ed. *Worth publishers, Inc.*
- Nemeroff ME, Barabino SML, Li YZ, Keller W, Krug RM. 1998. Influenza virus NS1 protein interacts with the cellular 30 KDa subunit of CPSF and inhibits 3' end formation of cellular pre-mRNAs. *Mol. Cell.* 1(7): 991-1000.
- Neumann AU, Lam NP, Dahari H, Davidian M, Wiley TE, Mika BP, Perelson AS, Layden TJ. 2000. Differences in viral dynamics between genotypes 1 and 2 of hepatitis C virus. *J. Infect. Dis.* 182(1): 28-35.

Neumann G, Castrucci MR, Kawaoka Y. 1997. Nuclear import and export of influenza virus nucleoprotein. *J. Virol.* 71(12): 9690-9700.

Neumann G, Hughes MT, Kawaoka Y. 2000. Influenza A virus NS2 protein mediates vRNP nuclear export through NES-independent interaction with hCRM1. *EMBO J.* 19(24): 6751-6758.

Nicholson KG, Webster RG, Hay AJ. 1998. Textbook of influenza. *Blackwell Science Ltd.*

Nowak M, May R. 2001. Virus Dynamics: Mathematical Principles of Immunology and Virology. *Oxford University Press, Inc.*

Nunes-Correia I, Ramalho-Santos J, Nir S, Pedroso de Lima MC. 1999. Interactions of influenza virus with cultured cells: detailed kinetic modeling of binding and endocytosis. *Biochemistry-US* 38(3):1095-1101.

O'Neill RE, Jaskunas R, Blobel G, Palese P, Moroianu J. 1995. Nuclear Import of Influenza Virus RNA Can Be Mediated by Viral Nucleoprotein and Transport Factors Required for Protein Import. *J. Biol. Chem.* 270: 22701-22704.

O'Neill RE, Talon J, Palese P. January, 1998. The influenza virus NEP (NS2 protein) mediates the nuclear export of viral ribonucleoproteins. *EMBO J.* 17(1): 288-96.

Olsen CW, Kehren JC, Dybdahl-Sissoko NR, Hinshaw VS. 1996a. Bcl-2 alters influenza virus yield, spread, and hemagglutinin glycosylation. *J. Virol.* 70(1): 663-666.

Olsen CW, Dybdahl-Sissoko N, Hinshaw VS. 1996b. The influence of calcium and reactive oxygen species on influenza virus-induced apoptosis. *Cell Death Differ.* 3: 191-197.

Ortin J. 1998. Multiple levels of posttranscriptional regulation of influenza virus gene expression. *Seminars in Virology*. 8(4): 335-342.

Park YW, Katze MG. 1995. Translational control by influenza virus: Identification of cis-acting sequences and trans-acting factors which may regulate selective viral mRNA translation. *J. Biol. Chem.* 270(47): 28433-28439.

Parodi AJ. 2000. Role of N-oligosaccharide endoplasmic reticulum processing reactions in glycoprotein folding and degradation. *Biochem. J.* 348(1): 1-13.

Perez DR, Donis RO. 1998. The matrix 1 protein of influenza A virus inhibits the transcriptase activity of a model influenza reporter genome in vivo. *Virology*. 249(1): 52-61.

Pinto LH, Holsinger LJ, Lamb RA. 1992. Influenza virus M2 protein has ion channel activity. *Cell*. 69(3): 517-528.

Portela A, Digard P. 2002. The influenza virus nucleoprotein: a multifunctional RNA-binding protein pivotal to virus replication. *J. Gen. Virol.* 83(Pt 4): 723-734.

Potten C, Wilson J. 2004. Apoptosis: The Life and Death of Cells. *Cambridge University Press*.

Power JF, Nielsen LK. 1996. Modelling baculovirus infection of insect cells in culture. *Cytotechnology*. 20(1-3): 209-219.

Reddy B, Yin J. 1999. Quantitative intracellular kinetics of HIV type 1. *AIDS Res. Hum. Retrov.* 15(3): 273-283.

Roy AM, Parker JS, Parrish CR, Whittaker GR. 2000. Early stages of influenza virus entry into Mv-1 lung cells: involvement of dynamin. *Virology* 267(1): 17-28.

- Rudneva IA, Il'yushina NA, Shilov AA, Varich NL, Sinitsyn BV, Kropotkina EA, Kaverin NV. 2003. Functional interactions of the influenza virus glycoproteins. *Molekulyarnaya Biologiya (Moscow)*. 37(1): 34-40.
- Rust MJ, Lakadamyali M, Zhang F, Zhuang X. 2004. Assembly of endocytic machinery around individual influenza viruses during viral entry. *Nat. Struct. Mol. Biol.* 11(6): 567-573.
- Sahai H, Khurshid A. 1995. Statistics in Epidemiology: Methods, Techniques, and Applications. *C R C Press LLC*.
- Saito T, Taylor G, Webster RG. 1995. Steps in maturation of influenza A virus neuraminidase. *J. Virol.* 69(8): 5011-5017.
- Schmid SL. 1997. Clathrin-coated vesicle formation and protein sorting: An integrated process. *Annu. Rev. Biochem.* 66: 511-548.
- Schreiber S, Ludwig K, Herrmann A, Holzhutter HG. 2001. Stochastic simulation of hemagglutinin-mediated fusion pore formation. *Biophys. J.* 81(3): 1360-1372.
- Schultz-Cherry S, Koci M, Thompson E, Tumpey TM. 2003. Examining the cellular pathways involved in influenza virus induced apoptosis. *Avian Dis.* 47(Special Issue): 968-971.
- Schwienhorst A, Lindemann BF, Eigen M. 1996. Growth kinetics of a bacteriophage in continuous culture. *Biotechnol. Bioeng.* 50(2): 217-221.
- Shapiro GI, Krug RM. 1988. Influenza virus RNA replication in-vitro: synthesis of viral template RNA species and virion RNA species in the absence of an added primer. *J. Virol.* 62(7): 2285-2290.
- Sidorenko Y, Reichl U. 2004. Structured model of influenza virus replication in MDCK cells. *Biotechnol. Bioeng.* 88(1): 1-14.

- Sieczkarski SB, Whittaker GR. 2002a. Dissecting virus entry via endocytosis. *J. Gen. Virol.* 83(Pt 7): 1535-1545.
- Sieczkarski SB, Whittaker GR. 2002b. Influenza virus can enter and infect cells in the absence of clathrin-mediated endocytosis. *J. Virol.* 76(20): 10455-10464.
- Singh UN. 1996. Polyribosome dynamics: Size-distribution as a function of attachment, translocation and release of ribosomes. *J. Theor. Biol.* 179(2): 147-159.
- Skehel JJ, Wiley DC. 2000. Receptor binding and membrane fusion in virus entry: The influenza hemagglutinin. *Annu. Rev. Biochem.* 69: 531-569.
- Srivastava R, You L, Summers J, Yin J. 2002. Stochastic vs. deterministic modeling of intracellular viral kinetics. *J. Theor. Biol.* 218: 309-321.
- Stoffler D, Fahrenkrog B, Aebi U. 1999. The nuclear pore complex: From molecular architecture to functional dynamics. *Curr. Opin. Cell Biol.* 11(3): 391-401.
- Stray SJ, Air GM. 2001. Apoptosis by influenza viruses correlates with efficiency of viral mRNA synthesis. *Virus Res.* 77(1): 3-17.
- Stryer L, Berg JM, Tymoczko JL. 2002. Biochemistry. 5th ed. *Worth publishers, Inc.*
- Traenkle F, Kienle A, Mohl KD, Zeitz M, Gilles ED. 1999. Object-oriented modeling of distillation processes. *Comput. Chem. Eng.* 23: 743-746.
- Traub LM, Kornfeld S. 1997. The trans-Golgi network: A late secretory sorting station. *Curr. Opin. Cell Biol.* 9(4): 527-533.
- Von Heijne G. 1990. Protein targeting signals. *Curr. Opin. Cell Biol.* 2(4): 604-608.
- Wagner R, Matrosovich M, Klenk HD. 2002. Functional balance between haemagglutinin and neuraminidase in influenza virus infections. *Rev. Med. Virol.* 12(3): 159-166.

Watanabe K, Takizawa N, Katoh M, Hoshida K, Kobayashi N, Nagata K. 2001. Inhibition of nuclear export of ribonucleoprotein complexes of influenza virus by leptomycin B. *Virus Res.* 77(1): 31-42.

Whittaker G, Bui M, Helenius A. 1996. The role of nuclear import and export in influenza virus infection. *Trends Cell Biol.* 6(2): 67-71.

Wickham TJ, Granados RR, Wood HA, Hammer DA, Shuler ML. 1990. General analysis of receptor-mediated viral attachment to cell surfaces. *Biophys. J.* 58(6): 1501-1516.

Wodarz D, Nowak MA, Bangham CR. 1999. The dynamics of HTLV-I and the CTL response. *Immunol. Today* 20(5): 220-227.

Yamanaka K, Ishihama A, Nagata K. 1988. Translational regulation of influenza virus mRNAs. *Virus Genes* 2(1): 19-30.

Zhirnov OP, Konakova TE, Garten W, Klenk HD. 1999. Caspase-dependent N-terminal cleavage of influenza virus nucleocapsid protein in infected cells. *J. Virol.* 73(12): 10158-10163.

Zhao S, Xu Z, Lu Y. 2000. A mathematical model of hepatitis B virus transmission and its application for vaccination strategy in china. *Int. J. Epidemiol.* 29(4): 744-752.

Zhou Q, Krebs JF, Snipas SJ, Price A, Alnemri ES, Tomaselli KJ, Salvesen GS. 1998. Interaction of the baculovirus anti-apoptotic protein P35 with caspases. Specificity, kinetics, and characterization of the caspase/p35 complex. *Biochemistry.* 37(30): 10757-10765.

Appendix

A1. Dynamics of the Assembly of Simple Components to Complex Particles

While modeling the given process, it can be often noticed that the description of some of events making up the process involved is itself an independent problem that possibly has more general cases and can arise in different applications. One typical problem, arising during the mathematical modeling of the influenza virus life cycle, is the quantitative description of the production of complex particles from simple precursors.

Consider a dynamic system consisting of $N+1$ types of particles, in which particles of $N+1$ -th type (complex particles) consist of particles of first N types (simple particles). Let $X_1 \dots X_N$ designate the numbers of particles of types $1 \dots N$ in the free state. The numbers of particles of types $1 \dots N$ in one complex particle will be denoted, correspondingly, by $Q_1 \dots Q_N$, and the number of complex particles will be, in turn, designated by X .

Suppose that particles of types $1 \dots N$ are produced from the external source at rates proportional to the m -th power of time with the rate coefficients $k_{synt,1} \dots k_{synt,N}$ (h^{-m-1}), respectively, and the particles of $N+1$ -th type are synthesized from particles of types $1 \dots N$ at the rate proportional to $X_1 \dots X_N$ with the rate coefficient of packaging k_{pck} (h^{-1}). Besides that, particles of types $1 \dots N$ will be supposed to undergo degradation with the rate coefficients $k_{degr,1} \dots k_{degr,N}$ (h^{-1}). Then the dynamic system can be described by the following system of ODEs:

$$(A1.1) \quad \frac{dX_i}{dt} = k_{synt,i} t^m - k_{pck,i} \prod_{l=1}^N X_l - k_{degr,i} X_i, \quad i = 1 \dots N$$

$$(A1.2) \quad \frac{dX}{dt} = k_{pck} \prod_{l=1}^N X_l$$

Here, the rate coefficients $k_{pck,i}$ (h^{-1}) are connected with the rate coefficient k_{pck} (h^{-1}) via the relation

$$k_{pck,i} = Q_i k_{pck}, \quad i = 1 \dots N$$

Equations (A1.1)-(A1.2) can be used to describe, for example the dynamics of chemical reactions of synthesis

$$A_1 + A_2 + \dots + A_N = A,$$

provided that the substrates A_1, A_2, \dots, A_N are continuously synthesized. Furthermore, in the detailed mathematical model of influenza virus replication developed in the present study, systems of equations, similar to (A1.1)-(A1.2) represent the formation of more complex viral components from simpler ones, e.g., the assembly of vRNP complexes from vRNA molecules and capsid proteins or the formation of new virions from vRNP complexes and viral envelope proteins. Since at the late stages of the infection simple viral components (e.g., NP proteins and polymerase complexes) are synthesized with the rate proportional to the first degree of time, the model of virus replication refers to the case of $m=1$ in $k_{syn,i} t^m$. Considered processes are, as a rule, accompanied by the complete consumption of particles of one type (i.e., particles of this type are limiting for the formation of complex particles) and the accumulation of particles of other types in the system. Nevertheless, the state of the system can also change according to other scenarios. In this section basic possible cases of the behavior of the system described by equations (A1.1)-(A1.2) will be discussed.

To better understand the behavior of the dynamic system involved, consider the simple case, when a complex particle consists of simple particles of four different types, present in equal amounts:

$$N = 4;$$

$$Q_1 = Q_2 = Q_3 = Q_4.$$

It is obvious that the results obtained for this particular case can be easily extended to the general case. For simulations it will be additionally assumed that

$$Q_1 = Q_2 = Q_3 = Q_4 = 1;$$

$$k_{degr,1} = k_{degr,2} = k_{degr,3} = k_{degr,4} = 1.0 \text{ h}^{-1};$$

$$k_{pck} = 1.0 \text{ h}^{-1}.$$

Evidently, at the late stages of the process the number of complex particles, similar to the numbers of simple particles produced, increases obeying a polynomial law. If a degradation of complex particles is not assumed, the increase of their number has the order equal to $m+1$ (integration of the m -th order law of the increase for the synthesis rate of simple particles):

$$X \sim t^{m+1}.$$

Suppose first that the rate coefficient of synthesis for particles of the 1st type is lower than that for particles of the 2nd, 3rd, and 4th types:

$$(A1.3) \quad k_{synt,1} < k_{synt,i}, \quad i = 2,3,4$$

It is clear that newly produced particles of the 2nd, 3rd, and 4th types are redundant and accumulate in the system. Their numbers increase proportionally to the m -th power of time:

$$X_i \sim t^m, \quad t \rightarrow \infty, \quad i = 2,3,4$$

The number of newly produced particles of the 1st type will be, in contrast, critical for the process. As follows from the numerical solution of system (A1.1)-(A1.2), after the initial increase due to a low rate of packaging their number in the system decreases, finally tending to zero (Fig. A1.1):

$$X_1 \rightarrow 0, \quad t \rightarrow \infty$$

It means that the whole amount of particles of the 1st type is consumed for the production of complex particles.

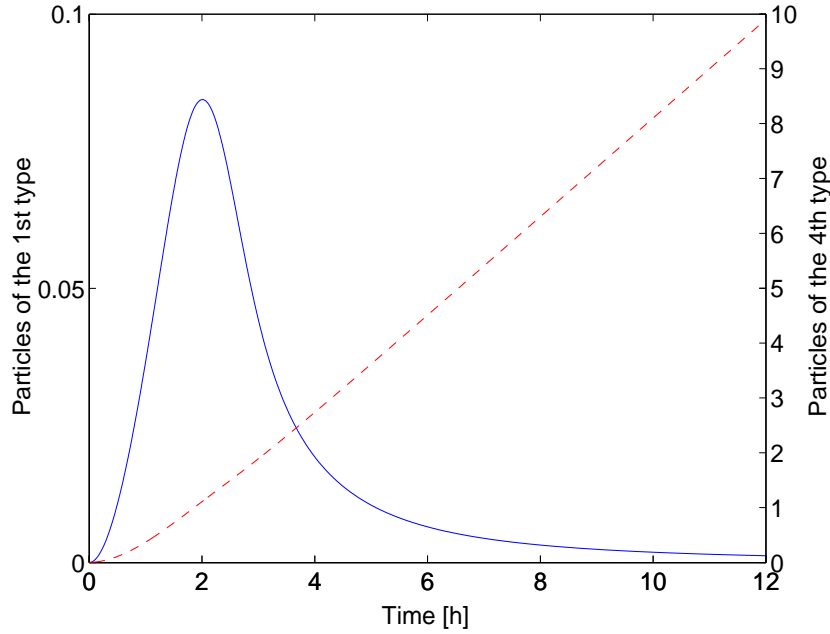


Figure A1.1 Dynamics of simple particles in the case of three redundant types. It is assumed that $m = 1$, $k_{\text{synt},1} = 0.1 \text{ h}^{-2}$, $k_{\text{synt},2} = k_{\text{synt},3} = k_{\text{synt},4} = 1.0 \text{ h}^{-2}$. Particles of the 1st type (X_1 , —) are completely consumed at the late stages of the process. The numbers of particles of the other types, e.g. the 4th type (X_4 , ---), in contrast, increase proportional to the 1st (m -th) power of time.

Let the rate coefficient of synthesis for particles of the 1st type be equal to that for particles of the 2nd type and less than that for particles of the 3rd and 4th types:

$$(A1.4) \quad k_{\text{synt},1} = k_{\text{synt},2}, \quad k_{\text{synt},1} < k_{\text{synt},i}, \quad i = 3,4$$

Simple particles critical for the production of complex particles (in the considered case, particles of the 1st and the 2nd types) are, like in the previous case, completely consumed:

$$X_i \rightarrow 0, \quad t \rightarrow \infty, \quad i = 1,2$$

However, the order of the decrease of their numbers is lower than that for the case considered before (the rate of packaging, expressed by $k_{\text{pck},i} \prod_{l=1}^N X_l$ in (A1.1), contains

only two increasing factors in comparison with three ones in the previous case) (Fig. A1.2). The numbers of redundant simple particles (those of the 3rd and 4th types) in the system increase proportional to the m -th power of time:

$$X_i \sim t^m, \quad t \rightarrow \infty, \quad i = 3,4$$

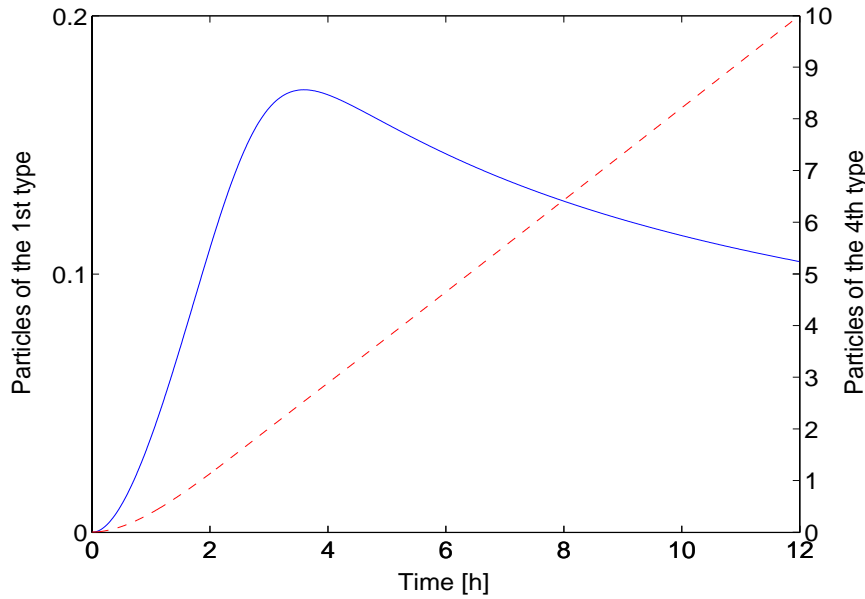


Figure A1.2 Dynamics of simple particles in the case of two redundant types. It is assumed that $m=1$, $k_{synt,1} = k_{synt,2} = 0.1 \text{ h}^{-2}$, $k_{synt,3} = k_{synt,4} = 1.0 \text{ h}^{-2}$. The numbers of particles of the 1st (X_1 , —) and 2nd types tend to zero, however, the order of the decrease is less by 1 (m) than it is in the case of one critical type. The numbers of particles of the 3rd and 4th (X_4 , ---) types increase proportional to the 1st (m -th) power of time.

It is remarkable that the considered situation is similar to the case of three different types of simple particles ($N=3$) with one critical type.

As shown above, for sufficiently high numbers of redundant types, simple particles of critical types are completely consumed for the assembly. However, according to the model it is not necessarily the case. Suppose now that simple particles of three types are critical for the production of complex particles, namely, that

$$(A1.5) \quad k_{synt,1} = k_{synt,2} = k_{synt,3}, \quad k_{synt,1} < k_{synt,4}$$

According to the numerical solution of system (A1.1)-(A1.2), particles of the 1st, 2nd, and 3rd types, despite being critical, are not completely incorporated into newly produced complex particles. Instead, their numbers tend to positive constants $X_{i,0}$:

$$X_i \rightarrow X_{i,0}, \quad t \rightarrow \infty, \quad i = 1,2,3$$

Such a solution results from the presence of only one increasing factor in the expression for the rate of packaging. At the constant numbers of critical components, the rates of their packaging have the same order as the rates of their synthesis

(correspondingly, the terms $k_{synt,i}t^m$ and $k_{pck,i}\prod_{l=1}^N X_l$ in (A1.1)), which provides the equality of the right- and the left-hand sides of equation (A1.1). The behavior of the function representing the number of a critical simple component depends on the relation between the rate coefficient of the synthesis of this component and the rate coefficient of its packaging. At small rate coefficients of packaging (k_{pck}), the number of a given component monotonously increases (Fig. A1.3), otherwise its initial increase due to the low rate of packaging is followed by the decrease (Fig. A1.4). However, as discussed above, in both cases the number of critical viral components tends to a positive constant.

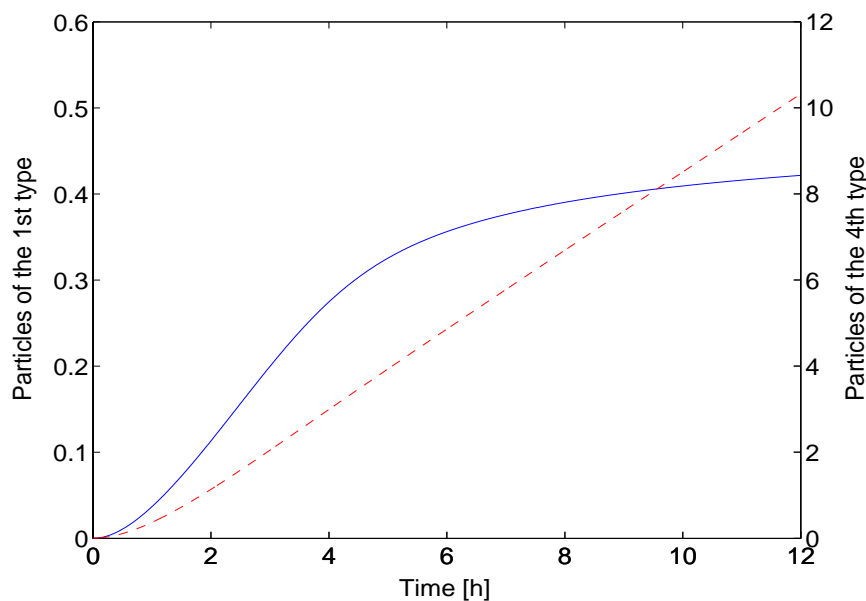


Figure A1.3 Dynamics of simple particles in the case of one redundant type. It is assumed that $m=1$, $k_{synt,1} = k_{synt,2} = k_{synt,3} = 0.1 \text{ h}^{-2}$, $k_{synt,4} = 1.0 \text{ h}^{-2}$. The numbers of particles of the 1st (X_1 , —), 2nd, and 3rd types monotonously increase tending to constant. The number of particles of the 4th type (X_4 , ---) increases proportional to the 1st (m -th) power of time.

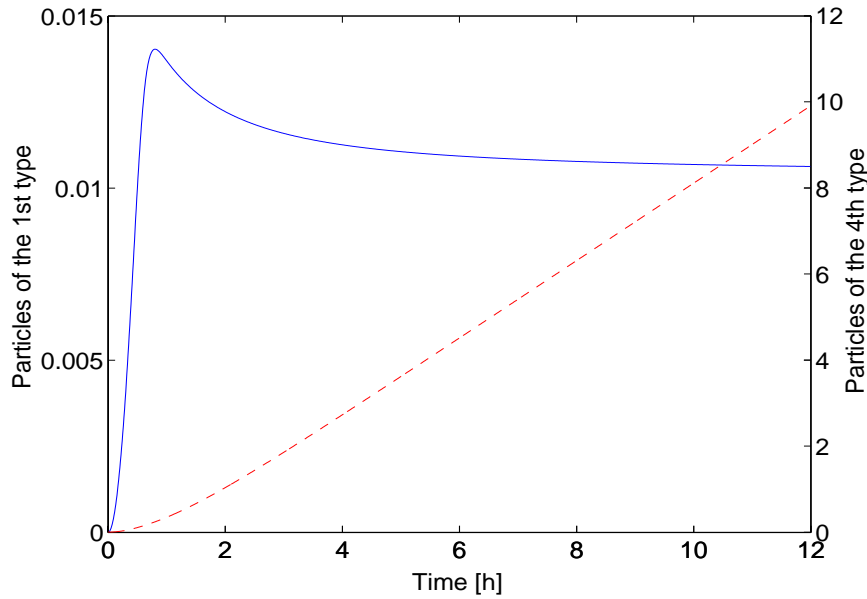


Figure A1.4 Dynamics of simple particles in the case of one redundant type (the rate coefficient of packaging is put to equal $k_{pck} = 10^5 \text{ h}^{-1}$). It is assumed that $m = 1$, $k_{synt,1} = k_{synt,2} = k_{synt,3} = 0.1 \text{ h}^{-2}$, $k_{synt,4} = 1.0 \text{ h}^{-2}$. The numbers of particles of the 1st (X_1 , —), 2nd, and 3rd types, after initial increase, decrease tending to constant. The number of particles of the 4th type (X_4 , ---) increases proportional to the 1st (m -th) power of time.

Consider the remaining possible scenario, when the rate coefficients of synthesis are equal for all simple particles:

$$(A1.6) \quad k_{synt,1} = k_{synt,2} = k_{synt,3} = k_{synt,4}$$

A numerical analysis of system (A1.1)-(A1.2) shows that in the considered case the numbers of simple components are represented by monotonous functions of time, increasing more slowly than the first order polynomial at the late stages of the process:

$$X_i(t) = o(t), \quad t \rightarrow \infty, \quad i = 1 \dots 4$$

It is also easy to see that in the general case the order of the increase of these functions is equal to m/N (at the given set of parameters it is $1/4$) (Fig. A1.5). At the same time, the number of complex particles, as it does in the previous cases, increases proportional to t^{m+1} .

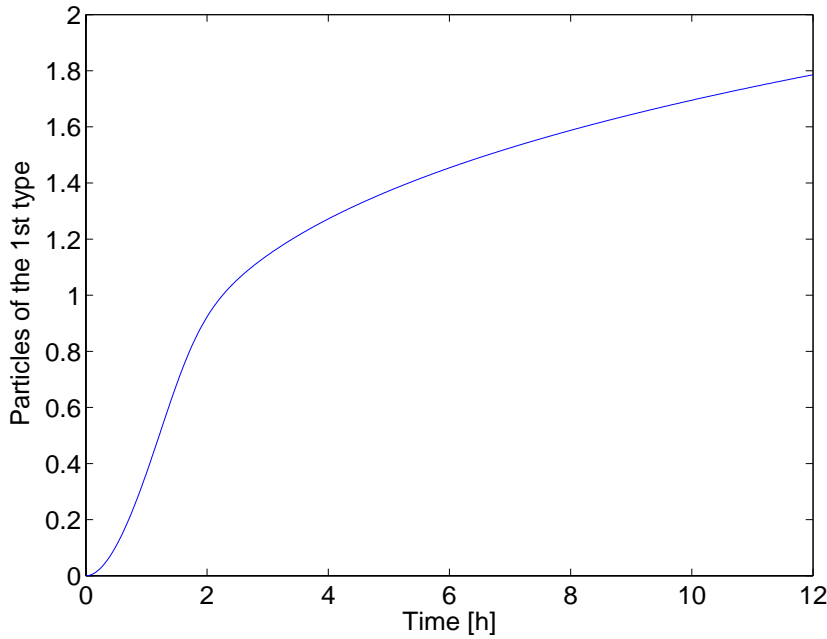


Figure A1.5 Dynamics of simple particles in the case of equal synthesis rates. It is assumed that $m=1$, $k_{synt,1} = k_{synt,2} = k_{synt,3} = k_{synt,4} = 1.0 \text{ h}^{-2}$. The numbers of particles of all types (—) monotonously increase as $o(t)$, $t \rightarrow \infty$.

It is remarkable that although this situation is similar to the case of only one type of simple particles ($N=1$), the order of the increase of the number of simple particles in the case of $N=1$ (Fig. A1.6) differs from that in the cases of $N=4$ (four equal types of simple particles) (Fig. A1.5). It can be also seen from equations (A1.1) and (A1.2) for both cases. In the case of $N=1$ the equations are satisfied by linearly increasing functions representing the numbers of simple particles, whereas in case of $N=4$ the order of the increase must be $1/4$.

It is also worth mentioning the particular case when there are only two types of simple particles making up a complex particle ($N=2$). In this situation only two possible scenarios are possible:

$$k_{synt,1} < k_{synt,2}$$

and

$$k_{synt,1} = k_{synt,2}$$

It is obvious that all the conclusions made above for the case (A1.5) concerning the system containing four types of particles can be applied to the former scenario, whereas the latter scenario corresponds to the case (A1.6) for the system described above. It means that in the system containing two types of particles, provided by the

presence of the degradation of simple particles, particles of all types involved (both critical and redundant) accumulate in the system. If the rate coefficients of synthesis are different for two types of simple particles, the number of particles of the redundant type increases proportional to t^m , whereas the number of particles of the critical type tends to constant.

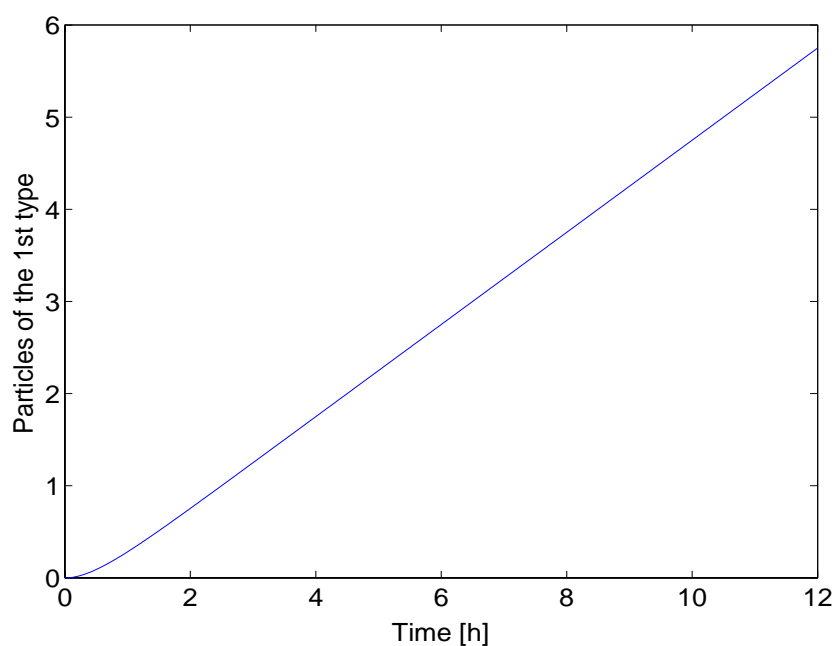


Figure A1.6 Dynamics of simple particles in the case of one type of simple particles ($N=1$). The number of simple particles (—) is a linearly increasing function of time ($m=1$).

Thus, at the late stages of the considered process, the number of complex particles invariably increases proportional to t^{m+1} , whereas the numbers of simple particles of redundant types increase proportional to the m -th power of time. As for the simple particles of critical types, their dynamics is highly sensitive to the number of redundant types in the system. At the absence of redundant types the number of simple particles monotonously increases; in the case of one redundant type the numbers of simple particles of critical types tend to constant; and in the case of several (more than one) redundant types the particles of critical types are completely consumed by the production of complex particles.

The model presented in this section can be easily modified to consider more complex expressions for synthesis rates of simple particles. For example, synthesis rates can be

assumed to be proportional to the number of simple particles of one of types (like polymerase complexes in the model for influenza virus replication, see section 2).

A2. Infection Probability for Virus Particles Containing Eight Genome Segments

Let N designate the total number of nucleotides, making up the genome segments produced. Since all 8 segments are produced by viral polymerase with the same rate (measured in nucleotides per second), the number of nucleotides belonging to the i -th segment is equal to $\frac{N}{8}$ for any i . The number of produced i -th segments is then

$$S_i = \frac{N}{8} \frac{1}{N_i},$$

where N_i is the number of nucleotides, making up one copy of the i -th segment. The total number of produced segments is, correspondingly,

$$S = \frac{N}{8} \sum_{i=1}^8 \frac{1}{N_i}.$$

Suppose that S and S_i ($i=1\dots 8$) are so big that taking away of several segments (less than eight) does not change them significantly. Then the number of all possible ways to choose 8 genome segments is

$$M_{all} = S^8.$$

However, only in

$$M_{dif} = 8! \prod_{i=1}^8 S_i$$

cases 8 chosen segments will be different ($\prod_{i=1}^8 S_i$ is the number of ordered selections, and $8!$ is the number of permutations). Taking the values for N_i from (Kneipe et al.,

2001), and calculating $\frac{1}{N_i}$ and $\frac{S_i}{S}$ (Table A2.1), the probability to produce an

infectious virion can be calculated as

$$P_{\text{inf}} = \frac{M_{\text{dif}}}{M_{\text{all}}} = 8! \prod_{i=1}^8 \frac{S_i}{S} = 8! \prod_{i=1}^8 \frac{1}{N_i} = 0.0015 \approx \frac{1}{667} .$$

Table A2.1 Calculations of the probability of infection for a virus particle containing 8 genome segments

	$\frac{1}{N_i}$	$\frac{S_i}{S}$
PB2	$4.27 \cdot 10^{-4}$	$8.04 \cdot 10^{-2}$
PB1	$4.27 \cdot 10^{-4}$	$8.04 \cdot 10^{-2}$
PA	$4.48 \cdot 10^{-4}$	$8.44 \cdot 10^{-2}$
HA	$5.62 \cdot 10^{-4}$	$10.59 \cdot 10^{-2}$
NP	$6.39 \cdot 10^{-4}$	$12.04 \cdot 10^{-2}$
NA	$7.08 \cdot 10^{-4}$	$13.34 \cdot 10^{-2}$
M	$9.74 \cdot 10^{-4}$	$18.35 \cdot 10^{-2}$
NS	$11.24 \cdot 10^{-4}$	$21.17 \cdot 10^{-2}$
Σ	$53.09 \cdot 10^{-4}$	
Π		$3.60 \cdot 10^{-8}$

A3. Method to Calculate the Average Lifetime of a Cell

Based on experimental data concerning the population of living cells after infection, the average lifetime of a cell can be calculated. Let $Z_d(t)$ (*cells/nL*) designate the number of dead¹³ cells at the time point t (h), which is the difference of the initial number of cells in the system (Z_0 (*cells/nL*)) and the total number of living cells (uninfected and infected). Then the number of cells that die at time interval $[t; t + dt]$ is $dZ_d(t)$, and the net lifetime of these cells at the considered interval is $t dZ_d(t)$.

¹³ Like in the population model, function Z_d represents the total number of dead and degraded cells.

If $\tau_{\max}(h)$ is the time point when all cells are dead, then the net lifetime of all cells in the system ($T_{\Sigma}(h)$) is

$$T_{\Sigma} = \int_0^{\tau_{\max}} t dZ_d(t),$$

and the initial number of living cells is, correspondingly,

$$Z_0 = \int_0^{\tau_{\max}} dZ_d(t).$$

Consequently, for the average lifetime of a cell ($T(h)$) the following formula can be written:

$$(A3.1) \quad T = \frac{T_{\Sigma}}{Z_0} = \frac{1}{Z_0} \int_0^{\tau_{\max}} t \frac{dZ_d(t)}{dt} dt.$$

This formula shows that required for the calculation of the average lifetime of a cell is the dependency of the number of dead cells on time. Such a dependency can be particularly obtained based on the population model (Fig. 4.23). Numerical integration in formula (A3.1) for the $MOI=0.1$ virions/cell provides the value of the average lifetime of a cell equal to approximately 22 h.

For high values of the MOI, e.g., $MOI=10.0$ virions/cell (all the cells are immediately infected) formula (A3.1) gives $T \approx 10$ h, which corresponds to the average lifetime of an infected cell.

A4. Estimation of Cellular Pools

Calculations of the numbers of free cellular amino acids and nucleotides, as well as the number of precursor mRNA molecules, are summarized in Table A4.1. Among the components the wet weight of the cell consists of 0.4 % falls to free nucleotides and 0.4 % is made up by free amino acids (Alberts et al., 2002). Precursor mRNA molecules make up about 5 % of the total number of RNA molecules constituting the

biomass of the cell, and the fraction of RNA molecules of the wet weight of the cell is, in turn, 1.1 %.

The percentage of the considered resources in the dry weight of the cell can be derived based on the data concerning the content of water: 70 % of the wet weight (Alberts et al., 2002). Cellular dry weight were taken equal to $5.41 \cdot 10^{-10}$ g (MDCK cells; U. Reichl, personal communication) and the relation between the units of mass involved is $1 \text{ Da} \approx 1.66 \cdot 10^{-24} \text{ g}$. The number of precursor mRNA molecules was calculated both in nucleotides and in molecules. In the latter case it was taken into account that the average length of the mRNA strand was approximately 6000 nucleotides (Kaufman et al., 2000).

Table A4.1 Calculations of the intracellular numbers of free nucleotides, amino acids, and precursor mRNA molecules

	Amino acids	Nucleotides	mRNA
% of cellular wet weight	0.4	0.4	0.05-1.1
Source	1	1	1
% of cellular dry weight	1.33	1.33	0.18
Weight in the cell, g/cell	$7.20 \cdot 10^{-12}$	$7.20 \cdot 10^{-12}$	$9.74 \cdot 10^{-13}$
Average molecular weight, Da	138	330	330
Source	2	3	3
Number of molecules	$3.14 \cdot 10^{10}$ aa	$1.31 \cdot 10^{10}$ nt	$1.78 \cdot 10^9$ nt $2.97 \cdot 10^5$ mlc

nt: Nucleotides

aa: Amino acids

mlc: Molecules

1: Alberts et al., 2002

2: Nelson et al., 2000

3: Stryer et al., 2002

A5. Experimental Data for Virus Release and Cell Detachment

The virus yield and the number of cells in the supernatant were investigated for the infection of cells in roller bottles at different MOI (Y. Genzel). Experimental data is presented in Figures A5.1 and A5.2.

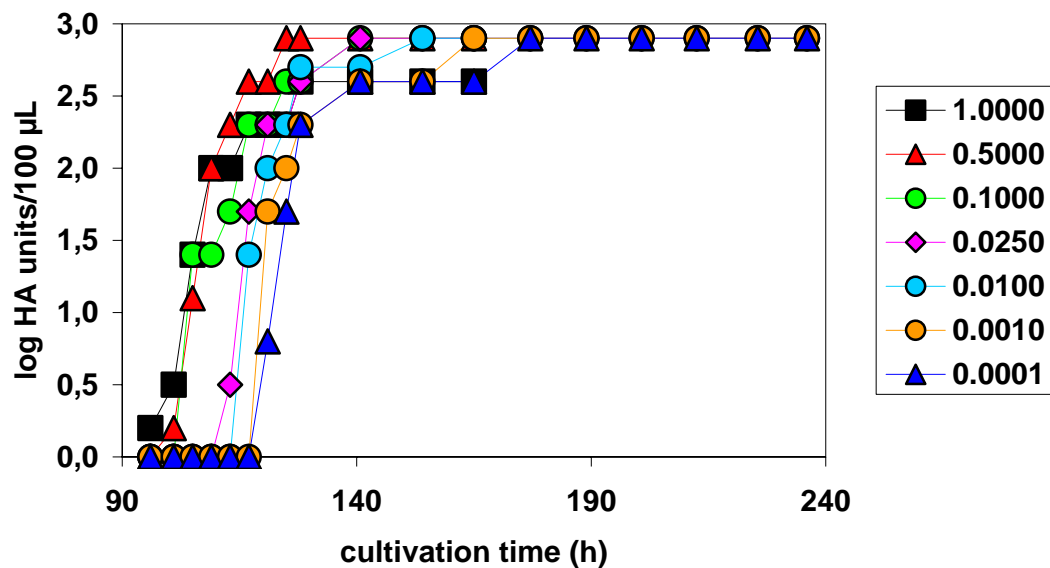


Figure A5.1 Virus yield (HA value) for different values of the MOI.

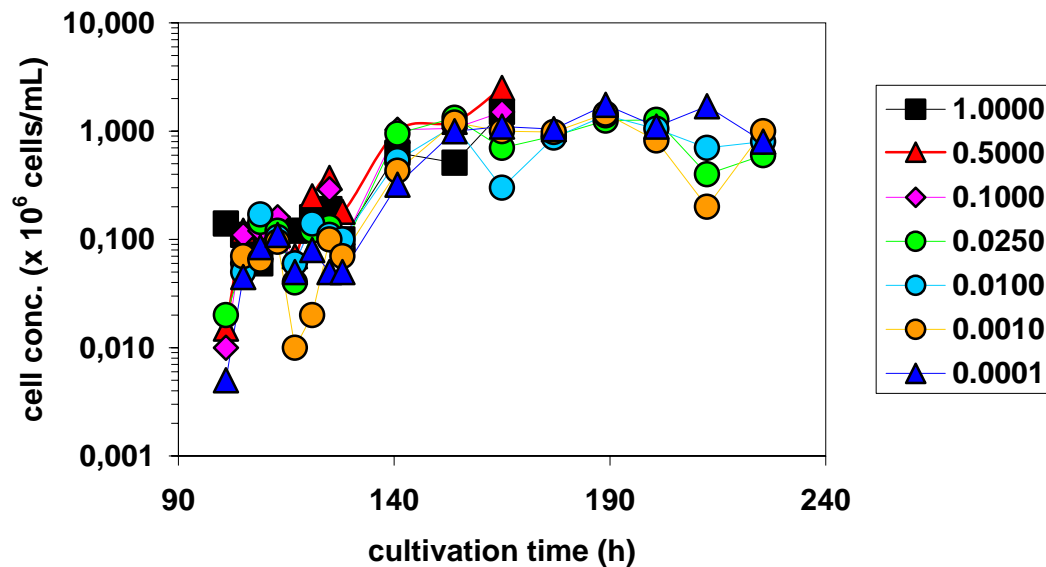


Figure A5.2 The number of cells in the supernatant (detached cells) for different values of the MOI.

This data indicates that at the early stages of the process the HA value (which can be assumed to be proportional to the virus yield) increases faster at higher MOI (Fig A5.1). On the other hand, the maximal number of released virions does not depend significantly on the MOI.

Figure A5.2 shows that within 48 h p.i. more than 90% of cells detach from microcarriers for all the MOI values considered.

Lebenslauf

Persönliche Daten:

Name: Yury Sidorenko
Anschrift: Listemannstr. 18
39104 Magdeburg
Deutschland
Tel.: 0179-9073059
zlaia@mpi-magdburg.mpg.de
Geburtsdatum: 03.03.1979
Geburtsort: Moskau
Familienstand: ledig
Staatsangehörigkeit: russisch

Schulische Entwicklung:

1985 – 1995 Mittelschule in Krasnojarsk
1986 – 1993 Musikschule in Krasnojarsk

Studium:

1995 – 1999 Institut der Physik und Technologie in
Moskau
Bachelorabschluss
1999 – 2001 Institut der Physik und Technologie in
Moskau
Magisterabschluss

Studienbegleitende Tätigkeiten:

1999 – 2001 Franko-Russisches Zentrum für
Rechnenmathematik in Moskau
Programmierer

Berufliche Tätigkeiten:

2001 – 2004 Max-Planck-Institut für Dynamik
komplexer technischer Systeme in
Magdeburg
Wissenschaftler
2004 – 2005 Otto-von-Guericke-Universität in
Magdeburg
Wissenschaftler

Magdeburg, 29.09.2005